Department of Physiology and Pharmacology "Vittorio Erspamer"
Sapienza University of Rome

The role of glial cells in neuropsychiatric disorders

A Dissertation in Fulfillment of the Requirements for the
Degree of Doctor of Philosophy in Pharmacology and Toxicology
Cycle XXXII

Roberta Facchinetti

Director of the Ph.D Program:

Prof. Maura Palmery

Thesis Advisor:

Dott. Caterina Scuderi

Thesis Committee:

Prof. Pietro Marini

Prof. Luca Romanelli

Prof. Viviana Trezza

Academic year 2018 - 2019

TABLE OF CONTENTS

Riassunto

I disturbi neuropsichiatrici rappresentano uno dei problemi principali dell'era moderna. L'incidenza di patologie come il morbo di Alzheimer (AD), il morbo di Parkinson (PD), la depressione e l'autismo sta aumentando, poiché la popolazione continua ad invecchiare ed i criteri diagnostici diventano sempre più accurati. Nonostante l'ampia conoscenza di queste patologie, numerosi disordini neuropsichiatrici sono, ad oggi, ancora incurabili.

La grande quantità di letteratura accumulata nel corso degli anni su questo argomento indica la disfunzione neuronale come principale responsabile dello sviluppo di tali disturbi; tuttavia, negli ultimi 15 anni numerosi studi hanno iniziato ad evidenziare il contributo di un'altra popolazione cellulare del sistema nervoso, denominata glia, nella fisiopatologia dei disturbi neuropsichiatrici. Suddetta popolazione cellulare comprende astrociti, oligodendrociti, cellule NG-2 e cellule microgliali, ognuna di esse dotata di specifiche funzioni volte a regolare l'omeostasi cerebrale.

Questa nuova percezione del funzionamento del sistema nervoso centrale (SNC) ha perciò spostato l'attenzione del mondo scientifico dal compartimento neuronale verso il campo, ancora poco conosciuto, delle interazioni glia-neuroni.

Le evidenze scientifiche che dimostrano il ruolo omeostatico delle cellule gliali nel SNC sono in continuo aumento. Diviene ragionevole ipotizzare, dunque, un loro ruolo nell'eziopatogenesi delle malattie neuropsichiatriche, tutte accomunate dalla presenza di un danno cerebrale, seppur di varia natura. In letteratura sono emersi i primi dati sulla presenza di una disfunzionalità gliale alla base di questi disturbi. Infatti, è stato ampiamente dimostrato che queste cellule, in seguito ad un insulto a carico del SNC, subiscano modificazioni morfologiche e funzionali di diverso tipo, innescando il processo di gliosi reattiva, frequentemente caratterizzato da attivazione gliale e neuroinfiammazione. Iniziato a scopo difensivo, tale processo può perdurare nel tempo, perturbando l'omeostasi cerebrale e generando effetti tossici sui neuroni e, conseguentemente, morte cellulare. Nonostante queste evidenze, i meccanismi molecolari inerenti il coinvolgimento della glia nei disturbi psichiatrici non sono stati ancora del tutto chiariti.

Pertanto, scopo del mio progetto di dottorato è stato quello di studiare il ruolo delle cellule gliali nell'insorgenza e/o nella progressione di alcune malattie neuropsichiatriche al fine d'identificare nuovi target da manipolare farmacologicamente. In particolare, avvalendomi di diversi modelli preclinici *in vitro* ed *in vivo,* ne ho studiato il coinvolgimento in modelli di AD, di disturbi dello spettro autistico (ASD) e di stress acuto (AS).

Studio sulle alterazioni gliali in diversi modelli preclinici di malattia di Alzheimer.

L'AD è un disturbo neurodegenerativo progressivo caratterizzato clinicamente, nella sua fase avanzata, da compromissione delle funzioni cognitive e da profonda perdita neuronale. I benefici degli attuali trattamenti sono limitati, quindi vi è una pressante richiesta di nuovi approcci terapeutici in grado di rallentare la progressione della malattia o, meglio, di prevenirne l'insorgenza. Negli ultimi decenni, l'alterazione delle cellule gliali e la presenza di un intenso stato infiammatorio sono state incluse tra le caratteristiche neuropatologiche dell'AD, insieme all'accumulo extracellulare di beta amiloide (Aβ) ed alla formazione intraneuronale di grovigli neurofibrillari. Quindi, risulta ragionevole pensare che la combinazione di trattamenti ad azione antinfiammatoria e neuroprotettiva possa rappresentare un approccio adeguato per il trattamento di questa patologia. In questo contesto, ha suscitato il mio interesse la palmitoiletanolamide (PEA), un'ammide endogena dell'etanolamide e dell'acido palmitico, dotata di numerose attività farmacologiche, comprese quella antinfiammatoria (anche se dimostrata in modelli d'infiammazione periferica) e neuroprotettiva. Pertanto, grazie ad una collaborazione scientifica con il Prof. Tommaso Cassano dell'Università di Foggia, durante il primo anno di dottorato, ho studiato gli effetti *in vitro* ed *in vivo* della PEA su un modello murino triplo transgenico di AD, denominato 3×Tg-AD. Gli esperimenti, dapprima effettuati *in vitro* su colture primarie di astrociti e neuroni corticali, hanno dimostrato la presenza di uno stato reattivo basale nelle cellule isolate dai topi 3×Tg-AD. Il trattamento con PEA ha contrastato efficacemente la reattività astrocitaria, determinando un miglioramento della vitalità neuronale.

Successivamente, ho eseguito gli esperimenti *in vivo*, trattando i topi non transgenici (Non-Tg) e 3×Tg-AD in cronico con PEA ultramicronizzata (um-PEA, 10 mg/kg/die per 90 giorni mediante un dispositivo a rilascio controllato), una formulazione che ne massimizza la biodisponibilità. Gli esperimenti sono stati effettuati su animali di due diverse età, giovani adulti (6 mesi al termine del trattamento) e anziani (12 mesi al termine del trattamento), per mimare la fase inziale e quella conclamata della patologia. Con la consapevolezza che le aree cerebrali non rispondono tutte simultaneamente agli insulti né con lo stesso grado d'intensità nella risposta, abbiamo studiato due differenti aree cerebrali: l'ippocampo e la corteccia prefrontale.

I risultati ottenuti con questo studio hanno dimostrato, per la prima volta, la capacità delle cellule gliali di comportarsi diversamente a seconda dello stadio della malattia investigato, passando da una condizione di reattività ad una di ipotrofia. Infatti, negli animali giovani, ho potuto rilevare la presenza di astrogliosi e neuroinfiammazione sia nella corteccia prefrontale che nell'ippocampo. Sorprendentemente, i topi che avevano ricevuto nei tre mesi precedenti la um-PEA non mostravano tali modifiche. Al contrario, negli animali anziani non ho riscontrato la presenza di reattività gliale ma alcuni parametri sembravano, invece, indicare un'iniziale condizione di atrofia cellulare.

È noto che l'invecchiamento rappresenta uno dei maggiori fattori di rischio per l'insorgenza dell'AD. Non è, invece, chiaro se le modifiche cellulari riscontrate nelle patologie correlate all'invecchiamento, incluso l'AD, siano dovute alla malattia o all'invecchiamento stesso. Cercando di chiarire questo aspetto, ho eseguito analisi molecolari volte a studiare gli effetti dell'invecchiamento sulla morfologia e sulle funzioni astrocitarie e microgliali, confrontando animali giovani (6 mesi) ed anziani (12 mesi) sani (Non-Tg) e malati (3×Tg-AD) per mimare, rispettivamente, l'invecchiamento sano e patologico. Sorprendentemente, questi studi hanno dimostrato che le alterazioni astrogliali osservate erano da attribuire all'invecchiamento piuttosto che alla patologia.

L'ultima parte dei miei studi sull'AD si è concentrata su una fase della malattia che in clinica viene definita prodromica. Questa fase è caratterizzata da alterazioni cellulari e molecolari, ma la persona affetta risulta, nella maggior parte dei casi, ancora asintomatica. Questo stadio è caratterizzato sia dall'iniziale accumulo di Aβ che da un precoce processo neuroinfiammatorio. Il National Institute of Aging da diversi anni sottolinea l'importanza di questa fase e spinge i ricercatori a studiarla. Difatti, risulta fondamentale comprendere quali vie determineranno il passaggio da una fase asintomatica a quella di manifesta patologia. La comprensione di questi meccanismi è cruciale per identificare un approccio terapeutico mirato a questo stadio dell'AD.
Per questi motivi, e tenendo in considerazione i risultati ottenuti con la PEA nel modello transgenico, durante il secondo anno di dottorato ho testato una nuova combinazione di PEA e luteolina (Lut - un noto flavonoide con proprietà antiossidanti), ultramicronizzati insieme in un'unica formulazione (co-ultra PEALut), in un modello chirurgico di AD in grado di ricapitolare questo stadio precoce della malattia. Recenti evidenze, infatti, dimostrano che questa nuova formulazione gode di maggiore biodisponibilità e che risulta più efficace rispetto ai due composti somministrati singolarmente. I risultati ottenuti hanno mostrato la capacità del composto co-ultra PEALut di contrastare l'astrogliosi e la microgliosi osservate nei ratti inoculati in ippocampo dorsale con Aβ, ma anche di prevenire l'aumento nell'espressione genica di citochine ed enzimi pro-infiammatori e di aumentare i livelli trascrizionali di alcuni fattori neurotrofici, promuovendo quindi la sopravvivenza neuronale.

Studio sulle alterazioni gliali in un modello di disturbo dello spettro autistico.
Grazie ad una collaborazione con la Prof. Viviana Trezza dell'Università di Roma Tre, durante il secondo anno di dottorato ho avuto la possibilità di ampliare i miei studi ad un'altra patologia neuropsichiatrica, il disturbo dello spettro autistico (ASD), un gruppo di alterazioni del neurosviluppo caratterizzate dalla compromissione della comunicazione e dell'interazione sociale.
Dal punto di vista fisiopatologico, i cervelli *post-mortem* di individui affetti da ASD rivelano cambiamenti nell'organizzazione sinaptica, nell'arborizzazione dendritica e nella neurotrasmissione,

oltre che alterazioni morfologiche e funzionali delle cellule gliali. In effetti, recenti studi suggeriscono un importante contributo della glia nello sviluppo dell'ASD; tuttavia, il ruolo funzionale ed i meccanismi molecolari alla base di tali alterazioni non sono ancora stati presi in esame dalla comunità scientifica. Per contribuire a colmare questo vuoto, in ratti maschi esposti in utero all'acido valproico ho analizzato l'espressione di specifici marcatori gliali e neuronali in aree cerebrali strettamente correlate ai comportamenti autistici (corteccia prefrontale, cervelletto ed ippocampo). Poiché questo disturbo viene diagnosticato durante l'infanzia ed accompagna il paziente nel corso della sua vita, ho effettuato gli esperimenti a tre diverse età, per riprodurre l'infanzia, l'adolescenza e l'età adulta. I dati ottenuti evidenziano marcate alterazioni morfologiche della neuroglia che ne suggeriscono, quindi, un ruolo nell'ASD. I risultati risultano complessi da interpretare, in quanto estremamente eterogenei (sia in relazione alle diverse aree cerebrali studiate che alle tre età). La corteccia prefrontale e l'ippocampo si sono rivelate le regioni cerebrali maggiormente interessate dai cambiamenti osservati.

Studio delle alterazioni gliali in un modello di stress acuto.

Ad oggi, lo stress cronico risulta ampiamente studiato e tra le numerose patologie ad esso correlate vengono annoverate alcune malattie neuropsichiatriche. In questo ambito, è stato dimostrato un coinvolgimento delle cellule gliali in modelli di stress duraturo nel tempo. Attualmente, invece, sono poche le evidenze che considerano un potenziale ruolo delle cellule gliali nel regolare la risposta ad uno stress di tipo breve ed improvviso. Durante l'ultimo anno di dottorato ho preso parte ad un progetto di ricerca, in collaborazione con il Prof. Giambattista Bonanno dell'Università di Genova ed il Prof. Maurizio Popoli dell'Università degli Studi di Milano, volto a chiarire quali siano le basi biologiche che predispongono alla vulnerabilità o resilienza ad uno stress acuto. Il protocollo sperimentale prevede l'esposizione di ratti maschi Sprague-Dawley al saccarosio all'1% per due ore ed al saccarosio allo 0,5% per un'ora due volte alla settimana per le successive tre settimane, al fine di valutare la loro assunzione basale di saccarosio. Successivamente, la metà degli animali viene esposta ad un evento di stress acuto (footshock stress) e dopo 24 ore sottoposta al test di preferenza al saccarosio per suddividere gli animali in resilienti (RES) e vulnerabili (VUL) (RES: soggetti con una diminuzione dell'assunzione di saccarosio < 10%; VUL: soggetti con una diminuzione di saccarosio > 25%). Il lavoro da me svolto si è focalizzato sullo studio, nella corteccia prelimbica di questi animali, delle alterazioni strutturali, cellulari e molecolari che colpiscono le cellule gliali 24 ore dopo il paradigma di stress acuto. Recentemente ho mostrato i dati fino ad ora ottenuti ad un congresso internazionale; essi, seppur preliminari, mostrano la capacità dello stress acuto di diminuire drasticamente il numero degli astrociti nell'area investigata, indipendentemente dalla resilienza o vulnerabilità degli animali all'evento stressorio. In maniera interessante, inoltre, si nota anche un

diverso coinvolgimento della componente astrocitaria stessa tra gli animali resilienti e quelli vulnerabili, dato che spinge a continuare gli esperimenti attualmente in corso.

Abstract

Glial cells are a large class of cells of ectodermal (astroglia, oligodendroglia, and peripheral glial cells) and mesodermal (microglia) origin, which provide basic homeostatic support, protection, and defense to the nervous tissue. For these reasons, the potential for glial cells involvement in pathological events has been acknowledged since their discovery. Only during the past decade, research evidence has shown the key role of these non-neuronal cells in the progression of several neurological diseases.

Neuropsychiatric disorders have always been widely ascribed to neuronal malfunction or loss, a "neurocentric view" that has dominated the neuropathology for a long time. However, because of the complexity of the physiological functions that glial cells perform, it is reasonable to state that they allow neurons to properly function; this "gliocentric view" has expanded the horizons to glial cells as new players to be studied and as potential pharmacological targets. This is a new and, for several aspects, undisclosed field of research. Indeed, despite a still growing body of evidence, the molecular mechanisms underlying glia involvement in psychiatric disorders have not yet been fully clarified. The present dissertation consists of an in-depth examination of glial cells in the onset and/or progression of three neuropsychiatric diseases: Alzheimer's disease, autism spectrum disorders and acute stress. To this aim, different *in vitro* and *in vivo* preclinical models mimicking these pathologies have been used.

All the results collected in this doctoral thesis demonstrate or contribute in demonstrating that glial cells are involved in the onset and in the progression of these neuropsychiatric disorders. The discovery of this common denominator among different brain pathologies represents an intriguing advance in the development of new therapeutic approaches to counteract these very frequent, but still incurable, diseases.

1. Introduction

1.1 General introduction

During my PhD in Pharmacology and Toxicology (cycle XXXII), carried out at the Department of Physiology and Pharmacology "V. Erspamer" at Sapienza University of Rome, I focused my studies on the involvement of glial cells in the onset and/or progression of some neuropsychiatric disorders. My interest in this topic arises from the studies I carried out for my Master's Degree thesis, when I investigated both the morphological and functional alterations of glial cells in a transgenic model of Alzheimer's disease (AD). The promising results obtained prompted me to pursue this line of research, deepening the issues addressed and opening new horizons in the intriguing world of glial cells.

Glial cells represent the most abundant cell type in the central nervous system (CNS) (Jäkel and Dimou, 2017). This heterogeneous cell population can be divided into two main groups: the macroglia and the microglia cells. The macroglia, which comprehends astrocytes, oligodendrocytes and NG-2 glia (not shown in the picture below), regulate the general homeostasis of the brain; microglia cells instead represent the immunocompetent portion of the CNS, executing functions related to those of macrophages (Di Benedetto and Rupprecht, 2013) (Fig.1).

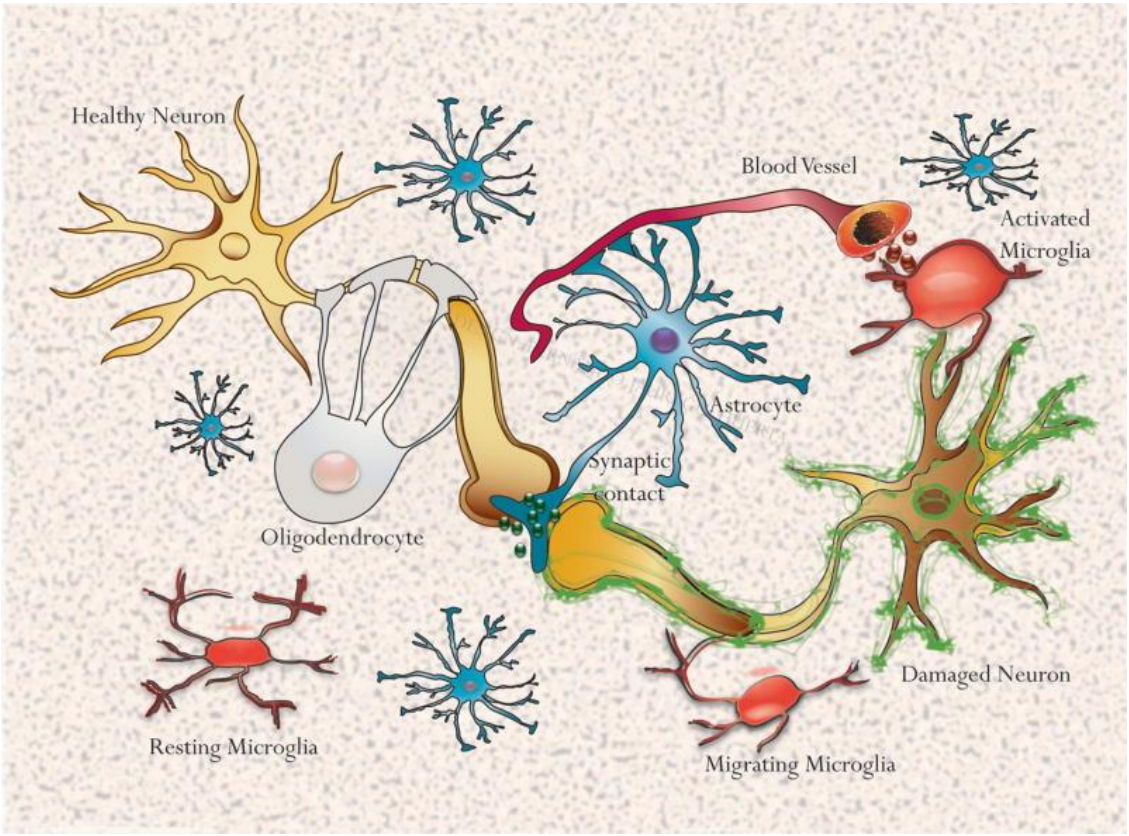

Fig. 1. Glial cells in the adult brain (Jauregui-Huerta et al., 2010).

The new available technological advances, such as high-resolution imaging or optogenetics, have allowed the study of glial cells *in vivo* in the brain, revealing their ability to perform several functions. While microglia cells act as the first form of immune defense in the brain, astrocytes are currently defined as cells responsible for CNS homeostasis at all levels of organization (molecular, cellular, network, organ and system levels) (Verkhratsky and Nedergaard, 2018). Among several functions, astrocytes finely control the environment by regulating pH, ion homeostasis, blood flow and counteracting oxidative stress. In addition, these cells contribute to synaptogenesis and dynamically modulate signal transmission, regulate neural and synaptic plasticity, and provide trophic and metabolic support to neurons (Butt and Verkhratsky, 2018).

Oligodendrocytes, which form the myelin sheath, regulate the transmission of action potentials through myelinated axons, profoundly affecting the functional connectome among neurons (Fields et al., 2015). Lastly, NG-2-positive cells are known to express a plethora of ion channels and receptors and to receive direct synaptic input from neurons, thus controlling myelination and brain plasticity (Eugenín-von Bernhardi and Dimou, 2016).

Neuropsychiatric diseases are widely ascribed to neuronal malfunction or loss of nerve cells. This "neurocentric view" has dominated the neuropathology for a long time, and almost all pharmacological therapies were designed to restore neuronal functions or ensure their survival.

Nowadays, it has become clear that this is a simplistic view; indeed, evidence accumulated in the last 15 years showed the crucial role of glial cells in allowing neurons to properly function. Therefore, possible alterations or modifications of these cells (or of their functions) could partially explain the pathogenesis and progression of many brain diseases.

It has been demonstrated that glial cells rapidly act in response to several brain injuries, undergoing important changes in their morphology and functioning. Such modifications are complex and still not well understood but, for simplicity, they are identified as hyperreactivity or atrophy (Burda and Sofroniew, 2014). For example, the coexistence of these two opposite events has been demonstrated in a transgenic model of AD, but in two different stages of the disease course (Scuderi et al., 2018).

The reactive response of astrocytes and microglia to brain damages represents a protective reaction aimed at removing the injurious stimuli. However, when an uncontrolled and prolonged activation of glial cells goes beyond physiological control, it brings detrimental effects that override the beneficial ones. In this condition, glial cells foster a neuroinflammatory response, accounting for the synthesis of different cytokines and proinflammatory mediators, self-perpetuating a condition called reactive gliosis (Mrak and Griffin, 2001).

Upon brain injury, two microglia activation states have been described: the M1, characterized by the production of various pro-inflammatory cytokines such as TNF-α, IL-1β and IL-6, as well as

superoxide, ROS and NO; the M2, deriving from a switch of the activation state towards an "alternatively activated" one, exerting a protective role against the brain injury through the release of neurotrophic factors including BDNF, IGF-1 and IL-4. It has been recently proposed to restrict the use of "alternative activation" for the description of microglial cells primarily exposed to IL-4 or IL-13. Indeed, it has been demonstrated that the M2 state is also represented by an "acquired deactivation" of these cells, consisting of a mixed-phenotype population in which IL-10, alone or together with TGF-β, initiates a cascade of cellular events eventually resulting in the inhibition of the production of proinflammatory cytokines, increased expression of scavenger receptors and further IL-10 release (Gordon, 2003; Gordon and Taylor, 2005) (Fig. 2).

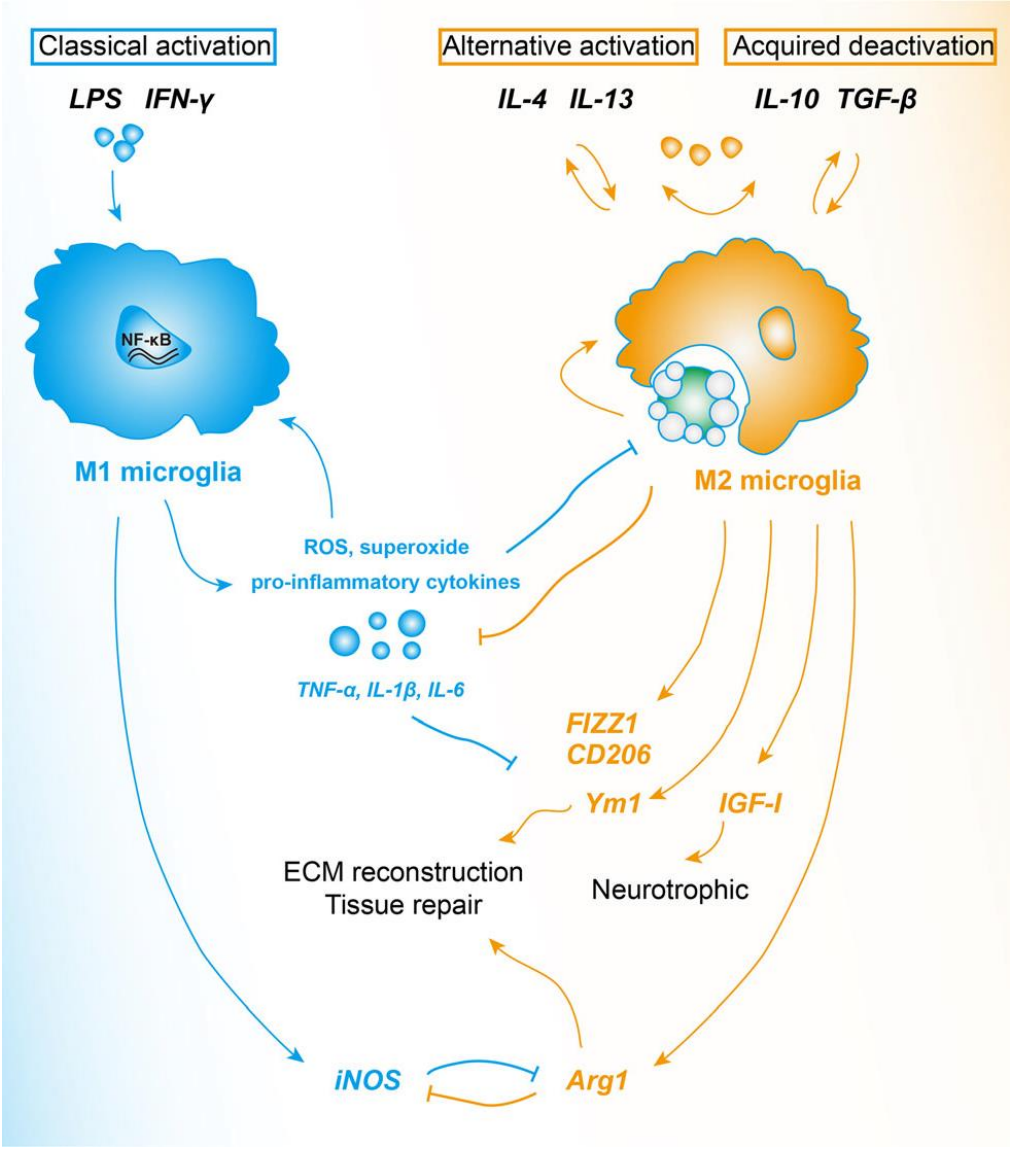

Fig. 2. M1 and M2 microglia (Tang and Le, 2016).

Regarding astrocytes, two activation states have been described upon brain injury: the A1 and A2 "reactive" behaviors. A1 astrocytes upregulate many genes ascribed to the classical complement cascade. They also secrete neurotoxins that induce a rapid death to neurons and oligodendrocytes. By contrast, A2 astrocytes upregulate many neurotrophic factors, promoting neuronal survival and tissue repair (Li et al., 2019) (Fig. 3).

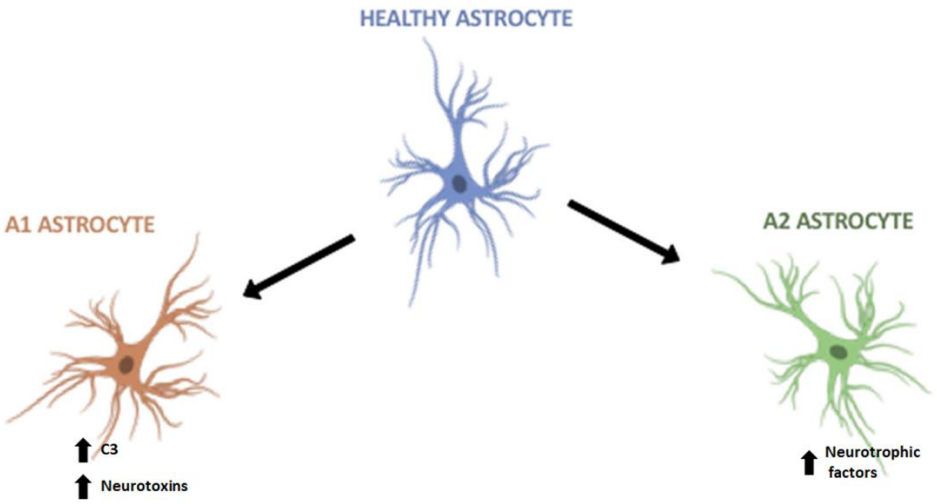

Fig. 3. Astroglia diversity in the adult brain (modified from Miller, 2018).

A recent study of Liddelow and collaborators (2017) demonstrated that the A1 astrocytic state is induced by classically activated microglia by secreting Il-1α, TNF and C1q (Liddelow et al., 2017), suggesting a strong link between astroglia and microglia activation and neuroinflammation.

Another element that support glial cells involvement in brain pathologies is their key role in regulating both synaptic-3D structure and functioning. Indeed, neuronal synapse formation is based on the interplay between neurons and glial cells. Microglia, the immune cells of the brain, regulate synapse formation and synapse engulfment via the complement system, which is included in the innate immune process (Parkhurst et al., 2013; Wu et al., 2015). In contrast, astrocytes take up and release neurotransmitters and provide structural support for neurons (Verkhratsky et al., 2010; Clarke and Barres, 2013). Lastly, oligodendrocytes are responsible for the myelin formation, guaranteeing fast movement of action potentials throughout axons (Dimou and Gallo, 2015).

Therefore, all the brain pathologies characterized by neurotransmitter dysfunctions like PD, AD, multiple sclerosis (MS) or depression, must have a rate of association with glial alterations. For these reasons, recent discoveries made possible to change the perspective regarding the "neurocentric view" of these brain diseases, expanding the horizon to glia as new players to be targeted to potentially counteract these disorders.

The role of glial cells in neuropsychiatric diseases is a new and, for several aspects, undisclosed field of research. Indeed, despite the aforementioned body of evidence, the molecular mechanisms underlying glia involvement in psychiatric disorders have not been fully clarified yet. Almost all epidemiological studies reported that these mental illnesses share several degrees of comorbidity, suggesting that common mechanisms might be causative of their etiopathogenesis and/or contribute to their progression (Di Benedetto and Rupprecht, 2013). Considering this evidence, during my PhD I intended to clarify the role of non-neuronal cells in some neuropsychiatric diseases; the main goal consisted in identifying novel possible pharmacological targets to counteract some of these very frequent, but still incurable, disorders. To do so, I investigated thoroughly the involvement of glial cells in three neuropsychiatric disorders such as AD, autism spectrum disorder (ASD) and acute stress (AS) using different animal models, each appropriate to mimic one of these diseases. I published the results obtained in three papers as first author, two papers as second author and one paper as third author, as shown in the list of publications included below. Moreover, I contributed in the writing of two book chapters, one as first author, and the other as second author.

1.2 List of publications

Papers:

I. Bronzuoli MR*, **Facchinetti R***, Steardo L, Scuderi C (2017). *Astrocyte: an innovative approach for Alzheimer's disease therapy*. Curr Pharm Des, 23(33):4979-4989. The authors marked with * contributed equally to the work.

II. Bronzuoli MR, **Facchinetti R**, Steardo jr L, Romano A, Passarella S, Steardo, Cassano T, Scuderi C (2018a). *Palmitoylethanolamide dampens reactive astrogliosis and improves neuronal trophic support in a triple transgenic model of Alzheimer's disease: in vitro and in vivo evidence.* Oxid Med Cell Longev, 2018:4720532.

III. Scuderi C, Bronzuoli MR, **Facchinetti R**, Pace L, Ferraro L, Broad K, Serviddio G, Bellanti F, Palombelli G, Carpinelli G, Canese R, Gaetani S, Steardo jr L, Steardo L, Cassano T (2018). *Ultramicronized Palmitoylethanolamide rescues learning and memory impairments in a triple transgenic mouse model of Alzheimer's Disease by exerting anti-inflammatory and neuroprotective effects*. Transl Psychiatry, 8(1):32.

IV. **Facchinetti R***, Bronzuoli MR*, Valenza M*, Ratano P, Steardo L, Campolongo P and Scuderi C (2019). *Preventing neuroinflammation with co-ultramicronized palmitoylethanolamide/luteolin in an animal model of prodromal Alzheimer's disease.* J Neuroinflamm, submitted. The authors marked with * contributed equally to the work.

V. Bronzuoli MR, **Facchinetti R**, Valenza M, Cassano T, Steardo L, Scuderi C (2019). *Astrocyte function is affected by aging and not Alzheimer's disease: a preliminary investigation in hippocampi of 3xTg-AD mice*. Front Pharmacol, 10:644.

VI. Bronzuoli MR*, **Facchinetti R***, Ingrassia D, Servadio M, Schiavi S, Steardo L, Verkhratsky A, Trezza V, Scuderi C (2018b). *Neuroglia in the autistic brain: evidence from a preclinical model*. Mol Autism, 9:66. The authors marked with * contributed equally to the work.

Book chapters:

I. **Facchinetti R**, Bronzuoli MR and Scuderi C (2018). *An animal model of Alzheimer disease based on the intrahippocampal injection of amyloid β-peptide (1-42).* Methods Mol Biol, 1727:343-352.

II. Bronzuoli MR**, Facchinetti R** and Scuderi C (2018c). *Preparation of rat hippocampal organotypic cultures and application to study amyloid-β peptide toxicity.* Methods Mol Biol, 1727:333-341.

1.3 Publications on the role of glial cells in Alzheimer's disease

Among neuropsychiatric disorders, AD represents the challenge of the second century (Holtzman et al., 2011). Indeed, AD is the most common cause of dementia (Lane et al., 2018), with an estimated prevalence of 44 million people worldwide, a number that is expected to triple by 2050 as the population ages (Prince et al., 2014).

The most important issue for AD patients, their families and caregivers, is the therapeutic intervention. There is an urgent need for more efficient therapeutic approaches, as currently available treatments provide minor and symptomatic relief, with only very negligible effects on the course of the disease. The identification of effective treatments requires a better understanding of the pathophysiological mechanisms implicated, and innovative approaches to drug development.

The vast majority of AD occurs on a sporadic basis (late onset AD), driven by a complex interplay between genetic and environmental factors, but mutations in the genes encoding for amyloid precursor protein (APP), presenilin 1 (PSEN1) and presenilin 2 (PSEN2) cause a rare (2-3%) familial form of AD (fAD). In this case, symptoms develop earlier than in the sporadic pathology, typically between 30 and 50 years of age (Bateman et al., 2010). Large-scale genome-wide association studies (GWASs) have identified single-nucleotide polymorphisms in multiple other genes associated with AD (Misra et al., 2018). Among them, the triggering receptor expressed on myeloid cells 2 (TREM2) and CD33 are primarily expressed in microglial cells (Griciuc et al., 2013; Jonsson et al., 2013).

The cardinal features of Alzheimer's pathology are amyloid plaques and neurofibrillary tangles, leading to neurodegeneration with synaptic and neuronal loss accompanied by macroscopic atrophy (Huang and Jiang, 2009; Querfurth and La Ferla, 2010) in vulnerable areas of the brain associated with memory and cognitive functions like prefrontal cortex (PfC) or hippocampus (HPC) (Sampath et al., 2017). During the last decades, also astrocyte dysfunction and the presence of an intense inflammatory state have been considered further hallmarks of AD (Rodriguez et al., 2009). Indeed, abnormally activated microglia and dysfunctional astrocytes are closely associated with amyloid deposits in brain parenchyma (Akiyama et al., 2000), an event which promotes further reactive gliosis, characterized by astrocytic activation and neuroinflammation (Pekny and Pekna, 2016). This phenomenon is normally engaged with the intent of defending the brain by removing injurious stimuli (e.g., Aβ fibrils phagocytosis). However, if prolonged, it exceeds normal physiological limits and can induce detrimental effects (Verkhratsky et al., 2010; Verkhratsky et al., 2012; Steardo et al., 2015) (Fig. 4).

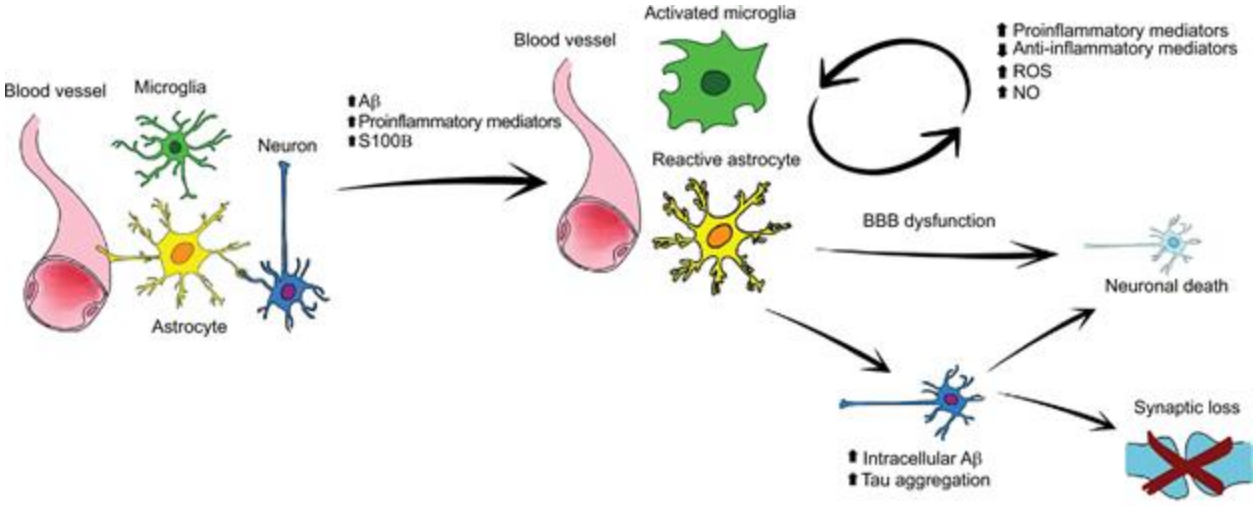

Fig. 4. Schematic representation of glial activation (Bronzuoli et al., 2016). Abbreviations: ROS, reactive oxygen species, NO, nitric oxide; Aβ, β-amyloid; NFTs, neurofibrillary tangles; BBB, blood–brain barrier.

Indeed, because of their crucial role in AD pathology, targeting astrocytes and neuroinflammation has been hypothesized to be a potential effective therapeutic strategy in AD.

The large amount of literature examined on this topic during my first year of the doctoral program allowed me to write a review paper discussing the currently available therapeutic approaches against astrocytic dysfunctions to counteract AD (**I**, **Bronzuoli et al., 2017**). Among them, the use of molecules acting on astrogliosis and neuroinflammation was included.

In this regard, in the last few years, my supervisor Dr. Caterina Scuderi has been investigating the pharmacological effects of palmitoyletanolamide (PEA), an endogenous amide of ethanolamide and palmitic acid also produced by glial cells, demonstrating its properties as an anti-inflammatory and neuroprotective molecule and proposing a mechanism for its action.

PEA, a naturally occurring amide of ethanolamide and palmitic acid, is a lipid messenger that mimics several endocannabinoid-driven actions, even though it does not bind to cannabinoid receptors (Lo Verme et al., 2005; Mackie and Stella, 2006; Re et al., 2007). PEA has been extensively studied for its anti-inflammatory and neuroprotective effects, mainly in model of peripheral neuropathies (Mazzari et al., 1996; Calignano et al., 1998; Calignano et al., 2001; Franklin et al., 2003). It displays analgesic and anti-epileptic properties (Jaggar et al., 1998; Sheerin et al., 2004), it inhibits food intake (Hansen and Diep, 2009), reduces gastrointestinal motility (Capasso et al., 2001), it counteracts cancer cell proliferation (De Petrocellis et al., 2002; Di Marzo et al., 2001), and it protects the vascular endothelium in the ischemic heart (Bouchard et al., 2003). Concerning the mechanism of action, some of its properties have been considered as dependent on the expression of peroxisome proliferator-activated receptor-alpha (PPAR-alpha) (Lo Verme et al., 2005, 2006; Re et al., 2007; Scuderi et al., 2011).

During the last few years, my mentor and other groups demonstrated the anti-inflammatory and neuroprotective effects of PEA, as well as its ability to attenuate memory impairment, in different *in vitro* and *in vivo* models of AD able to reproduce the sporadic form of the disease (Scuderi et al., 2011, 2012, 2014; D'Agostino et al., 2012; Tomasini et al., 2015).

Oddo and collaborators, in 2003, developed a genetic model of AD, the triple transgenic model (3×Tg-AD), currently considered the closest to the fAD. These mice harbor three human transgenes strongly correlated with AD (APPswe, PS1M146V and tauP301L), and express both senile plaques and neurofibrillary tangles (Oddo et al., 2003) (Fig. 5).

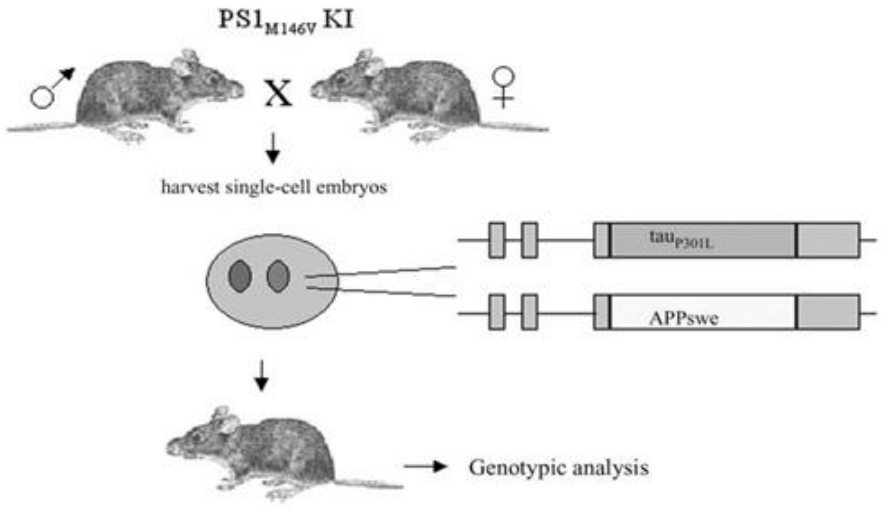

Fig. 5. Generation of 3×Tg-AD mouse model (Oddo et al., 2003).

Compared to other transgenic AD models, this is the first able to develop both plaques and tangle pathology in AD-relevant brain regions, exhibiting deficits in synaptic plasticity, including long term potentiation (LTP) (Oddo et al., 2003**)**. All these alterations occurr in an age and brain-dependent manner. The following representative scheme retraces in detail the development of the AD-like alterations in 3×Tg-AD mice (Fig. 6).

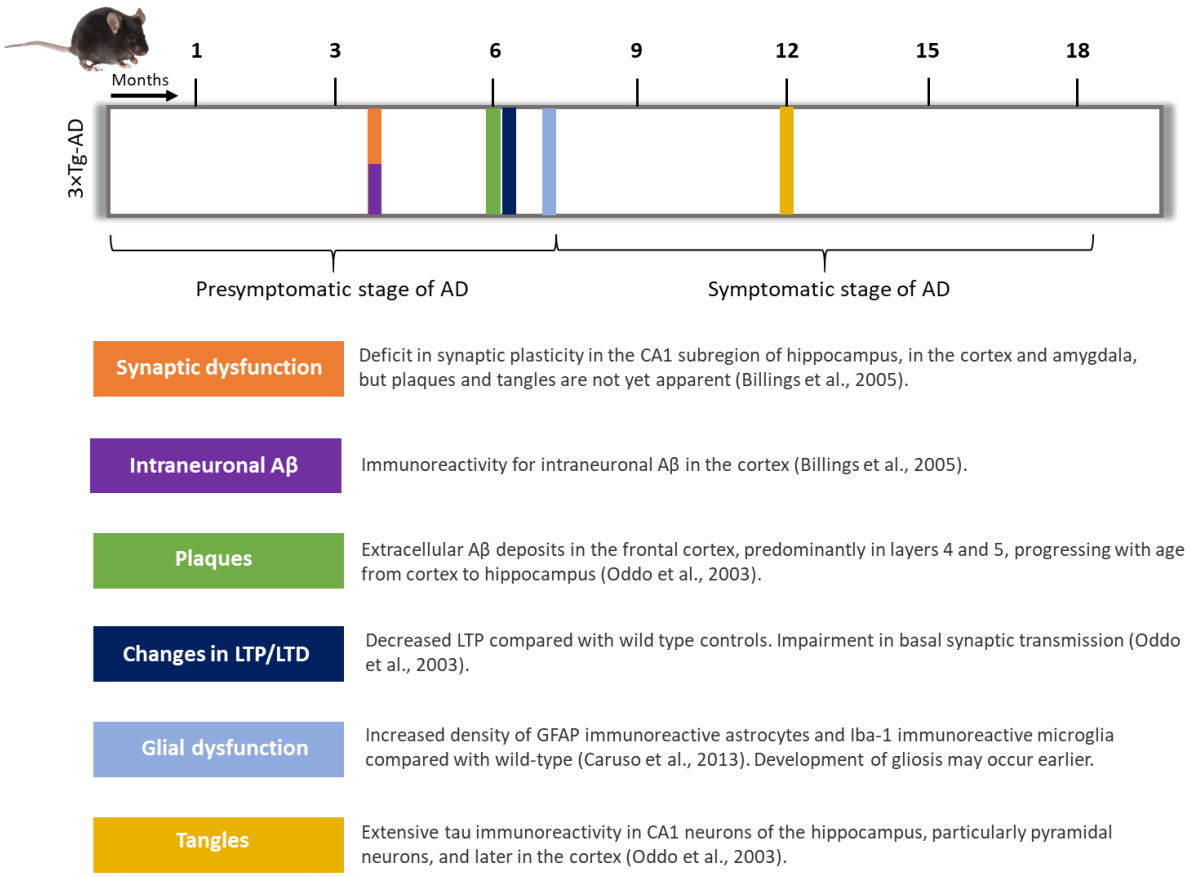

Fig. 6. Representative scheme of the onset of each AD-like alteration modelled in 3×Tg-AD mice (modified from Alzforum, 2018)

Investigations with transgenic animal models have strongly supported the assumption that inflammation is a key component of the pathology of AD and have risen the hypothesis that, besides the sustained production of pathogenic substances, astrocytes in transition to the inflammatory state fail to provide their supportive functions to neurons, making them vulnerable to toxic molecules (Rodriguez et al., 2009; Olabarria et al., 2010).

During the first year of my PhD program, I carried out experiments on this genetic model of AD with the effort to expand the knowledge acquired during my studies for the Master of Science Degree thesis. Specifically, I performed molecular analyses to investigate the *in vitro* and *in vivo* effects of PEA in the PfC of 3×Tg-AD mice (**II, Bronzuoli et al., 2018a**). To reduce the statistical variability linked to the use of female mice (due to their hormonal cycle), as well as the number of animals used, the study was restricted to males. However, since recent epidemiological studies show that the incidence of the disease is higher in women than in men (OMS, 2016), future studies need to be performed on females. *In vitro* results demonstrated an intense activation and inflammation in primary 3×Tg-AD astrocytes, as well as the ability of PEA to counteract them and promote neuronal viability.

For the *in vivo* experiments, male 3-month-old 3×Tg-AD and sex- and age-matched non transgenic (non-Tg) mice were subcutaneously implanted with a pellet releasing either ultramicronized-PEA (um-PEA - 10 mg/kg/die for 90 days using a controlled release device) or placebo for three months. The choice to use an ultramicronized formulation of PEA was supported by the evidence that it is endowed with both superior absorption and efficacy compared to naïve formulations (Impellizzeri et al., 2014; Petrosino et al., 2018). Results demonstrated the precocious presence of reactive astrogliosis and neuroinflammation in the PfC of transgenic animals, and the ability of chronic um-PEA to alleviate both indices.

One of the major risk factors for the onset of AD is represented by aging, and scientists are debating on which could be the best phase of the disease to therapeutically intervene. At present, there are not enough data to answer this question. Based on these considerations and on the promising results obtained using the 3×Tg-AD mice, I evaluated the effects of chronic um-PEA administration (10 mg/kg/die for 90 days using a device for controlled release) in 3×Tg-AD mice at two different stages (mild and severe) of AD-like pathology, by subcutaneously administering the drug in a pellet form for 3 consecutive months (**III, Scuderi et al., 2018**). In particular, I compared PEA effects on hippocampi of 6-month-old (corresponding to a pre-symptomatic stage) and 12-month-old (corresponding to full-blown disease) 3×Tg-AD mice. Data obtained demonstrated the first *in vivo* evidence that chronic um-PEA has a beneficial effect on neuroinflammation and neuronal survival in the 3×Tg-AD model, improving cognitive and neural functions during both the early presymptomatic and later symptomatic stages of AD. As previously mentioned, astrocytes behaved differently between the two stages of the pathology investigated: 6 months old 3×Tg-AD mice showed hyperreactive astrocytes, accompanied by an intense inflammatory status, while the same mice at 12 months of age demonstrated a slight astrocyte atrophy not accompanied by neuroinflammation.

Originally, two AD stages were described: the first named mild cognitive impairment (MCI), with an accelerated cognitive decline, and the second characterized by dementia with complete loss of independence in activities of daily living. In 2012, the National Institute on Aging (NIA) published new guidelines according to which AD is preceded by an early stage of dementia, named prodromal AD, starting before the MCI stage (Hyman et al., 2012). At this stage the cellular and molecular alterations leading to the disease have been already triggered, but an affected person can be still asymptomatic (Jack et al., 2013; Irwin et al., 2018). In particular, this preclinical stage can be divided in three substages, named 1, 2 and 3. The individuals in stage 1 have evidence of Aβ deposits as biomarker, demonstrated by positron emission tomography (PET), but no detectable evidence of cognitive or behavioral symptomatology. Stage 2 is characterized by amyloid positivity and, in addition, neuronal injury evidenced by brain atrophy on structural magnetic resonance imaging

(MRI). In the last stage of preclinical AD, the individuals have amyloid accumulation, early neurodegeneration, as well as the evidence of subtle cognitive decline (Tan et al., 2014) (Fig. 7).

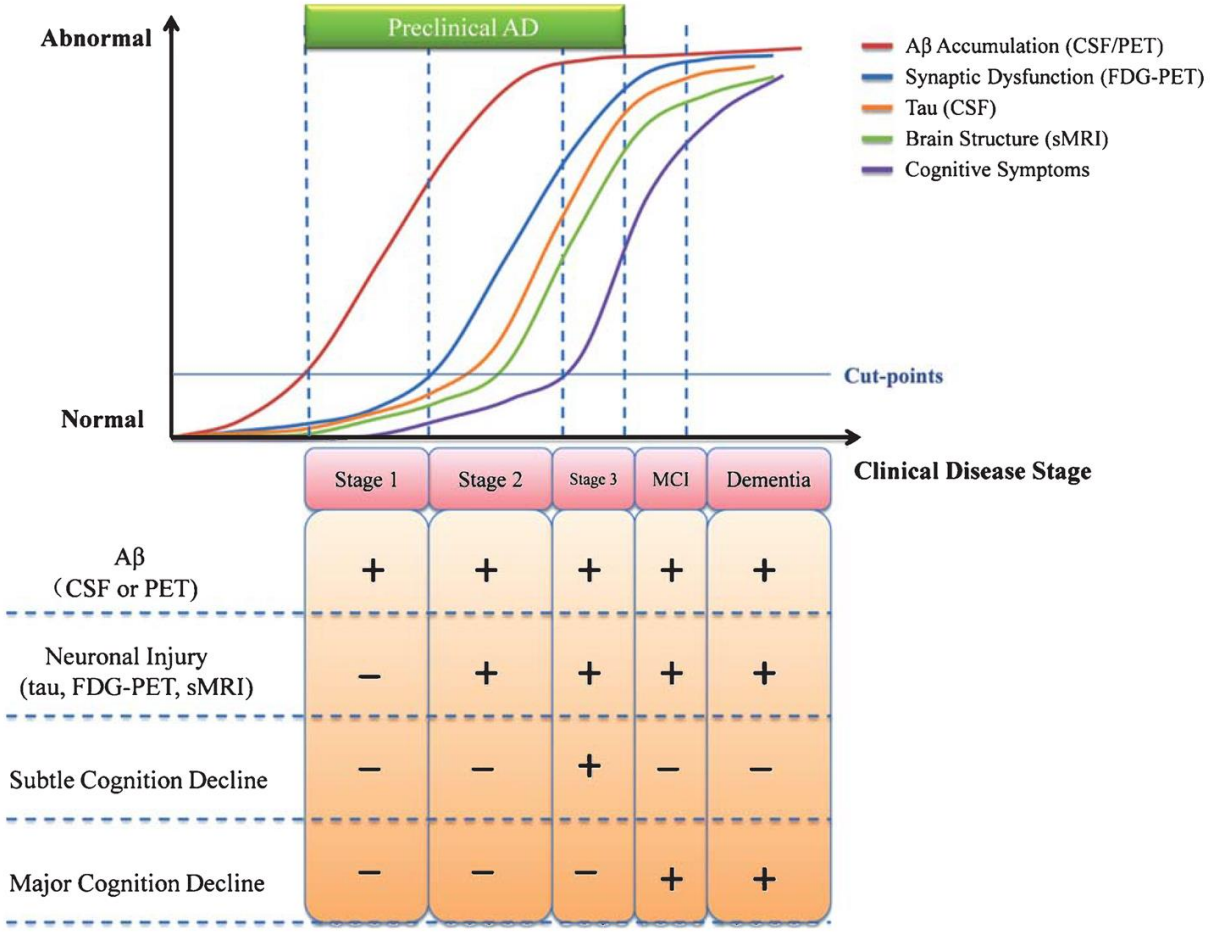

Fig. 7. The brain pathology of preclinical AD, subdivided into three stages: the stage of asymptomatic amyloidosis (1), amyloid deposition plus evidence of synaptic dysfunction and/or early neurodegeneration (2), and amyloid deposition plus evidence of neurodegeneration (3) (Tan et al., 2014).

Current research in the field of AD is focusing the attention on the earliest stage of dementia. In fact, it is fundamental to understand the pathways potentially responsible of the passage from an asymptomatic phase to that of blown pathology. During this phase of the disease, both beta amyloid (Aβ) accumulation and a neuroinflammatory process have been documented (Price et al., 2009). Therefore, neuroinflammation at this earliest phase of the disease may be a valuable therapeutic strategy to prevent the onset of the pathology. In literature, there are currently few preclinical data available using this specific time point as a potential window of treatment.

For these reasons, with the aim to contribute in filling this gap, during the second year of my PhD program, I tested a new combination of PEA and luteolin (Lut), ultramicronized together as a single

formulation (co-ultra PEALut), in an *in vivo* surgical model of AD, obtained by a single intrahippocampal inoculation of $A\beta_{(1-42)}$ in adult rats. Occurrence of the main hallmarks of AD in 3×Tg-AD mice appears controversial in literature; thus, identifying precisely the different stages of AD in 3×Tg-AD mice is difficult. On the contrary, the experimenter-controlled surgical inoculation of $A\beta_{(1-42)}$ in adults rats allows to model a very first $A\beta_{(1-42)}$ deposit. Since we aimed at testing the potential beneficial effect of a therapeutic intervention at the prodromal stage of the disease, I started the pharmacological administration on the same day of the $A\beta_{(1-42)}$ insult given surgically.

This model has shown the ability to recapitulate the features of the preclinical stage. Indeed, these animals show glial dysfunctions soon after the peptide inoculation, but exhibit modest learning and memory deficits only 21 days after Aβ injection (Scuderi et al., 2014). In the past, my mentor and her group had already studied the effect of PEA alone administration to the same surgical model. Another reason of the choice to carry my investigations in the surgical model again, instead of transgenic mice, arises from the consideration that it has the great advance of reproducing some features of the sporadic form of AD, the most frequent in patients (Chakrabarti et al., 2015). Further the surgical model has face, structure and predictive validities among international scientists (Scuderi et al., 2014).

Lut is a well-known flavonoid, found in different edible plants, with antioxidant, anti-inflammatory as well as memory-improving properties (Seelinger et al., 2008; Lopez-Lazaro et al., 2009; Nabavi et al., 2015). The choice of using this compound arose from recent studies showing that this new formulation exhibits greater bioavailability and that it is more effective than the two compounds alone (Impellizzeri et al., 2013; Skaper et al., 2015; Parrella et al., 2016).

At the end of the study, I drafted a manuscript which is currently under consideration in Journal of Neuroinflammation (**IV**, **Facchinetti et al., submitted**). Such paper reports the first *in vivo* evidence that co-ultra PEALut, administered daily from the day of the surgical $A\beta_{(1-42)}$ peptide infusion for 14 consecutive days, prevents the Aβ-induced upregulation in gene expression of pro-inflammatory cytokines and enzymes. Moreover, in our model of prodromal AD, this molecule is able to reduce mRNA levels of two neurotrophic factors, the brain derived neurotrophic factor (BDNF) and the glial derived neurotrophic factor (GDNF), ultimately promoting neuronal survival.

Most AD cases have a late onset (usually after 65 years), indeed AD incidence is known to increase with age (Guerreiro and Bras, 2015). What it is still not clear is whether the cellular changes found in aging-related diseases, including AD, are due to the consequences of these disorders or to aging itself. With the aim to clarify this, I investigated the effects of aging on morphology and functions of hippocampal astrocytes and microglia by comparing young adult (6-month-old) and aged (12-month-old) healthy (Non-Tg) and AD-like (3×Tg-AD) mice to model, respectively, healthy and pathological aging. The results are discussed in the brief-research report here attached (**V, Bronzuoli et al., 2019**).

This paper reveals, for the first time, that the responsible actor for astrocytic dysfunction is aging. Indeed, surprisingly, a main effect of aging and not of genotype was detected in all astrocytic markers investigated, suggesting that the observed alterations to astroglia functions were related to aging itself rather than AD.

Figure 8 shows a schematic representation to compare the different studies carried out during my PhD program, related to the *in vivo* models used and the respective stages of AD investigated, as well as the different formulations of PEA tested.

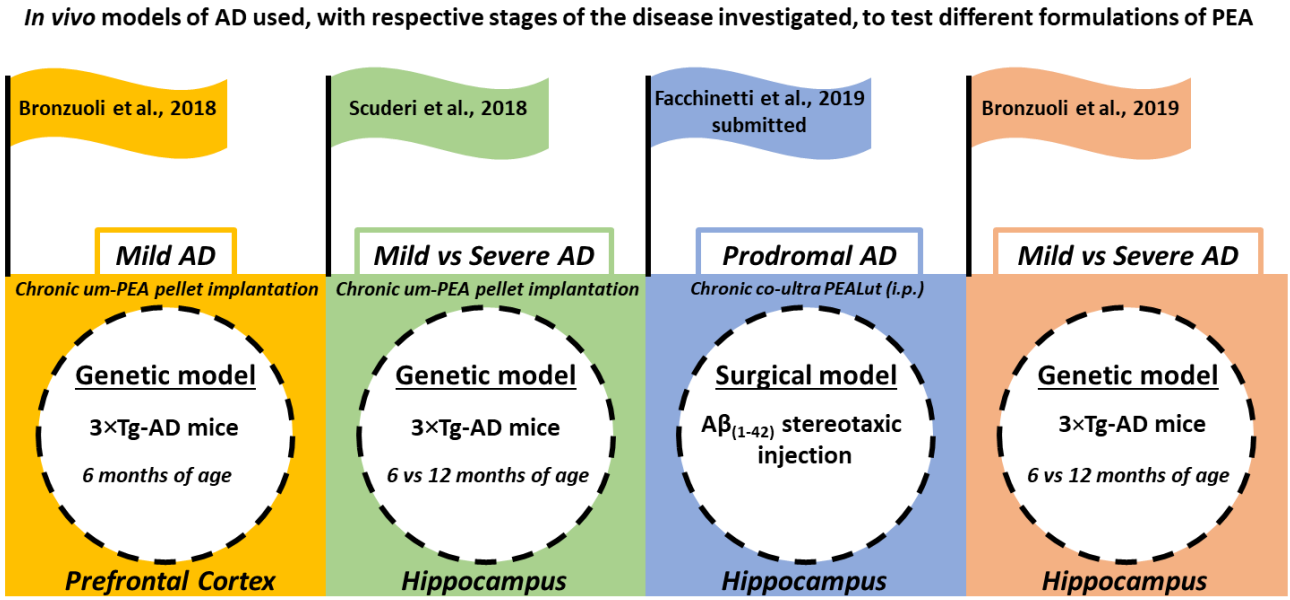

Fig. 8. Schematic representation of the *in vivo* preclinical models of AD used to test different formulations of PEA in different stages of the disease course.

1.4 Publication on the role of glial cells in autism spectrum disorders

The global burden of neuropsychiatric disorders is one of the main problems afflicting the modern society and a growing number of researchers are studying the molecular mechanisms underlying the pathogenesis of these brain diseases, but few looking at glial cells. Thanks to the collaboration with the Prof. Viviana Trezza of Roma Tre University, during the second year of my PhD program I could deepen the topic regarding the involvement of glial cells in neuropsychiatric disorders moving towards another serious mental disease as the autism spectrum disorder (ASD).

ASD is a heterogeneous set of neurodevelopmental disorders characterized by the impairment of social communication and social interaction, presence of stereotypies, and reduced patterns of behaviors. Symptoms generally appear in infancy and early childhood and last a lifetime (Vahia, 2013). These conditions profoundly affect the quality of life of the child and, consequently, the family (Payakachat et al., 2012). Epidemiological studies conducted over the past 50 years have detected that 1 out of 160 children worldwide suffers from ASD, and the prevalence of this condition seems to be globally increasing (WHO, 2018). To date, there are only symptomatic treatments and non-pharmacological tools to intervene on the disease course. Thus, improved understanding of the comparative effectiveness of different pharmacological, behavioral, medical and alternative treatments for children (Payakachat et al., 2012) are needed.

Several risk factors are involved in the development of ASD, including genetic background, environmental conditions, maternal stressors, infectious agents, and the prenatal exposure to specific drugs. For example, maternal exposure during pregnancy to valproic acid (VPA), an antiepileptic and mood stabilizer, induces congenital malformations (Kozma, 2001; Kini et al., 2006) and autistic-like features in the exposed children, such as impaired communication, reduced sociability and appearance of stereotyped behaviors (Williams and Hersh, 1997; Williams et al., 2001). This can be easily modelled in animals. The *in vivo* VPA model displays important structural and behavioral features that can be observed in individuals with ASD; thus, it is an excellent animal model for testing new drug targets and developing novel behavioral and pharmacological therapies with translational power, as well as face and construct validity (Mabunga et al., 2015).

From a physiopathological point of view, *post-mortem* brains from ASD individuals reveal changes in synaptic organization, dendritic arborization, neurotransmission as well as morphological and functional alterations of glial cells. Indeed, recent studies suggest an important contribution of neuroglia in the development of ASD (Petrelli et al., 2016) (Fig. 9).

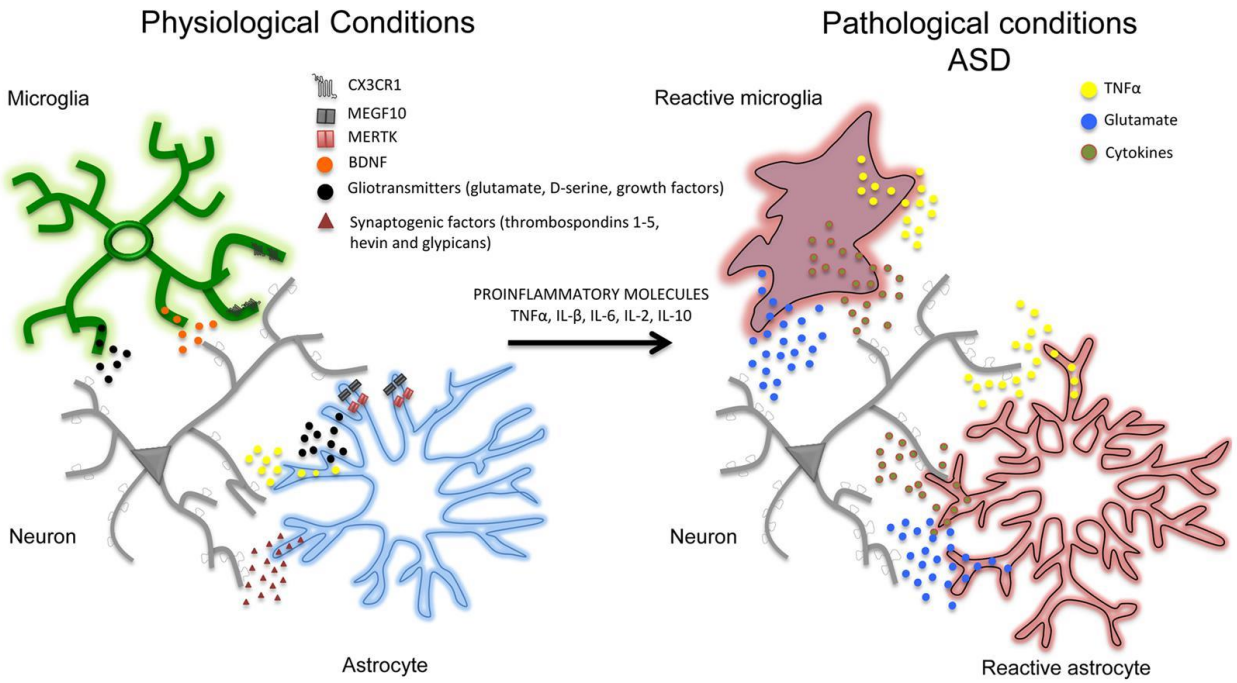

Fig. 9. Glial cells alterations and ASD (Petrelli et al., 2016).
In physiological conditions astrocytes and microglia release a number of neuroactive substances such as gliotransmitters together with growth factors (such as TNFα, BDNF, glutamate, D-serine; *black dots*) and synaptogenic factors (such as thrombospondins 1-5, hevin, and glypicans; *red dots*) that can promote the formation and maturation of synapses. Glial cells can also contribute to synapse remodeling and pruning through CX3CR1, multiple EGF-like domains 10 (MEGF10), c-mer proto-oncogene tyrosine kinase (MERTK) phagocytic pathways. In pathological conditions (i.e., in autistic brains) pro-inflammatory factors (including cytokines TNFα, IL-β, IL-6, IL-2, IL-10) may lead to a chronic neuroinflammation in which astrocytes and microglia become reactive (*red*), release pro-inflammatory mediators (such as TNFα, glutamate and pro-inflammatory cytokines) and may exacerbate the initial inflammatory condition.

However, the functional role and the molecular mechanisms underlying these alterations have not yet been examined by the scientific community.

Therefore, my colleagues and I, under the supervision of Dr. Caterina Scuderi, investigated the role of glial cells in ASD by performing an in-depth molecular analysis of specific markers of astrocytes, oligodendrocytes, and microglial cells in rats prenatally exposed to VPA. The analysis was performed on brain areas critically involved in ASD: the HPC, the PfC and the cerebellum (Cb) (Dichter et al., 2012; Donovan and Basson, 2017; Reim et al., 2017). Since this disorder is diagnosed during childhood and accompanies the patient throughout the course of his/her life (Matson et al., 2016), analyses were carried out at three different ages, postnatal day (PND)13, PND35 and PND90, to account for human infancy, adolescence, and adulthood, respectively. As several epidemiological studies report a higher incidence of ASD in boys than in girls (Kim et al., 2013; Melancia et al., 2018) we focused our studies on male littermates.

I published as co-first author the results (**VI, Bronzuoli et al., 2018b**). In our experimental condition we were able to confirm ASD-like behavioral features of the *in vivo* VPA model, performing the isolation-induced ultrasonic vocalizations (USVs) test at PND13, the three-chamber test at PND35,

and the hole board test at PND90. VPA exposed pups, separated from the dam, vocalized significantly less compared to control pups. Adolescent animals showed decreased sociability in the three-chamber test, spending less time sniffing the stimulus animal compared to vehicle-exposed rats. At adulthood, VPA-exposed rats showed stereotypic behaviors in the hole board test, since they made more head dipping at PND90.

Results obtained from the molecular analyses extend the knowledge on the involvement of glial cells in ASD and indicate that prenatal VPA exposure affects all types of neuroglia, mainly causing transcriptional modifications. The most significant changes occur in the PfC and in the HPC of ASD-like animals, and the alterations are mostly evident during infancy and adolescence, while they appear to be mitigated in adulthood. In particular, the altered expression of neuroglial markers seems to be rather mild, with neuroinflammatory phenotype being present mainly in young ages and less in adulthood. These results demonstrate a strong heterogeneity of glial involvement in this neurodevelopmental disorder, both in the different ages examined and in the different areas investigated.

1.5 Ongoing experiments on the role of glial cells in acute stress

Stress is largely recognized as one of the main risk factors in neuropsychiatric diseases (Radley et al., 2011). It involves the activation of the hypothalamic-pituitary-adrenal (HPA) axis (Fig. 10), deeply affecting neurotransmission and synaptic morphology in brain areas associated with behavioral responses.

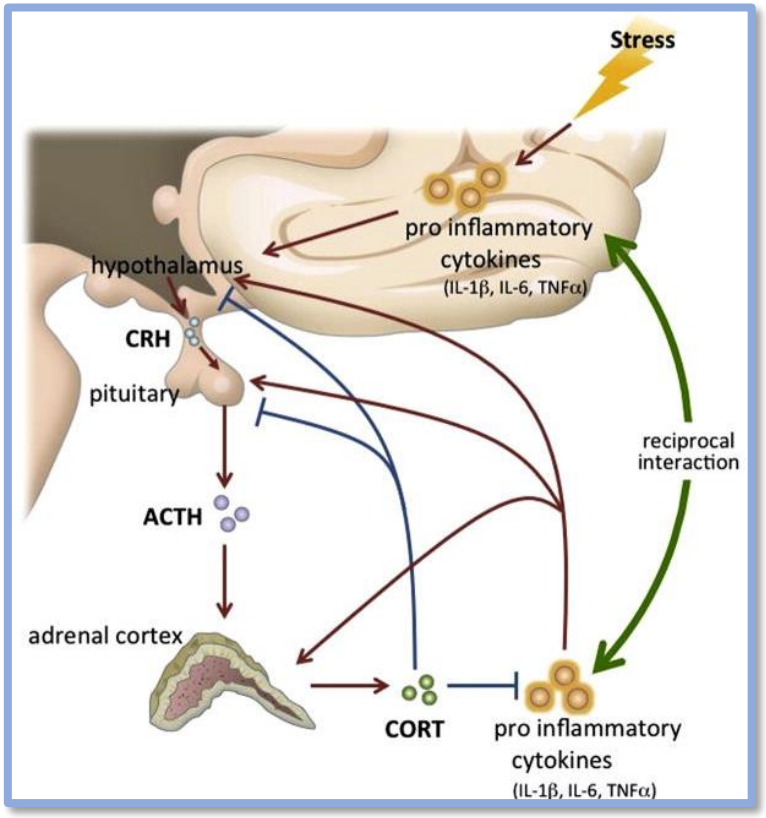

Fig. 10. Activation of the HPA axis after a stressful event (Iwata et al., 2013).

Clinical and preclinical studies have demonstrated that the impact of a stressful life on emotional and cognitive behaviors may vary depending on the nature of stress, its intensity or duration, and the age at which the stress exposure occurs (perinatally, adolescence, adulthood, or advanced age) (Musazzi and Marrocco, 2016).

When the stress response is physiologically activated, it can induce adaptive plasticity and improve cognition, and then it is inactivated. However, when the stress response is maladaptive, it is not shut down and can have detrimental effects, leading to epigenetic changes associated with impaired brain functions that may ultimately trigger the development of neuropsychiatric disorders (Fig. 11). Therefore, the identification of the molecular mechanisms underlying resilience and vulnerability to stress is of crucial importance in understanding the pathophysiology of mental illnesses and in developing treatments (Musazzi and Marrocco, 2016).

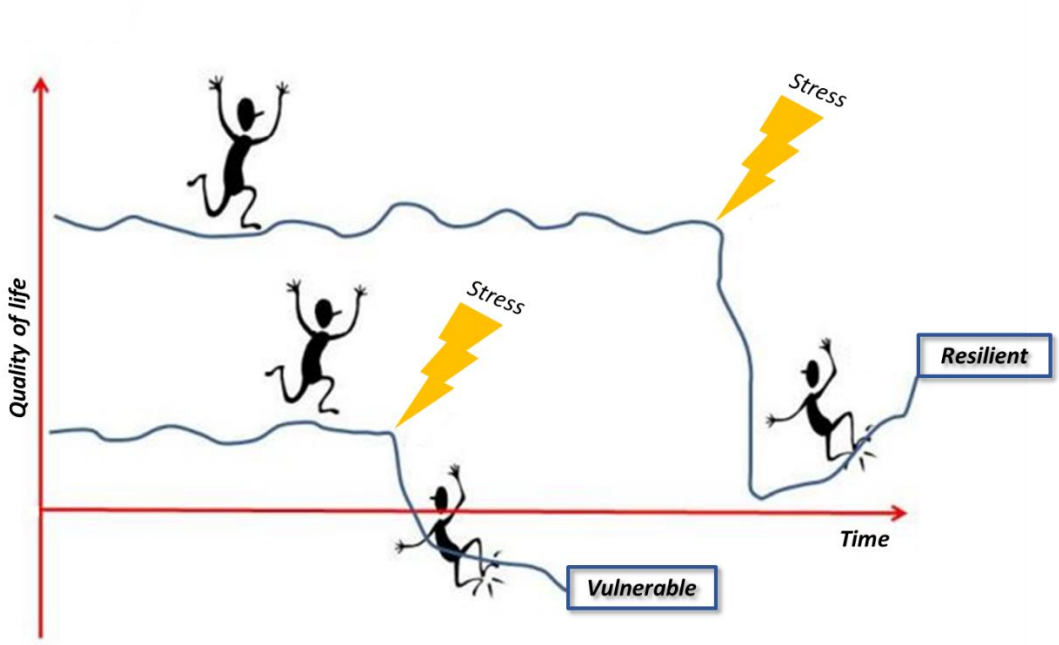

Fig. 11. Schematic representation of individual resilience or vulnerability to stress.

Changes in the neuroarchitecture of brain areas, including HPC and PfC, have been consistently found in psychiatric patients and rodents exposed to chronic stress (CS) (Musazzi et al., 2017). For example, CS induces a profound structural remodeling of PfC pyramidal neurons, including dendritic shortening, spine loss, and neuronal atrophy (Nava et al., 2014). Findings suggest that these modifications, including dendritic atrophy, are caused by the enhancement of glutamate release and excitatory transmission induced by stress, but clear demonstration of that is still missing. However, recent evidence demonstrated that glial cells impairment after CS directly affects the glutamatergic homeostasis (Tynan et al., 2013; Mayhew et al., 2015).

Unlike the effects of CS, which have been extensively studied, the short- and long-term consequences of AS, defined as a single exposure to stress scaling from minutes to hours without cycles of re-exposure (Kirby et al., 2013), are still poorly investigated. What is known is that also AS induces rapid and sustained changes in brain neuroarchitecture, but the effects of AS on glial cells and, mostly, the role of these cells in the differential response of resilience or vulnerability to this paradigm, are still understudied. In this context, it is reasonable to hypothesize that glial cells, clearly involved in the effects of CS, take part in the cellular and molecular changes also caused by AS.

Nowadays, the possibility of mitigating the detrimental consequences of AS through the administration of antidepressant drugs has already been demonstrated (Nava et al., 2014), but the efficacy of these drugs is limited. Therefore, it is fundamental to study the mechanisms capable of

modifying an adaptive physiological response in a maladaptive one, in order to identify new and innovative therapeutic strategies.

During the last year of my PhD program I contributed to a study, carried out in collaboration with Prof. Giambattista Bonanno of the University of Genoa and Prof. Maurizio Popoli of the University of Milan, investigating the role of glia in the adaptive/maladaptive response to AS. To this aim, the University of Genoa provided us with the brain areas extracted from adult male Sprague-Dawley rats exposed to a single foot-shock stress session. Those rats were screened for their anhedonia-like behavior 24 hour after stress by the sucrose preference test. Based on the results, animals were then considered either resilient (RES) or vulnerable (VUL) to acute stress (VUL: subjects with a decrease in sucrose intake > 25% compared to baseline consumption; RES: subjects with a variation < 10%). I performed several molecular analyses on the prelimbic cortex (PrL) of these rats and I recently showed data obtained from this study in an international congress. Although preliminary, my results show the ability of AS to dramatically decrease the number of astrocytic cells in the PrL, independently from the resilient or vulnerable response of animals to AS. Interestingly, data show a different involvement of the astrocytic component between RES and VUL animals; in particular, we observed a rearrangement of the three astrocytic subpopulations investigated in these two experimental groups. Further experiments are currently ongoing.

1.6 Book chapters

My mentor and her group previously published several papers on the role of glial cells in AD, using different *in vitro* and *in vivo* preclinical models. They demonstrated the anti-inflammatory and neuroprotective effects of PEA treatment on both astrocyte activation and neuronal loss, observed in organotypic hippocampal slices challenged with $A\beta_{(1-42)}$ (Scuderi et al., 2012). Based on those promising *in vitro* results, they tested PEA administration *in vivo* using a surgical model of AD, obtained by a single intrahippocampal injection of $A\beta_{(1-42)}$.

During the first year of my PhD, we were invited to write in detail the experimental procedures used to develop these AD models in the book "Methods in Molecular Biology". Therefore, I contributed in the drafting of the chapter regarding the preparation of rat hippocampal organotypic cultures **(I, Bronzuoli et al., 2018c**). On the other hand, considering the laboratory experience acquired on the topic, I personally wrote the book chapter concerning the intrahippocampal stereotaxic injection of $A\beta_{(1-42)}$, combining our laboratory practice and expertise with the available literature, discussing the advantages and disadvantages of using this murine model of AD (**II, Facchinetti et al., 2018**).

1.7 References

Akiyama H, Barger S, Barnum S, et al. Inflammation and Alzheimer's disease. *Neurobiol Aging*. 2000; 21(3):383–421.

Bateman RJ, Aisen PS, De Strooper B, et al. Autosomal-dominant Alzheimer's disease: a review and proposal for the prevention of Alzheimer's disease. *Alzheimers Res Ther*. 2011; 3(1):1.

Bélanger M, Magistretti PJ. The role of astroglia in neuroprotection. *Dialogues Clin Neurosci*. 2009; 11(3):281–295.

Billings LM, Oddo S, Green KN et al. Intraneuronal Abeta causes the onset of early Alzheimer's disease-related cognitive deficits in transgenic mice. *Neuron*. 2005; 45(5):675-88.

Bouchard JF, Lépicier P, Lamontagne D. Contribution of endocannabinoids in the endothelial protection afforded by ischemic preconditioning in the isolated rat heart. *Life Sci*. 2003; 72(16):1859-70.

Bronzuoli MR, Facchinetti R, Steardo L et al. Astrocyte: an innovative approach for Alzheimer’s disease therapy. *Curr. Pharm. Des*. 2017; 23(33):4979-4989.

Bronzuoli MR, Facchinetti R, Steardo L Jr, et al. Palmitoylethanolamide Dampens Reactive Astrogliosis and Improves Neuronal Trophic Support in a Triple Transgenic Model of Alzheimer's Disease: In Vitro and In Vivo Evidence. *Oxid Med Cell Longev*. 2018; 2018:4720532.

Burda JE, Sofroniew MV. Reactive gliosis and the multicellular response to CNS damage and disease. *Neuron*. 2014; 81(2):229–248.

Butt A, Verkhratsky A. Neuroglia: Realising their true potential. *BNA.* 2018; 2: 1–6.

Calignano A, La Rana G, Giuffrida A et al. Control of pain initiation by endogenous cannabinoids. *Nature*. 1998; 394(6690), 277-281.

Calignano A, La Rana G, Piomelli D. Antinociceptive activity of the endogenous fatty acid amide, palmitylethanolamide. *Eur J Pharmacol*. 2001; 419(2-3):191-8.

Capasso R, Izzo AA, Fezza F, et al. Inhibitory effect of palmitoylethanolamide on gastrointestinal motility in mice. *Br J Pharmacol*. 2001; 134(5):945–950.

Caruso D, Barron AM, Brown MA et al. Age-related changes in neuroactive steroid levels in 3xTg-AD mice. *Neurobiol Aging*. 2013; 34(4):1080–1089.

Chakrabarti S, Khemka VK, Banerjee A, Chatterjee G, Ganguly A, Biswas A. Metabolic Risk Factors of Sporadic Alzheimer's Disease: Implications in the Pathology, Pathogenesis and Treatment. *Aging Dis*. 2015; 6(4):282–299.

Clarke LE, Barres BA. Emerging roles of astrocytes in neural circuit development. *Nat Rev Neurosci*. 2013; 14(5):311–321.

D'Agostino G, Russo R, Avagliano C, Cristiano C, Meli R, Calignano A. Palmitoylethanolamide protects against the amyloid-β25-35-induced learning and memory impairment in mice, an experimental model of Alzheimer disease. *Neuropsychopharmacol*. 2012; 37(7):1784–1792.

De Petrocellis L, Bisogno T, Ligresti A et al. Effect on cancer cell proliferation of palmitoylethanolamide, a fatty acid amide interacting with both the cannabinoid and vanilloid signalling systems. *Fundam Clin Pharmacol*. 2002; 16(4):297-302.

Di Benedetto B, Rupprecht R. Targeting glia cells: novel perspectives for the treatment of neuropsychiatric diseases. *Curr Neuropharmacol*. 2013; 11(2):171–185.

Di Marzo V, Melck D, Orlando P, et al. Palmitoylethanolamide inhibits the expression of fatty acid amide hydrolase and enhances the anti-proliferative effect of anandamide in human breast cancer cells. *Biochem J*. 2001; 358(Pt 1):249–255.

Dichter GS, Felder JN, Green SR et al. Reward circuitry function in autism spectrum disorders. *Soc Cogn Affect Neurosci*. 2012; 7(2):160–172.

Dietert RR, Dietert JM, Dewitt JC. Environmental risk factors for autism. *Emerg Health Threats J.* 2011; 4:7111.

Dimou L, Gallo V. NG2-glia and their functions in the central nervous system. *Glia*. 2015; 63(8):1429–1451.

Donovan AP, Basson MA. The neuroanatomy of autism - a developmental perspective. *J Anat.* 2017; 230(1):4–15.

Esposito G, Scuderi C, Valenza M, et al. Cannabidiol reduces Aβ-induced neuroinflammation and promotes hippocampal neurogenesis through PPARγ involvement. *PLoS One*. 2011; 6(12): e28668.

Eugenín-von Bernhardi J, Dimou L. NG2-glia, More Than Progenitor Cells. *Adv Exp Med Biol.* 2016; 949:27-45.

Fields RD, Woo DH, Basser PJ. Glial Regulation of the Neuronal Connectome through Local and Long-Distant Communication. *Neuron*. 2015; 86(2):374–386.

Franklin A, Parmentier-Batteur S, Walter L, Greenberg DA, Stella N. Palmitoylethanolamide increases after focal cerebral ischemia and potentiates microglial cell motility. *J Neurosci*. 2003; 23(21):7767–7775.

Gordon S. Alternative activation of macrophages. *Nat Rev Immunol*. 2003; 3:23–35.

Gordon S, Taylor PR. Monocyte and macrophage heterogeneity. *Nat Rev Immunol*. 2005; 5:953–964.

Griciuc A, Serrano-Pozo A, Parrado AR, et al. Alzheimer's disease risk gene CD33 inhibits microglial uptake of amyloid beta. *Neuron*. 2013; 78(4):631–643.

Guerreiro R, Bras J. The age factor in Alzheimer's disease. *Genome Med*. 2015; 7:106.

Hansen HS, Diep TA. N-acylethanolamines, anandamide and food intake. *Biochem Pharmacol*. 2009; 78(6):553-60.

Holtzman DM, Morris JC, Goate AM. Alzheimer's disease: the challenge of the second century. *Sci Transl Med*. 2011; 3(77):77sr1.

Huang HC, Jiang ZF. Accumulated amyloid-beta peptide and hyperphosphorylated tau protein: relationship and links in Alzheimer's disease. *J Alzheimers Dis*. 2009; 16(1):15-27.

Hyman BT, Phelps CH, Beach TG, et al. National Institute on Aging-Alzheimer's Association guidelines for the neuropathologic assessment of Alzheimer's disease. *Alzheimers Dement*. 2012; 8(1):1–13.

Impellizzeri D, Bruschetta G, Cordaro M, et al. Micronized/ultramicronized palmitoylethanolamide displays superior oral efficacy compared to nonmicronized palmitoylethanolamide in a rat model of inflammatory pain. J *Neuroinflammation*. 2014; 11:136.

Impellizzeri D, Esposito E, Di Paola R, et al. Palmitoylethanolamide and luteolin ameliorate development of arthritis caused by injection of collagen type II in mice. Arthritis Res Ther. 2013; 15: R192.

Irwin K, Sexton C, Daniel T, Lawlor B, Naci L. Healthy Aging and Dementia: Two Roads Diverging in Midlife?. *Front Aging Neurosci*. 2018; 10:275.

Jack CR Jr, Knopman DS, Jagust WJ, et al. Tracking pathophysiological processes in Alzheimer's disease: an updated hypothetical model of dynamic biomarkers. *Lancet Neurol*. 2013; 12(2):207–216.

Jaggar SI, Hasnie FS, Sellaturay S et al. The anti-hyperalgesic actions of the cannabinoid anandamide and the putative CB2 receptor agonist palmitoylethanolamide in visceral and somatic inflammatory pain. *Pain*. 1998; 76(1-2):189-99.

Jäkel S, Dimou L. Glial Cells and Their Function in the Adult Brain: A Journey through the History of Their Ablation. *Front Cell Neurosci*. 2017; 11:24.

Jauregui-Huerta F, Ruvalcaba-Delgadillo Y, Gonzalez-Castañeda R et al. Responses of glial cells to stress and glucocorticoids. *Curr Immunol Rev*. 2010; 6(3):195–204.

Jonsson T, Stefansson H, Steinberg S, et al. Variant of TREM2 associated with the risk of Alzheimer's disease. *N Engl J Med*. 2013; 368(2):107–116.

Kim KC, Kim P, Go HS et al. Male-specific alteration in excitatory post-synaptic development and social interaction in pre-natal valproic acid exposure model of autism spectrum disorder. *J Neurochem*. 2013; 124(6):832-43.

Kini U, Adab N, Vinten J, Fryer A, Clayton-Smith J; Liverpool and Manchester Neurodevelopmental Study Group. Dysmorphic features: an important clue to the diagnosis and severity of fetal anticonvulsant syndromes. *Arch Dis Child Fetal Neonatal Ed*. 2006; 91(2): F90–F95.

Kirby ED, Muroy SE, Sun WG, et al. Acute stress enhances adult rat hippocampal neurogenesis and activation of newborn neurons via secreted astrocytic FGF2. *Elife*. 2013; 2: e00362.

Kozma C. Valproic acid embryopathy: report of two siblings with further expansion of the phenotypic abnormalities and a review of the literature. *Am J Med Genet*. 2001; 98(2):168-75.

Lane CA, Hardy J, Schott J. Alzheimer's disease. *Eur J Neurol*. 2018; 25(1):59-70.

Li T, Chen X, Zhang C et al. An update on reactive astrocytes in chronic pain. *J Neuroinflammation.* 2019; 16, 140.

Liddelow S, Guttenplan K, Clarke L et al. Neurotoxic reactive astrocytes are induced by activated microglia. *Nature*. 2017; 541**,** 481–487.

Lo Verme J, Fu J, Astarita G et al. The nuclear receptor peroxisome proliferator-activated receptor-alpha mediates the anti-inflammatory actions of palmitoylethanolamide. *Mol Pharmacol*. 2005; 67(1):15-9.

López-Lázaro M. Distribution and biological activities of the flavonoid luteolin. *Mini Rev Med Chem*. 2009; 9(1):31-59.

LoVerme J, La Rana G, Russo R et al. The search for the palmitoylethanolamide receptor. *Life Sciences*. 2005; 77(14), 1685-1698.

LoVerme J, Russo R, La Rana G et al. Rapid broad-spectrum analgesia through activation of peroxisome proliferator-activated receptor-alpha. *J Pharmacol Exp Ther*. 2006; 319(3):1051-61.

Mabunga DF, Gonzales EL, Kim JW et al. Exploring the Validity of Valproic Acid Animal Model of Autism. *Exp Neurobiol*. 2015; 24(4):285–300.

Mackie K, Stella N. Cannabinoid receptors and endocannabinoids: evidence for new players. *AAPS J*. 2006; 8(2): E298–E306.

Matson JL, Cervantes PE, Peters WJ. Autism spectrum disorders: management over the lifespan. *Expert Rev Neurother*. 2016; 16(11):1301-1310.

Mayhew J, Beart PM, Walker FR. Astrocyte and microglial control of glutamatergic signalling: a primer on understanding the disruptive role of chronic stress. *J Neuroendocrinol*. 2015; 27(6):498-506.

Mazzari S, Canella R, Petrelli L, Marcolongo G, Leon A. N-(2-hydroxyethyl) hexadecanamide is orally active in reducing edema formation and inflammatory hyperalgesia by down-modulating mast cell activation. *Eur J Pharmacol*. 1996; 300(3):227-36.

Melancia F, Schiavi S, Servadio M, et al. Sex-specific autistic endophenotypes induced by prenatal exposure to valproic acid involve anandamide signalling. *Br J Pharmacol*. 2018; 175(18):3699 3712.

Miller SJ. Astrocyte Heterogeneity in the adult central nervous system. *Front Cell Neurosci*. 2018; 12:401.

Misra A, Chakrabarti SS, Gambhir IS. New genetic players in late-onset Alzheimer's disease: Findings of genome-wide association studies. *Indian J Med Res*. 2018; 148(2):135–144.

Mrak RE, Griffin WS. The role of activated astrocytes and of the neurotrophic cytokine S100B in the pathogenesis of Alzheimer’s disease. *Neurobiol Aging*. 2001; 22(6):915–922.

Musazzi L, Marrocco J. The Many Faces of Stress: Implications for Neuropsychiatric Disorders. *Neural Plast*. 2016; 2016:8389737.

Musazzi L, Tornese P, Sala N et al. Acute or Chronic? A Stressful Question. *Trends Neurosci*. 2017; 40(9):525-535.

Nabavi SF, Braidy N, Gortzi O et al. Luteolin as an anti-inflammatory and neuroprotective agent: A brief review. *Brain Res Bull*. 2015; 119(Pt A):1-11.

Nava N, Treccani G, Liebenberg N, et al. Chronic desipramine prevents acute stress-induced reorganization of medial prefrontal cortex architecture by blocking glutamate vesicle accumulation and excitatory synapse increase. *Int J Neuropsychopharmacol*. 2014; 18(3): pyu085.

Oddo S, Caccamo A, Shepherd JD et al. Triple-transgenic model of Alzheimer's disease with plaques and tangles: intracellular Abeta and synaptic dysfunction. *Neuron*. 2003; 39(3):409-21.

Olabarria M, Noristani HN, Verkhratsky A et al. Concomitant astroglial atrophy and astrogliosis in a triple transgenic animal model of Alzheimer's disease. *Glia*. 2010; 58(7):831-8.

Parkhurst CN, Yang G, Ninan I, et al. Microglia promote learning-dependent synapse formation through brain-derived neurotrophic factor. *Cell*. 2013; 155(7):1596–1609.

Parrella E, Porrini V, Iorio R, et al. PEA and luteolin synergistically reduce mast cell-mediated toxicity and elicit neuroprotection in cell-based models of brain ischemia. *Brain Res*. 2016; 1648:409-417.

Payakachat N, Tilford JM, Kovacs E, Kuhlthau K. Autism spectrum disorders: a review of measures for clinical, health services and cost-effectiveness applications. *Expert Rev Pharmacoecon Outcomes Res*. 2012; 12(4):485–503.

Pekny M, Pekna M. Reactive gliosis in the pathogenesis of CNS diseases. *Biochim Biophys Acta.* 2016; 1862(3):483-91

Petrelli F, Pucci L, Bezzi P. Astrocytes and Microglia and Their Potential Link with Autism Spectrum Disorders. *Front Cell Neurosci.* 2016; 10:21.

Petrosino S, Cordaro M, Verde R, et al. Oral Ultramicronized Palmitoylethanolamide: Plasma and Tissue Levels and Spinal Anti-hyperalgesic Effect. *Front Pharmacol*. 2018; 9:249.

Price JL, McKeel DW Jr, Buckles VD, et al. Neuropathology of nondemented aging: presumptive evidence for preclinical Alzheimer disease. *Neurobiol Aging*. 2009; 30(7):1026–1036.

Prince M, Albanese E, Guerchet M, et al. *World Alzheimer Report 2014*: Dementia and Risk Reduction an Analysis of Protective and Modifiable Factors, 2014.

Querfurth HW, LaFerla FM. Alzheimer's disease. *N Engl J Med.* 2010; 362(4):329-44.

Radley JJ, Kabbaj M, Jacobson L, Heydendael W, Yehuda R, Herman JP. Stress risk factors and stress-related pathology: neuroplasticity, epigenetics and endophenotypes. *Stress*. 2011; 14(5):481–497.

Re G, Barbero R, Miolo A, Di Marzo V. Palmitoylethanolamide, endocannabinoids and related cannabimimetic compounds in protection against tissue inflammation and pain: potential use in companion animals. *Vet J*. 2007; 173(1):21-30.

Reim D, Distler U, Halbedl S, et al. Proteomic Analysis of Post-synaptic Density Fractions from Shank3 Mutant Mice Reveals Brain Region Specific Changes Relevant to Autism Spectrum Disorder. *Front Mol Neurosci*. 2017; 10:26.

Rodríguez JJ, Olabarria M, Chvatal A et al. Astroglia in dementia and Alzheimer's disease. *Cell Death Differ*. 2009; 16: 378–385.

Sampath D, Sathyanesan M, Newton SS. Cognitive dysfunction in major depression and Alzheimer's disease is associated with hippocampal-prefrontal cortex dysconnectivity. *Neuropsychiatr Dis Treat*. 2017; 13:1509–1519.

Scuderi C, Bronzuoli MR, Facchinetti R, et al. Ultramicronized palmitoylethanolamide rescues learning and memory impairments in a triple transgenic mouse model of Alzheimer's disease by exerting anti-inflammatory and neuroprotective effects. *Transl Psychiatry*. 2018; 8(1):32.

Scuderi C, Esposito G, Blasio A, et al. Palmitoylethanolamide counteracts reactive astrogliosis induced by β-amyloid peptide. *J Cell Mol Med*. 2011; 15(12):2664–2674.

Scuderi C, Steardo L. Neuroglial roots of neurodegenerative diseases: therapeutic potential of palmitoylethanolamide in models of Alzheimer's disease. *CNS Neurol Disord Drug Targets*. 2013a; 12(1):62-9.

Scuderi C, Stecca C, Bronzuoli MR, et al. Sirtuin modulators control reactive gliosis in an in vitro model of Alzheimer's disease. *Front Pharmacol*. 2014; 5:89.

Scuderi C, Stecca C, Iacomino A, Steardo L. Role of astrocytes in major neurological disorders: the evidence and implications. *IUBMB Life*. 2013b; 65(12):957-61.

Scuderi C, Stecca C, Valenza M, et al. Palmitoylethanolamide controls reactive gliosis and exerts neuroprotective functions in a rat model of Alzheimer's disease. *Cell Death Dis*. 2014; 5(9): e1419.

Scuderi C, Valenza M, Stecca C, Esposito G, Carratù MR, Steardo L. Palmitoylethanolamide exerts neuroprotective effects in mixed neuroglial cultures and organotypic hippocampal slices via peroxisome proliferator-activated receptor-α. *J Neuroinflammation*. 2012; 9:49.

Seelinger G, Merfort I, Schempp CM. Anti-oxidant, anti-inflammatory and anti-allergic activities of luteolin. 2008; 74(14):1667-77.

Sheerin AH, Zhang X, Saucier DM et al. Selective antiepileptic effects of N-palmitoylethanolamide, a putative endocannabinoid. *Epilepsia*. 2004; 45(10):1184-8.

Skaper SD, Facci L, Barbierato M, et al. N-palmitoylethanolamine and neuroinflammation: a novel therapeutic strategy of resolution. *Mol Neurobiol*. 2015; 52:1034-1042.

Steardo L Jr, Bronzuoli MR, Iacomino A, Esposito G, Steardo L, Scuderi C. Does neuroinflammation turn on the flame in Alzheimer's disease? Focus on astrocytes. *Front Neurosci*. 2015; 9:259.

Tan CC, Yu JT, Tan L. Biomarkers for preclinical Alzheimer's disease. *J Alzheimers Dis*. 2014; 42(4):1051-69.

Tang Y and Le W. Differential Roles of M1 and M2 Microglia in Neurodegenerative Diseases. *Mol Neurobiol*. 2016; 53:1181–1194.

Tomasini MC, Borelli AC, Beggiato S et al. Differential Effects of Palmitoylethanolamide against Amyloid-β Induced Toxicity in Cortical Neuronal and Astrocytic Primary Cultures from Wild-Type and 3×Tg-AD Mice. *J Alzheimers Dis*. 2015; 46(2):407-21.

Tynan RJ, Beynon SB, Hinwood M, et al. Chronic stress-induced disruption of the astrocyte network is driven by structural atrophy and not loss of astrocytes. *Acta Neuropathol*. 2013; 126(1):75-91.

Vahia VN. Diagnostic and statistical manual of mental disorders 5: A quick glance. *Indian J Psychiatry*. 2013; 55(3):220–223.

Verkhratsky A, Nedergaard M. Physiology of Astroglia. *Physiol Rev*. 2018; 98(1):239–389.

Verkhratsky A, Olabarria M, Noristani HN, Yeh CY, Rodriguez JJ. Astrocytes in Alzheimer's disease. *Neurotherapeutics*. 2010; 7(4):399–412.

Verkhratsky A, Sofroniew MV, Messing A, et al. Neurological diseases as primary gliopathies: a reassessment of neurocentrism. *ASN Neuro*. 2012; 4(3): e00082.

Williams G, King J, Cunningham M et al. Fetal valproate syndrome and autism: additional evidence of an association. *Dev Med Child Neurol*. 2001; 43(3):202-6.

Williams PG, Hersh JH. A male with fetal valproate syndrome and autism. *Dev Med Child Neurol*. 1997; 39(9):632-4.

Wu Y, Dissing-Olesen L, MacVicar BA, Stevens B. Microglia: Dynamic Mediators of Synapse Development and Plasticity. *Trends Immunol*. 2015; 36(10):605–613.

2. Publications

Send Orders for Reprints to reprints@benthamscience.ae

Current Pharmaceutical Design, 2017, *23*, 1-11

REVIEW ARTICLE

Astrocyte: An Innovative Approach for Alzheimer's Disease Therapy

Maria Rosanna Bronzuoli[#], Roberta Facchinetti[#], Luca Steardo and Caterina Scuderi[1*]

[1]*Department of Physiology and Pharmacology "Vittorio Erspamer", Faculty of Pharmacy and Medicine, SAPIENZA University of Rome, P.le A. Moro, 5 - 00185 Rome - Italy*

ARTICLE HISTORY

Received: May 2, 2017
Accepted: June 22, 2017

DOI:
10.2174/1381612823666170710163411

Abstract: Alzheimer's disease is a devastating neurological illness with a heavy economic impact. Further co-morbidity in combination with the social impact of this disorder increases the urgency of a clearer comprehension of its etiopathogenesis, allowing the execution of novel therapeutic strategies. Despite astrocytes have been widely described as active participant in the regulation of cerebral circuits, available data are still poor. Even less information is available about their precise role in the pathogenesis of illness. Moreover, the scant knowledge about the astrocyte-neuron interplay in health and disease still impede pioneering discoveries.

The focus of this review is to look for new and innovative pharmacological approaches against AD. In order to perform this, we used following keywords in PubMed search engine: astrocytes, therapy, Alzheimer's disease, AD, treatment and glia in different combinations.

With this review, we collected data available in literature describing how also astrocytes besides neurons might be new potential targets for drug discovery. Different approaches currently being studied include modulation of glutamate transporters expression, astroglial genetic manipulation, free radicals inhibition, up-regulation of neurotrophins, and regulation of astrogliosis and neuroinflammation.

Since several studies already demonstrated that astrocytes are definitely involved in AD pathogenesis, these cells can represent a promising new therapeutic target.

Keywords: Astrocytes, Alzheimer's disease, pharmacotherapy, reactive gliosis, genetic manipulation, neurotrophins.

1. INTRODUCTION

1.1. Alzheimer's Disease and Astrocytes

1.1.1. Alzheimer's Disease

Dementia is a neurodegenerative condition resulting from a variety of cerebral disorders whose incidence has expanded in parallel with the lifespan increase. The incidence of dementia is evaluated to be 46.8 million people worldwide in 2015 and this number is expected to reach 131.5 million in 2050 [1]. Alzheimer's disease (AD) accounts up to 80% of dementia cases [2] and is one of the biggest economically burdensome health conditions in current society. At the clinical level, a subtle decline in episodic memory is followed by a general impairment in overall cognitive abilities [3], beginning with an inability to recall recent past, followed by loss of long-term memories, change in personality and loss of other cognitive functions, including language and attention [4]. Histopathologically, the two major AD neuropathological hallmarks are the accumulation of extracellular beta-amyloid peptide (Aβ) that induces the creation of senile plaques (SPs) mainly in hippocampal and cortical areas, and the production of intracellular neurofibrillary tangles (NFTs) in the cytoplasm of pyramidal neurons [5, 6]. Furthermore, an intense inflammation has been shown to be closely associated with amyloid deposits in brain parenchyma, as confirmed by the presence of microglia and astrocytes abnormally activated [7]. Studies of *post mortem* brain tissues from AD patients demonstrated the presence of a generalized astrogliosis, mainly manifested by cell dysfunction and increased expression of the cytoskeletal glial fibrillary acidic protein (GFAP) and the neurotrophin S100B, guided by increased pro-inflammatory mediators [8].

*Address correspondence to this author at the Department of Physiology and Pharmacology "Vittorio Erspamer", SAPIENZA University of Rome P.le A. Moro, 5 - 00185 Rome Italy; Tel: +39 06 49912713; Fax: +39 06 49912480; E-mail: caterina.scuderi@uniroma1.it

[#]*These two authors equally contributed to this work.*

1.1.2. Physiological Functions of Astrocytes

Astrocytes (also termed astroglia) are the most heterogeneous type of glial cells in the central nervous system (CNS). These cells are crucially involved in the organization of the brain structures, and actively participate in the brain function maintenance [9, 10]. The term astrocyte derives from the Greek words *astron* (plural *astra*), due to their characteristic star shape, and *kytos*, meaning vessel. More than a century ago, Camillo Golgi and Santiago Ramòn Y Cajal proposed astrocytes as functionally important beyond simple structural support [11, 12]. Indeed, astrocytes largely differ according to their localization, developmental stage, and subtype. So, in the gray matter there is a clear prevalence of protoplasmic astrocytes, characterized by short branches, whilst fibrous astrocytes with long unbranched processes are abundant in the white matter [13].

Astrocytes coordinate several functions aimed at regulating synaptic activity and preventing injury spreading. Indeed, astrocytes can sense neuronal inputs through membrane ion channels, transporters, and receptors. They can also respond by transduction pathways that involve mainly calcium (Ca^{2+}) signaling, and modulate in turn adjacent neuronal elements through various mechanisms, including neuroactive factors uptake or release [14, 15]. Although astrocytes are not considered excitable cells, however, they display well-organized increases in intracellular Ca^{2+} ($[Ca^{2+}]_i$) levels that may be considered a form of astrocyte excitability [16]. Such $[Ca^{2+}]_i$ increase is crucial for the communication among astrocytes, and between astrocytes and neurons [17]. For example, many studies demonstrate that a great variety of G-protein coupled receptors are located on astrocytes, and such receptors, once activated by neurotransmitters released from presynaptic terminals, regulate astrocytic $[Ca^{2+}]_i$ levels [18].

Interestingly, astrocytes can regulate synapses organization, stability, and activity through the release of gliotransmitters (e.g., glutamate, ATP or D-serine) acting on pre- or post-synaptic recep-

1381-6128/17 $58.00+.00

tors [14]. These cells finely regulate the extracellular glutamate concentration, improving its clearance through their transporters, or by changing the volume of the extracellular space, as a result of plastic physical coverage of neurons. By this way, astrocytes improve the efficacy of synapses [19]. Indeed, astrocyte processes, together with neuronal pre- and post-synaptic regions, form the tripartite synapse necessary not only for functional synapses maturation, but also to maintain them [20]. The regulation of glutamate levels managed by astrocytes is fundamental to correctly coordinate the neurotransmission and to avoid the extracellular glutamate levels from reaching excitotoxic concentrations [21]. The synaptic glutamate re-uptake is operated by the astrocytic excitatory amino acid transporters (EAATs), EAAT1 (GLAST) and EAAT2 (GLT-1). By this manner, these cells protect neurons preventing the excessive accumulation of glutamate in the synaptic cleft [22]. In astrocytes, glutamate is metabolized to glutamine by glutamine synthetase (GS), an enzyme mainly localized on membrane. The glutamine is then given back to neurons to be reconverted to glutamate or GABA, primarily by phosphate-activated glutaminase [23].

The glutamate uptake performed by astrocytic drives glycolysis and consequently the lactate shuttling from astrocytes to neurons that needs it for the oxidative metabolism. Neuronal impulses generation and transmission are biochemical activities that require a huge amount of energy, guaranteed by the solid bidirectional interconnection between neurons and astrocytes. Indeed, these latter allow the creation of a nourishing environment for neurons mainly by the regulation of glucose metabolism [24, 25]. Glucose enters directly neurons by the glucose transporter 3 (GLUT3) or through the astrocytic GLT-1 transporter present in their end-foot processes. [26]. In astrocytes, glucose is stored as glycogen and, when is needed, it is metabolized to produce lactate. Glycogen stores can be mobilized only after signaling coming from few neurotransmitters, including molecule deriving from neurons [27]. Most of these conclusions are based on *in vitro* evidence; anyway, a recent *in vivo* study based on a $GLAST^{CreERT2}$: $Cox10^{flox/flox}$ mouse model that lacks the mitochondrial respiration in astrocytes showed that, in healthy conditions, at last Bergmann glial cells can survive by aerobic glycolysis for a protracted period of time [28].

It is widely accepted that astrocytes play an important role in the function and maintenance of the blood brain barrier (BBB) [29]. Because their processes both enwrap synapses and contact the endothelial cells of the BBB, they are able to modulate cerebral blood flow based on neural activity [30].

Astrocytes are also fundamental for the clearance of CNS. They express a specific water transporter called aquaporin-4 (AQP4), which facilitates the bulk of glymphatic flow through the CNS [31, 32], utilizing a network of perivascular channels that promote efficient elimination of soluble proteins and metabolites of the CNS [33].

Many other physiological functions are regulated by astrocytes. These include the control of fluids composition and ions (e.g., K^+) concentration, pH regulation, detoxification, free-radical scavenging, metal sequestration, and neurotransmitter homeostasis in the synaptic cleft [17]. For example, astrocytes counteract oxidative stress by contributing to the formation of glutathione, the main cellular antioxidant, increasing the intracellular levels of its precursor cysteine through the activation of the cystine/glutamate antiporter and other transporters [34]. Moreover, astrocytes secrete an enormous variety of neurotrophic factors, like nerve growth factor, brain-derived neurotrophic factor (BDNF), ciliary neurotrophic factor, glia-derived nexin, epidermal growth factor, and hepatocyte growth factor [35, 29]. They are also capable of synthesizing cytokines, including tumor necrosis factor-α (TNF-α), interleukin (IL)-1β, IL-6 and transforming growth factor-β (TGF-β) [36].

Table 1. Astrocytes functions.

Astrocytes functions	References
Glutamate/GABA-glutamine cycle regulation	Araque *et al.*, 2014 [14] Pannasch *et al*., 2011 [19] Pellerin *et al*., 1994 [21] Rothstein *et al.*, 1996 [22] Wang *et al*., 2008 [24]
Capillary blood flow regulation	Zlokovic *et al*., 2005 [63]
Neurotrophic factors production	Markiewicz *et al.*, 2006 [93] Jana *et al*., 2013 [94]
Synaptogenesis and neurogenesis	Diniz *et al*., 2014 [53]
Immune modulation with microglia	Wang *et al*., 2008 [24]
BBB regulation	Alvarez *et al*., 2013 [28] Zonta *et al.,* 2003 [30]
Energetic substrates	Gavillet *et al.,* 2008 [27]
Potassium buffering	Sattler *et al*., 2006 [17]
Neurotransmitters uptake and regulation	Araque *et al*., 2014 [14] Bernardinelli *et al*., 2014 [15]
Tripartite synapse regulation	Christopherson *et al*., 2005 [20]
Stress defense	Shih *et al*., 2006 [34]
Cholesterol metabolism	Kanekiyo *et al*., 2014 [47]

1.1.3. Astrocytes and AD

Several studies showed the benefits and neuroprotective effects of reactive astrocytes on surrounding neurons that try to limit damage, repair BBB, remodel tissues and provide energy substrates [37] (main astrocytes functions are summarized in table 1). Dysregulation of communication at the level of the tripartite synapse may be implicited in the cumulative effects of disease progression seen in neurodegenerative diseases such as AD.

The pathological potential of neuroglia has been hypostasized already by Alois Alzheimer. He discovered glial cells in close connection with damaged neurons, and observed that these cells were components of SPs. In line with these observations, the presence of reactive astrocytes in the brains of AD animal models is now well-documented [38]. However, it is still under debate how much astrocytes dysfunctions contribute to neurodegenerative diseases. Although significant progress in studying astrocytes functions in the brain has been made over the last twenty years [39], the molecular and functional modifications of these cells after injuries occurring in AD are still not completely understood [40, 41].

Consistent with the hypothesis of the amyloid cascade, Aβ deposition in the brain starts the sequence of pathological events that give rise to inflammation, synaptic impairment and neuronal loss [42]. Especially neuroinflammation, mainly fostered by the activation of both astrocytes and microglia surrounding SPs and neurons carrying NFTs, is a peculiar feature of AD brains [43]. In particular, this activation is limited to cells closely related and localized to protein deposits, especially for microglia that needs to be physically in contact with Aβ to be activated, unlike microglia located in the parenchyma far from Aβ deposits that remains ramified

and inactivated. This behavior of microglial cells has been seen also in human *post mortem* AD brains [44, 45]. The lack of this activation and the reduction of microglia in AD human brains could be considered pathogenic factors themselves. The genetic profile of astrocytes in AD reveals alterations in stress defense, cholesterol metabolism, and gene transcription [46-49].

As previously described, astrocytes are crucial for the removal and recycling of neurotransmitters, in particular glutamate. The deletion of GLT-1, the predominant glutamate transporter in the mature mammalian brain [50], leads to pathological conditions like spontaneous seizures and increased susceptibility to acute cortical injury [51]. Compromised glutamate homeostatic mechanisms were found, for example, in a triple transgenic model of AD, the 3×Tg-AD mouse, that shows a decrease in GS expression not necessarily coupled with reduction in GLT-1 presence [52]. Disruption in the glutamate/GABA-glutamine cycle leads to this inhibition by limiting the metabolic substrate provided by astrocytes to interneurons, essential to maintain the release of GABA at active inhibitory synapses. In physiological conditions, TGF-β from astrocytes regulates inhibitory GABAergic synapse formation in a glutamatergic dependent manner [53]. Increased TGF-β is found in AD patients; the levels detected correlate strongly with plaques deposition and cerebral amyloid angiopathy, and promote Aβ production and deposition in transgenic mice [54]. Astrocytes membranes have a high K^+ conductance mainly due to their abundant expression of inwardly rectifying K^+ channels, predominantly Kir4.1 and Kir5.1 [55, 56]. This inward rectification is the main determinant of the low resting membrane potential of astrocytes, close to the equilibrium potential for K^+. Furthermore, a single astrocyte contacts thousands of synapses and is directly electrically coupled with neighboring astrocytes into a large syncytium. The combination of these characteristics makes astrocytes optimal for K^+ uptake. This mechanism is named "potassium buffering" and it minimizes the deleterious effects of local prolonged increases in $[K^+]_o$ resulting from neuronal activity [56]. The impairment of astrocytic K^+ buffering can deeply impact neuronal survival. For instance, down-regulation of Kir4.1 has consequences for glutamate uptake, since the electrogenic transport of this neurotransmitter is intimately linked to Na^+ and K^+ ionic gradients [57].

Ca^{2+} signaling is an extremely important multifunctional process in all cells that can be regulated by different stimuli. This process is fundamental in astrocytes, too. For instance, noradrenalin, coming from neuronal projections of locus coeruleus (LC), is able to activate astroglia in the cortex through α- and β-adrenergic receptors [58]. The result is $[Ca^{2+}]_i$ increase that, together with cAMP increase, determines astrocytic metabolism, excitation-energy coupling, morphology and vesicle trafficking. In neurodegeneration, especially in the early stage of the disease, loss of LC neurons causes alterations in the noradrenergic system that deregulates main astrocytic functions playing an additional role in facilitating the course of neurodegeneration [59, 60] and this is mediated by aberrant Ca^{2+} signaling.

Generally, murine AD astrocytes show a higher frequency of spontaneous Ca^{2+} oscillations, anomaly also observed in response to intravenous Aβ administration. *In vivo* Ca^{2+} imaging of APP/PS1 transgenic mice, presenting SPs deposition, also showed increased spontaneous Ca^{2+} activity, including waves spreading out radially starting from plaques [61].

Another peculiar AD feature is the presence of cerebrovascular dysregulation that is closely connected with ischemic injury and BBB damage [62]. In fact, it has been demonstrated that the synaptic and neuronal dysfunctions in AD are also caused by the accumulation of toxic compounds due to the failure of the efflux transport provoked by the deposition of Aβ in the cerebral microvessels [63].

In line with the observations that activated astrocytes are generally present in the brains of patients with AD as well as in transgenic models of the pathology [64], a close relationship between astrocyte activation and Aβ deposition has been demonstrated. The Aβ-induced activation of astrocytes is characterized by morpho-functional changes detectable, for example, by the increased expression of GFAP and S100B [65]. The latter protein is crucially involved in the amplification of the neuroinflammatory process. Indeed, after brain injuries, a large quantity of S100B is released by astrocytes into cerebrospinal fluid (CSF) and blood brain and, by this manner, it recruits and activates further glial cells [66, 67]. Astrogliosis is more often associated with the increased production of factors that may either be beneficial or harmful to neighboring cells. This astrocytic production is accompanied by microglial cytokines production, finely modulating the immune response of the brain [24].

The process of astrogliosis is gradual [10]. It starts with a wide range of stimuli that trigger it in response to Aβ production. These stimuli can be ATP, secreted mediators like endothelin-1, pro-inflammatory cytokines like IL-1β and TNF-α, etc… [37]. Many of these factors are secreted by both microglia and astrocytes that start a vicious neuroinflammatory cycle in which glial cells amplify the neuropathological injury through the direct killing of neurons and the simultaneous perpetuation of reactive gliosis [68, 69]. By this manner, astrocytes lose their physiological neurosupportive functions, and actively foster a chronic inflammatory state that overrides its initial and beneficial intent, promoting exclusively the detrimental effects.

Recent evidence suggests that astrocyte changes do not occur only with hyperactivation that often precedes SPs and NFTs formation, but also with atrophy [39]. This has been first showed in 3×Tg-AD mice in 2010 from Olabarria and colleagues who found a reduction in both surface and volume of GFAP profiles. This phenomenon was patent since the early stages of the disease and persisted up to 18 months of age in the dentate gyrus; while in the CA1 region of the hippocampus astrocyte atrophy was seen only starting from 18 months of age [70]. This atrophy is widely detectable in the brain parenchima but not near SPs where surrounding astrocytes keep their hypertrophic phenotype [70]. Astroglial atrophy has been seen also in PDAPP-J20 mice [71] and in familiar AD human *post-mortem* tissues [72]. So, also astrocytes are susceptible to degeneration that can be named "astrodegeneration" [72].

On the basis of all these considerations, astrocytes may be realistically view as a new encouraging target for future AD therapies.

2. TARGETING ASTROCYTES IN AD

Despite scientific efforts, treatments currently used in AD therapy give moderate benefits only to a subgroup of patients and valid therapeutics are lacking [73]. Given the complexity of this disorders, actually innovative and promising therapeutic tools should simultaneously counteract the several pathogenic mechanisms involved in AD. The fact that astrocytes may serve both adaptive and pathological functions is one of the recurrent themes concerning their functions in disease and difficulties in targeting these cells to treat neurological disease.

The morpho-functional changes that astrocytes undergo during several neuropsychiatric conditions, including AD, often become detrimental mainly because of the loss of their homeostatic actions. By this way, astrocytes play crucial roles in the pathogenesis of such disorders. So, they can be legitimately considered as promising therapeutic target. Glia-addressed drugs are still in an embryonic state, and their discovery still represents a challenge.. As result, a wide-range of treatments targeting astrocytes is now under investigation. They range from environmental stimulation, dietary modifications, up to genetic manipulation (Fig. **1**). This latter seems to be one of the most promising approaches.

Current and under investigation therapies targeting astrocytes in AD are summarized in Table **2**.

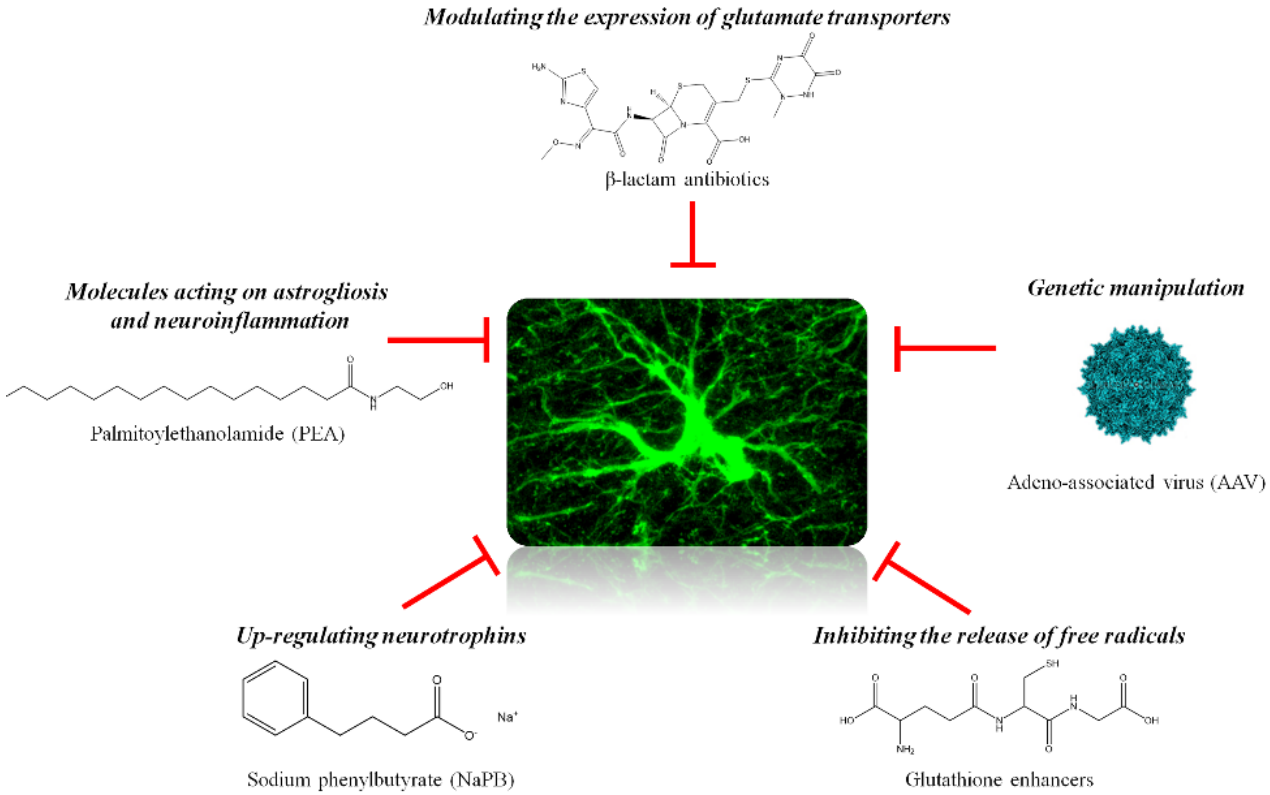

Fig. (1). Schematic view of approaches targeting astrocytes in Alzheimer's disease.
Dysfunctional astrocytes can be rescued by modulating the expression of glutamate transporters (e.g., Cefatriaxone or Riluzole) [77, 78], by genetic manipulation (e.g., using adeno-associated virus - AAV) [80, 84, 85], by inhibiting the release of free radicals (e.g., glutathione enhancers, anti-oxidative drugs, NADPH inhibitors, iNOS inhibitors) [86, 88, 91], by up-regulating neurotrophins in astrocytes (e.g., NaPB) [95] or via molecules acting on astrogliosis and neuroinflammation (e.g., PEA, RSV, AGK-2, MW-151, pentamidine isethionate) [74, 111, 113, 132].

Table 2. Approaches targeting astrocytes in Alzheimer's disease.

Astrocyte Dysregulated Function	Mechanism of Action	Therapy	References
Glutamate excitotoxicity	Increase of expression of astroglial glutamate transporters	Riluzole	Ji *et al.*, 2005 [77]
	Promotion of EAAT2 activation through hetero-dimeric transcription (NF-kB) signaling	Ceftriaxone	Lee *et al.*, 2014 [78]
Gene trascription	Use of adeno-associated virus (AAV) to deliver vehicles into astrocytes	Driving the expression of VIVIT through the human GFAP specific promoter (Gfa2)	Foust *et al.*, 2009 [80]
	Use of adeno-associated virus (AAV) to deliver vehicles into astrocytes	Inducing overexpression of TGF-α	White *et al.*, 2011 [84]
		Displaying anti-GLAST IgG on lentivirus surfaces	Fassler *et al.*, 2015 [85]
Impaired oxidative defense system	Enhancement of molecular properties	Glutathione enhancers	Hensley *et al.*, 2000 [86]

(Table 2) Contd....

Astrocyte Dysregulated Function	Mechanism of Action	Therapy	References
	Inhibition of pro-inflammatory redox signaling	Antioxidative drugs	Fuller *et al*., 2010 [88] Crespo *et al*., 2017 [89]
	Inhibition of pro-inflammatory redox signaling	Inhibitors of NADPH and iNOS	Pahan *et al*., 1998 [91]
Reduced levels of neurotrophic factors in the brain	Increasing the levels of BDNF through the activation of the PKC-CREB signaling pathway	Sodium phenylbutyrate (NaPB)	Butler *et al*., 2006 [95]
Astrocyte disfunction and neuroinflammation	Anti-inflammatory and neuroprotective activities dependent on PPAR-α activation	Palmitoylethanolamide (PEA)	Scuderi *et al*., 2011 [111]
	Modulating sirtuins (SIRTs)	Resveratrol (RSV), a SIRT1 activator, and AGK-2, a SIRT2-selective inhibitor	Scuderi *et al*., 2014 [113]
	Downregulation of astrocytic IPAF inflammasome	ASC-mediated activation of the inflammasome on phagocytic activity of astrocytes	Liu *et al*., 2013 [122]
	Abolition of Aβ-induced glia proinflammatory cytokine production	MW-151	Hu *et al*., 2007 [74]
	Blockade of S100B/p53 interaction	Pentamidine isethionate	Hartman *et al*., 2013 [132]
	Reduction of the expression and secretion of TNF-α and IL-6	Hepcidin	Urrutia *et al*., 2017 [121]
Activation of the complement system	Antagonizing C3aR		Lian *et al*., 2014 [134]

2.1. Modulating the Expression of Glutamate Transporters

Deficiencies in astrocyte uptake of glutamate have been linked to various neurodegenerative disorders, such as amyotrophic lateral sclerosis (ALS), epilepsy, oligodendrocyte death, tauopathies and schizophrenia [74, 75]; some others, like stroke, lead to an increased expression of glutamate transporters [76]. Therefore, modifying the action or expression of these proteins may provide a therapeutic target for these conditions. Various molecules have entered clinical trials to test the feasibility of manipulating astrocyte-mediated glutamate uptake in reducing neurodegeneration. In particular, astroglial glutamate uptake has been proposed as an alternative approach to decrease neuronal toxicity and regulate synaptic function. Modifying the action or expression of astrocytic glutamate transporters may provide a therapeutic strategy for these conditions. In line with this hypothesis, it has been observed that the expression of glutamate transporters (in particular GLT-1) increases after treatment with β-lactam antibiotics or the neuroprotective drug riluzole [22, 77], suggesting these drugs as candidates to target glutamate excitotoxicity. In fact, β-lactam antibiotics are FDA-approved drugs since 1984. One of these antibiotics, ceftriaxone, promotes EAAT2 activation through heterodimeric transcription nuclear factor-kappa B (NF-κB) signaling [78].

2.2. Genetic Manipulation of Astrocytes

An alternative therapeutic target to consider as a pharmacological approach against AD is astroglial gene expression [79]. Recently, the use of adeno-associated virus (AAV) as vector able to modify astrocytic genes has been proposed. For example, AVV vectors bringing human GFAP specific promoter (Gfa2) have been used to reach the hippocampal astrocytes of APP/PS1 mice. By this way, such population of glial cells express VIVIT, a peptide able to erase the inflammatory calcineurin/NFAT pathway that is importantly involved in astrocyte activation. Such gene-related approach further demonstrated the pathological role of astrocytes in AD. Indeed, because of the induced expression of GFAP-VIVIT, researchers found a reduction of Aβ load as well as improved synaptic functions and cognitive activities [80, 81].

Because of their reported benefits after injury and their important role in normal physiology, astrocytes have been used in transplantation studies to try to improve functional recovery. In particular, immature astrocytes have been used because of their growth-permissive properties without the negative effects of scar formation. In fact, transplanted immature, but not mature, astrocytes suppress glial scar formation and thereby enhance neurite outgrowth in the mouse brain [82]. Transplanted immature astrocytes are also more motile and better associate with blood vessels than mature astrocytes, which may account for their ability to suppress scar formation. A previous study suggested that adult cortical astrocytes retain the ability to revert to a more immature, even radial-glial like, state that can direct the migration of transplanted immature neurons [83]. Enhancing the beneficial neuroprotective effects of astrocytes after injury, while minimizing the negative effects on regeneration, is

one of the major interests in the field. One study used an intraparenchymal AAV injection at the site of the injury to induce overexpression of TGF-α [84]. TGF-α was able to transform astrocytes neighboring the injury to a growth permissive phenotype that enhanced cell proliferation, altered their distribution and led to increased regeneration in the rostral end of the lesion [85]. This suggests that astrocytes manipulation, rather than their ablation, may provide a promising way for AD therapy in the next future.

Many studies have focused on the possibility of astrocytes to form bridges across the lesion core after injury. It has been demonstrated that microtransplanting immature astrocytes along with the enzyme chondroitinase ABC to aid proteoglycan degradation provides a bridge across the lesion environment that allows axonal regeneration. The microlesion was done in the cingulate gyrus [86].

Among the possible approaches to selectively target subpopulations of astrocytes in the CNS (e.g., transgenic mice, imaging, and molecular genetic), the viral-mediated one remains the more beneficial for investigating neurodegenerative disorders. Interestingly, Fassler and collaborators demonstrated the possibility to use engineered lentiviruses, with a modified Sindbis envelope presenting on their surface anti-GLAST IgG, to reach specific astrocytes, by either *in vitro* and *in vivo* experiments [85]. This encouraging approach could be applied to target not only astrocytes but also other CNS cell populations in the near future [87]. The gene-delivery approach is difficult to make routinely in a short time, mainly for the structural and functional complexity of the brain. However, this method is very promising and of crucial importance for farther comprehension of the role of astrocytes in brain physiology and pathology.

2.3. Inhibiting the Release of Free Radicals

Astrocytes during AD are profoundly modified in both structure and functions. These changes are particularly evident in proximity of SPs, where astrocytes exhibit energy metabolism alteration, modification in their ability to regulate the levels of glutamate in the synaptic cleft, and produce and release a huge amount of mediators of inflammation and oxidative stress (reactive oxygen species, ROS, and reactive nitrogen species, RNS). So, it is reasonable to assume that all these astrocytic pathological modifications could have a role in AD progression and that drugs ameliorating such alterations could counteract the disease. Among the potential inhibitors of astroglial activation, glutathione enhancers are the most promising and the closest to clinical practice.

A close connection between oxidative stress and astrocyte activation has been established, and free radicals are regarded as activating agents. For this reason, drugs able to reduce their levels thus blocking the pro-inflammatory redox signaling are under consideration [86, 88].

Among antioxidant molecules, recently it has been demonstrated also that hydroxytyrosol (HT), a polyphenol olives- and olive oil-derived, could exert beneficial effects in AD controlling $A\beta_{(25-35)}$ toxicity in astrocytes, through the insulin signaling pathway; indeed, there is a link between insulin resistance (diabetes) and AD [89].

Also inhibitors of nicotinamide adenine dinucleotide phosphate (NADPH) oxidase and inducible nitric oxide synthase (iNOS) have been proposed as potential agents able to reduce astroglial activation. NADPH oxidase is a plasma membrane enzyme that catalyzes the production of superoxide (O_2^-) [80]. The biochemical pathways responsible for NADPH oxidase activation are complex, so the pharmacological modulation is feasible at different steps. As a results, inhibitory agents have been proposed [90]. [90]. iNOS is an inducible enzyme responsible for the glial synthesis of NO, and is considered an important factor in the inflammatory diseases course. After activation, glial cells produce cytokines, such as IL-1β, TNF-α, and interferon-γ (INF-γ), that induce iNOS whose end-product is NO [91]. Therefore, the inhibition of these enzymes that produce free radicals may prove to be effective in counteracting further astroglial activation.

2.4. Up-Regulating Neurotrophins in Astrocytes

An alternative approach to target astrocytic functions against pathological brain conditions is to design modalities that could enhance or mimic the "good" astrocytes functionality . For instance, several studies tested the administration of astrocyte-derived neuroprotective factors, like the glial-derived neurotrophic factor (GDNF) and the erythropoietin (EPO), with the aim to enhance neuroprotection in neurological disorders. Interestingly, it has been demonstrated that GDNF efficiently reduces neuronal loss generally recorded in animal models of ALS, PD, and stroke [92]. Given the relative lack of permeability of the BBB to these neurotrophic factors, a more promising methodology may involve the development of small molecules able to induce the expression of such factors endogenously by astrocytes, instead of the exogenous administration of the neurotrophins [93]. The idea of administering neurotrophins in neurodegenerative diseases, such as AD, PD, and HIV-associated dementia comes from the need to protect neurons since in these pathological conditions the levels of some neurotrophins are extremely reduced in the cerebral tissues. For instance, it has been demonstrated that the levels of both BDNF and the growth factor NT-3, needed to support neuronal survival and differentiation, are significantly down-regulated in AD brains [94]. Accordingly, these neurotrophic factors exhibit protective effects *in vitr*o, as well as *in vivo* models of numerous neurodegenerative disorders. In physiological conditions, neurotrophic factors are, for the most part, produced by neurons. Conversely, glial cells release much more neurotrophins in neurodegenerative conditions mainly because of the neuronal loss and surviving cells do not produce these essential trophic factors. Although such mechanisms are poorly understood, increasing the levels of neurotrophins in astrocytes could represent an important area of research. Sodium phenylbutyrate (NaPB), for example, is a salt of short chain fatty acid that gained the clinical attraction since several lines of evidence support the idea that this compound and its metabolite NaPA are able to up-regulate neurotrophins production in astrocytes [95]. Indeed, NaPB induces the expression of both BDNF and NT-3 in primary murine and human astrocytes in a dose-dependent manner. Its action is mediated by the activation of the PKC-CREB signaling pathway. These results revealed some NaPB properties that indicate such FDA-approved drug as a promising tool in improving synaptic plasticity in neurodegenerative diseases not only as an adjunct therapy, but also as a primary approach [96].

2.5. Molecules Acting on Astrogliosis and Neuroinflammation

In physiological conditions, astrogliosis is a dynamic and essential process needed for CNS functions [97]. In this context, subsequently to $[Ca^{2+}]_i$ increase, astrocytes become transiently reactive, so they can perform their functions that include neuronal interactions and blood flow regulation. This activated state is not just a response to insults. So, it is possible to differentiate this physiological activation from the disease-correlated one by using the term 'reactive' that includes a wider spectrum of responses [98]. Even during the pathological states, it is important to highlight that astrocyte activation is a protective process that starts with the aim to circumscribe and erase the initial insult. Indeed, Pekny and collaborators demonstrated that GFAP and vimentin murin KO depletes the reactive astrocyte state, exacerbating AD-associated changes [99].

In AD brains, together with the abundant production of pathogenic molecules, astrocytes acquire a reactive state that let them failing in providing their supportive functions to neurons, thus rendering them more exposed to harmful stimuli. Every compound that has the ability to control astrocyte activation together with neuroinflammation, and simultaneously able to prevent neuronal impair-

ment, has to be taken into consideration as a novel potential therapeutic drug. For instance, the fatty acid amide palmitoylethanolamide (PEA) has raised much interest for its important anti-inflammatory and neuroprotective activities, demonstrated in different neuropathological conditions [100-103]. Despite PEA displays several cannabinoid-like effects, it shows very low affinity for cannabinoid receptors [104, 105]. Instead, the activation of peroxisome proliferator-activated receptor-α (PPAR-α) mainly mediates its molecular mechanism [68, 101, 106]. Glial cells produce and hydrolase PEA [107, 108], and the presence of both PEA and PPAR-α has been observed in the CNS, as well as their changes during some pathological states [109, 110]. The biological significance of these modifications is still poorly understood. What is known is that Aβ exposure down-regulates the expression of PPAR-α and, under the same circumstances, enhances the levels of PEA and oleoylethanolamide, another potent PPAR-α agonist, in activated astrocytes [111]. Our group showed the therapeutic potential of exogenous PEA, demonstrating its ability in counteracting astrocyte activation and the inflammatory process through the inhibition of NF-κB pathway [111]. Later we demonstrated, in an *in vivo* rat model of AD, the capability of PEA to control AD neuropathology by simultaneously exerting anti-inflammatory and neuroprotective effects. These results support the hypothesis that astrocyte activation can be regarded as a novel and proper target for developing novel AD treatments [73].

We also showed that is also possible to control astroglial activation through an epigenetic approach, in particular by modulating sirtuins (SIRTs). Seven isoforms of these NAD+-dependent enzymes have been identified, and are involved in regulating key biological processes like chromosomal stability, transcriptional silencing, cell metabolism and cycle progression, autophagy, stress response and inflammation [112]. Moreover, we recently established SIRTs involvement in brain protection in Aβ-challenged primary astrocytes, where the selective SIRT1 activation or SIRT2 inhibition (made by resveratrol (RSV) and AGK-2, respectively) controlled astrocyte activation, negatively modulating GFAP and S100B expression, and suppressed the production of proinflammatory mediators. Our results indicate SIRTs as key regulators of the reactive gliosis, suggesting RSV or AGK-2 as innovative agents suitable for the treatment of neurodegenerative disorders presenting inflammation, including AD [113].

As previously mentioned, the inflammatory process is sustained by glial cells through the release of cytokines. In presence of stress or cellular infection, the creation of a molecular platforms named inflammasome takes place. This event prompts the release of proinflammatory cytokines like the pro-IL-1β to begin the innate immune defenses [114]. The abnormal signaling of the inflammasome can contribute itself to etiopathogenesis of infectious brain injuries, and neurodegenerative and autoimmune diseases [115, 116]. However, inflammasome role in brain disorders requires further investigations. The presence of IL-1β and its receptor on microglia and astrocytes makes the CNS highly sensitive to this signaling [117, 118]. Indeed, in both AD patients and *in vivo* models of AD, a high proliferation and activation of these cells is actually induced by this signaling [119, 120]. Also IL-6 and TNF-α are detected in cultured astrocytes and microglia after $A\beta_{1-42}$-insult, and recent data showed that hepcidin, an hormone that physiologically regulates iron metabolism, can mediate an anti-inflammatory action, accompanied by antioxidative and neuroprotective outcomes [121]. It has been recently demonstrated that the inflammasome, containing LRR, NACHT and PYD domains-containing protein 3 (also known as cryopyrin), can be activated by Aβ *in vitro*, causing the induction of the inflammatory process and, as a consequence, tissue damage [119]. Furthermore, the absence of NALP3 in the APP/PS1 mouse model of AD is able to reduce Aβ deposition and to prevent memory loss. The expression of astrocytic IPAF inflammasome and the adaptor protein ASC results significantly augmented in a subgroup of patients affected by the sporadic form of AD. On the contrary, it has been demonstrated that the downregulation of such astrocytic inflammasome is able to reduce $A\beta_{1-42}$ production deriving from primary neurons [122]. Couturier and colleagues [123] investigated the effect of the inflammasome activation ASC-mediated on phagocytosis performed by astrocytes and its further implications in a 5×FAD transgenic murine model of AD. They firstly found that ASC is essential for the induction of IL-1β release from primary astrocytes $A\beta_{1-42}$-exposed and, moreover, that ASC expressed in heterozygosity is enough to reduce the amyloid load, rescuing the impairment of the long-term spatial memory [124]. So, also these evidence suggest astrocytes as potent actors in Aβ clearance, demonstrating the improved phagocytic efficiency of these cells in presence of ASC heterozygosity, after Aβ-challenge. By this manner, inflammasome activation in astrocytes can be considered as a new therapeutic target against Aβ -induced pathology.

In relation to the progression of the disease, the overproduction of proinflammatory cytokines, like IL-1β, causes damages not only perpetuating neuroinflammation, but also directly impairing neuronal functionality. In fact, Hu and colleagues demonstrated the possibility to ameliorate the neuronal dysfunction induced by cytokines through a therapeutic intervention [74]. They developed MW01-2-151SRM, a small therapeutic molecule, named MW-151, which was able to selective suppress glial production of proinflammatory cytokines induced by Aβ, thus attenuating the loss of synaptic markers (e.g., synaptophysin and PSD-95) and the resulting cognitive deficits. These results showed the beneficial effects on synaptic functionality obtained by the selective and precocious inhibition of the glial proinflammatory response, suggesting the relevance of taking into consideration the precise timing for starting the anti-inflammatory therapies. Indeed, they observed that MW-151 treatment was more performing when tested in a preventative paradigm. In addition, analysis of data from the Alzheimer's Disease Anti-inflammatory Prevention Trial (ADAPT) randomized clinical trial suggests that the effects of nonsteroidal anti-inflammatory drug (NSAIDs) treatment differ according to the stage of the disease. So, also these data confirm the potential beneficial effects of starting drug administration in asymptomatic AD patients with little or no cognitive decline and, on the contrary, the harmful effects of starting in later stages [125]. Even though MW-151 is not an NSAID, the results here reported are in agreement with the idea that suppressing inflammation in the CNS can be effective if considered as a prevention strategy. However, we have to report that MW-151 effectiveness in blocking cytokine production and in preventing synaptic impairment was also showed in later stage of the pathology [126].

The terms "reactive gliosis" refer to overexpression of glial-derived factors. As above described, one of the most interesting is the neurotrophin S100B [124, 127], a soluble protein belonging to the family of EF-related Ca^{2+} and Zn^{2+} binding proteins. According to its concentration, it can operate different effects. When presented at nanomolar concentration, S100B function is to provide a pro-survival effect on neurons and stimulate neurite outgrowth; at higher (micromolar) concentration S100B is responsible for promoting inflammation and, simultaneously, neuronal loss [128]. In fact, the overexpression of S100B has been linked to the typical hallmarks of reactive gliosis in AD [129]. Surprisingly, pentamidine isethionate, an old drug currently used for the treatment of protozoal diseases [130], is able to control both reactive gliosis and neuroinflammation in an *in vivo* model of AD by specifically inhibiting S100B-mediated effects [131]. The assumed pentamidine isethionate mechanism of action depends on its ability to prevent S100B/p53 interaction [132].

Like S100B, also GFAP is a marker of astrocyte activation making the control of its expression another possible therapeutic strategy, although the outcomes of this approach remain controversial.

Data reported in this paragraph, about molecules with various chemical structure and different mechanisms of action, converge in demonstrating that astrogliosis and neuroinflammation represent a valid target to design novel drugs.

2.6. Targeting the Complement System

The activation of the complement system as a consequence of neuronal damage has been well documented. Moreover, the observation that such system is activated after Aβ challenge and that the complement receptor 1 is regarded as a genetic AD risk factor suggest that the complement activation could be involved in AD etiopathogenesis and progression [133, 134]. The complement system counts more than 30 soluble factors that participate to the immune system functioning, through three different pathways (the classical, the alternative, and the lectin pathways) all culminating in the cleavage of C3 and subsequent release of the peptide C3a and the opsonin C3b [135]. Besides these immune activities, complement factors C3 and C1q are involved in the coordination of important CNS functions, including the microglia-driven synaptic remodeling and the neuronal survival and protection [135]. Lian and collaborators demonstrated that the C3 release from Nf-κB-activated astrocytes modifies neuronal morphology and synaptic function [134]. Indeed, astroglia-derived C3 through the interaction with the neuronal C3aR receptor allows a correct interaction between astrocytes and neurons, permitting the correct dendritic architecture and synaptic function [134]. NF-κB abnormal activation has been described in several neurological disorders including AD. In absence of pro-inflammatory insults, NF-κB is inactive because sequestered by its inhibitor protein IκB in the cytoplasm. Stimuli able to induce IκB degradation activate NF-κB cascade allowing its translocation into the nucleus where it promotes target genes transcription [136]. The abnormal activation of NF-κB/C3/C3aR pathway results in important modifications of the synaptic cytoarchitecture and brain functions. In line with this evidence, the blockade of C3aR rescues morphological and functional defects resulting from NF-κB aberrant activation, and almost completely restores cognitive impairments in APP transgenic mice [134]. These results are of great interest because they disclose new information about the intricate homeostatic interaction between neurons and glia, and provide novel and therapeutically suitable targets.

CONCLUSION

The data collected in this review support the hypothesis that astrocytes may represent a promising target for the development of new therapeutics. Involvement of astrocytes in the pathogenesis of AD is becoming increasingly studied. It is now clear that these cells physiologically control a plethora of essential functions that are modified or abolished in many neuropsychiatric disorders, including AD. Under these circumstances, astrocytes can turn into harmful cells. Despite the great scientific effort, there are still many issues that need to be clarified. These include astrocyte differences in properties among brain regions, and a better knowledge of cellular mechanisms that control the neuron-astrocyte interplay. Further investigation of these issues may suggest new drugs for AD treatment.

In conclusion, with this review we hope to have highlighted how important is the designing of novel pharmacological treatments that directly act on astrocytes in addition to neurons.

CONSENT FOR PUBLICATION

Not applicable.

CONFLICT OF INTEREST

Authors declare no conflict of interest. This work was supported by the SAPIENZA University Grant to CS (prot. C26A15X58E).

ACKNOWLEDGEMENTS

All authors contributed equally to the design and writing of this work contributing at both intellectual content and drafting the manuscript.

REFERENCES

[1] Prince M, Comas-Herrera A, Knapp M, *et al.* World Alzheimer Report 2016. Improving healthcare for people living with dementia: coverage, quality and costs now and in the future. Alzheimer's disease International 2016.

[2] Gaugler J, James B, Johnson T, *et al.* Alzheimer's Association 2015. Alzheimer's disease facts and figures. Alzheimer's Dementia 2015.

[3] Querfurth HW, LaFerla FM. Alzheimer's disease. N Engl J Med 2010; 362: 329-44.

[4] Osborn LM. Astrogliosis: An integral player in the pathogenesis of Alzheimer's disease. Prog Neurobiol 2016; 144: 121-41.

[5] Braak H, Braak E. Neuropil threads occur in dendrites of tangle-bearing nerve cells. Neuropathol Appl Neurobiol 1988; 14: 39-44.

[6] Merz P, Wisniewski H, Somerville R, *et al.* Ultrastructural morphology of amyloid fibrils from neuritic and amyloid plaques. Acta Neuropathol 1983; 60: 113-24.

[7] Akiyama H, Barger S, Barnum S, *et al.* Inflammation and Alzheimer's disease. Neurobiol Aging 2000; 21: 383-421.

[8] Verkhratsky A, Olabarria M, Noristani HN, *et al.* Astrocytes in Alzheimer's disease. Neurotherapeutics 2010; 7: 399-412.

[9] Maragakis NJ, Rothstein JD. Mechanisms of Disease: astrocytes in neurodegenerative disease. Nat Clin Pract Neurol 2006; 2: 679-89.

[10] Sofroniew MV. Molecular dissection of reactive astrogliosis and glial scar formation. Trends Neurosci 2009; 32: 638-47.

[11] García-Marín V, García-López P, Freire M. Cajal's contributions to glia research. Trends Neurosci 2007; 30: 479-787.

[12] Kettenmann H, Verkhratsky A. Neuroglia: the 150 years after. Trends Neurosci 2008; 31: 653-9.

[13] Verkhratsky A, Parpura V. Astroglia dynamics in ageing and Alzheimer's disease. Curr Opin Pharmacol 2016; 26: 74-9.

[14] Araque A, Carmignoto G, Haydon PG, *et al.* Gliotransmitters travel in time and space. Neuron 2014; 81: 728-39.

[15] Bernardinelli Y, Randall J, Janett E. *et al.* Activity-dependent structural plasticity of perisynaptic astrocytic domains promotes excitatory synapse stability. Curr Biol 2014; 24: 1679-88.

[16] Seifert G, Schilling K, Steinhauser C. Astrocyte dysfunction in neurological disorders: a molecular perspective. Nat Rev Neurosci 2006; 7: 194-206.

[17] Sattler R, Rothstein JD. Regulation and dysregulation of glutamate transporters. Handb Exp Pharmacol 2006; (175): 277-303.

[18] Agulhon C, Petravicz J, McMullen AB, *et al.* What is the role of astrocyte calcium in neurophysiology? Neuron 2008; 59: 932-46.

[19] Pannasch U, Vargova L, Reingruber J, *et al.* Astroglial networks scale synaptic activity and plasticity. Proc Natl Acad Sci 2011; 108: 8467-72.

[20] Christopherson KS, Ullian EM, Stokes CC, *et al.* Thrombospondins are astrocyte-secreted proteins that promote CNS synaptogenesis. Cell 2005; 120: 421-33.

[21] Pellerin L, Magistretti P. Glutamate uptake into astrocytes stimulates aerobic glycolysis: a mechanism coupling neuronal activity to glucose utilization. Proc Natl Acad Sci 1994; 91: 10625-9.

[22] Rothstein JD, Dykes-Hoberg M, Pardo CA, *et al.* Knockout of glutamate transporters reveals a major role for astroglial transport in excitotoxicity and clearance of glutamate. Neuron 1996; 16: 675-86.

[23] Yudkoff M, Nissim I, Pleasure D. Astrocyte metabolism of glutamine: implications for the glutamine-glutamate cycle. J Neurochem 1988; 51: 843-50.

[24] Wang DD, Bordey A. The astrocyte odyssey. Prog Neurobiol. 2008; 86: 342-67.

[25] Benarroch E. Neuron-astrocyte interactions: partnership for normal function and disease in the central nervous system. Mayo Foundation 2005; 80: 1326-38.

[26] Kayano T, Fukumoto H, Eddy RL, *et al.* Evidence for a family of human glucose transporter-like proteins. Sequence and gene local-

ization of a protein expressed in fetal skeletal muscle and other tissues. J Biol Chem 1988; 263: 15245-8.
[27] Gavillet M, Allaman I, Magistretti P. Modulation of astrocytic metabolic phenotype by proinflammatory cytokines. Glia 2008; 56: 975-89.
[28] Supplie LM, Düking T, Campbell G, *et al*. Respiration-deficient astrocytes survive as glycolytic cells in vivo. J Neurosci 2017.
[29] Alvarez J, Katayama T, Prat A. Glial influence on the blood brain barrier. Glia 2013; 61: 1939-58.
[30] Zonta M, Angulo MC, Gobbo S, *et al.* Neuron-to-astrocyte signaling is central to the dynamic control of brain microcirculation. Nat Neurosci 2003; 6: 43-50.
[31] Iliff JJ, Wang M, Liao Y, *et al.* A paravascular pathway facilitates CSF flow through the brain parenchyma and the clearance of interstitial solutes, including amyloid β. Sci Transl Med 2012; 4: 147ra111.
[32] Papadopoulos MC, Verkman AS. Aquaporin water channels in the nervous system. Nat Rev Neurosci 2013; 14: 265-77.
[33] Jessen NA, Munk ASF, Lundgaard I, *et al.* The glymphatic system-a beginner's guide. Neurochem Res 2015; 40: 2583-99.
[34] Shih AY, Erb H, Sun X, *et al.* Cysteine/glutamate exchanger modulates glutathione supply for neuroprotection from oxidative stress and cell proliferation. J Neurosci 2006; 26: 10514-23.
[35] Nedergaard M, Takano T, Hansen AJ. Beyond the role of glutamate as a neurotransmitter. Nat Rev Neurosci 2002; 3: 748-55.
[36] Lau LT, Yu AC. Astrocytes produce and release interleukin-1, interleukin-6, tumor necrosis factor alpha and interferon-gamma following traumatic and metabolic injury. J Neurotrauma 2001; 18: 351-9.
[37] Buffo A, Rolando C, Ceruti S. Astrocytes in the damaged brain: molecular and cellular insights into their reactive response and healing potential. Biochem Pharmacol 2010; 79: 77-89.
[38] Rodriguez-Arellano JJ, Parpura V, Zorec R, *et al.* Astrocytes in physiological aging and Alzheimer's disease. Neuroscience 2016; 323: 170-82.
[39] Dallérac G, Rouach N. Astrocytes as new targets to improve cognitive functions. Prog Neurobiol 2016; 144: 48-67.
[40] Attwell D, Buchan AM, Charpak S, *et al.* Glial and neuronal control of brain blood flow. Nature 2010; 468: 232-43.
[41] Halassa MM, Haydon PG. Integrated brain circuits: astrocytic networks modulate neuronal activity and behavior. Annu Rev Physiol 2010; 72: 335-55.
[42] Walsh DM, Selkoe DJ. Deciphering the molecular basis of memory failure in Alzheimer's disease. Neuron 2004; 44: 181-93.
[43] Sastre M, Klockgetherm T, Henekam MT. Contribution of inflammatory processes to Alzheimer's disease: molecular mechanisms. Int J Dev Neurosci 2006; 24: 167-76.
[44] Itagaki S, McGeer PL, Akiyama H, Zhu S, Selkoe D. Relationship of microglia and astrocytes to amyloid deposits of Alzheimer disease. J Neuroimmunol 1989; 24: 173-82.
[45] Streit W J, Xue Q S, Tischer J, Bechmann I. Microglial pathology. Acta Neuropathol Commun 2014; 2: 142.
[46] Allaman I, Gavillet M, Bélanger M, *et al.* Amyloid-beta aggregates cause alterations of astrocytic metabolic phenotype: impact on neuronal viability. J Neurosci 2010; 30: 3326-38.
[47] Kanekiyo T, Xu H, Bu G. ApoE and Aβ in Alzheimer's disease: accidental encounters or partners? Neuron 2014; 81: 740-54.
[48] Ben Haim L, Ceyzériat K, Carrillo-de Sauvage MA, *et al.* The JAK/STAT3 pathway is a common inducer of astrocyte reactivity in Alzheimer's and Huntington's diseases. J Neurosci 2015; 35: 2817-29.
[49] Femminella G, Nicola Ferrara N, Rengo G. The emerging role of microRNAs in Alzheimer's disease. Front Physiol 2015; 6: 40.
[50] Danbolt NC, Glutamate uptake. Prog Neurobiol 2001; 65: 1-105.
[51] Tanaka K, Watase K, Manabe T, *et al.* Epilepsy and exacerbation of brain injury in mice lacking the glutamate transporter GLT-1. Science 1997; 276: 1699-702.
[52] Olabarria M, Noristani HN, Verkhratsky A, *et al.* Age-dependent decrease in glutamine synthetase expression in the hippocampal astroglia of the triple transgenic Alzheimer's disease mouse model: mechanism for deficient glutamatergic transmission? Mol Neurodegener 2011; 6: 55.
[53] Diniz B, Teixeira A, Machado-Vieira R, *et al.* Reduced cerebrospinal fluid levels of brain-derived neurotrophic factor is associated with cognitive impairment in late-life major depression. J Gerontol B Psychol Sci Soc Sci 2014; 69: 845-51.
[54] Wyss-Coray T. Inflammation in Alzheimer disease: driving force, bystander or beneficial response? Nat Med 2006; 12: 1005-15.
[55] Butt A, Kalsi A. Inwardly rectifying potassium channels (Kir) in central nervous system glia: a special role for Kir4.1 in glial functions. J Cell Mol Med 2006; 10: 33-44.
[56] Hibino H, Inanobe A, Furutani K. Inwardly rectifying potassium channels: their structure, function, and physiological roles. Physiol Rev 2010; 90: 291-366.
[57] Kucheryavykh YV, Kucheryavykh LY, Nichols CG, *et al.* Downregulation of Kir4.1 inward rectifying potassium channel subunits by RNAi impairs potassium transfer and glutamate uptake by cortical astrocytes. Glia 2007; 55: 274-81.
[58] Aoki C. β-Adrenergic receptors: Astrocytic localization in the adult visual cortex and their relation to catecholamine axon terminals as revealed by electron microscopic immunocytochemistry. J. Neurosci 1992; 12: 781-92.
[59] Vardjan N, Verkhratsky A, Zorec R. Calcium Homeostasis and Impaired Vesicle Trafficking in Neurodegeneration. Int J Mol Sci 2017; 18.
[60] Gannon M, Che P, Chen Y, Jiao K, Roberson ED, Wang Q. Noradrenergic dysfunction in Alzheimer's disease. Front Neurosci 2015; 9: 220.
[61] Delekate A, Füchtemeier M, Toni Schumacher T, *et al.* Metabotropic P2Y1 receptor signaling mediates astrocytic hyperactivity in vivo in an Alzheimer's disease mouse model. Nat Commun 2014; 5: 5422.
[62] Kalaria RN. The role of cerebral ischemia in Alzheimer's disease. Neurobiol Aging 2000; 21: 321-30.
[63] Zlokovic B, Rashid D, Sallstrom J, *et al.* Neurovascular pathways and Alzheimer amyloid β-peptide. Brain Pathol 2005; 15: 78-83.
[64] Kraft AW, Hu X, Yoon H, *et al.* Attenuating astrocyte activation accelerates plaque pathogenesis in APP/PS1 mice. FASEB J 2013; 27: 187-98.
[65] Nagele RG, Wegiel J, Venkataraman V, *et al.* Contribution of glial cells to the development of amyloid plaques in Alzheimer's disease. Neurobiol Aging 2004; 25: 663-74.
[66] Donato R, Heizmann CW. S100B protein in the nervous system and cardiovascular apparatus in normal and pathological conditions. Cardiovasc Psychiatry Neurol 2010; 2010: 929712.
[67] Steiner J, Bogerts B, Schroeter ML, *et al.* S100B protein in neurodegenerative disorders. Clin Chem Lab Med 2011; 49: 409-24.
[68] Scuderi C, Stecca C, Valenza M*, et al.* Palmitoylethanolamide controls reactive gliosis and exerts neuroprotective functions in a rat model of Alzheimer's disease. Cell Death Dis 2014; 5: e1419.
[69] Heneka MT, O'Banion MK, Terwel D, *et al.* Neuroinflammatory processes in Alzheimer's disease. J Neural Transm (Vienna) 2010; 117: 919-47.
[70] Olabarria M, Noristani HN, Verkhratsky A, Rodríguez JJ. Concomitant astroglial atrophy and astrogliosis in a triple transgenic animal model of Alzheimer's disease. Glia 2010; 58: 831-8.
[71] Beauquis J, Pavia P, Pomilio C, *et al*. Environmental enrichment prevents astroglial pathological changes in the hippocampus of APP transgenic mice, model of Alzheimer's disease. Exp Neurol 2013; 239: 28-37.
[72] Rodríguez-Arellano JJ, Parpura V, Zorec R, Verkhratsky A. Astrocytes in physiological aging and Alzheimer's disease. Neuroscience 2016; 323: 170-82.
[73] Steardo L Jr, Bronzuoli MR, Iacomino A, *et al.* Does neuroinflammation turn on the flame in Alzheimer's disease? Focus on astrocytes. Front Neurosci 2015; 9: 259.
[74] Hu W, Ralay Ranaivo H, Roy SM, *et al.* Development of a novel therapeutic suppressor of brain proinflammatory cytokine upregulation that attenuates synaptic dysfunction and behavioral deficits. Bioorg Med Chem Lett 2007; 17: 414-18.
[75] Toro CT, Deakin JFW. Adult neurogenesis and schizophrenia: a window on early brain development? Schizophrenia Res 2006; 90: 1-14.

[76] Hazell AS. Excitotoxic mechanisms and the role of astrocytic glutamate transporters in traumatic brain injury. Neurochem Int 2006; 48: 394-403.

[77] Ji HF, Shen L, Zhang HY. Beta-lactam antibiotics are multipotent agents to combat neurological diseases. Biochem Biophys Res Commun. 2005; 333: 661-3.

[78] Lee R, Walker S, Savery K, *et al*. Fold change of nuclear NF-κB determines TNF-induced transcription in single cells. Molecular Cell 2014; 53: 867-79.

[79] Furman J, Sama D, Gant J. Targeting astrocytes ameliorates neurologic changes in a mouse model of Alzheimer's disease. J Neurosci 2013; 32: 16129-40.

[80] Foust KD, Nurre E, Montgomery CL, *et al.* Intravascular AAV9 preferentially targets neonatal neurons and adult astrocytes. Nat Biotechnol 2009; 27: 59-65.

[81] Furman J, Sompol P, Kraner S, *et al*. Blockade of astrocytic calcineurin/NFAT signaling helps to normalize hippocampal synaptic function and plasticity in a rat model of traumatic brain injury. J Neurosci 2016; 36: 1502-15.

[82] Filous A, Silver J. Targeting astrocytes in CNS injury and disease: a translational research approach. Prog Neurobiol 2016; 144: 173-87.

[83] Filous A, Miller J, Coulson-Thomas Y, *et al.* Immature astrocytes promote CNS axonal regeneration when combined with chondroitinase ABC. Dev Neurobiol 2010; 70: 826-41.

[84] White R, Rao M, Gensel J, *et al.* Transforming growth factor α transforms astrocytes to a growth-supportive phenotype after spinal cord injury. J Neurosci 2011; 31: 15173-87.

[85] Fassler M, Weissberg I, Levy N, *et al*. Preferential lentiviral targeting of astrocytes in the central nervous system. PLoS One 2013; 8: e76092.

[86] Hensley K, Robinson K, Gabbita S, *et al.* Reactive oxygen species, cell signaling, and cell injury. Free Radic Biol Med 2000; 28: 1456-62.

[87] Babior B. NADPH oxidase: an update. Blood 1999; 93: 1464-76.

[88] Fuller S, Steele M, Münch G. Activated astroglia during chronic inflammation in Alzheimer's disease-do they neglect their neurosupportive roles? Mutat Res 2010; 690: 40-9.

[89] Crespo MC, Tomé-Carneiro J, Pintado C, Dávalos A, Visioli F, Burgos-Ramos E. Hydroxytyrosol restores proper insulin signaling in an astrocytic model of Alzheimer's disease. Biofactors 2017.

[90] Holland J, O'Donnell R, Chang M, *et al.* Endothelial cell oxidant production: effect of NADPH oxidase inhibitors, Endothelium: 2000; 7(2): 109-19.

[91] Pahan K, Sheikh F, Namboodiri A, *et al*. Inhibitors of protein phosphatase 1 and 2A differentially regulate the expression of inducible nitric-oxide synthase in rat astrocytes and macrophages. J Biol Chem 1998; 273: 12219-26.

[92] Rempe DA, Nedergaard M. Targeting glia for treatment of neurological disease. Neurotherapeutics 2010; 7: 335-7.

[93] Markiewicz I, Lukomska B. The role of astrocytes in the physiology and pathology of the central nervous system. Acta Neurobiol Exp 2006; 66: 343-58.

[94] Jana A, Modi K, Roy A, *et al.* Up-regulation of neurotrophic factors by cinnamon and its metabolite sodium benzoate: therapeutic implications for neurodegenerative disorders. J Neuroimmune Pharmacol 2013; 8: 739-55.

[95] Butler R, Bates GP. Histone deacetylase inhibitors as therapeutics for polyglutamine disorders. Nat Rev Neurosci 2006; 7: 784-96.

[96] Corbett G, Roy A, Pahan K. Sodium phenylbutyrate enhances astrocytic neurotrophin synthesis via protein kinase C (PKC)-mediated activation of cAMP-response element-binding protein (CREB). J Biol Chem 2013; 288(12): 8299-312.

[97] Sofroniew MV, Vinters HV. Astrocytes: biology and pathology. Acta Neuropathol 2010; 1190 : 7-35.

[98] Burda JE, Sofroniew MV. Reactive gliosis and the multicellular response to CNS damage and disease. Neuron 2014; 81: 229-48.

[99] Kamphuis W, Kooijman L, Orre M, Stassen O, Pekny M, Hol EM. GFAP and vimentin deficiency alters gene expression in astrocytes and microglia in wild-type mice and changes the transcriptional response of reactive glia in mouse model for Alzheimer's disease. Glia 2015; 63 : 1036-56.

[100] Duncan RS, Chapman KD, Koulen P. The neuroprotective properties of palmitoylethanolamine against oxidative stress in a neuronal cell line. Mol Neurodegener 2009; 4: 50.

[101] LoVerme J, Russo R, La Rana G. Rapid broad-spectrum analgesia through activation of peroxisome proliferator-activated receptor-alpha. J Pharmacol Exp Ther 2006; 319: 1051-61.

[102] Calignano A, La Rana G, Giuffrida A. Control of pain initiation by endogenous cannabinoids. Nature 1998; 394: 277-81.

[103] Skaper SD, Buriani A, Dal Toso R, *et al.* The ALIAmide palmitoylethanolamide and cannabinoids, but not anandamide, are protective in a delayed postglutamate paradigm of excitotoxic death in cerebellar granule neurons. Proc Natl Acad Sci USA 1996; 93: 3984-9.

[104] LoVerme J, La Rana G, Russo R, *et al*. The search for the palmitoylethanolamide receptor. Life Sci 2005; 77: 1685-98.

[105] Mackie K, Stella N. Cannabinoid receptors and endocannabinoids: evidence for new players. AAPS J 2006; 8: E298-306.

[106] Scuderi C, Valenza M, Stecca C, Esposito G, Carratù MR, SteardoL. Palmitoylethanolamide exerts neuroprotective effects in mixed neuroglial cultures and organotypic hippocampal slices via peroxisome proliferator-activated receptor-α. J Neuroinflammation 2012; 9: 49.

[107] Muccioli GG, Stella N. Microglia produce and hydrolyze palmitoylethanolamide. Neuropharmacology 2008; 54(1): 16-22.

[108] Skaper SD, Facci L, Giusti P. Mast cells, glia and neuroinflammation: partners in crime? Immunology 2014; 141(3): 314-27.

[109] Calignano A, La Rana G, Piomelli D, Antinociceptive activity of the endogenous fatty acid amide, palmitoylethanolamide. Eur J Pharmacol 2001; 419: 191-8.

[110] Franklin A, Parmentier-Batteur S, Walter L, *et al.* Palmitoylethanolamide increases after focal cerebral ischemia and potentiates microglial cell motility. J Neurosci 2003; 23: 7767-75.

[111] Scuderi C, Esposito G, Blasio A, *et al.* Palmitoylethanolamide counteracts reactive astrogliosis induced by β-amyloid peptide. J Cell Mol Med 2011; 15: 2664-74.

[112] Gan L, Mucke L. Paths of convergence: sirtuins in aging and neurodegeneration. Neuron 2008; 58: 10-4.

[113] Scuderi C, Stecca C, Bronzuoli MR, *et al*. Sirtuin modulators control reactive gliosis in an in vitro model of Alzheimer's disease. Frontiers in Pharmacology. 2014; 5: 89.

[114] Shroder K, Tschopp J. The inflammasomes. Cell 2010; 140: 821-32.

[115] Lamkanfi M, Dixit VM. Mechanisms and functions of inflammasomes. Cell 2014; 157: 1013-22.

[116] Walsh JG, Muruve DA, Power C. Inflammasomes in the CNS. Nat Rev Neurosci 2014; 15: 84-97.

[117] Allan S, Tyrrel P. Interleukin-1 and neuronal injury. Nat Rev Immunol 2005; 5: 629-40.

[118] John GR, Lee SC, Song X, *et al.* IL-1-regulated responses in astrocytes: relevance to injury and recovery. Glia 2005; 49: 161-76.

[119] Halle A, Hornung V, Petzold GC, *et al.* The NALP3 inflammasome is involved in the innate immune response to amyloid-beta. Nat Immunol 2008; 9: 857-65.

[120] Rothwell NJ, Luheshi GN. Interleukin 1 in the brain: biology, pathology and therapeutic target. Trends Neurosci 2000; 23: 618-25.

[121] Urrutia PJ, Hirsch EC, González-Billault C, Núñez MT. Hepcidin attenuates amyloid beta-induced inflammatory and pro-oxidant responses in astrocytes and microglia. J Neurochem 2017.

[122] Liu L, Chan C. IPAF inflammasome is involved in interleukin-1beta production from astrocytes, induced by palmitate; implications for Alzheimer's disease. Neurobiol Aging 2014; 35: 309-21.

[123] Couturier J, Stancu I, Schakman O, *et al.* Octave Activation of phagocytic activity in astrocytes by reduced expression of the inflammasome component ASC and its implication in a mouse model of Alzheimer disease. J Neuroinflam 2016; 13: 20.

[124] Mrak RE, Griffin WS. Interleukin-1, neuroinflammation, and Alzheimer's disease. Neurobiol Aging 2001; 22: 903-8.

[125] Leoutsakos J-MS, Muthen BO, Breitner JCS, *et al.* Effects of nonsteroidal anti-inflammatory drug treatments on cognitive decline vary by phase of pre-clinical Alzheimer disease: findings from the randomized controlled Alzheimer's disease anti-inflammatory prevention trial. Int J Geriatr Psychiatry 2012; 27: 364-74.

[126] Bachstetter A, Norris C, Sompol P, *et al.* Early stage drug treatment that normalizes proinflammatory cytokine production attenuates synaptic dysfunction in a mouse model that exhibits age-dependent progression of Alzheimer's disease-related pathology. J Neurosci 2012; 32: 10201-10.

[127] Pekny M, Wilhelmsson U, Pekna M. The dual role of astrocyte activation and reactive gliosis. Neurosci. Lett 2014: 565: 30-8.

[128] Eldik LJ, Wainwright MS. The Janus face of glial-derived S100B: beneficial and detrimental functions in the brain. Restor Neurol Neurosc 2003; 21: 97-10.

[129] Sheng JG, Mrak RE, Griffin WST. S100beta protein expression in Alzheimer disease: potential role in the pathogenesis of neuritic plaques. J Neurosci Res 1994; 39(4): 398-404.

[130] Drake S, Lampasona V, Nicks HL, *et al.* Pentamidine isethionate in the treatment of Pneumocystis carinii pneumonia. Clin Pharm 1985; 4: 507-16.

[131] Cirillo C, Capoccia E, Iuvone T, *et al.* S100B inhibitor pentamidine attenuates reactive gliosis and reduces neuronal loss in a mouse model of Alzheimer's disease. Biomed Res Int 2015; 2015: 508342.

[132] Hartman KG, Mcknight LE, Liriano MA, *et al*. The evolution of S100B inhibitors for the treatment of malignant melanoma. Future Med Chem 2013; 5: 97-109.

[133] Crehan H, Holton P, Wray S, *et al.* Complement receptor 1 (CR1) and Alzheimer's disease, Immunobiology. 2012; 217: 244-50.

[134] Lian H, Yang L, Cole A, *et al.* NFκB-activated astroglial release of complement C3 compromises neuronal morphology and function associated with Alzheimer's disease. Neuron 2015; 85: 101-15.

[135] Benoit ME, Tenner AJ. Complement protein C1q-mediated neuroprotection is correlated with regulation of neuronal gene and microRNA expression J Neurosci 2011; 31: 3459-69.

[136] Oeckinghaus A, Ghosh S. The NF-kappaB family of transcription factors and its regulation, Cold Spring Harb Perspect Biol 2009; 1: a000034.

Hindawi
Oxidative Medicine and Cellular Longevity
Volume 2018, Article ID 4720532, 14 pages
https://doi.org/10.1155/2018/4720532

Research Article

Palmitoylethanolamide Dampens Reactive Astrogliosis and Improves Neuronal Trophic Support in a Triple Transgenic Model of Alzheimer's Disease: *In Vitro* and *In Vivo* Evidence

Maria Rosanna Bronzuoli,[1] Roberta Facchinetti,[1] Luca Steardo Jr.,[2] Adele Romano,[1] Claudia Stecca,[1] Sergio Passarella,[1] Luca Steardo,[1] Tommaso Cassano,[3] and Caterina Scuderi[1]

[1]*Department of Physiology and Pharmacology "V. Erspamer", Sapienza University of Rome, Rome, Italy*
[2]*Department of Psychiatry, University of Naples SUN, Naples, Italy*
[3]*Department of Clinical and Experimental Medicine, University of Foggia, Foggia, Italy*

Correspondence should be addressed to Tommaso Cassano; tommaso.cassano@unifg.it

Received 25 May 2017; Revised 2 October 2017; Accepted 23 October 2017; Published 16 January 2018

Academic Editor: Bruno Meloni

Alzheimer's disease (AD) is a neurodegenerative disorder responsible for the majority of dementia cases in elderly people. It is widely accepted that the main hallmarks of AD are not only senile plaques and neurofibrillary tangles but also reactive astrogliosis, which often precedes detrimental deposits and neuronal atrophy. Such phenomenon facilitates the regeneration of neural networks; however, under some circumstances, like in AD, reactive astrogliosis is detrimental, depriving neurons of the homeostatic support, thus contributing to neuronal loss. We investigated the presence of reactive astrogliosis in 3×Tg-AD mice and the effects of palmitoylethanolamide (PEA), a well-documented anti-inflammatory molecule, by *in vitro* and *in vivo* studies. *In vitro* results revealed a basal reactive state in primary cortical 3×Tg-AD-derived astrocytes and the ability of PEA to counteract such phenomenon and improve viability of 3×Tg-AD-derived neurons. *In vivo* observations, performed using ultramicronized- (um-) PEA, a formulation endowed with best bioavailability, confirmed the efficacy of this compound. Moreover, the schedule of treatment, mimicking the clinic use (chronic daily administration), revealed its beneficial pharmacological properties in dampening reactive astrogliosis and promoting the glial neurosupportive function. Collectively, our results encourage further investigation on PEA effects, suggesting it as an alternative or adjunct treatment approach for innovative AD therapy.

1. Introduction

Alzheimer's disease (AD) accounts for more than 80% of dementia cases worldwide in elderly people and leads to the progressive loss of mental, behavioral, and learning abilities and to functional decline [1]. Histopathologically, AD is characterized by two major protein deposits affecting mainly hippocampal and cortical regions: extracellular neuritic β-amyloid peptide (Aβ), which induces the creation of senile plaques (SPs), and the production of intracellular neurofibrillary tangles (NFTs) due to tau hyperphosphorylation that occupies much of the cytoplasm of pyramidal neurons [2, 3]. The presence of abnormally activated microglia and astrocytes is a feature of AD of more recent discovery [4]. It is followed by an intense inflammation, closely associated with amyloid deposits in the brain parenchyma [4, 5]. Indeed, studies of post mortem brain tissues from AD patients demonstrated the presence of a generalized astrogliosis, mainly manifested by astrocytic dysfunction, detectable by an increased expression of both glial fibrillary acidic protein (GFAP) and S100B, and accompanied by an increased production of proinflammatory mediators [6]. Many authors name this complex phenomenon as reactive astrogliosis [6, 7]. GFAP is a specific cytoskeletal

marker, whose expression is higher during astrogliosis [8]. S100B is a neurotrophin that, at physiological concentrations (nanomolar), exerts prosurvival effects on neurons and stimulates neurite outgrowth [9]. However, at higher (micromolar) concentrations, S100B becomes neurotoxic, promoting inflammation and neuronal apoptosis [10]. Aβ itself induces the expression of proinflammatory cytokines by glial cells [11] and the induction of proinflammatory enzymes, such as the inducible nitric oxide synthase (iNOS) and the isoenzyme cyclooxygenase type-2 (COX-2). Several lines of evidence suggest that all these factors may contribute to neuronal dysfunction and cell death, either alone or in concert [12]. The reactive astrogliosis has the initial intent of defence of removing injurious stimuli. However, if this phenomenon goes beyond physiological control, it may cause several detrimental effects. Under these circumstances, both neuronal and synaptic loss are detectable, because structural and functional modifications of neurons and astrocytes occur [13, 14]. Alterations of the neuronal marker microtubule-associated protein 2 (MAP-2), as well as modifications of the neurotrophin brain-derived neurotrophic factor (BDNF) content, have also been demonstrated [15, 16]. Considering the crucial actions of BDNF, especially in controlling neuronal survival, differentiation, neurotransmitter release, dendritic remodeling, axon growth, and synaptic plasticity [17, 18], the detrimental consequences of its alterations by reactive astrogliosis may be dramatic.

Based on this evidence, it is reasonable to assume that an early combination of neuroprotective and anti-inflammatory treatments may represent an efficacious approach to counteract AD. In this context, palmitoylethanolamide (PEA), an endogenous lipid mediator, seems to be a promising pharmacological agent. The anti-inflammatory and neuroprotective effects of PEA, as well as its ability to attenuate memory impairment in surgical models of AD, have already been demonstrated [15, 19–22].

In this work, we provide novel evidence on the ability of PEA to counteract reactive astrogliosis and neuronal impairment both *in vitro* and *in vivo*. For the *in vitro* studies, we used primary cortical neurons and astrocytes from 3×Tg-AD mice, a triple transgenic model of AD currently considered the closest to the familial human disease, and from wild-type littermates (non-Tg). The same AD model was used for the *in vivo* experiments, in which male 3-month-old 3×Tg-AD and sex- and age-matched non-Tg mice were subcutaneously implanted with a pellet, releasing either ultramicronized-PEA (um-PEA) or placebo, for three months. This treatment schedule was designed to reproduce a chronic treatment (as needed for this type of disease), administered starting from the early stage of the AD pathology.

In vitro results highlighted an intense activation and inflammation in primary 3×Tg-AD astrocytes, as well as the ability of PEA to counteract them and promote neuronal viability. Moreover, *in vivo* biochemical experiments demonstrated that chronic um-PEA treatment resulted in a beneficial control of the astrocyte activation and neuroinflammation. In addition, um-PEA interestingly increased BDNF levels, confirming its neuroprotective/neurotrophic effects.

Our results confirm the therapeutic potential of PEA, demonstrating its ability to counteract some of the detrimental effects occurring in AD, since the earliest stage of the pathology. PEA is already on the market for the treatment of pain. Therefore, these observations, in addition to the information regarding its safety and tolerability also in humans, prompt us to hypothesize a rapid translation into clinical practice.

2. Materials and Methods

All the procedures involving animals were conducted in conformity with the guidelines of the Italian Ministry of Health (D.L. 26/2014) and performed in compliance with the European Parliament directive 2010/63/EU.

2.1. Animals and Experimental Design. 3×Tg-AD mice [23] expressing APP_{swe}, $PS1_{M146V}$, and tau_{P301L} human transgenes were compared to non-Tg littermates. The background strain of 3×Tg-AD mice was C57BL6/129SvJ hybrid [23]. Animals were group housed and raised in controlled conditions ($22 \pm 2^{\circ}$C temperature, 12 h light/12 h dark cycle, 50%–60% humidity) in an enriched environment, with food and water ad libitum.

For *in vitro* experiments, we used newborn mice at postnatal day (PND) 1 or 2. Astrocytes were isolated from both non-Tg (total pups used = 12) and 3×Tg-AD (total pups used = 24) mice. Neurons were isolated from 3×Tg-AD mice (total pups used = 12).

For *in vivo* experiments, 3-month-old male non-Tg ($n = 18$) and 3×Tg-AD ($n = 18$) mice were used. Animals were surgically implanted with a 90-day-release pellet containing either 28 mg um-PEA, a formulation that improves its bioavailability [24], or placebo (catalogue number NX-999 and NC-111, resp.; Epitech Group SpA). Both pellets were made by Innovative Research of America (Sarasota, Florida) that homogeneously distributed um-PEA in the matrix, keeping its original crystalline form of micrometric size. Therefore, mice received 10 mg/kg/day for 3 consecutive months. Experimental dosage was chosen according to literature [25, 26].

To subcutaneously implant the pellet, mice were anesthetized with ketamine hydrochloride (1 mg/10 g) and xylazine (0.1 mg/10 g). After shaving the shoulder blades, the implantation area was sterilized with 70% alcohol. A dorsal midline incision of 1-2 cm was executed to create a subcutaneous pocket with a blunt probe. One pellet, containing um-PEA or placebo, was placed into the pocket and the surgical incision was closed with sterile absorbable sutures. Non-Tg and 3×Tg-AD mice were then left in their home cages for the next three months, and their weight monitored daily. No weight differences among all experimental groups were detected (data not shown). At the end of the chronic treatment, 6-month-old mice were killed by decapitation, and their brains were rapidly excised and either immediately frozen on dry ice for the immunofluorescence experiments or freshly dissected

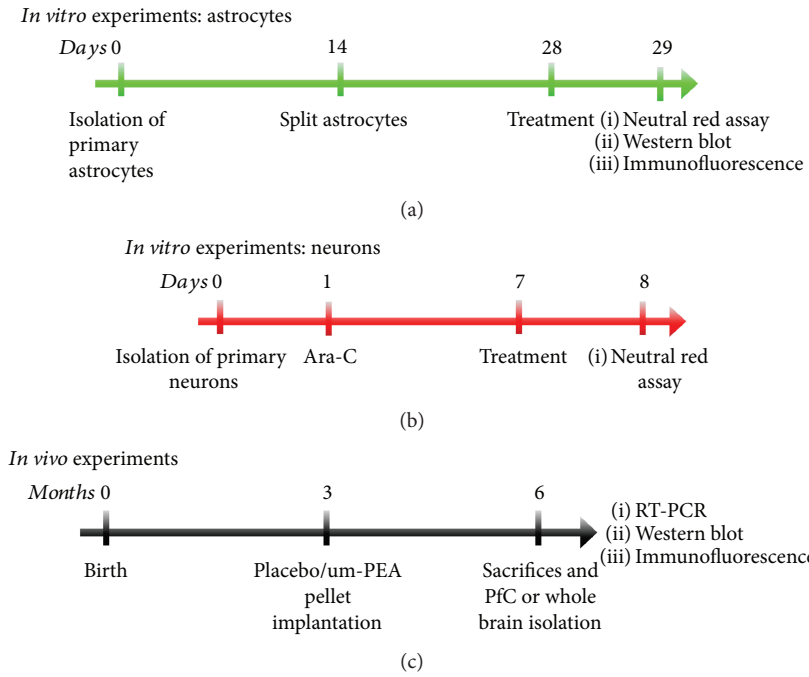

Figure 1: Study designs. Schematic representation of the experimental designs in (a) primary 3×Tg-AD and non-Tg astrocytes, (b) primary 3×Tg-AD neurons, and (c) *in vivo* experiments in 3×Tg-AD and non-Tg mice.

to isolate the frontal cortex (FC) for RT-PCR and Western blot analyses.

The experimental timelines are summarized in Figure 1.

2.2. Astroglial Primary Cultures. Astroglial primary cultures were obtained as previously described [27]. Cortices were isolated from non-Tg and 3×Tg-AD newborn mice (PND 1 or 2) sacrificed by decapitation. Tissues were manually homogenized in Dulbecco's modified Eagle's medium (DMEM) supplemented with 5% inactivated fetal bovine serum (FBS), 100 U/ml penicillin and 100 μg/ml streptomycin and then chemically dissociated with a solution containing 0.25% trypsin, 0.2% ethylenediaminetetraacetic acid (EDTA), and 0.2 mg/ml of DNAse I (all from Sigma-Aldrich, Milan, Italy) to obtain single cells. After a centrifugation at 403 ×g for 5 minutes, the medium was replaced, and surviving cells were counted using a Burker chamber with a 0.2% trypan blue solution and seeded at a density of 3×10^{-6} cells/75 cm^2 flask. Cell cultures were at +37°C in humidified atmosphere containing 5% CO_2. DMEM supplemented with 20% inactivated FBS and 100 U/ml penicillin, and 100 μg/ml streptomycin was replaced 24 h and one week after isolation. Approximately 14-15 days after the dissection, when a monolayer of cells was created, astrocytes were separated from microglia by mechanical shacking. Then, astrocytes were detached from the plates with a solution containing 0.25% trypsin and 0.2% EDTA and then seeded into 10 cm diameter petri dishes at a density of 1×10^6 cells/dish for Western blot analysis, into eight chambers polystyrene culture slides at a density of 3×10^4 cells/chamber (Thermo Fisher Scientific, MA, USA) for immunofluorescence, or into 24-well plates at a density of 1×10^5 cells/well for neutral red viability assay. Experiments were performed 28 days after cells isolation, when astrocytes are considered completely mature [22].

2.3. Neuronal Primary Cultures. Cortices from newborn 3×Tg-AD mice (PND 1 or 2) were used to obtain primary neuronal cultures as previously described [20]. Multiwells were previously coated with poly-L-lysine (Sigma-Aldrich) to allow neurons to adhere to the bottom of the wells. Mice were sacrificed by decapitation and cerebral cortices dissected in Hank's balanced salt solution (HBSS) containing 25 mM 4-(2-hydroxyethyl)-1-piperazineethanesulfonic acid (Hepes), 100 U/ml penicillin, and 100 μg/ml of streptomycin in cold conditions. Tissues were mechanically and chemically homogenized in a solution containing 0.25% trypsin, 0.2% EDTA, and 0.2 mg/ml of DNAse I (all from Sigma). After a centrifugation at 403 ×g for 5 minutes, cells were suspended in neurobasal media supplemented with 2% B27, 100 U/ml penicillin, and 100 μg/ml streptomycin. Then, they were counted using a Burker chamber while suspended in 0.2% trypan blue solution and then seeded in 24-well multiplates at a density of 5×10^{-5} cells/well. Neuronal cultures were maintained at +37°C in humidified atmosphere containing 5% CO_2. Twenty-four hours later, cells were treated with 10 μM of cytosine arabinoside (ara-C) to suppress glial cell growth. One week later, primary 3×Tg-AD-derived neurons were treated with PEA.

2.4. Chemicals and Cell Treatments. Mature astrocytes and neurons derived from 3×Tg-AD mice were treated with PEA (Epitech Group SpA, Saccolongo, Italy), at three different concentrations (0.01, 0.1, and 1 μM), chosen according to our previous works [19, 20, 22]. PEA was suspended in 5% pluronic F-68 (Sigma-Aldrich) and solubilized in 95%

Table 1: Experimental conditions for immunofluorescence.

Primary antibody	Brand primary antibody	Primary antibody dilution	Secondary antibody	Brand secondary antibody
Rabbit α-GFAP	Abcam	1 : 1000 0.5% BSA in TBS/0.25% triton X-100	FITC conjugated goat anti-rabbit IgG (H+L) 1 : 200, 0.5% BSA in TBS/0.25% triton X-100	Jackson ImmunoResearch
Rabbit α-S100B	Novus Biologicals	1 : 250 0.5% BSA in TBS/0.25% triton X-100	TRITC conjugated goat anti-rabbit IgG (H+L) 1 : 200, 0.5% BSA in TBS/0.25% triton X-100	Jackson ImmunoResearch
Mouse α-MAP2	Novus Biologicals	1 : 250 0.5% BSA in TBS/0.25% triton X-100	TRITC conjugated goat anti-mouse IgG (H+L) 1 : 200, 0.5% BSA in TBS/0.25% triton X-100	Jackson ImmunoResearch

DMEM. First, we added pluronic F-68 to PEA powder and sonicated the emulsion for 20 min protecting it from light, and then we included DMEM to complete the solution. Viability assay, Western blot analysis, and immunofluorescence were performed 24 h after treatments.

2.5. Analysis of Astrocyte and Neuronal Viability by Neutral Red Uptake Assay. Astrocyte and neuronal viability was tested 24 h after treatment by neutral red uptake assay, as previously described [27]. Cells were incubated with a neutral red working solution, containing 50 μg/ml in Ca^{2+} and Mg^{2}-free PBS (Sigma-Aldrich), for 3 h at +37°C. Cells were then rinsed in Ca^{2+}- and Mg^{2}-free PBS and the dye removed from the inside of the cells through a rinse in destaining solution (ethanol : deionized water : glacial acetic acid, 50 : 49 : 1 *v*/*v*). The absorbance, whose value is proportional to the number of living cells, was read at 540 nm using a microplate spectrophotometer (Epoch, BioTek, Winooski, VT, USA). The values obtained were referred to control medium-exposed cultures (CTRL) and expressed as percentage variation of CTRL. Three independent experiments were performed in triplicate.

2.6. Immunofluorescence. Both primary astrocytes, 24 h after treatment, and non-Tg and 3×Tg-AD coronal slices (12 μm thickness), deriving from 6-month-old mice containing the FC, were rinsed in PBS and postfixed for 10 minutes at +4°C with 4% paraformaldehyde (PFA) prepared in PBS. Then, samples were blocked with 1% bovine serum albumin (BSA) prepared in PBS/0.25% triton X-100 for 90 minutes at room temperature. Cells were incubated overnight at +4°C in 0.5% BSA in Tris-buffered saline (TBS)/0.25% triton X-100 solution containing the primary antibodies rabbit anti-GFAP (1 : 1000, Abcam, Cambridge, USA) or rabbit anti-S100B (1 : 250, Novus Biologicals, Littleton, CO, USA). FC slices, instead, were incubated overnight at +4°C with mouse anti-MAP2 (1 : 250, Novus Biologicals, Littleton, CO, USA) in 0.5% BSA in TBS/0.25% triton X-100 solution. The following day, cells and tissues were thoroughly rinsed in PBS and then incubated for 2 hours at room temperature with the appropriate secondary antibody (fluorescein- (FITC-) conjugated AffiniPure goat anti-rabbit IgG (H+L), rhodamine- (TRITC-) conjugated AffiniPure goat anti-rabbit IgG (H+L), 1 : 200, or rhodamine- (TRITC-) conjugated AffiniPure goat anti-mouse IgG (H+L); Jackson ImmunoResearch, Suffolk, UK). Nuclei were stained with 4′,6-diamidino-2-phenylindole, dihydrochloride (DAPI) (1 : 75000, Sigma-Aldrich) in 0.5% BSA in TBS/0.25% triton X-100, added to the solution of the secondary antibodies. Samples were rinsed with PBS and coverslipped using Fluoromount aqueous mounting medium (Sigma-Aldrich). Experimental conditions are summarized in Table 1.

Pictures were captured with a wide-field microscope (Eclipse E600; Nikon Instruments, Rome, Italy) and densitometric analysis performed using ImageJ software. Data are expressed as ratio ($\Delta F/F_0$) of the difference between the mean of fluorescence sample and its background (ΔF) and the non-immunoreactive regions (F_0). To prevent the observation of differences among experimental groups due to artifacts, the exposure parameters, such as gain and time, were kept constant during image acquisitions. For each analysis, three replicates were used, and at least three independent experiments were performed.

2.7. RNA Isolation and RT-PCR. Total mRNA from FC of both non-Tg and 3×Tg-AD mice was extracted using the NZY total RNA isolation kit (NZYTech, Lisboa, Portugal) following the manufacturer's protocol. Total mRNA was quantified by Nanodrop 1000 spectrophotometer (Thermo Fisher Scientific, MA, USA). Revers transcription of 1 μg mRNA was performed to obtain cDNA adding oligo(dT) and random primers to the first-strand cDNA synthesis kit (NZYTech, Lisboa, Portugal). All PCRs were performed using the supreme NZYTaq DNA polymerase (NZYTech, Lisboa, Portugal) in the presence of specific primers (Sigma-Aldrich) for the target genes: GFAP, GAPDH, S100B, iNOS, and COX-2. GAPDH was used as reference gene. Three independent experiments were performed in triplicate. Primer sequences and PCR details are reported in Table 2.

2.8. Protein Extraction and Western Blot Analysis. Western blot analysis was performed on protein extracts obtained from primary astrocytic cultures as well as from FC samples, as previously described [15]. Samples were suspended in ice-cold hypotonic lysis buffer containing 50 mM Tris/HCl pH 7.5, 150 mM NaCl, 1 mM EDTA, 1% triton X-100, 1 mM phenylmethylsulfonyl fluoride (PMSF), 10 μg/ml aprotinin, and 0.1 mM leupeptin (all from Sigma-Aldrich). After 40 min of incubation at +4°C, homogenates were centrifuged at 18440 ×g for 30 min and the supernatant collected and stored in aliquots at −80°C until use. An equivalent

Table 2: Primer sequences used for RT-PCR.

Sequence of interest		Primer $5'\rightarrow3'$	Annealing temperature (°C)	Number of cycles
GFAP	Forward	GAAGAGGGACAACTTTGCAC	61	32
	Reverse	GCTCTAGGGACTCGTTCGTG		
S100B	Forward	TAATGTGAGTGGCTGCGGAA	63	32
	Reverse	CCTCACCAAGGGCTAAGCAG		
iNOS	Forward	CAAGCTGATGGTCAAGATCCAGAG	64	40
	Reverse	GTGCCCATGTACCAACCATTGAAG		
COX-2	Forward	GCTGTACAAGCAGTGGCAAA	62	30
	Reverse	CCCCAAAGATAGCATCTGGA		
GAPDH	Forward	GCTACACTGAGGACCAGGTTGTC	64	30
	Reverse	CCATGTAGGCCATGAGGTCCAC		

Table 3: Experimental conditions for Western blot from 3×Tg-AD mice astrocytes and FC.

Primary antibody	Brand primary antibody	Dilution	Secondary antibody	Brand secondary antibody
GFAP	Abcam	1 : 50000 5% milk in TBS-T 0.1%	HRP conjugated goat anti-rabbit IgG 1 : 30000 5% milk in TBS-T 0.1%	Jackson ImmunoResearch
S100B	Novus Biologicals	1 : 1000 5% BSA in TBS-T 0.1%	HRP conjugated goat anti-rabbit IgG 1 : 10000 5% BSA in TBS-T 0.1%	Jackson ImmunoResearch
COX-2	Cell Signaling	1 : 1000 5% milk in TBS-T 0.1%	HRP conjugated goat anti-rabbit IgG 1: 10000 5% milk in TBS-T 0.1%	Jackson ImmunoResearch
iNOS	Sigma-Aldrich	1 : 8000 1% BSA in TBS-T 0.1%	HRP conjugated goat anti-rabbit IgG 1 : 10000 1% BSA in TBS-T 0.1%	Jackson ImmunoResearch
BDNF	Santa Cruz	1 : 500 5% milk in TBS-T 0.1%	HRP conjugated goat anti-rabbit IgG 1 : 10000 5% milk in TBS-T 0.1%	Jackson ImmunoResearch
MAP2	Novus Biologicals	1 : 250 5% BSA in TBS-T 0.1%	HRP conjugated goat anti-rabbit IgG 1 : 10000 5% BSA in TBS-T 0.1%	Jackson ImmunoResearch
$A\beta_{(1-42)}$	Millipore	1 : 1000 5% BSA in TBS-T 0.1%	HRP conjugated goat anti-mouse IgG 1 : 10000 5% BSA in TBS-T 0.1%	Jackson ImmunoResearch
β-actin	Santa Cruz	1 : 1500 5% milk in TBS-T 0.1%	HRP conjugated goat anti-rabbit IgG 1 : 10000 5% milk in TBS-T 0.1%	Jackson ImmunoResearch

amount of each sample (50 μg), calculated by Bradford assay, was resolved through 12% acrylamide SDS-PAGE precast gels (Bio-Rad Laboratories, Segrate, Italy). Then, with a trans-blot SD semidry transfer cell (Bio-Rad Laboratories), proteins were transferred onto nitrocellulose membranes that were then blocked with 5% no-fat dry milk powder or 5% BSA in TBS 0.1% Tween 20 (TBS-T) (Tecnochimica Moderna, Rome, Italy) for 1 h before overnight incubation at +4°C with the appropriate primary antibodies. After appropriate rinses in 0.05% TBS-T, membranes were incubated for 1 h at room temperature with a specific secondary horseradish peroxidase- (HRP-) conjugated antibody. The experimental conditions are summarized in Table 3.

Immunocomplexes were detected by an ECL kit (GE Healthcare Life Sciences, Milan, Italy), exposed to X-ray film (GE Healthcare Life Sciences, Milan, Italy) and quantified using ImageJ software. Protein expression level of β-actin was used as loading control. For each antibody, three replicates were used, and at least three independent experiments were performed.

2.9. Statistical Analysis. Analysis was performed using GraphPad Prism software (GraphPad Software, San Diego, CA, USA). Student's *t*-test was used to compare two groups. One-way analysis of variance (ANOVA) was used to determine statistical differences among experimental groups in *in vitro* experiments. *In vivo* results were analyzed by two-way ANOVA, with genotype and treatment as factors. Bonferroni's post hoc test was used upon detection of a main significant effect. Differences between mean values were considered statistically significant when $P < 0.05$.

3. Results

3.1. 3×Tg-AD Primary Astrocytes Present Reactive Astrogliosis. Reactive astrogliosis is a phenomenon commonly detectable in AD brains and characterized by both astrocyte activation and neuroinflammation [6]. Here, we decided to test parameters connected with such events in both non-Tg and 3×Tg-AD primary astrocytes.

To study astrocyte activation, we tested the expression of GFAP, a specific cytoskeletal marker, and S100B, a neurotrophin that when present at high concentrations becomes neurotoxic [6, 28, 29]. Results obtained from both immunofluorescence and Western blot analysis showed a significantly higher GFAP immunoreactivity in primary 3×Tg-AD astrocytes than non-Tg cells (immunofluorescence: $P < 0.05$; Western blot $P < 0.01$) (Figures 2(a), 2(b), 2(e), and 2(f)), while we did not detect changes in S100B signal ($P > 0.05$) (Figures 2(c), 2(d), 2(e), and 2(g)).

A neuroinflammatory environment is mainly characterized by the production and activation of two inducible enzymes: the prostanoid-generating enzyme COX-2 and iNOS [15]. Here, we tested the expression of these two enzymes in non-Tg and 3×Tg-AD primary astrocytes. Results showed that iNOS expression is significantly higher in transgenic-derived primary astrocytes than non-Tg cells ($P < 0.01$) (Figures 2(e) and 2(h)). We did not find any statistical difference in COX-2 expression between the two experimental groups ($P > 0.05$) (Figures 2(e) and 2(i)).

Collectively, these results show that reactive astrogliosis is detectable in mature 3×Tg-AD cortical astrocytes.

3.2. PEA Improves Neuronal Viability and Counteracts Reactive Astrogliosis In Vitro. To test whether PEA treatment could have any toxic effect on astrocyte and neuronal viability, we performed the neutral red assay. Results showed that PEA did not affect astrocytes or neuronal viability at all concentrations tested ($P > 0.05$) (Figures 3(a) and 3(b)). Surprisingly, the highest PEA concentration significantly improved neuronal viability (+5.35%; $P < 0.001$) (Figure 3(b)).

Next, we tested the ability of PEA, at different concentrations (0.01, 0.1, and 1 μM), to counteract reactive astrogliosis. Western blot analyses showed that PEA treatment prevented GFAP increase in primary astrocytes derived from newborn 3×Tg-AD mice in a concentration-dependent manner ($P < 0.05$) (Figures 3(c) and 3(d)). Results by immunofluorescence confirmed this trend, although only the highest dose of PEA reached statistical significance ($P < 0.05$) (Figures 3(f) and 3(g)). Moreover, by Western blot, we found that 1 μM PEA was able to significantly reduce iNOS expression ($P < 0.05$) (Figures 3(c) and 3(e)).

These results show that PEA has no toxicity in both astrocytes and neurons from 3×Tg-AD mice, at the concentrations tested; rather, it promotes neuron viability. Moreover, PEA counteracts reactive astrogliosis in mature 3×Tg-AD primary astrocytes.

3.3. Chronic Um-PEA Normalizes Reactive Astrogliosis in the Frontal Cortex of 3×Tg-AD Mice. Given the interesting *in vitro* results, and with the aim of further exploring PEA effectiveness in the triple transgenic model of AD, we decided to translate the study *in vivo*. Specifically, we tested the effect of chronic um-PEA treatment on reactive astrogliosis and neuronal functionality in FCs of 6-month-old 3×Tg-AD mice, compared to their age-matched non-Tg littermates.

Confirming our *in vitro* observations, we found astrocyte activation in FC of 3×Tg-AD mice when compared with their age-matched non-Tg littermates. Indeed, we found, by RT-PCR and Western blot, an increase of both GFAP and S100B expression in placebo-treated 3×Tg-AD mice in comparison with placebo-treated non-Tg mice ($P < 0.05$) (Figures 4(a), 4(b), 4(c), 4(f), 4(g), and 4(h)). Um-PEA chronic treatment greatly controlled such astrocytic activation, significantly decreasing GFAP mRNA and protein expression ($P < 0.05$) (Figures 4(a), 4(b), 4(f), and 4(g)). Moreover, the two-way ANOVA showed a significant genotype-by-treatment interaction effect on GFAP transcription ($F_{\text{genotype}\times\text{treatment}(1,23)} = 7.872$, $P = 0.0062$) (Figure 4(g)) and expression ($F_{\text{genotype}\times\text{treatment}(1,23)} = 4.829$, $P = 0.0337$) (Figure 4(g)). Surprisingly, um-PEA also induced a trend toward a decrease (−20%) of S100B protein expression in 3×Tg-AD mice compared to placebo-treated 3×Tg-AD ones (Figures 4(a), 4(c), 4(f), and 4(h)).

Regarding the parameters related to the inflammatory process, RT-PCR and Western blot results showed a significant increase of iNOS transcription ($P < 0.001$) (Figures 4(a) and 4(d)) and expression ($P < 0.05$) (Figures 4(f) and 4(i)) in the FC of placebo-treated 3×Tg-AD mice in comparison with placebo-treated non-Tg animals. Interestingly, chronic um-PEA treatment greatly controlled the induced production of this proinflammatory enzyme (RT-PCR: $P < 0.001$; Western blot: $P < 0.05$) (Figures 4(a), 4(d), 4(f), and 4(i)). In addition, two-way ANOVA showed a significant genotype-by-treatment interaction effect in iNOS transcription ($F_{\text{genotype}\times\text{treatment}(1,23)} = 28.37$, $P < 0.0001$) (Figure 4(d)) and protein expression ($F_{\text{genotype}\times\text{treatment}(1,23)} = 4.894$, $P = 0.0306$) (Figure 4(i)). As in *in vitro* results, neither genotype nor treatment induced changes in COX-2 transcript and protein expression (Figures 4(a), 4(e), 4(f), and 4(j)).

Interestingly, using Western blot experiments, we found a trend toward an increase of $A\beta_{(1-42)}$ (+20%) in the FCs of transgenic mice in comparison with the non-Tg animals. This trend, which follows the observed changes in parameters related to astrocyte activation and neuroinflammation, is in line with the evidence available in literature indicating that 6-month-old 3×Tg-AD mice show $A\beta$ overexpression predominantly in FC layers 4 to 5 [23]. Moreover, chronic um-PEA treatment dampened the expression of $A\beta$ in 3×Tg-AD mice, although this failed to reach significance (−34.23%) (Figures 4(f) and 4(k)). Despite this evidence, further experiments will be required to demonstrate the existence of a causative correlation between the reduction of $A\beta$ load and the control of neuroinflammation.

Combined, our results demonstrate the presence of activated astrocytes and a proinflammatory environment in the FCs of 3×Tg-AD mice at 6 months of age. Additionally, we show that chronic um-PEA treatment efficaciously controls these alterations in the AD brain.

3.4. Chronic um-PEA Normalizes Astrocyte Support to Neuronal Functionality in the Frontal Cortex of 3×Tg-AD Mice. Finally, we wanted to explore if there was any impairment in neuronal functionality guided by astrocytes

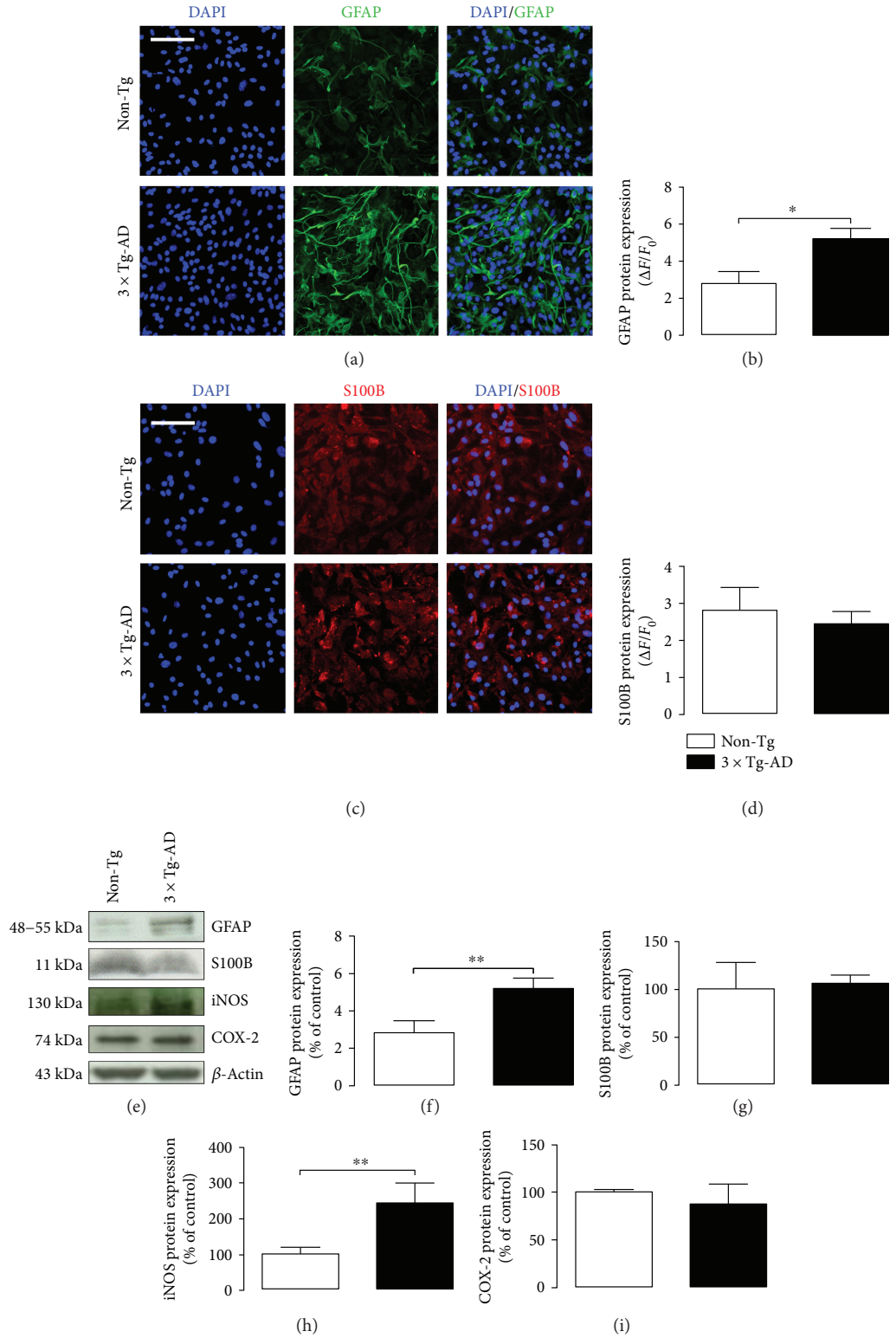

FIGURE 2: Study of parameters related to reactive astrogliosis in 3×Tg-AD and non-Tg primary astrocytes. (a) Representative fluorescent photomicrographs of GFAP (green) and (b) signal quantification in both non-Tg (white bar) and 3×Tg-AD (black bar) primary astrocytes. (c) Representative fluorescent photomicrographs of S100B (red) and (d) signal quantification in both non-Tg (white bar) and 3×Tg-AD (black bar) primary astrocytes. Nuclei were stained with DAPI (blue). Scale bar is 50 μm. Fluorescence analysis is expressed as $\Delta F/F_0$. (e) Representative bands and Western blot densitometric analysis of (f) GFAP, (g) S100B, (h) iNOS, and (i) COX-2. β-Actin was used as loading control. Results are expressed as percentage of the mean control value (non-Tg cells). Experiments were performed three times in triplicate. Data are presented as mean ± SEM. The statistical analysis was performed by Student's t-test ($^*P < 0.05$ and $^{**}P < 0.01$ versus non-Tg group).

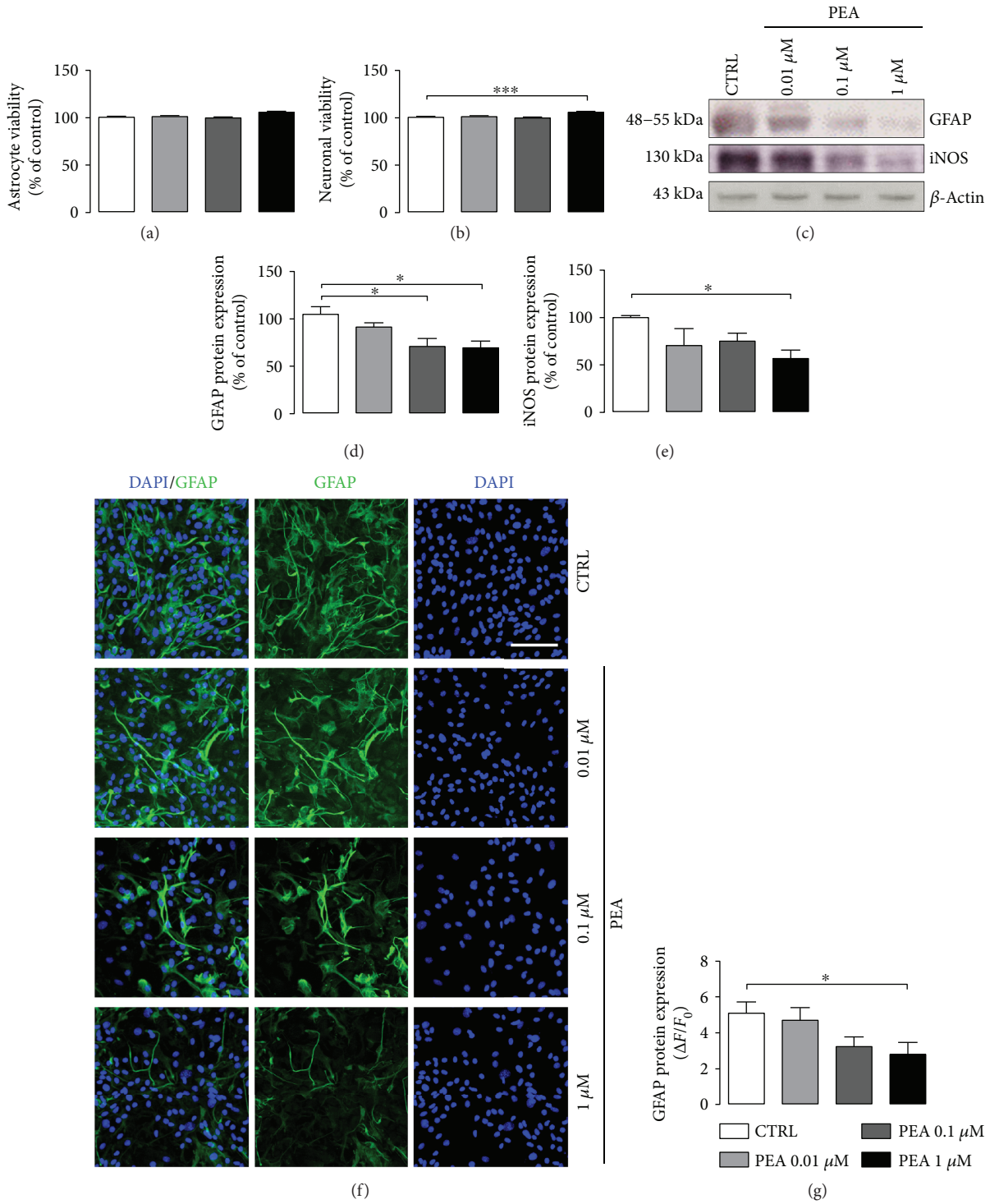

Figure 3: Effect of PEA treatment on astrocyte and neuronal viability and reactive astrogliosis in 3×Tg-AD cells. Evaluation of (a) astrocyte and (b) neuronal viability tested by neutral red uptake assay after 24 h PEA treatment (0.01–0.1–1 μM). (c) Representative immunoreactive signals and Western blot densitometric analysis of (d) GFAP and (e) iNOS. β-Actin was used as loading control. Results are expressed as percentage of the mean control value (CTRL). (f) Representative fluorescent photomicrographs of GFAP (green) staining in 3×Tg-AD primary astrocytes. Nuclei were stained with DAPI (blue). Scale bar is 50 μm. (g) Fluorescence analysis is expressed as $\Delta F/F_0$. Experiments were performed three times in triplicate. Data are presented as mean ± SEM. The statistical analysis was performed by one-way ANOVA followed by Bonferroni's post hoc multiple comparison test ($^{*}P < 0.05$ and $^{***}P < 0.001$ versus CTRL group).

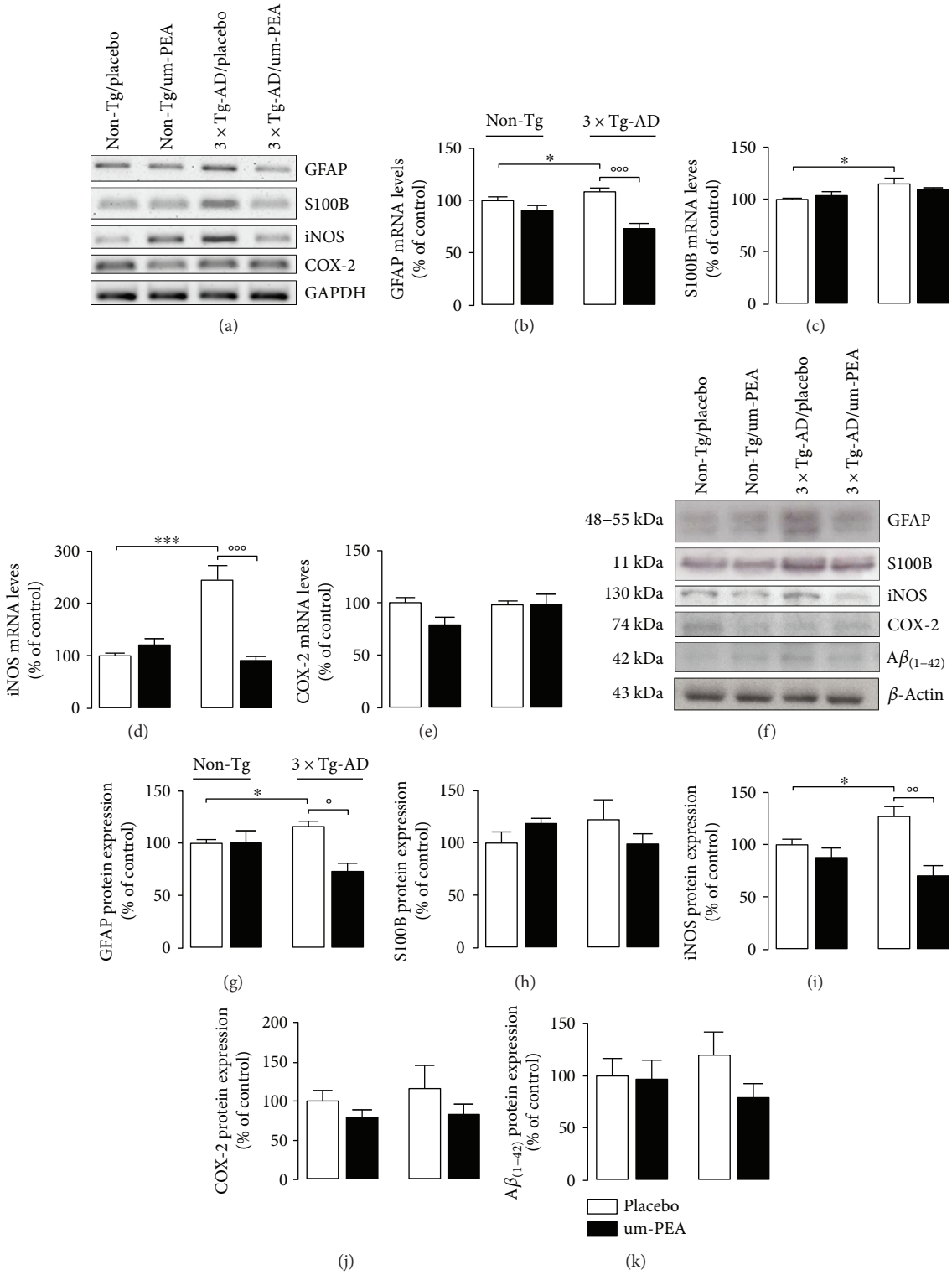

Figure 4: Effect of chronic um-PEA on reactive astrogliosis and $A\beta_{(1-42)}$ expression in the FC of 3×Tg-AD and non-Tg mice. (a) Representative bands from RT-PCR performed in FC homogenates for GFAP, S100B, iNOS, and COX-2, and (b–e) densitometric analysis of the corresponding signals normalized to GAPDH. (f) Representative immunoreactive species and Western blot densitometric analysis of (g) GFAP, (h) S100B, (i) COX-2, (j) iNOS, and (k) $A\beta_{(1-42)}$. β-Actin was used as loading control. Results are expressed as percentage of the mean control value (non-Tg/placebo). Experiments were performed three times in triplicate. Data are presented as mean ± SEM. The statistical analysis was performed by two-way ANOVA followed by Bonferroni's post hoc multiple comparison test ($^{*}P < 0.05$ and $^{***}P < 0.001$ versus non-Tg/placebo group; $^{\circ}P < 0.05$, $^{\circ\circ}P < 0.01$, and $^{\circ\circ\circ}P < 0.001$ versus 3×Tg-AD/placebo group).

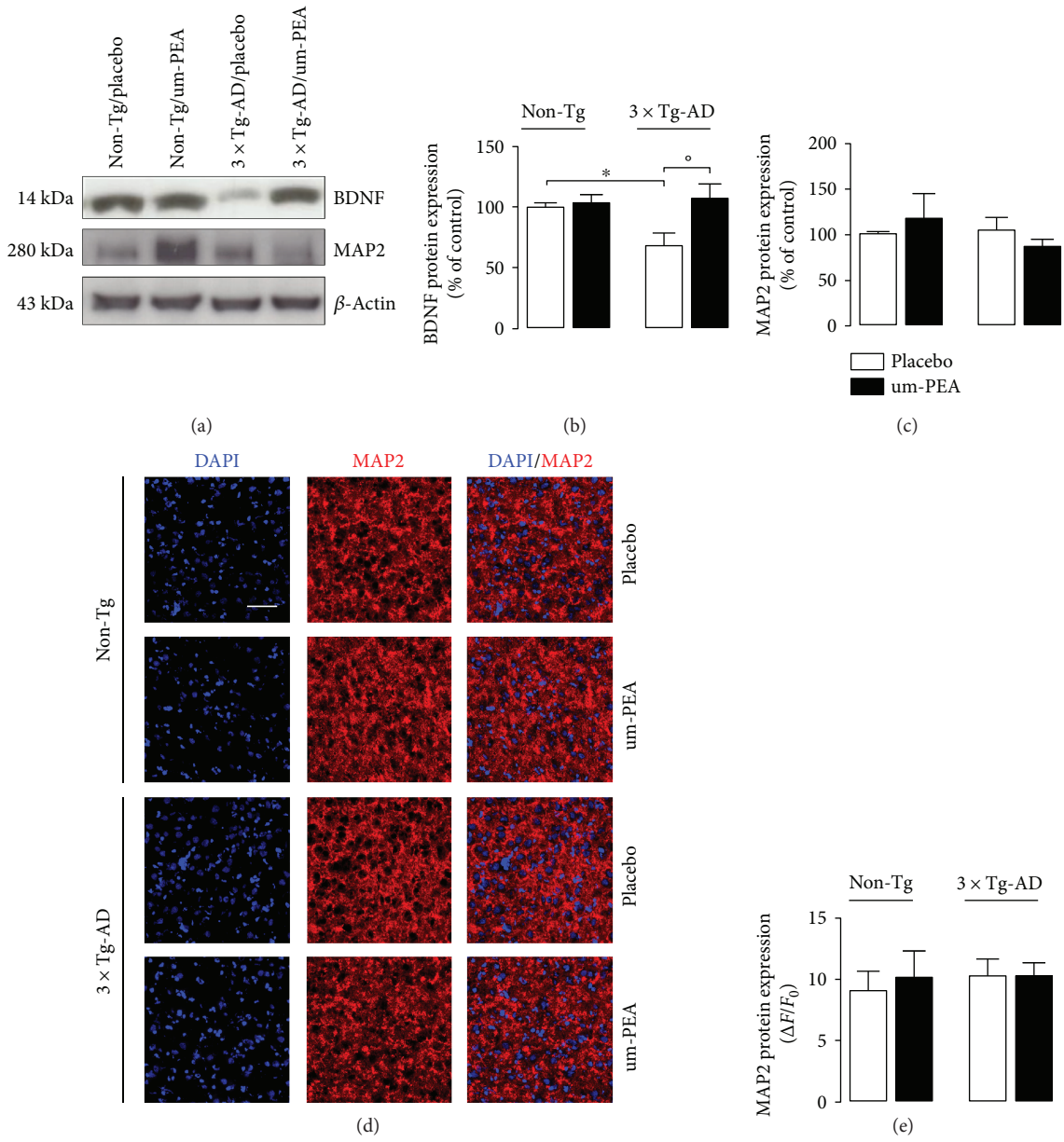

Figure 5: Effect of chronic um-PEA on neuronal support and survival in FC of 3×Tg-AD and non-Tg mice. (a) Representative immunoreactive species and Western blot densitometric analysis of (b) BDNF and (c) MAP2. β-Actin was used as loading control. Results are expressed as percentage of the mean control value (non-Tg/placebo). (d) Representative fluorescent photomicrographs of MAP2 (red) staining in FC of 6-month-old non-Tg and 3×Tg-AD mice, placebo- or um-PEA-treated. Nuclei were stained with DAPI (blue). Scale bar is 50 μm. (e) Fluorescence analysis is expressed as $\Delta F/F_0$. Experiments were performed three times in triplicate. Data are presented as mean ± SEM. The statistical analysis was performed by two-way ANOVA followed by Bonferroni's post hoc multiple comparison test ($^*P < 0.05$ versus non-Tg/placebo group; $^\circ P < 0.05$ versus 3×Tg-AD/placebo group).

that is responsible for BDNF production [30]. To address this goal, we tested both BDNF and MAP2 expression. Western blot analysis showed an impaired production of BDNF in the FC of placebo-treated 3×Tg-AD animals compared to placebo-treated non-Tg littermates. Interestingly, um-PEA significantly counteracted such decrease ($P < 0.05$) (Figures 5(a) and 5(b)). Surprisingly, these modifications did not affect neuronal survival. Indeed, by both Western blot and immunofluorescence, we did not observe modifications in MAP2 expression in placebo-treated transgenic mice in comparison with placebo-treated non-Tg animals (Figures 5(a), 5(c), 5(d), and 5(e)).

Altogether, these results demonstrate the presence of reduced trophic support to FC neurons in 6-month-old 3×Tg-AD mice; this has not yet impaired neuronal viability. Chronic um-PEA treatment restores the neuronal trophic support.

4. Discussion

Astrocytes represent the crucial element of a defensive system of CNS. Cerebral insults trigger reactive astrogliosis, which represents a conserved defensive reprogramming of astroglial cells. It is a very heterogeneous phenomenon that limits damage and facilitates postlesion regeneration of neural networks [31–33], although it may become neurotoxic in some circumstances [34]. In fact, astrogliosis involves complex biochemical and functional remodelling and produces multiple reactive cellular phenotypes. The common feature of pathological astroglial change is the morphological cellular remodelling towards atrophy or hypertrophy [35, 36]. This sometimes occurs at early pathological stages preceding (and possibly precipitating) neuronal death. Such an early activation is observed in AD, when astrocytes, in proximity of plaques and β-amyloid deposits, acquire a reactive phenotype detectable by an increased expression of intermediate filaments and overproduction of proinflammatory mediators [23, 35, 37]. By this way, astrocytes contribute to neurodegeneration, becoming interesting targets for the development of innovative therapies [38–41]. Here, we provide the first *in vitro* evidence of the presence of a basal reactive state in primary astrocytes derived from 3×Tg-AD mice cortices, as well as of the capability of PEA to counteract such a phenomenon and improve neuronal viability. We also obtained important data on the beneficial pharmacological properties of this compound by testing the effect of a chronic treatment with um-PEA in 3×Tg-AD mice. Our *in vivo* results indicate that, during the mild stage of the disease, both reactive astrogliosis and neuroinflammation are already detectable in the FCs of transgenic animals, and that chronic um-PEA is able to alleviate both indices.

Several clinical studies have shown that an impairment of hippocampus, entorhinal cortex, posterior cingulate gyrus, amygdala, and parahippocampal gyrus occur in early AD [42–45]. When AD becomes severe, atrophy progresses from the hippocampus to the FC [46]. Interestingly, our results revealed the absence of neuronal atrophy in 6-month-old 3×Tg-AD mice (age that corresponds to a mild stage of pathology), but detected the early presence of reactive astrogliosis, confirming that such phenomenon is precocious and comes before neuronal loss in this animal model.

Since glial cells, previously considered only space-filling support cells of the CNS, are indeed highly involved in the maintenance of CNS homeostasis, we wondered whether cells in the FC were abnormally activated during the mild stage of the disease, before atrophy occurs. To this aim, we first performed an *in vitro* screening of 3×Tg-AD cortical astrocytes and compared them with non-Tg-derived cells, for signs of astrocyte activation and inflammation. In the absence of any exogenous insult, 3×Tg-AD primary astrocytes showed a basal reactive and proinflammatory phenotype, as demonstrated by the increased expression of GFAP and iNOS, a cytoskeletal astrocyte marker and a proinflammatory inducible enzyme, respectively. Since reactive gliosis may occur before plaque formation, these results suggest that astrocytes can contribute to AD progression before the development of the main AD hallmarks [40]. Since some astrocytes express little or no GFAP [47], we used an additional astrocytic marker, such as S100B, a Ca^{2+}-binding protein. S100B is a neurotrophic factor that improves neuronal survival during CNS development [48]. In adulthood, levels of S100B increase after brain damage and can be neurotoxic and proinflammatory [49]. We did not find any genotypic difference in S100B expression, in our experimental condition. Therefore, it is possible that this protein maintains trophic functionality in the cell population analysed in the absence of an actual injury. Moreover, to further evaluate the inflammatory component in this animal model, we studied a proinflammatory enzyme, COX-2, responsible for prostanoid formation. Its involvement in the cascade of events leading to neurodegeneration in AD is still controversial [50]. COX-2 expression did not change in 3×Tg-AD cortical astrocytes, confirming the hypothesis that COX-2 induction could be connected with neurotoxicity [51], but this was not assessed in this *in vitro* study.

In the last few years, increasing evidence has confirmed the effectiveness of PEA treatment against inflammation in different models of neurodegeneration [15, 21, 52, 53]. Here, we tested the effectiveness of this compound on those parameters that we found to be influenced by the 3×Tg-AD genotype. Therefore, first we demonstrated the absence of astrocytic and neuronal toxicity of PEA at three different concentrations (0.01, 0.1, and 1 μM). Then, we performed the neutral red assay, a viability test, in both primary astrocytes and primary neurons, confirming that PEA is not cytotoxic and fosters neuronal viability at the highest concentration investigated. This result agrees with the already proven neuroprotective effects of PEA in different preclinical models of neurological disorders [15, 54, 55]. In a surgical rat model of AD, we recently demonstrated the ability of PEA to counteract the reactive gliosis caused by $A\beta_{(1-42)}$ hippocampal infusion [15]. Here, we demonstrated that PEA exerts this pharmacological effect in a transgenic model of AD, expanding the range of pathological targets treatable with this compound. In fact, the present *in vivo* experiments confirmed the therapeutic potential of chronic PEA administration. Moreover, such experiments were designed to simulate a clinic-like treatment schedule; for this reason, 3-month-old 3×Tg-AD and sex- and age-matched non-Tg animals were chronically treated for three months with placebo or um-PEA, a crystalline form on micrometric size, which improves its pharmacokinetics properties [24, 56]. Consistent with our *in vitro* observations, in the FC of 3×Tg-AD mice, we detected the presence of reactive gliosis in the mild stage of the disease, as shown by the increased transcription and expression of both GFAP and iNOS. The expression of both S100B and COX-2 were not affected by the genotype. Only S100B mRNA was increased in transgenic cortices. Interestingly, chronic um-PEA treatment dampened such alterations, confirming its effectiveness against reactive gliosis *in vivo*. Another interesting result was the detection of lower levels of BDNF in the FC of transgenic mice in comparison with non-Tg littermates, and, even more significant, the discovery of the ability of chronic um-PEA at increasing the expression of BDNF. Despite the fact that we found a

decreased expression of BDNF together with the presence of reactive gliosis, known to be able to amplify CNS damages [14, 47], we did not detect any impairment of neuronal viability in FC of 3×Tg-AD mice. Such evidence was surprising because it is widely accepted that at 6 months of age these transgenic mice show early symptoms of AD-like pathology and behavioural alterations [23, 57–59]. However, since CNS impairment in AD travels broadly from hippocampus to FC, we can speculate that the massive alteration of this brain region has not occurred as yet, and neurons can somehow survive these insults. In fact, Castello and colleagues demonstrated that BDNF reduction does not exacerbate Aβ and tau pathology, but is a consequence of the pathology itself [60]. If this is true, the improvement in BDNF production that we found in mice after chronic um-PEA treatment can be a positive sign of the control that such a molecule has on the pathology in its entirety, and not only against reactive gliosis.

5. Conclusions

In the present study, we expand the knowledge on glial activity in a triple transgenic model of AD that closely mimics the main features of the pathology. Here, we provide the first evidence that 3×Tg-AD mice present signs of reactive gliosis in the FC at an early stage of the disease. Moreover, we demonstrate for the first time that acute PEA *in vitro*, as well as chronic um-PEA *in vivo*, may counteract such phenomenon, improving the trophic support to neurons, in absence of astrocytes and neuronal toxicity. By the virtue of its safety [61], and considering the growing body of evidence regarding its efficacy, we foresee a possible translation of the results collected in animal models into the clinical practice, in the near future.

Conflicts of Interest

The authors report no financial interests or potential conflicts of interest.

Acknowledgments

This research was supported by the Italian Ministry of Education, University and Research (MIUR) to Luca Steardo (PON01-02512 and PRIN Protocol 2009NKZCNX) and Sapienza University of Rome to Caterina Scuderi (Protocol C26A15X58E) and Maria Rosanna Bronzuoli (Protocol C26N15BHZZ).

References

[1] R. Anand, K. D. Gill, and A. A. Mahdi, "Therapeutics of Alzheimer's disease: past, present and future," *Neuropharmacology*, vol. 76, pp. 27–50, 2014.

[2] H. Braak and E. Braak, "Neuropil threads occur in dendrites of tangle—bearing nerve cells," *Neuropathology and Applied Neurobiology*, vol. 14, no. 1, pp. 39–44, 1988.

[3] P. Merz, H. Wisniewski, R. Somerville, S. A. Bobin, C. L. Masters, and K. Iqbal, "Ultrastructural morphology of amyloid fibrils from neuritic and amyloid plaques," *Acta Neuropathology*, vol. 60, no. 1-2, pp. 113–124, 1983.

[4] J. J. Rodríguez, M. Olabarria, A. Chvatal, and A. Verkhratsky, "Astroglia in dementia and Alzheimer's disease," *Cell Death & Differentiation*, vol. 16, no. 3, pp. 378–385, 2009.

[5] H. Akiyama, S. Barger, S. Barnum, B. Bradt, J. Bauer, and G. M. Cole, "Inflammation and Alzheimer's disease," *Neurobiology of Aging*, vol. 21, no. 3, pp. 383–421, 2000.

[6] A. Verkhratsky, M. Olabarria, H. N. Noristani, C. Y. Yeh, and J. J. Rodriguez, "Astrocytes in Alzheimer's disease," *Neurotherapeutics*, vol. 7, no. 4, pp. 399–412, 2010.

[7] A. Verkhratsky, M. V. Sofroniew, A. Messing et al., "Neurological diseases as primary gliopathies: a reassessment of neurocentrism," *ASN Neuro*, vol. 4, no. 3, article AN20120010, 2012.

[8] Z. Yang and K. K. W. Wang, "Glial fibrillary acidic protein: from intermediate filament assembly and gliosis to neurobiomarker," *Trends in Neurosciences*, vol. 38, no. 6, pp. 364–374, 2015.

[9] G. Esposito, C. Scuderi, J. Lu, C. Savani, D. De Filippis, and T. Iuvone, "S100B induces tau protein hyperphosphorylation via Dickopff-1 up-regulation and disrupts the Wnt pathway in human neural stem cells," *Journal of Cellular and Molecular Medicine*, vol. 12, no. 3, pp. 914–927, 2008.

[10] L. J. van Eldik and M. S. Wainwright, "The Janus face of glial-derived S100B: beneficial and detrimental functions in the brain," *Restorative Neurology and Neuroscience*, vol. 21, no. 3-4, pp. 97–108, 2003.

[11] C. Lindberg, E. Hjorth, C. Post, B. Winblad, and M. Schultzberg, "Cytokine production by a human microglial cell line: effects of ßamyloid and α-melanocyte-stimulating hormone," *Neurotoxicity Research*, vol. 8, no. 3-4, pp. 267–276, 2005.

[12] G. C. Brown and A. Bal-Price, "Inflammatory neurodegeneration mediated by nitric oxide, glutamate, and mitochondria," *Molecular Neurobiology*, vol. 27, no. 3, pp. 325–355, 2003.

[13] J. E. Burda and M. V. Sofroniew, "Reactive gliosis and the multicellular response to CNS damage and disease," *Neuron*, vol. 81, no. 2, pp. 229–248, 2014.

[14] L. Steardo Jr., M. R. Bronzuoli, A. Iacomino, G. Esposito, L. Steardo, and C. Scuderi, "Does neuroinflammation turn on the flame in Alzheimer's disease? Focus on astrocytes," *Frontiers in Neuroscience*, vol. 9, p. 259, 2015.

[15] C. Scuderi, C. Stecca, M. Valenza et al., "Palmitoylethanolamide controls reactive gliosis and exerts neuroprotective functions in a rat model of Alzheimer's disease," *Cell Death & Disease*, vol. 5, no. 9, article e1419, 2014.

[16] S. E. O'Bryant, V. Hobson, J. R. Hall et al., "Brain-derived neurotrophic factor levels in Alzheimer's disease," *Journal of Alzheimer's Disease*, vol. 17, no. 2, pp. 337–341, 2009.

[17] A. N. Voineskos, J. P. Lerch, D. Felsky, S. Shaikh, T. K. Rajji, and D. Miranda, "The brain-derived neurotrophic factor Val66Met polymorphism and prediction of neural risk for Alzheimer disease," *Archives of General Psychiatry*, vol. 68, no. 2, pp. 198–206, 2011.

[18] V. K. Sandhya, R. Raju, R. Verma et al., "A network map of BDNF/TRKB and BDNF/p75NTR signaling system," *Journal of Cell Communication and Signaling*, vol. 7, no. 4, pp. 301–307, 2013.

[19] C. Scuderi, G. Esposito, A. Blasio, M. Valenza, P. Arietti, and L. Steardo Jr., "Palmitoylethanolamide counteracts reactive astrogliosis induced by β-amyloid peptide," *Journal of*

Cellular and Molecular Medicine, vol. 15, no. 12, pp. 2664–2674, 2011.

[20] C. Scuderi, M. Valenza, C. Stecca, G. Esposito, M. R. Carratù, and L. Steardo, "Palmitoylethanolamide exerts neuroprotective effects in mixed neuroglial cultures and organotypic hippocampal slices via peroxisome proliferator-activated receptor-α," *Journal of Neuroinflammation*, vol. 9, no. 1, 2012.

[21] G. D'Agostino, R. Russo, C. Avagliano, C. Cristiano, R. Meli, and A. Calignano, "Palmitoylethanolamide protects against the amyloid-β25-35-induced learning and memory impairment in mice, an experimental model of Alzheimer disease," *Neuropsychopharmacology*, vol. 37, no. 7, pp. 1784–1792, 2012.

[22] M. C. Tomasini, A. C. Borelli, S. Beggiato, L. Ferraro, T. Cassano, and S. Tanganelli, "Differential effects of palmitoylethanolamide against amyloid-β induced toxicity in cortical neuronal and astrocytic primary cultures from wild-type and 3xTg-AD mice," *Journal of Alzheimer's Disease*, vol. 46, no. 2, pp. 407–421, 2015.

[23] S. Oddo, A. Caccamo, J. D. Shepherd et al., "Triple-transgenic model of Alzheimer's disease with plaques and tangles: intracellular Aβ and synaptic dysfunction," *Neuron*, vol. 39, no. 3, pp. 409–421, 2003.

[24] S. Petrosino and V. Di Marzo, "The pharmacology of palmitoylethanolamide and first data on the therapeutic efficacy of some of its new formulations," *British Journal of Pharmacology*, vol. 174, no. 11, pp. 1349–1365, 2017.

[25] B. Costa, S. Conti, G. Giagnoni, and M. Colleoni, "Therapeutic effect of the endogenous fatty acid amide, palmitoylethanolamide, in rat acute inflammation: inhibition of nitric oxide and cyclo-oxygenase systems," *British Journal of Pharmacology*, vol. 137, no. 4, pp. 413–420, 2002.

[26] S. L. Grillo, J. Keereetaweep, M. A. Grillo, K. D. Chapman, and P. Koulen, "*N*-Palmitoylethanolamine depot injection increased its tissue levels and those of other acylethanolamide lipids," *Drug Design, Development and Therapy*, vol. 7, pp. 747–752, 2013.

[27] C. Scuderi, C. Stecca, M. R. Bronzuoli et al., "Sirtuin modulators control reactive gliosis in an in vitro model of Alzheimer's disease," *Frontiers in Pharmacology*, vol. 5, p. 89, 2014.

[28] J. Baudier, C. Delphin, D. Grunwald, S. Khochbin, and J. J. Lawrence, "Characterization of the tumor suppressor protein p53 as a protein kinase C substrate and a S100b-binding protein," *Proceedings of the National Academy of Sciences of the United States of America*, vol. 89, no. 23, pp. 11627–11631, 1992.

[29] C. Scotto, J. C. Deloulme, D. Rousseau, E. Chambaz, and J. Baudier, "Calcium and S100B regulation of p53-dependent cell growth arrest and apoptosis," *Molecular and Cellular Biology*, vol. 18, no. 7, pp. 4272–4281, 1998.

[30] Y. Sato, Y. Chin, T. Kato et al., "White matter activated glial cells produce BDNF in a stroke model of monkeys," *Neuroscience Research*, vol. 65, no. 1, pp. 71–78, 2009.

[31] V. Parpura, M. T. Heneka, V. Montana et al., "Glial cells in (patho)physiology," *Journal of Neurochemistry*, vol. 121, no. 1, pp. 4–27, 2012.

[32] A. Verkhratsky, R. Zorec, J. J. Rodríguez, and V. Parpura, "Astroglia dynamics in ageing and Alzheimer's disease," *Current Opinion in Pharmacology*, vol. 26, pp. 74–79, 2016.

[33] M. Pekny and M. Pekna, "Reactive gliosis in the pathogenesis of CNS diseases," *Biochimica et Biophysica Acta (BBA) - Molecular Basis of Disease*, vol. 1862, no. 3, pp. 483–491, 2016.

[34] S. A. Liddelow, K. A. Guttenplan, L. E. Clarke et al., "Neurotoxic reactive astrocytes are induced by activated microglia," *Nature*, vol. 541, no. 7638, pp. 481–487, 2017.

[35] M. Olabarria, H. N. Noristani, A. Verkhratsky, and J. J. Rodriguez, "Concomitant astroglial atrophy and astrogliosis in a triple transgenic animal model of Alzheimer's disease," *Glia*, vol. 58, no. 7, pp. 831–838, 2010.

[36] V. C. Jones, R. Atkinson-Dell, A. Verkhratsky, and L. Mohamet, "Aberrant iPSC-derived human astrocytes in Alzheimer's disease," *Cell Death & Disease*, vol. 8, no. 3, article e2696, 2017.

[37] A. Verkhratsky, V. Parpura, M. Pekna, M. Pekny, and M. Sofroniew, "Glia in the pathogenesis of neurodegenerative diseases," *Biochemical Society Transactions*, vol. 42, no. 5, pp. 1291–1301, 2014.

[38] P. C. Chen, M. R. Vargas, A. K. Pani et al., "Nrf2-mediated neuroprotection in the MPTP mouse model of Parkinson's disease: critical role for the astrocyte," *Proceedings of the National Academy of Sciences of the United States of America*, vol. 106, no. 8, pp. 2933–2938, 2009.

[39] J. Bradford, J. Y. Shin, M. Roberts et al., "Mutant huntingtin in glial cells exacerbates neurological symptoms of Huntington disease mice," *Journal of Biological Chemistry*, vol. 285, no. 14, pp. 10653–10661, 2010.

[40] C. Acosta, H. D. Anderson, and C. M. Anderson, "Astrocyte dysfunction in Alzheimer disease," *Journal of Neuroscience Research*, vol. 95, no. 12, pp. 2430–2447, 2017.

[41] M. R. Bronzuoli, A. Iacomino, L. Steardo, and C. Scuderi, "Targeting neuroinflammation in Alzheimer's disease," *Journal of Inflammation Research*, vol. 9, pp. 199–208, 2016.

[42] M. Basso, J. Yang, L. Warren et al., "Volumetry of amygdala and hippocampus and memory performance in Alzheimer's disease," *Psychiatry Research: Neuroimaging*, vol. 146, no. 3, pp. 251–261, 2006.

[43] D. P. Devanand, G. Pradhaban, X. Liu et al., "Hippocampal and entorhinal atrophy in mild cognitive impairment: prediction of Alzheimer disease," *Neurology*, vol. 68, no. 11, pp. 828–836, 2007.

[44] C. Pennanen, M. Kivipelto, S. Tuomainen et al., "Hippocampus and entorhinal cortex in mild cognitive impairment and early AD," *Neurobiology of Aging*, vol. 25, no. 3, pp. 303–310, 2004.

[45] H. Wolf, A. Hensel, F. Kruggel et al., "Structural correlates of mild cognitive impairment," *Neurobiology of Aging*, vol. 25, no. 7, pp. 913–924, 2004.

[46] R. I. Scahill, J. M. Schott, J. M. Stevens, M. N. Rossor, and N. C. Fox, "Mapping the evolution of regional atrophy in Alzheimer's disease: unbiased analysis of fluid-registered serial MRI," *Proceedings of the National Academy of Sciences of the United States of America*, vol. 99, no. 7, pp. 4703–4707, 2002.

[47] M. V. Sofroniew and H. V. Vinters, "Astrocytes: biology and pathology," *Acta Neuropathologica*, vol. 119, no. 1, pp. 7–35, 2010.

[48] A. Bhattacharyya, R. W. Oppenheim, D. Prevette, B. W. Moore, R. Brackenbury, and N. Ratner, "S100 is present in developing chicken neurons, and Schwann cells, and promotes neuron survival in vivo," *Journal of Neurobiology*, vol. 23, no. 4, pp. 451–466, 1992.

[49] H. Zetterberg, D. H. Smith, and K. Blennow, "Biomarkers of mild traumatic brain injury in cerebrospinal fluid and blood," *Nature Reviews Neurology*, vol. 9, no. 4, pp. 201–210, 2013.

[50] L. Minghetti, "Cyclooxygenase-2 (COX-2) in inflammatory and degenerative brain diseases," *Journal of Neuropathology and Experimental Neurology*, vol. 63, no. 9, pp. 901–910, 2004.

[51] M. A. Meraz-Ríos, D. Toral-Rios, D. Franco-Bocanegra, J. Villeda-Hernández, and V. Campos-Peña, "Inflammatory process in Alzheimer's disease," *Frontiers in Integrative Neuroscience*, vol. 7, p. 59, 2013.

[52] E. Esposito, D. Impellizzeri, E. Mazzon, I. Paterniti, and S. Cuzzocrea, "Neuroprotective activities of palmitoylethanolamide in an animal model of Parkinson's disease," *PLoS One*, vol. 7, no. 8, article e41880, 2012.

[53] A. Rahimi, M. Faizi, F. Talebi, F. Noorbakhsh, F. Kahrizi, and N. Naderi, "Interaction between the protective effects of cannabidiol and palmitoylethanolamide in experimental model of multiple sclerosis in C57BL/6 mice," *Neuroscience*, vol. 290, pp. 279–287, 2015.

[54] S. D. Skaper, A. Buriani, R. Dal Toso et al., "The ALIAmide palmitoylethanolamide and cannabinoids, but not anandamide, are protective in a delayed postglutamate paradigm of excitotoxic death in cerebellar granule neurons," *Proceedings of the National Academy of Sciences of the United States of America*, vol. 93, no. 9, pp. 3984–3989, 1996.

[55] D. M. Lambert, S. Vandevoorde, G. Diependaele, S. J. Govaerts, and A. R. Robert, "Anticonvulsant activity of *N*-palmitoylethanolamide, a putative endocannabinoid, in mice," *Epilepsia*, vol. 42, no. 3, pp. 321–327, 2001.

[56] D. Impellizzeri, G. Bruschetta, M. Cordaro et al., "Micronized/ultramicronized palmitoylethanolamide displays superior oral efficacy compared to nonmicronized palmitoylethanolamide in a rat model of inflammatory pain," *Journal of Neuroinflammation*, vol. 11, no. 1, p. 136, 2014.

[57] K. R. Stover, M. A. Campbell, C. M. Van Winssen, and R. E. Brown, "Analysis of motor function in 6-month-old male and female 3xTg-AD mice," *Behavioural Brain Research*, vol. 281, pp. 16–23, 2015.

[58] S. Oddo, A. Caccamo, M. Kitazawa, B. P. Tseng, and F. M. LaFerla, "Amyloid deposition precedes tangle formation in a triple transgenic model of Alzheimer's disease," *Neurobiology of Aging*, vol. 24, no. 8, pp. 1063–1070, 2003.

[59] L. M. Billings, S. Oddo, K. N. Green, J. L. McGaugh, and F. M. LaFerla, "Intraneuronal Aβ causes the onset of early Alzheimer's disease-related cognitive deficits in transgenic mice," *Neuron*, vol. 45, no. 5, pp. 675–688, 2005.

[60] N. A. Castello, K. N. Green, and F. M. LaFerla, "Genetic knockdown of brain-derived neurotrophic factor in 3xTg-AD mice does not alter aβ or tau pathology," *PLoS One*, vol. 7, no. 8, article e39566, 2012.

[61] E. R. Nestmann, "Safety of micronized palmitoylethanolamide (microPEA): lack of toxicity and genotoxic potential," *Food Science & Nutrition*, vol. 5, no. 2, pp. 292–309, 2017.

Scuderi et al. Translational Psychiatry (2018)8:32
DOI 10.1038/s41398-017-0076-4

Translational Psychiatry

ARTICLE Open Access

Ultramicronized palmitoylethanolamide rescues learning and memory impairments in a triple transgenic mouse model of Alzheimer's disease by exerting anti-inflammatory and neuroprotective effects

Caterina Scuderi[1], Maria Rosanna Bronzuoli[1], Roberta Facchinetti[1], Lorenzo Pace[2], Luca Ferraro[3], Kevin Donald Broad[4], Gaetano Serviddio[5], Francesco Bellanti[5], Gianmauro Palombelli[6], Giulia Carpinelli[6], Rossella Canese[6], Silvana Gaetani[1], Luca SteardoJr[7], Luca Steardo[1] and Tommaso Cassano[2]

Abstract

In an aging society, Alzheimer's disease (AD) exerts an increasingly serious health and economic burden. Current treatments provide inadequate symptomatic relief as several distinct pathological processes are thought to underlie the decline of cognitive and neural function seen in AD. This suggests that the efficacy of treatment requires a multitargeted approach. In this context, palmitoylethanolamide (PEA) provides a novel potential adjunct therapy that can be incorporated into a multitargeted treatment strategy. We used young (6-month-old) and adult (12-month-old) 3×Tg-AD mice that received ultramicronized PEA (um-PEA) for 3 months via a subcutaneous delivery system. Mice were tested with a range of cognitive and noncognitive tasks, scanned with magnetic resonance imaging/magnetic resonance spectroscopy (MRI/MRS), and neurochemical release was assessed by microdialysis. Potential neuropathological mechanisms were assessed postmortem by western blot, reverse transcription–polymerase chain reaction (RT-PCR), and immunofluorescence. Our data demonstrate that um-PEA improves learning and memory, and ameliorates both the depressive and anhedonia-like phenotype of 3×Tg-AD mice. Moreover, it reduces Aβ formation, the phosphorylation of tau proteins, and promotes neuronal survival in the CA1 subregion of the hippocampus. Finally, um-PEA normalizes astrocytic function, rebalances glutamatergic transmission, and restrains neuroinflammation. The efficacy of um-PEA is particularly potent in younger mice, suggesting its potential as an early treatment. These data demonstrate that um-PEA is a novel and effective promising treatment for AD with the potential to be integrated into a multitargeted treatment strategy in combination with other drugs. Um-PEA is already registered for human use. This, in combination with our data, suggests the potential to rapidly proceed to clinical use.

Introduction

Alzheimer's disease (AD) is the primary cause of dementia in the elderly, but currently prescribed medications provide only modest and transient benefits to a subset of patients.

Histopathologically, the major features of AD include the extracellular accumulation of beta amyloid (Aβ) fibrils in senile plaques (SPs) and intraneuronal neurofibrillary

Correspondence: Luca Steardo (luca.steardo@uniroma1.it)
[1]Department of Physiology and Pharmacology "V. Erspamer", SAPIENZA University of Rome, Rome, Italy
[2]Department of Clinical and Experimental Medicine, University of Foggia, Foggia, Italy
Full list of author information is available at the end of the article
Caterina Scuderi and Maria Rosanna Bronzuoli contributed equally to this work

tangles (NFTs), whose precise role in the progression of AD remains to be clarified[1, 2]. Interestingly, preclinical and clinical data have demonstrated that both SPs and NFTs are colocalized close to activated glial cells, suggesting that a dysfunction in glia homeostasis is a key pathogenetic mechanism in AD[3–5]. In the context of AD, both astrocytes and microglia can be activated by Aβ which promotes further reactive gliosis[6]. This phenomenon is normally engaged with the intent of defending the brain by removing injurious stimuli (e.g., Aβ fibrils phagocytosis). However, if prolonged, this response exceeds normal physiological limits and can induce detrimental effects[7–10].

Our hypothesis is that an early combination of neuroprotective and anti-inflammatory treatments represents a promising treatment approach for the treatment of AD. The endogenous lipid mediator palmitoylethanolamide (PEA) demonstrates exceptional potential as a novel treatment for AD. We have previously demonstrated PEA anti-inflammatory and neuroprotective properties, as well as its ability to preserve memory function in rodent models of AD[11–16]. At present, we lack precise information concerning both the effects of chronic PEA administration on the progression of AD and the optimal time to begin treatment. This is an important consideration as one of the major problems with the development of effective treatments for AD is that diagnosis is normally made at an advanced stage of the disease which may mean many therapeutic interventions begin too late to be effective.

In this paper, we evaluated the effects of chronic um-PEA administration in 3×Tg-AD mice at two different stages (mild and severe) of AD-like pathology and cognitive deficits, by subcutaneously administering the drug to two age groups of animals for 3 months. 3×Tg-AD mice were chosen because they present both Aβ deposits and tau pathology, as well as synaptic dysfunction, thus representing a widely used and validated model which closely mimics the neuropathological alterations seen in human AD[17, 18]. The animals were then tested using a range of cognitive and noncognitive tasks, followed by an assessment of neuropathology.

Our data demonstrate the first in vivo evidence that chronic treatment with ultramicronized-PEA (um-PEA), a formulation which maximizes its bioavailability[19, 20], induces considerable improvements in cognitive and neural function during both the early presymptomatic and later symptomatic stages of AD in a triple transgenic mouse model of AD (3×Tg-AD mice).

Our data suggest that PEA demonstrates exceptional potential as a novel treatment for AD and in combination with the fact that is already licensed for the use in humans, where it demonstrates high safety and tolerability, provides an opportunity for its rapid translation in clinical pactice.

Materials and methods

Animals and pellet implantation

3×Tg-AD (harboring APP_{swe}, $PS1_{M146V}$, and tau_{P301L} transgenes) male mice and their sex- and age-matched wild-type littermates (Non-Tg) (C57BL6/129SvJ) were maintained in controlled conditions (12-h light/12-h dark cycle, temperature 22 °C, humidity 50–60%, fresh food, and water ad libitum). All procedures were conducted in accordance with the guidelines of the Italian Ministry of Health (D.L. 26/2014) and the European Parliamentary directive 2010/63/EU.

Mice of 3 and 9 months were anesthetized by i.p. injection of ketamine hydrochloride (1 mg/10 g) and xylazine (0.1 mg/10 g). The area between the shoulder blades was shaved and the surgical area was sterilized with alcohol. A small (1–2 cm) dorsal midline incision was made and a subcutaneous pocket was created with a blunt probe. An um-PEA or a placebo pellet was placed into the pocket and the incision was closed with sterile sutures.

Drugs and protocols

Um-PEA (EPT2110/1) was obtained from Epitech group (Saccolongo, Italy). A 90-day-release pellet containing either 28 mg of um-PEA (Innovative Research of America, Sarasota, Florida; cat. #NX-999) or placebo (cat. #NC-111) was subcutaneously implanted. During pellet inclusion process, um-PEA was homogeneously distributed in the matrix, maintaining its original crystalline form and micrometric size; both dosage and administration route were chosen according to previous data[20, 21]. Both Non-Tg and 3 × Tg-AD mice were randomly assigned to either placebo or um-PEA group. No animals were excluded from the analysis. Behavioral sample size (N) is specified in open and black bars of Fig. 1. For molecular analyses, the sample size (N) for all experimental groups/condition is specified in the figure legends.

Behavioral, microdialysis/HPLC, and MRI/MSI experiments were performed as previously described[22–29], and conducted at the end of 90-day treatment. Mice were then killed, and hippocampi were isolated for western blot (WB), cytokine assays, and RT-PCR analyses, whereas whole brains for immunohistochemistry were flash-frozen in 2-methylbutane. Biochemical analyses were performed as previously described[12]. The timeline of the experiments is described in Fig. 1a.

Behavioral tests

The minimum interval between two consecutives procedures was 2 days. All tests were performed between 8:00 a.m. and 3:00 p.m., in a dimly lit condition. On the day of testing, the mice were acclimated for about 60 min in the

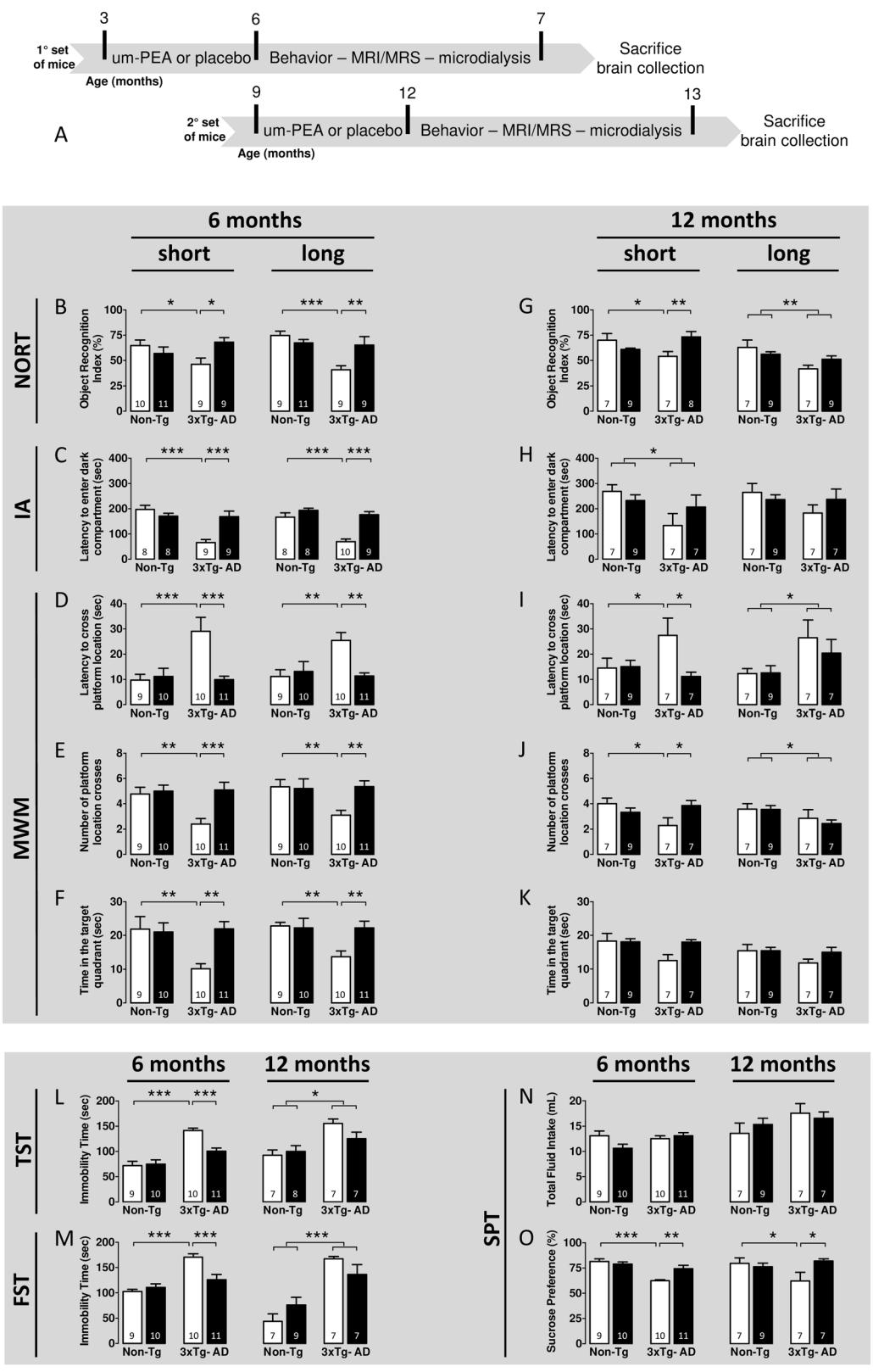

Fig. 1 (See legend on next page.)

(see figure on previous page)
Fig. 1 Um-PEA rescues early memory deficits and ameliorates the depressive-like phenotype in the 3×Tg-AD mice. (**a**) Schematic representation of the experimental design. Evaluation of the (**b–k**) cognitive and (**l–o**) emotional phenotype of 6- and 12-month-old 3×Tg-AD and age-matched Non-Tg mice chronically treated with placebo (open bars) or um-PEA (black bars). Short- and long-term memory of mice was evaluated by (**b**, **g**) novel object recognition test (NORT), (**c**, **h**) inhibitory passive avoidance (IA), and (**d**–**f**, **i**–**k**) Morris water maze (MWM). Moreover, the emotional phenotype of mice was evaluated by (**l**) tail suspension test (TST), (**m**) forced swim test (FST), and (**n**, **o**) sucrose preference test (SPT). Sample size is indicated in the bars. The data are presented as means ± SEM. Statistical analysis was performed by two-way ANOVA followed by Tukey multiple- comparison test (*$p < 0.05$; **$p < 0.01$; ***$p < 0.001$)

behavioral room before the procedures were initiated. Mice were weighed every day during the entire period of the experiment. All behavioral tasks were analyzed by a blinded investigator.

Novel object recognition test (NORT)

Each mouse was habituated to an empty Plexiglas arena (45 × 25 × 20 cm) for 3 consecutive days. On training (day 4), mice were exposed to two identical objects (A+A) placed at opposite ends of the arena for 5 min. After 30 min and 24 h, the animals were subjected to a 5-min retention session where they were exposed to one object A and to a novel object B (after 30 min) and object C (after 24 h). Exploration was considered as pointing the head toward an object at a distance of <2.5 cm from the object, with its neck extended and vibrissae moving. Turning around, chewing, and sitting on the objects were not considered exploratory behaviors. Behavior was recorded with a MV750i camera (1024 × 768 resolution, Canon, Tokyo, Japan) and scored by a blinded investigator. Videotapes were analyzed as MPEG files using a behavioral tracking system furnished with infrared lighting-sensitive CCD cameras. Animal performances were monitored with the EthoVision XT version 7 video-tracking software system (Noldus Information Technology Inc., Leesburg, VA). The time of exploration was recorded, and an object recognition index (ORI) was calculated, such that $ORI = (TN-TF)/(TN + TF)$, where TN and TF represent times of exploring the familiar and novel object, respectively. Mice that did not explore both objects during training were discarded from further analysis.

Inhibitory passive avoidance (IA)

On training, mice were placed in the fear-conditioning chamber and were allowed to explore for 2 min before receiving three electric foot shocks (1 s, 0.1 mA; inter-shock interval, 2 min). Animals were returned to the home cage 30 s after the last footshock. The animals were subsequently tested 24 h or 7 days after the training phase to assess the short- and long-term memory. During this phase, the behavior in the conditioning chamber was video recorded for 5 min and subsequently was analyzed for freezing behavior, which was defined as the absence of all movements except for respiration.

Morris water maze (MWM)

The test was conducted in a circular tank of 1.2 m in diameter, and locates in a room with several extra maze cues. Mice were trained to swim to a 14-cm-diameter circular Plexiglas platform submerged 1.5 cm beneath the surface of water and invisible to the mouse while swimming. The water temperature was kept at 25 °C throughout the duration of the test. The platform was fixed in place, equidistant from the center of the tank and its walls. Mice were subjected to four training trials per day and were alternated among four random starting points for 5 consecutive days. Mice were allowed to find and escape onto the submerged platform. If the mice failed to find the platform within 60 s, they were manually guided to the platform and were allowed to remain on it for 10 s. After this, each mouse was placed into a holding cage under a warming lamp for 25 s until the start of the next trial. Retention of the spatial memory (the probe trial) was assessed 1.5 and 24 h after the last training session and consisted of a 60 s trial without the platform. Mice were monitored by a camera mounted in the ceiling directly above the pool, and all trials were stored on videotape for subsequent analysis. The parameters measured during the probe trial included initial latency to cross the platform location, number of platform location crosses, and time spent in the target quadrant.

Tail suspension test (TST)

Mice were suspended for 6 min by the tail and the duration of immobility was measured during the last 4 min.

Forced swim test (FST)

Mice were individually placed in a Plexiglas cylinder (20 cm diameter, 50 cm high) containing 20 cm of water (25 °C). The experiment lasted for 6 min and the duration of immobility was analyzed during the last 4 min.

Sucrose preference test (SPT)

Singularly caged mouse had free access to two drinking bottles, the first filled with tap water, while the other with

a 2% sucrose solution. Before the test, there was a period of adaptation that lasted for 48 h. The animals were then deprived of food and liquids for 3 h. During the next 24 h, free consumption of water and 2% sucrose solution took place, in the presence of *ad libitum* food. Fluid intake was measured afterward by weighing the drinking bottles. The sucrose preference (%) was determined as follows: sucrose solution intake (g)/total fluid intake (g) × 100.

Biochemical testing procedures

RNA isolation and RT-PCR

Total RNA from hemi-hippocampi homogenates was extracted by using the NZY total RNA isolation kit (NZYTech, Lisboa, Portugal) following the company's datasheet. The total RNA was measured by Nanodrop 1 000 spectrophotometer (Thermo Fisher Scientific, MD, USA), so, 1 μg of RNA was reverse transcribed to obtain cDNA by using oligo(dT) and random primers of the first-strand cDNA synthesis kit (NZYTech, Lisboa, Portugal). All PCRs were performed using supreme NZYTaq DNA polymerase (NZYTech, Lisboa, Portugal) with specific primers (Sigma-Aldrich, Milan, Italy) for tumor necrosis factor-α (TNF-α, forward primer 5′-CAGCCGATGGGTTGTACCTT-3′ and reverse primer 5′-CCGGACTCCGCAAAGTCTAA-3′), interleukin-1β (IL-1β, forward primer 5′-GGACCCCAAAAGATGAAGGGC-3′ and reverse primer 5′-GGAAAAGAAGGTGCTCATGTCC-3′), and IL-10 (forward primer 5′-GCCCTTTGCTATGGTGTCCT-3′ and reverse primer 5′-CTCTGAGCTGCTGCAGGAAT-3′). Glyceraldehyde 3-phosphate dehydrogenase (GAPDH, forward primer 5′-GCTACACTGAGGACCAGGTTGTC-3′ and reverse primer 5′-CCATGTAGGCCATGAGGTCCAC-3′) was used as reference gene.

Protein extraction and western blot analysis

Hemi-hippocampi were homogenized in ice-cold hypotonic lysis buffer (50 mM Tris/HCl, pH 7.5, 150 mM NaCl, 1 mM ethylenediaminetetraacetic acid (EDTA), 1% triton X-100, 1 mM phenylmethylsulfonyl fluoride (PMSF), 10 μg/ml aprotinin, and 0.1 mM leupeptin, all from Sigma-Aldrich, Milan, Italy) and incubated for 40 min at +4 °C. Protein dephosphorylation was avoided by adding a phosphatase inhibitor cocktail. The homogenates were then centrifuged, cellular membranes discarded, and the obtained supernatant was aliquoted and stored at −80 °C. Bradford assay was performed to calculate protein concentration. An equal amount of proteins (50 μg) was resolved on 12% acrylamide SDS-PAGE precast gels (Bio Rad Laboratories, Milan, Italy) and transferred onto nitrocellulose membranes through a semidry system (Bio Rad Laboratories, Milan, Italy). Membranes were blocked for 1 h either with no-fat dry milk or bovine serum albumin (BSA) powders in tris-buffered saline–0.1% tween 20 (TBS-T) (Tecnochimica, Rome, Italy).

Overnight incubation at +4 °C was performed with one of the following primary antibodies: rabbit anti-amyloid precursor protein (anti-APP 1:1 000, Cell Signaling, Danvers, MA, USA), rabbit anti-β-secretase (anti-BACE1 1:1 000, Cell Signaling, Danvers, MA, USA), mouse anti-β-amyloid (1:200, Millipore, Darmstad, Germany), rabbit anti-Akt (1:500, Cell Signaling, Danvers, MA, USA), rabbit anti-p[Thr308]Akt (1:5 000, Cell Signalling, Danvers, MA, USA), rabbit anti-glycogen synthase kinase-3β (anti-Gsκ-3β 1:1 000, Cell Signaling, Danvers, MA, USA), rabbit anti-p[Ser9]GSκ-3β (1:1 000, Cell Signaling, Danvers, MA, USA), rabbit anti-p[Ser396]tau (1:1 000, Thermo Fisher Scientific, Waltham, MA, USA), mouse anti-microtubule-associated protein 2 (anti-MAP2 1:250, Novus Biologicals, Littleton, CO, USA), rabbit anti-S100B (1:1 000, Epitomics, Burlingame, CA, USA), rabbit anti-glial fibrillary acidic protein (anti-GFAP 1:25 000, Abcam, Cambridge, UK), rabbit anti-p[Ser536]nuclear factor kappa-light-chain enhancer of activated B cells (anti-p[Ser536]NF-κB p65 1:2 000, Cell Signaling, Danvers, MA, USA), rabbit anti-inducible nitric oxide synthase (anti-iNOS, 1:8 000, Sigma-Aldrich, Milan, Italy), rabbit anti-glutamate transporter GLT-1 (1:1 000, Tocris, Bristol, UK), and mouse anti-glutamine synthetase clone GS-6 (1:1 000, Millipore, Darmstad, Germany). Rabbit anti-β-actin (1:1 500, Santa Cruz, Dallas, TX, USA) was used as loading control.

Membranes were incubated with a specific secondary horseradish peroxidase (HRP)-conjugated antibody (HRP-conjugated goat anti-rabbit IgG, 1:10 000–1:30 000; HRP-conjugated goat anti-mouse, 1:10 000; all from Jackson ImmunoResearch, Suffolk, UK) either in no-fat dry milk or BSA TBS-T. Immunocomplexes were detected by an enhanced chemiluminescence (ECL) kit (GE Healthcare Life Sciences, Milan, Italy) and the signal obtained was quantified by ImageJ software after densitometric scanning of the X-ray films (GE Healthcare Life Sciences, Milan, Italy).

Immunohistochemistry

Immunohistochemistry for GFAP and MAP2 was performed on coronal slices (12 μm thickness) containing the hippocampal regions, collected, and postfixed with 4% paraformaldehyde in 0.1 M phosphate buffer solution (PBS) (Tecnochimica, Rome, Italy). Slices were incubated with blocking solution and then incubated overnight in blocking solution containing either rabbit anti-GFAP (1:1 000, Abcam, Cambridge, UK) or mouse anti-MAP2 (1:250, Novus Biologicals, Littleton, CO, USA). Sections were incubated with the proper secondary antibody (1:200, fluorescein-affinipure goat anti-rabbit IgG (H+L); 1:300–1:400, rhodamine-affinipure goat anti-mouse IgG (H+L), Jackson ImmunoResearch, Suffolk, UK) and 4′,6-

Table 1 Results from the statistical analysis of data obtained from the behavioral tests of 6- and 12-month-old mice

Behavioral tests	Parameter	Genotype (G)	Treatment (T)	Interaction G × T
6 month old				
NORT	Object recognition index––30 min	F (1,38) = 0.377, n.s.	F (1,38) = 1.389, n.s.	F (1,38) = 6.406 $p < 0.05$
	Object recognition index––24 h	F (1,37) = 11.993, $p < 0.01$	F (1,37) = 2.617, n.s.	F (1,37) = 9.214, $p < 0.01$
IA	Latency to enter dark compartment—24 h	F (1,33) = 16.499, $p < 0.001$	F (1,33) = 5.513, $p < 0.05$	F (1,33) = 15.951, $p < 0.001$
	Latency to enter dark compartment—7 days	F (1,34) = 21.239, $p < 0.001$	F (1,34) = 29.431, $p < 0.001$	F (1,34) = 10.556, $p < 0.01$
MWM	Latency to cross platform location—1.5 h	F (1,39) = 6.842, $p < 0.05$	F (1,39) = 6.481, $p < 0.05$	F (1,39) = 8.757, $p < 0.01$
	Latency to cross platform location—24 h	F (1,39) = 4.698, $p < 0.05$	F (1,39) = 4.325, $p < 0.05$	F (1,39) = 7.879, $p < 0.01$
	Time in the target quadrant—1.5 h	F (1,39) = 4.441, $p < 0.05$	F (1,39) = 4.474, $p < 0.05$	F (1,39) = 6.050, $p < 0.05$
	Time in the target quadrant—24 h	F (1,39) = 4.836, $p < 0.05$	F (1,39) = 3.812, n.s.	F (1,39) = 4.994, $p < 0.05$
	Number of platf location crosses—1.5 h	F (1,39) = 4.835, $p < 0.05$	F (1,39) = 7.845, $p < 0.01$	F (1,39) = 5.634, $p < 0.05$
	Number of platf location crosses—24 h	F (1,39) = 3.454, n.s.	F (1,39) = 3.660, n.s.	F (1,39) = 4.633, $p < 0.05$
TST	Immobility	F (1,39) = 44.062, $p < 0.001$	F (1, 39) = 7.203, $p < 0.05$	F (1, 39) = 9.308, p < 0.01
FST	Immobility	F (1,39) = 28.558, p < 0.001	F (1, 39) = 5.473, p < 0.05	F (1, 39) = 11.442, $p < 0.01$
SPT	Total fluid intake	F (1,39) = 0.349, n.s.	F (1,39) = 0.382, n.s.	F (1,39) = 1.991, n.s.
	Sucrose preference	F (1,39) = 22.547, $p < 0.001$	F (1,39) = 3.608, n.s.	F (1,39) = 8.933, $p < 0.01$
12 month old				
NORT	Object recognition index—30 min	F (1,30) = 0.154, n.s.	F (1,30) = 1.251, n.s.	F (1,30) = 9.460, $p < 0.01$
	Object recognition index—24 h	F (1,31) = 9.310, $p < 0.01$	F (1,31) = 0.112, n.s.	F (1,31) = 3.431, n.s.
IA	Latency to enter dark compartment—24 h	F (1,29) = 4.799, $p < 0.05$	F (1,29) = 0.261, n.s.	F (1,29) = 2189, n.s.
	Latency to enter dark compartment—7 days	F (1,29) = 1653, n.s.	F (1,29) = 0179, n.s.	F (1,29) = 1723, n.s.
MWM	Latency to cross platform location—1.5 h	F (1,29) = 1273, n.s.	F (1,29) = 3.760, n.s.	F (1,29) = 4.326, $p < 0.05$
	Latency to cross platform location—24 h	F (1,29) = 5.725, $p < 0.05$	F (1,29) = 0.388, n.s.	F (1,29) = 0.464, n.s.
	Time in the target quadrant—1.5 h	F (1,29) = 3.715, $p = 0.065$	F (1,29) = 3.022, $p = 0.094$	F (1,29) = 3.437, $p = 0.07$
	Time in the target quadrant—24 h	F (1,29) = 2.107,n.s	F (1,29) = 1.303, n.s.	F (1,29) = 1.277, n.s.
	Number of platf location crosses—1.5 h	F (1,29) = 1.783, n.s.	F (1,29) = 1.030, n.s.	F (1,29) = 6.303, $p < 0.05$
	Number of platf location crosses—24 h	F (1,29) = 4.474, $p < 0.05$	F (1,29) = 0.261, n.s.	F (1,29) = 0.225. n.s.
TST	Immobility	F (1,28) = 11.873, $p < 0.01$	F (1,28) = 0.363, n.s.	F (1,28) = 1.681, n.s.
FST	Immobility	F (1,29) = 39.686, $p < 0.001$	F (1,29) = 0.00321, n.s.	F (1, 29) = 4.690, $p < 0.05$
SPT	Total fluid intake	F (1,29) = 2.638, n.s.	F (1,29) = 0.0558, n.s.	F (1,29) = 0.733, n.s.
	Sucrose preference	F (1,29) = 1.126, n.s.	F (1,29) = 2.319, n.s.	F (1,29) = 4.563, $p < 0.05$

Two-way analyses of variance (ANOVA) with genotype (3×Tg-AD *vs* Non-Tg) and treatment (um-PEA *vs* placebo) as between-subject factors ($n = 10–12$ per group). Details are reported in the text

NORT novel object recognition test, *IA* inhibitory passive avoidance, *MWM* Morris water maze, *TST* tail suspension test, *FST* forced swim test, *SPT* sucrose preference test

diamidino-2-phenylindole (DAPI 1:75 000, Sigma-Aldrich, Milan, Italy) in BSA at room temperature. Fluorescent signal was detected by an Eclipse E600 microscope (Nikon, Tokyo, Japan) using both Nikon Plan 10X/10.25 and Nikon Plan Fluor 20X/0.5 objectives. Pictures were captured by a QImaging camera (Canada) with NISelements BR 3.2 64-bit software with pixel resolution of 1024 × 1024.

Analysis was performed by ImageJ software and data were expressed as a ratio of the difference between the

mean of fluorescence signal and the background (ΔF), and the non-immunoreactive regions (F_0). To prevent any change in the fluorescent signal due to artifacts, the gain and time exposure were kept constant during all image acquisitions.

Cytokine array

Hippocampal homogenates were analyzed for cytokines presence using a mouse cytokine array panel A (R&D Systems, Minneapolis). A total of 100 µg for each hippocampal lysate were processed following the manufacturer's instructions.

In vivo microdialysis and HPLC analysis

In vivo microdialysis was performed in awake and freely moving mice. Anesthetized mice were stereotaxically implanted with a CMA/7 guide cannula with stylet (CMA Microdialysis, Stockholm, Sweden) into the ventral hippocampus (anterior–posterior, −3.0 mm; lateral, +3.0 mm; and ventral, −1.8 mm from bregma). Following a 2-day recovery period, the CMA/7 probe was inserted and dialyses were carried out perfusing the probe with Krebs-Ringer phosphate (KRP) buffer at flow rate of 1 µl/min. The constituents of the KRP buffer were (in mM) NaCl 145, KCl 2.7, $MgCl_2$ 1, $CaCl_2$ 2.4, and Na_2HPO_4 2, buffered at pH 7.4. After a 2-h stabilization period, four baseline samples were collected every 20 min. Probe position was verified histologically and glutamate was quantified by HPLC coupled to fluorescence detection.

Magnetic resonance imaging (MRI)/magnetic resonance spectroscopy (MRS)

Mice of 6 and 12 months undergo MRI and MRS scanning to evaluate genotype- and treatment-induced differences in brain metabolism. Animals were anesthetized with 2.5–1.5% isoflurane (IsoFlo, Abbott SpA, Berkshire, UK) in oxygen at flow rate of 1 l/min. MRI/MRS experiments were conducted on a 4.7T Agilent Inova preclinical system (Agilent Technologies Inc., Palo Alto, CA, USA) equipped with a combination of volume and surface coils (Rapid Biomedical GmbH, Rimpar, Germany). Fast spin-echo sagittal anatomical images (Repetition Time (TR)/Echo Time (TE) = 3200/60 ms, 13 slices of 0.8-mm thickness, Field of View (FOV) 20 × 25 mm^2, matrix 256 × 256, 2 averages, and scan time 12 min) were acquired for positioning of the voxel for MRS. Single voxel localized 1H MR spectra (PRESS, TR/TE = 4 000/23 ms, NS = 256) were collected from hippocampus (volume 9.5 µl) according to a quantitative protocol, which includes water T2 measurements and LCModel fitting routine for spectral analysis[29]. We adopted the spectral analysis which considers Glx as the combined signal that mainly comes from glutamate plus glutamine because, at field strength generally used in human MRS studies, they have overlapping signals.

Statistical analysis

Sample size was determined on the basis of our previous experiments and by using the software GPower. All data were expressed as mean ± standard error of measurement (SEM). Behavioral, biochemical, and MRI/MRS data were analyzed by two-way analyses of variance (ANOVA) with genotype (3×Tg-AD *vs* Non-Tg) and treatment (um-PEA *vs* placebo) as between-subject factors. Tukey's honestly significant difference (HSD) test or Bonferroni's test were used for multiple *post hoc* comparisons when required. The threshold for statistical significance was set at $p < 0.05$.

Data availability

The data that support the findings of this study are available from the corresponding author upon reasonable request.

Results

Behavioral tasks

Statistical details are reported in Table 1.

Um-PEA improves learning and memory in 6-month-old 3×Tg-AD mice

We tested the effects of um-PEA on both short- (30 min) and long-term (24 h) memory with a novel object recognition test (NORT). Two-way ANOVA analysis revealed significant changes in the time mice spent exploring the new object across the four different groups. At 30 min, we found significant genotype-by-treatment interaction effects, while no significant differences were found for the main effects of genotype and treatment. *Post hoc* comparisons showed a significant higher object recognition index (ORI) for 3×Tg-AD mice treated with um-PEA with respect to placebo-treated 3×Tg-AD mice (Fig. 1b). Performing this trial 24 h later, we observed a significant genotype and genotype-by-treatment interaction effect of ORI in the exploration session among the four groups. *Post hoc* analysis demonstrated that um-PEA-treated 3×Tg-AD mice performed significantly better than the placebo-treated 3×Tg-AD group, and indicated that, at both time points, um-PEA had no effect on the performance of Non-Tg mice (Fig. 1b).

Contextual learning and memory were then evaluated by an inhibitory passive avoidance task (IA), and the retention test was then conducted 24 h or 7 days after the training trial to assess short- and long-term memory. Statistical analysis indicated, at both time points, a significant main effect of genotype, treatment, and genotype-by-treatment interaction. Multiple *post hoc* comparisons indicated that um-PEA-treated transgenic mice

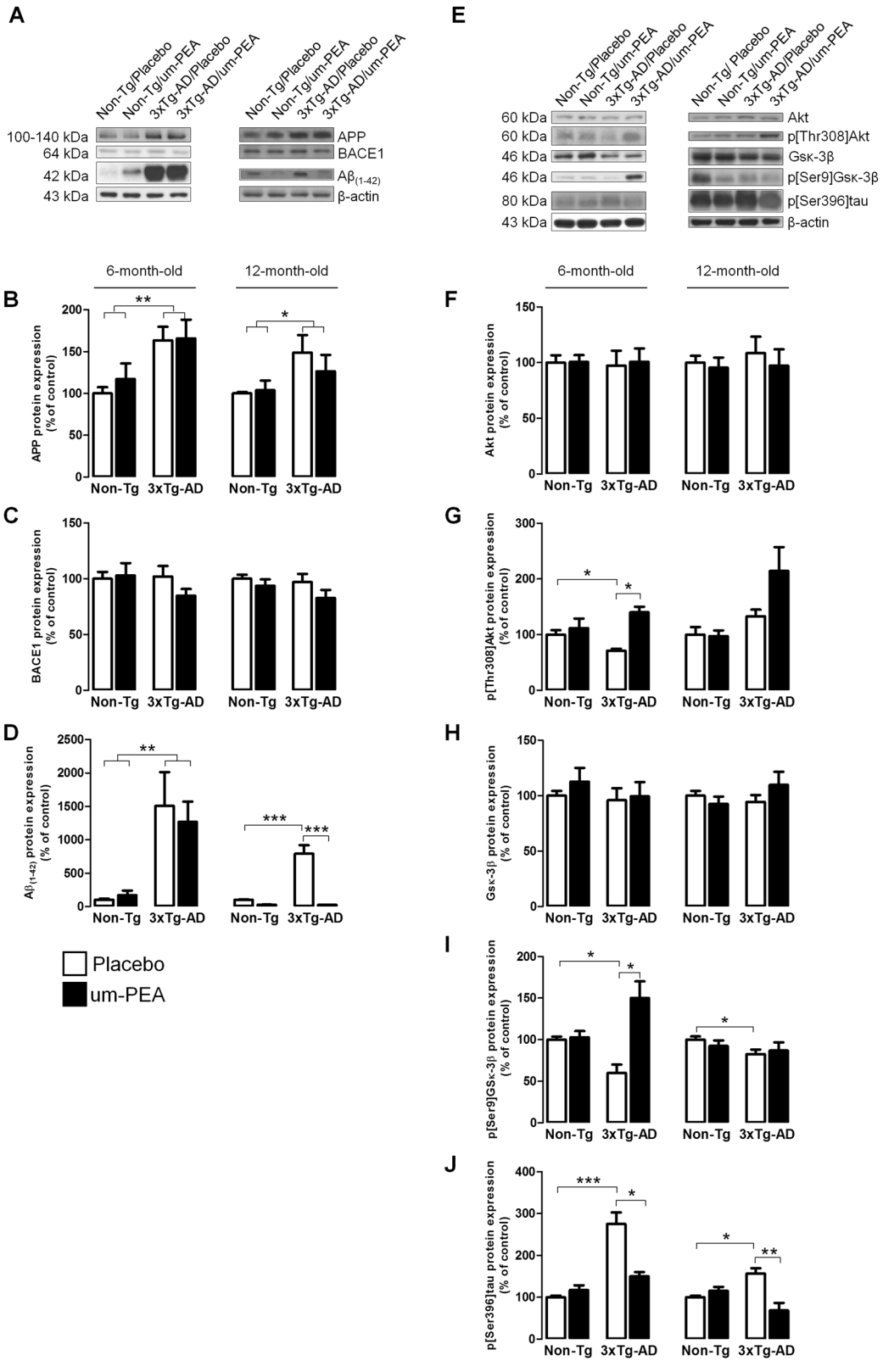

Fig. 2 (See legend on next page.)

(see figure on previous page)
Fig. 2 Um-PEA effects on AD pathology. Evaluation of protein expression in hippocampi of 6- and 12-month-old 3×Tg-AD and age-matched Non-Tg mice chronically treated with placebo (open bars) or um-PEA (black bars). (**a**) Representative western blots for APP, BACE1, and $A\beta_{(1-42)}$ proteins and (**b–d**) densitometric analyses normalized to β-actin used as loading controls ($N = 3$, in triplicate). (**e**) Representative western blots for Akt, p[Thr308]Akt, Gsk-3β, p[Ser9]Gsk-3β, p[Ser396]tau, and (**f–j**) densitometric analysis normalized to β-actin used as loading control ($N = 3$, in triplicate). The results are expressed as percentage of control (Non-Tg/placebo groups). The data are presented as means ± SEM. Statistical analysis was performed by two-way ANOVA followed by Bonferroni's multiple-comparison test (*$p < 0.05$; **$p < 0.01$; ***$p < 0.001$)

performed better than placebo-treated 3×Tg-AD mice, and reached the same performance level of Non-Tg animals (Fig. 1c). This was not due to differences in or enhanced sensitivity to the footshock, as all mice had similar jump responses upon shock administration.

Spatial learning was measured by the Morris water maze (MWM). Mice received four training trials/day for 5 consecutive days to locate the hidden platform. Statistics demonstrated no difference in spatial memory during 5 days of training among all groups measured (data not shown). To determine the effects of um-PEA on memory, the platform was removed from the maze, and tests were conducted 1.5 or 24 h following the last training trial to independently assess both short- and long-term memory, respectively. Um-PEA rescued the early spatial memory deficits present in 6-month-old 3×Tg-AD mice, as indicated by a significantly decreased latency to cross the platform location of the 3×Tg-AD mice treated with um-PEA compared to placebo-treated 3×Tg-AD (Fig. 1d). Moreover, the number of platform location crosses, as well as the time spent in the target quadrant were significantly increased in um-PEA-treated 3×Tg-AD compared to placebo-treated 3×Tg-AD mice. Multiple *post hoc* comparisons showed that 3×Tg-AD mice treated with um-PEA performed similarly to the Non-Tg mice in all probe trials and at both time points. Finally, um-PEA had no significant effects on learning or memory retention in Non-Tg mice (Fig. 1e, f).

Overall, these data indicate that um-PEA treatment rescues early learning and memory deficits in 6-month-old 3×Tg-AD mice.

Um-PEA improves short-term learning and memory alone in 12-month-old 3×Tg-AD mice

Two-way ANOVA for the ORI at a time point of 30 min (short memory) in 12-month-old mice revealed a significant genotype-by-treatment interaction effect, while no significant main effects of genotype and treatment were found. Multiple *post hoc* comparisons showed a significant higher ORI in um-PEA-treated 3×Tg-AD with respect to placebo-treated 3×Tg-AD mice (Fig. 1g).

When the probe trial was performed 24 h after the exploration session (long-term memory), we observed a significant main effect of genotype only among the four groups (Fig. 1g).

In 12-month-old mice, IA showed significant main effects only for genotype 24 h after the training trial, whereas at 7 days, no significant main effects were observed (Fig. 1h).

The results from MWM in 12-month-old mice demonstrated that no significant differences were observed during 5 days of training among the four different groups (data not shown). When the probe trial was performed 1.5 h after the last training session (short-term memory), statistical analysis showed that um-PEA significantly decreased the latency to cross the platform location and increased the number of platform location crosses in 3×Tg-AD compared to placebo-treated 3×Tg-AD mice (Fig. 1i, j). Regarding the time spent in the target quadrant at 1.5 h after the last training session, no significant differences were observed among the four groups, although um-PEA induced a trend toward an increase (+43%) in the 3×Tg-AD compared to placebo-treated 3×Tg-AD mice (Fig. 1k). Moreover, when testing was performed at 24 h after the last training session (long-term memory), statistical analysis showed a significant main effect of genotype alone for both latency to cross the platform location and the number of platform location crosses (Fig. 1i–k).

Overall, these data indicate that um-PEA improves the short-term memory of 12-month-old 3×Tg-AD mice, with no significant effects on long-term memory. Moreover, um-PEA exerts no significant effects on learning or memory in aged Non-Tg mice.

Um-PEA ameliorates the depressive- and anhedonia-like behaviors in 3×Tg-AD mice

Depressive-like behaviors were measured by the tail suspension test (TST) and forced swim test (FST). At 6 months of age, significant main effects of treatment, genotype, and genotype-by-treatment interactions were observed. *Post hoc* comparisons revealed that the immobility time in both tests was higher in placebo-treated 3×Tg-AD than in placebo-treated Non-Tg mice. Moreover, um-PEA significantly decreased the immobility time in the 3×Tg-AD for both tests (Fig. 1l, m). Interestingly, we found a significant main effect of genotype alone in 12-month-old mice, with no significant main effects of treatment and genotype-by-treatment interaction (Fig. 1l, m).

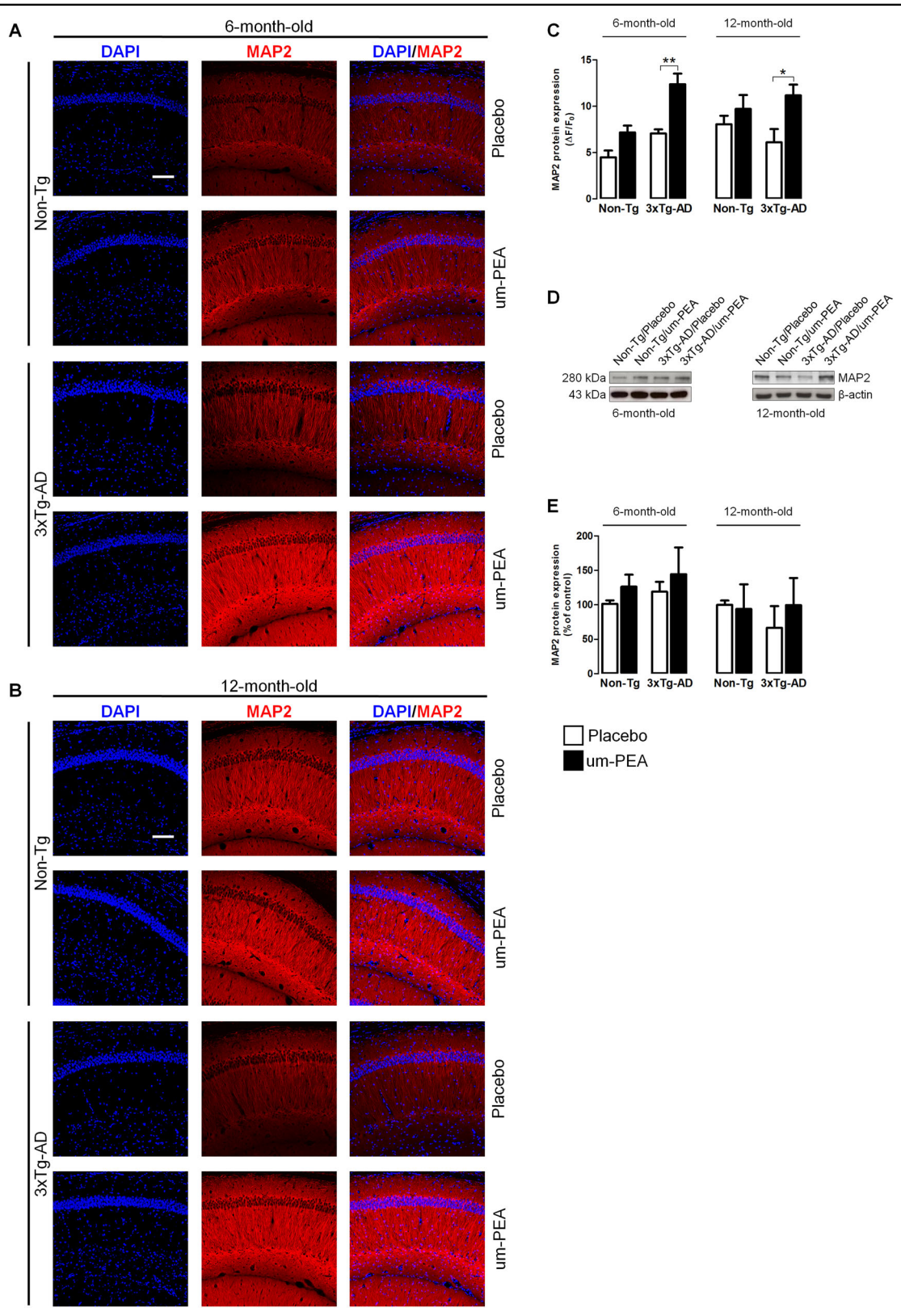

Fig. 3 (See legend on next page.)

(see figure on previous page)

Fig. 3 Um-PEA effects on neuronal viability in hippocampus of 3×Tg-AD and Non-Tg mice. Evaluation of neuronal marker expression in hippocampi of 6- and 12-month-old 3×Tg-AD and age-matched Non-Tg mice chronically treated with placebo (open bars) or um-PEA (black bars). (**a**, **b**) Representative fluorescent photomicrographs of microtubule-associated protein 2 (MAP2) (red) staining in the CA1 region of hippocampi at both 6 and 12 months of age, and (**c**) fluorescence analysis expressed as $\Delta F/F_0$. Nuclei were stained with DAPI (blue) ($N = 3$, in triplicate). (**d**) Representative western blots for MAP2 and (**e**) densitometric analyses normalized with β-actin used as loading controls ($N = 3$, in triplicate). The results are expressed as percentage of control (Non-Tg/placebo groups). The data are presented as means ± SEM. Statistical analysis was performed by two-way ANOVA followed by Bonferroni's multiple-comparison test (*$p < 0.05$; p** < 0.01). Scale bar 100 µm

Anhedonia-like behaviors were measured by a sucrose preference test (SPT). SPT revealed a significant main effect of genotype and genotype-by-treatment interaction at 6 months of age, and other significant main effects included a genotype-by-treatment interaction at 12 months of age (Fig. 1n, o). Multiple *post hoc* comparisons demonstrated a significantly increased preference for sucrose in the placebo-treated Non-Tg mice compared to placebo-treated 3×Tg-AD mice. Interestingly, um-PEA restored the preference for the sweet solution in the 3×Tg-AD group at both 6 and 12 months of age. This effect was not accounted for by a difference in total fluid intake among all groups (Fig. 1n, o).

Altogether, these results suggest that 3×Tg-AD mice show a depressive-like phenotype that is reversed by um-PEA treatment only at 6 months of age, while no significant effect is observed at 12 months of age. Differently, um-PEA treatment attenuates the anhedonia-like phenotype of both 6- and 12-month-old 3×Tg-AD mice. Moreover, um-PEA has no significant effect on Non-Tg mice.

Um-PEA reduces Aβ formation in aged 3×Tg-AD mice

To evaluate the effect of um-PEA on AD-like pathology, we studied the expression of APP, BACE1, and $A\beta_{(1–42)}$. Placebo-treated 3×Tg-AD mice of 6 and 12 months compared with placebo-treated Non-Tg littermates showed a significant increase of APP and, despite no changes in BACE1 expression, exhibited a massive increase in $A\beta_{(1–42)}$ levels. At both ages, um-PEA did not change the expression of full-length APP. Interestingly, um-PEA strongly reduced $A\beta_{(1–42)}$ expression in 3×Tg-AD mice only at 12 months of age (Fig. 2a–d).

Together, these results show that chronic um-PEA treatment reduces hippocampal $A\beta_{(1–42)}$ expression in aging 12-month-old 3×Tg-AD mice, while inducing no significant effects in younger 6-month-old 3×Tg-AD mice.

Um-PEA reduces tau phosphorylation and promotes neuronal survival in 3×Tg-AD mice

The expression of Gsκ-3β and the downstream abnormally phosphorylated (p[Ser396]tau) tau protein, both closely related to NFT formation and its associated neuronal impairments, were evaluated[30–34]. We also assessed the expression of the Akt, a kinase whose active form p[Thr308]Akt is responsible for Gsκ-3β inactivation through Ser9 phosphorylation[35]. The results showed, despite no changes in the total Akt quantity, a significant decrease of p[Thr308]Akt in 6-month-old placebo-treated 3×Tg-AD mice in comparison with placebo-treated Non-Tg littermates. Although no differences in Gsκ-3β total amount were detected, placebo-treated 3×Tg-AD demonstrated a significant p[Ser9]Gsκ-3β reduction at both ages compared to placebo-treated Non-Tg mice. Um-PEA increased both p[Thr308]Akt and p[Ser9]Gsκ-3β in 6-month-old 3×Tg-AD compared to age-matched Non-Tg mice. Moreover, in placebo-treated 3×Tg-AD mice at both ages, we observed a significant p[Ser396]tau increase that was substantively reduced by um-PEA (Fig. 2e–j).

As a consequence of these observations, we investigated neuronal survival by testing the expression of MAP2. Western blot experiments did not show any difference between expression in any of these groups at both ages (Fig. 3d, e). However, immunofluorescence experiments, which were performed to examine subtle differences in expression between different hippocampal subregions, revealed a significant increase in MAP2 immunoreactivity in the CA1 of um-PEA-treated 3×Tg-AD mice at both ages (Fig. 3a–c).

Altogether, these data suggest that um-PEA reduces abnormal tau phosphorylation in the hippocampus of 3×Tg-AD mice at 6 and 12 months of age, and that such an effect may be partially mediated by the Gsκ-3β/Akt pathway. Moreover, um-PEA promotes MAP2 expression and hence neuronal survival in the CA1 subregion of the hippocampus of 3×Tg-AD mice.

Um-PEA normalizes astrocyte function and restrains neuroinflammation

We examined the effects of chronic um-PEA treatment on astrocyte function. Specifically, the expression of the cytoskeletal GFAP and S100B, a glial-derived neurotrophin whose levels are affected in AD[6], was tested. We did not detect any significant difference in 6-month-old 3×Tg-AD mice compared to Non-Tg littermates in the expression of both GFAP and S100B (Fig. 4a–d, f).

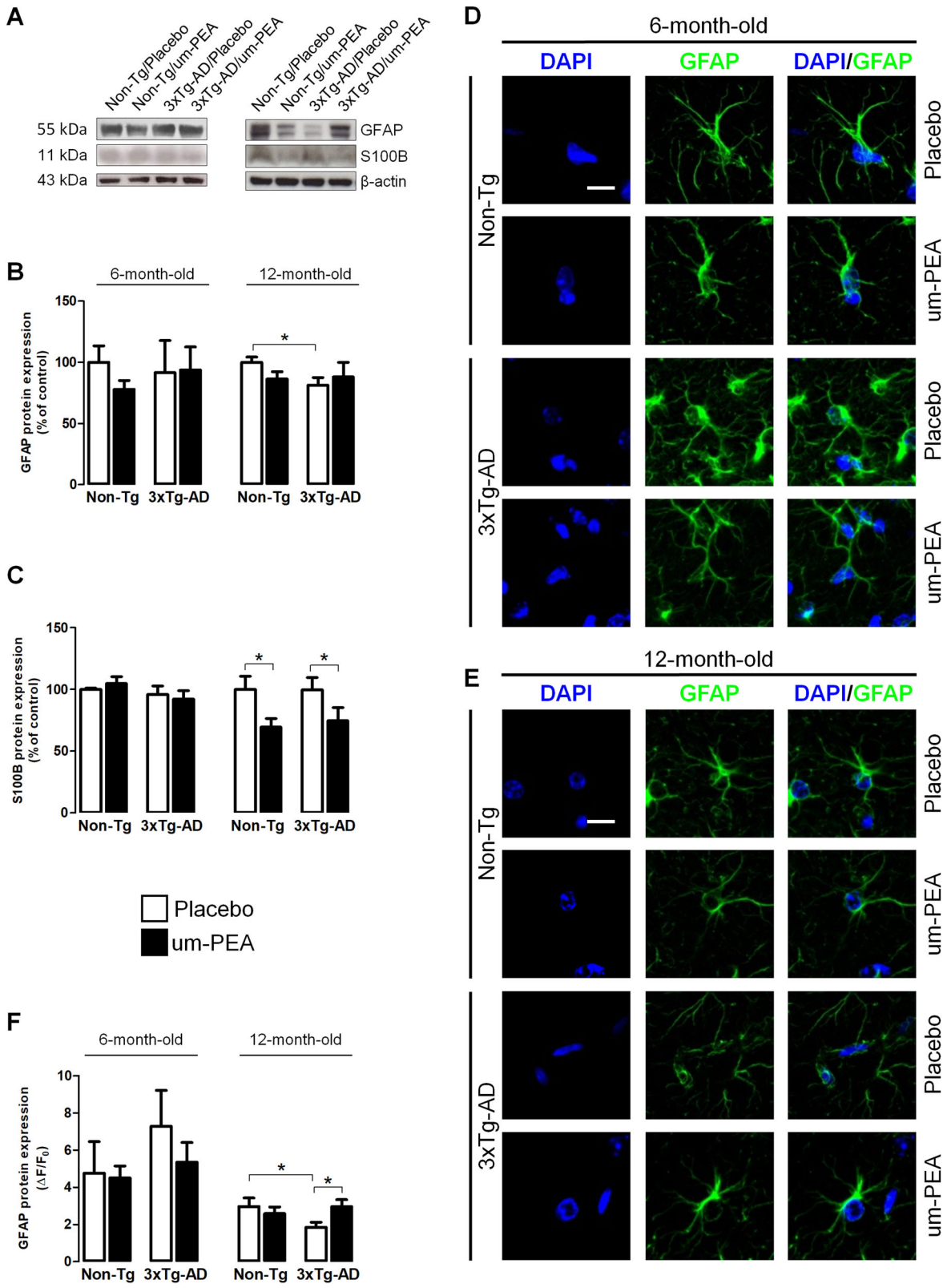

Fig. 4 (See legend on next page.)

(see figure on previous page)

Fig. 4 Um-PEA effects on astrocyte functionality in hippocampus of 3×Tg-AD and non-Tg mice. Evaluation of astrocytic markers in hippocampi of 6- and 12-month-old 3×Tg-AD and age-matched Non-Tg mice chronically treated with placebo (open bars) or um-PEA (black bars). (**a**) Representative western blots for GFAP and S100B proteins and (**b**, **c**) densitometric analyses normalized with β-actin used as loading controls. Results are expressed as percentage of control (Non-Tg/placebo groups) ($N = 3$, in triplicate). (**d**, **e**) Representative fluorescent photomicrographs of GFAP (green) staining in the CA1 subregion of hippocampi at both 6 and 12 months of age, and (**f**) fluorescence analysis expressed as $\Delta F/F_0$. Nuclei were stained with DAPI (blue) ($N = 3$, in triplicate). The data are presented as means ± SEM. Statistical analysis was performed by two-way ANOVA followed by Bonferroni's multiple-comparison test (*$p < 0.05$). Scale bar 10 μm

We then examined the expression of a range of cytokines which revealed that 3×Tg-AD mice exhibit a transition to an increased proinflammatory state. It is notable that placebo-treated 6-month-old 3×Tg-AD mice displayed an increased transactivation of NF-κB p65 subunit, an overproduction of proinflammatory mediators, including iNOS, TNF-α, IL-1β, IL-16, and IL-5, macrophage colony-stimulating factor (M-CSF), monocyte chemotactic protein 5 (MCP-5), and reduction of the anti-inflammatory IL-10. Chronic treatment with um-PEA almost completely abolished the increase in inflammatory markers observed in 6-month-old 3×Tg-AD mice, and suppressed the expression of p[Ser536]p65, IL-1β, M-CSF, IL-16, MCP-5, and IL-5 but not iNOS and TNF-α, while enhancing IL-10 transcription (Fig. 5).

Contrasting results were obtained in aging animals. Indeed, placebo-treated 12-month-old 3×Tg-AD mice exhibited a significant reduction of GFAP expression compared to placebo-treated Non-Tg (Fig. 4a, b), and immunofluorescence revealed that um-PEA restored GFAP expression in the CA1 subregion of the hippocampus (Fig. 4e, f). Moreover, we did not observe any genotype-related difference in S100B expression. Interestingly, um-PEA significantly decreased S100B levels in both genotypes (Fig. 4a, c). Finally, in 12-month-old mice, we did not detect a transition to a proinflammatory state. However, at this age, um-PEA reduced iNOS expression in 3×Tg-AD, and enhanced IL-10 transcript in Non-Tg (Fig. 5a, c, l, m).

Collectively, these results show that 6-month-old 3×Tg-AD mice exhibit mild astrocyte activation but displayed an intense inflammatory status. In contrast, 12-month-old 3×Tg-AD mice did not demonstrate astrocyte activation but a slight astrocyte atrophy not accompanied by neuroinflammation. Um-PEA stabilizes the altered parameters related to astrocyte function, bringing them to more physiological levels, and restrains neuroinflammation.

Um-PEA effect on glutamatergic transmission

Quantitative magnetic resonance spectroscopy (MRS) analyses demonstrated that 6-month-old 3×Tg-AD mice had reduced hippocampal levels of both Glx (a combined measure of glutamate and glutamine) and N-acetyl-aspartate (NAA) compared to age-matched Non-Tg littermates. Interestingly, um-PEA significantly increased Glx levels only in the 3×Tg-AD mice (Fig. 6a–d). As Glx concentration reflects both intracellular and extracellular glutamate and glutamine pools, we attempted to gain deeper insights into the functional state of glutamatergic transmission by microdialysis. The results showed that basal extracellular glutamate levels in the hippocampus of 6-month-old 3×Tg-AD were significantly higher compared to age-matched Non-Tg mice (Fig. 6e). Westren blot analyses indicated that the higher extracellular glutamate levels in transgenic mice may be partially due to the reduced expression of GLT-1, while the expression of GS remained unaffected (Fig. 6f–i). Even though our results were not statistically significant, um-PEA treatment induced a trend toward an increase of GLT-1 (+35%) in 6-month-old 3×Tg-AD mice compared to placebo-treated Non-Tg ones (Fig. 6g, h).

In 12-month-old mice, we did not record any genotype-related differences in Glx, NAA, or extracellular glutamate levels despite a reduction in GLT-1 being evident (Fig. 6).

Collectively, these results indicate that 6-month-old 3×Tg-AD mice exhibit a disruption to glutamatergic function and that um-PEA increases Glx levels.

Discussion

This study, employing a multidisciplinary approach, provides compelling evidence that a chronic um-PEA treatment exerts anti-inflammatory and neuroprotective effects in a murine model of AD that recapitulates the salient neural and cognitive impairments seen in this disease. It also demonstrates that um-PEA exerts these effects in both mildly declining young (6-month-old) and severely declining aging (12-month-old) 3×Tg-AD mice, which suggests its potential to arrest the decline in neural and cognitive function at two separate stages of the disease. These data also provide novel insights into the molecular mechanisms involved in AD. We comprehensively examined a number of pathways underlying astrocyte function, neuroinflammation, and neuronal integrity in 6- and 12-month-old 3×Tg-AD mice chronically receiving um-PEA or placebo for 3 months. Our results confirm that important behavioral and molecular

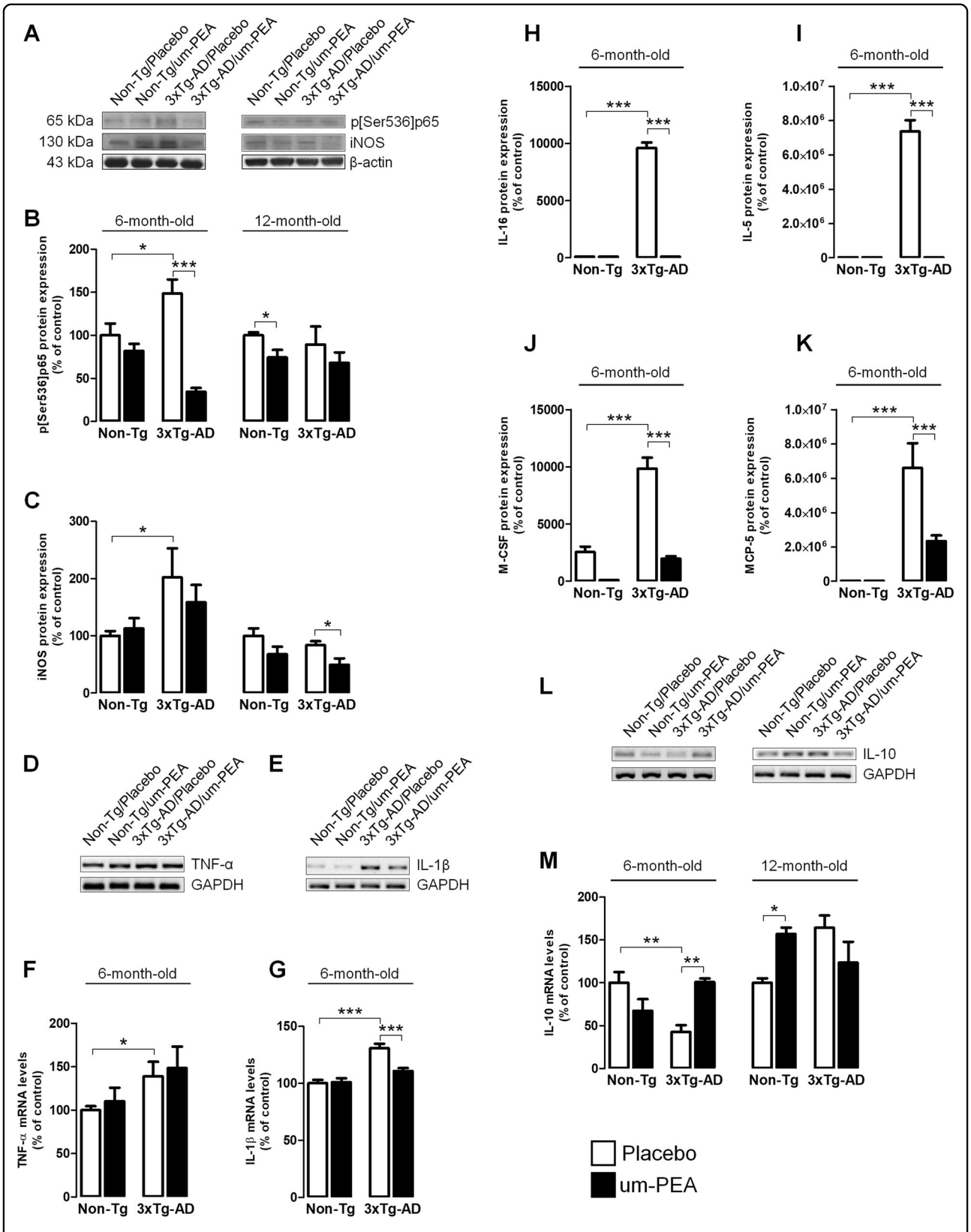

Fig. 5 (See legend on next page.)

(see figure on previous page)

Fig. 5 Um-PEA effects on neuroinflammation in hippocampus of 3×Tg-AD and Non-Tg mice. Evaluation of proinflammatory markers in hippocampi of 6- and 12-month-old 3×Tg-AD and age-matched Non-Tg mice chronically treated with placebo (open bars) or um-PEA (black bars). (**a**) Representative western blots for p[Ser536]p65 and iNOS proteins and (**b**, **c**) densitometric analyses normalized with β-actin used as loading controls. Results are expressed as percentage of control (Non-Tg/placebo groups) ($N = 3$, in triplicate). (**d**, **e**) Representative results obtained from RT-PCR in 6-month-old mice for tumor necrosis factor-α (TNF-α) and interleukin-1β (IL-1β), and (**f**, **g**) densitometric analysis of corresponding bands normalized with glyceraldehyde 3-phosphate dehydrogenase (GAPDH). Results are expressed as percentage of control (Non-Tg/placebo groups) ($N = 3$, in triplicate). (**h–k**) Densitometric analysis of cytokine array for IL-16, IL-5, macrophage colony-stimulating factor (M-CSF), and monocyte chemotactic protein 5 (MCP-5). Results are expressed as percentage of control (Non-Tg/placebo groups) ($N = 3$, in triplicate). (**l**) Representative results obtained from RT-PCR in 6- and 12-month-old mice for IL-10 and (**m**) densitometric analysis of corresponding bands normalized with glyceraldehyde 3-phosphate dehydrogenase (GAPDH). Results are expressed as percentage of control (Non-Tg/placebo groups) ($N = 3$, in triplicate). The data are presented as mean ± SEM. Statistical analysis was performed by two-way ANOVA followed by Bonferroni's multiple-comparison test (*$p < 0.05$; **$p < 0.01$; ***$p < 0.001$)

modifications occur during the early stages of AD, and demonstrate that chronically administered um-PEA restrains or reverses most of them.

These results are important as AD has important public health and economic consequences and there is a need to develop novel effective therapeutic strategies to complement or replace those in current use. It has been apparent for a long time that PEA displays marked anti-inflammatory properties in peripheral inflammation models and it has demonstrated high effectiveness in a number of neurodegenerative disorders that present with an inflammatory component, including AD, Parkinson's disease, and multiple sclerosis[10,14,36, 37]. The recent availability of um-PEA, a crystalline form on micrometric size which improves both its pharmacokinetics and bioavailability[19, 38], prompted us to test its anti-inflammatory and neuroprotective effects in 3×Tg-AD mice.

First, we found that um-PEA rescued the early hippocampal, cortex, and amygdala-dependent memory impairments seen in 3×Tg-AD mice. The youngest mice (6-month old) demonstrated the largest significant improvement of both short- and long-term memory. Less clear-cut effects were seen in the oldest mice (12-month old), where um-PEA improved short-term memory (or at least some behavioral parameters, e.g., ORI, and latency and number of crosses in the MWM), but did not induce significant effects on long-term memory. This study also demonstrates that um-PEA induces other noncognitive effects that are relevant to AD. In this regard, following the observation that a depressive-like phenotype is present in the same strain of 18-month-old 3×Tg-AD mice[24], we identified that this phenotype is already present by 6 months of age and is reversible at 6 but not at 12 months of age. However, we found that um-PEA attenuates a similar anhedonia-like phenotype of both young (6-month-old) and aging (12-month-old) 3×Tg-AD mice.

It is widely accepted that glia mediate the response to several brain injuries, including the deposition of Aβ, and undergo important morphological and functional changes that can, in turn, influence the progression of the disease. These modifications are intricate and heterogeneous, and can be crudely classified into hyperreactivity or atrophy[39, 40]. Moreover, a direct correlation has been established between glial dysfunction and the induction of proinflammatory pathways[41]. In younger mice, although we did not detect significant alterations of GFAP and S100B, the best-known markers of astrocytic activation, we found that a range of parameters suggesting an increase in neuroinflammation occurred. These were reduced by um-PEA, suggesting that it restrains the transition to a neuroinflammatory environment. A comparison of results suggests that um-PEA effects are completely different in 3×Tg-AD mice at 6 and 12 months of age. At 12 months, mice do not show any noteworthy signs of neuroinflammation and merely displayed moderate astrocyte atrophy.

Based on our results and the hypothesis that neuroinflammation accelerates the development of the AD phenotype, increasing Aβ accumulation, we explored the main elements involved in the pro-amyloidogenic pathway[42]. 3×Tg-AD mice express a mutant APP_{swe} transgene, and we recorded an accumulation of this protein in these mice at both 6 and 12 months. No accumulation of BACE1 protein occurred, however, a 15-fold higher increase in $Aβ_{(1–42)}$ expression was observed in the 3×Tg-AD compared to Non-Tg mice. Our results demonstrated the ability of um-PEA to strongly suppress $Aβ_{(1–42)}$ expression in 12-month-old 3×Tg-AD mice, suggesting an important pathway by which it can restrain the disease progression. Another iconic hallmark of AD is the formation of NFTs which are mainly caused by the abnormal phosphorylation of tau. Tau protein is a microtubule-associated protein that facilitates microtubule assembly and stabilization as a function of its phosphorylation state[30]. However, under pathological conditions, including AD, enhanced phosphorylation (known as "hyperphosphorylation") occurs, which leads to microtubule dissociation, aggregation into paired helical filaments, and

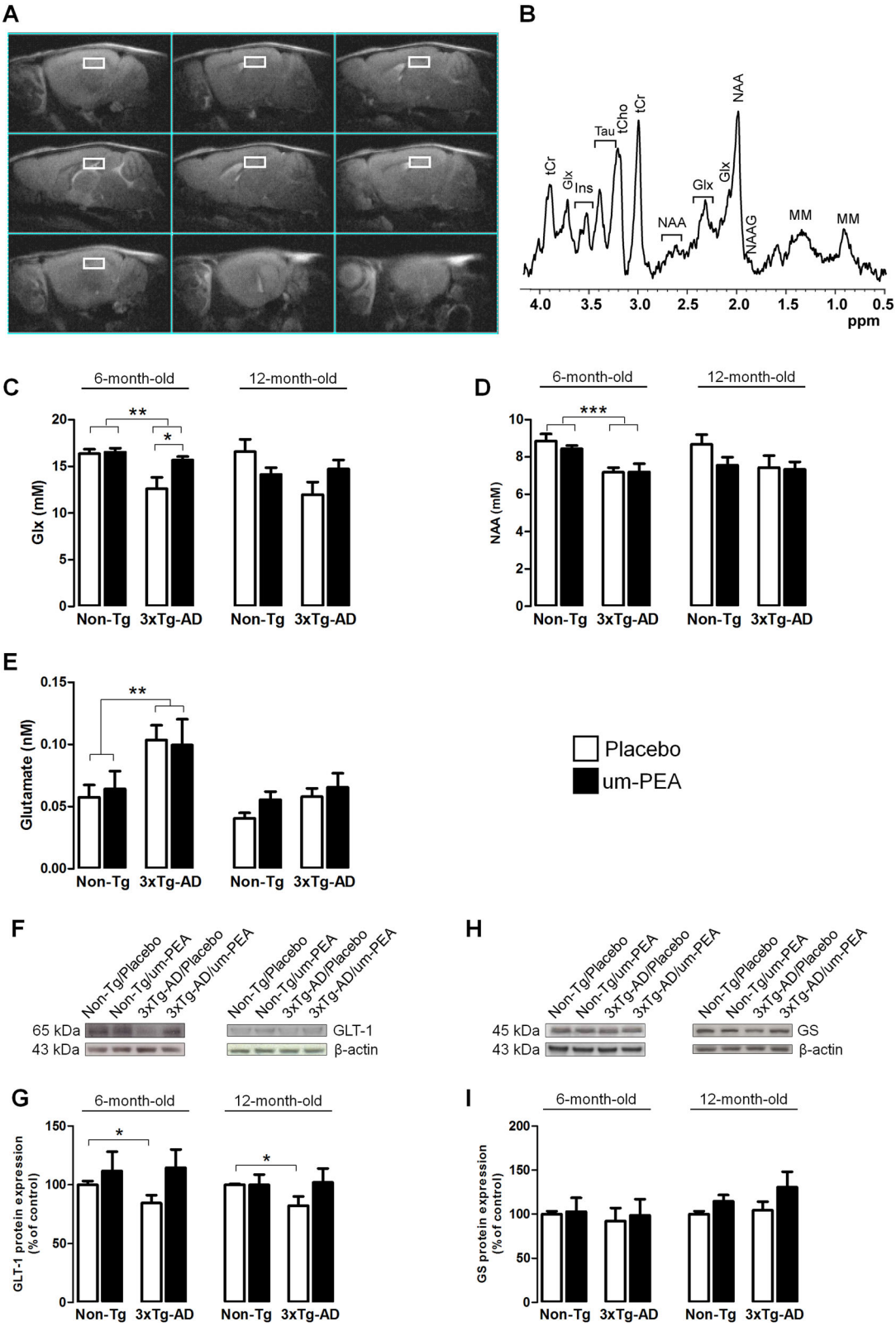

Fig. 6 (See legend on next page.)

(see figure on previous page)

Fig. 6 Um-PEA effects on brain metabolism and the glutamatergic system. Evaluation of the glutamatergic system in hippocampi of 6- and 12-month-old 3×Tg-AD and age-matched Non-Tg mice chronically treated with placebo (open bars) or um-PEA (black bars). (**a**) MRI panel—Example of *in vivo* fast spin-echo sagittal anatomical images (Repetition Time (TR)/Echo Time (TE) = 3200/60 ms, consecutive slices). Voxels localized on hippocampus are indicated by the white rectangles. (**b**) MRS panel—Examples of in vivo 1 H spectra (PRESS, TR/TE = 4000/23 ms, NS = 256). Metabolite assignments: inositol (Ins), total creatine (tCr), glutamine + glutamate (Glx), taurine (Tau), total choline (tCho), N-acetyl-aspartate (NAA), N-acetyl-aspartyl-glutamate (NAAG), and macromolecules (MM). Histograms showing (**c**) Glx and (**d**) NAA hippocampal concentrations at 6 and 12 months of age, respectively, expressed in nM ($N = 12$). (**e**) Results from HPLC on extracellular glutamate hippocampal concentrations at 6 and 12 months of age of Non-Tg and 3×Tg-AD mice. (**f**, **h**) Representative western blots for glutamate transporter 1 (GLT-1) and glutamine synthetase (GS) proteins at 6 and 12 months of age, and (**g**, **i**) densitometric analyses normalized with β-actin used as loading controls ($N = 3$, in triplicate). Results are expressed as percentage of control (Non-Tg/placebo groups). Data are presented as means ± SEM. Statistical analysis was performed by two-way ANOVA followed by Bonferroni's multiple-comparison test (*$p < 0.05$; **$p < 0.01$; ***$p < 0.001$)

the subsequent production of insoluble NFTs[43, 44]. These events worsen axonal transport and synaptic function, which facilitates the development of a neurotoxic environment and cognitive impairments[31, 32]. Several kinases add phosphate groups to tau-specific amino acids and Gsκ-3β is one of the primary kinases that are involved[30] and its activity is regulated by Akt, a serine/threonine-specific kinase[34]. We observed significant alterations of the Akt/Gsκ-3β pathway in 3×Tg-AD mice, at both mild (6-month-old) and severe (12-month-old) stages of pathology, and have also demonstrated for the first time in an *in vivo* model the ability of um-PEA to prevent such alterations, thus reducing the abnormal phosphorylation of tau. Besides the deposition of NFTs, it has been demonstrated that a disruption of astrocyte function contributes to neuronal death[39]. In this study, we also investigated the expression of the neuron-specific cytoskeletal marker, MAP2. By immunofluorescence, we show that um-PEA increases MAP2 expression in the CA1 zone of the hippocampus in 3×Tg-AD mice at 6 and 12 months of age, suggesting that um-PEA increases neuronal viability in this region, a key area for the mediation of memory formation and recall.

Alterations in both the glutamatergic system and the metabolism of the brain are well documented in AD patients[45, 46]. Employing both *in vivo* MRI/MRS scanning and microdialysis sampling, we evaluated the effects of um-PEA on neural metabolism and glutamatergic transmission in the hippocampus of mice. MRI/MRS revealed that 6-month-old 3×Tg-AD mice show a robust reduction of both Glx and NAA content compared to Non-Tg mice. This observation may underlie the substantial cognitive deficits observed at this age. Interestingly, um-PEA increased Glx content and improved the cognitive performance and behavioral abnormalities observed in 3×Tg-AD mice. Our data also highlight some intriguing potential mechanisms by which AD affects glutaminergic transmission. In younger (6-month-old) 3×Tg-AD mice, we observed a marked increase in the levels of extracellular glutamate, which is probably due to a reduced expression of a glial transporter mainly responsible for glutamate reuptake (GLT-1). Despite observing a similar trend in aging (12-month-old) mice, we did not detect any statistical difference in brain metabolites and extracellular glutamate levels, but a reduction of GLT-1 expression was still evident.

Our data extend the knowledge of the mechanisms underlying the progression of AD-like pathology in 3×Tg-AD mice and demonstrate the exceptional therapeutic potential of um-PEA in restraining the development of AD-like pathology and cognitive/behavioral declines by exerting a combination of anti-inflammatory and neuroprotective effects. Given the numerous and multitargeted effects of um-PEA that we observed, we can speculate that many molecular mechanisms are involved in mediating the actions of this compound. Despite we have already demonstrated, in other preclinical models of AD, that PEA exerts its pharmacological effects through the peroxisome proliferator-activated receptors alpha (PPARα) involvement[11–13, 47], other molecular targets should be taken into account, including PPARγ, transient receptor potential vanilloid type-1 channel, orphan G-protein-coupled receptor 55, and the so-called entourage effect on the endocannabinoid system[19]. Therefore, further experiments will be needed to address this issue. Our results indicate an interesting interaction of um-PEA treatment and the aging process, which may suggest its use as a potential preventive therapy. In aging mice, um-PEA treatment induces an effect on pathways involved in AD pathology, but the most interesting data were derived from younger mice. Indeed, changes in neural function in mice precociously treated with um-PEA (starting from 3 months of age, before any overt signs of disease) seemed to be less pronounced, suggesting the benefits of starting drug treatment at an early stage.

From the perspective of the translational potential of um-PEA in human AD, our data strongly suggest its exceptional potential as a therapy that provides clinically considerable benefits if started early enough in the continuum toward dementia. It is noteworthy that PEA,

which is already licensed for use in humans, displays a high tolerability and safety profile and would be an ideal candidate for long-term use lasting several years, as potential AD treatments require.

Summarizing, our data suggest that um-PEA exerts a robust therapeutic effect in a transgenic mouse model (3×Tg-AD) of AD, since it ameliorates both cognitive deficits and a range of neuropathological features. Despite the limits of our preclinical experimental study and avoiding any simplistic extrapolation of data from the animal model to the human condition, the results of this research suggest that um-PEA demonstrates considerable potential to have an impact on the progression of AD.

Acknowledgements
This work was supported by the Italian Ministry of Instruction, University, and Research (MIUR) to LS, and the SAPIENZA University of Rome to CS and MRB.

Author details
[1]Department of Physiology and Pharmacology "V. Erspamer", SAPIENZA University of Rome, Rome, Italy. [2]Department of Clinical and Experimental Medicine, University of Foggia, Foggia, Italy. [3]Department of Life Sciences and Biotechnology, University of Ferrara, Ferrara, Italy. [4]UCL Institute of Opthalmology, University College, University College London, London, UK. [5]C.U.R.E. Centre for Liver Diseases Research and Treatment, Institute of Internal Medicine, Department of Medical and Surgical Sciences, University of Foggia, Foggia, Italy. [6]Department of Cell Biology and Neurosciences, Istituto Superiore di Sanità, Rome, Italy. [7]Department of Psychiatry, University of Naples SUN, Naples, Italy

Conflict of interest
The authors declare that they have no competing interests.

Received: 3 November 2017 Accepted: 13 November 2017
Published online: 31 January 2018

References

1. Huang, H. C. & Jiang, Z. F. Accumulated amyloid-beta peptide and hyperphosphorylated tau protein: relationship and links in Alzheimer's disease. *J. Alzheimers Dis.* **16**, 15–27 (2009).
2. Querfurth, H. W. & LaFerla, F. M. Alzheimer's disease. *N. Engl. J. Med.* **362**, 329–344 (2010).
3. Craft, J. M., Watterson, D. M. & Van Eldik, L. J. Human amyloid beta-induced neuroinflammation is an early event in neurodegeneration. *Glia* **53**, 484–490 (2006).
4. McGeer, P. L. & McGeer, E. G. The amyloid cascade-inflammatory hypothesis of Alzheimer disease: implications for therapy. *Acta Neuropathol.* **126**, 479–497 (2013).
5. Osborn, L. M., Kamphuis, W., Wadman, W. J. & Hol, E. M. Astrogliosis: An integral player in the pathogenesis of Alzheimer's disease. *Prog. Neurobiol.* **144**, 121–141 (2016).
6. Verkhratsky, A. et al. Neurological diseases as primary gliopathies: a reassessment of neurocentrism. *ASN Neuro* **4**, e00082 (2012).
7. Burda, J. E. & Sofroniew, M. V. Reactive gliosis and the multicellular response to CNS damage and disease. *Neuron* **81**, 229–248 (2014).
8. Steardo, L. et al Does neuroinflammation turn on the flame in Alzheimer's disease? Focus on astrocytes. *Front. Neurosci.* **9**, 259 (2015).
9. Verkhratsky, A., Olabarria, M., Noristani, H. N., Yeh, C. Y. & Rodriguez, J. J. Astrocytes in Alzheimer's disease. *Neurotherapeutics* **7**, 399–412 (2010).
10. Bronzuoli, M. R., Facchinetti, R., Steardo, L. & Scuderi, C. Astrocyte: an innovative approach for Alzheimer's disease therapy. *Curr. Pharm. Des.* (2017) https://doi.org/10.2174/1381612823666170710163411.
11. Scuderi, C. et al. Palmitoylethanolamide counteracts reactive astrogliosis induced by beta-amyloid peptide. *J. Cell. Mol. Med.* **15**, 2664–2674 (2011).
12. Scuderi, C. et al. Palmitoylethanolamide controls reactive gliosis and exerts neuroprotective functions in a rat model of Alzheimer's disease. *Cell. Death Dis.* **5**, e1419 (2014).
13. Scuderi, C. et al. Palmitoylethanolamide exerts neuroprotective effects in mixed neuroglial cultures and organotypic hippocampal slices via peroxisome proliferator-activated receptor-alpha. *J. Neuroinflamm.* **9**, 49 (2012).
14. D'Agostino, G. et al. Palmitoylethanolamide protects against the amyloid-β25-35-induced learning and memory impairment in mice, an experimental model of Alzheimer disease. *Neuropsychopharmacol* **37**, 1784–1792 (2012).
15. Tomasini, M. C. et al. Differential effects of palmitoylethanolamide against amyloid-β induced toxicity in cortical neuronal and astrocytic primary cultures from wild-type and 3xTg-AD mice. *J. Alzheimers Dis.* **46**, 407–421 (2015).
16. Bronzuoli, M. R. et al. Palmitoylethanolamide dampens reactive astrogliosis and improves neuronal trophic support in a triple transgenic model of Alzheimer's disease: *in vitro* and *in vivo* evidence. *Oxid. Med. Cell. Longev.* (Article id: 4720532) Accepted 23 October 2017 (2017).
17. Oddo, S. et al. Triple-transgenic model of Alzheimer's disease with plaques and tangles: intracellular Abeta and synaptic dysfunction. *Neuron* **39**, 409–421 (2003).
18. Blázquez,G.et al.Modeling behavioral and neuronal symptoms of Alzheimer's disease in mice: a role for intraneuronal amyloid.*Neurosci. Biobehav. Rev.***31**,125–147(2007).
19. Petrosino, S. & Di Marzo, V. The pharmacology of palmitoylethanolamide and first data on the therapeutic efficacy of some of its new formulations. *Br. J. Pharmacol.* **174**, 1349–1365 (2017).
20. Grillo, S. L., Keereetaweep, J., Grillo, M. A., Chapman, K. D. & Koulen, P. N-Palmitoylethanolamine depot injection increased its tissue levels and those of other acylethanolamide lipids. *Drug. Des. Devel Ther.* **7**, 747–752 (2013).
21. Costa, B., Conti, S., Giagnoni, G. & Colleoni, M. Therapeutic effect of the endogenous fatty acid amide, palmitoylethanolamide, in rat acute inflammation: inhibition of nitric oxide and cyclo-oxygenase systems. *Br. J. Pharmacol.* **137**, 413–420 (2002).
22. Cassano, T. et al. Glutamatergic alterations and mitochondrial impairment in a murine model of Alzheimer disease. *Neurobiol. Aging* **33**, 1121.e1–12 (2012).
23. Martinez-Coria, H. et al. Memantine improves cognition and reduces Alzheimer's-like neuropathology in transgenic mice. *Am. J. Pathol.* **176**, 870–880 (2010).
24. Romano, A. et al. Depressive-like behavior is paired to monoaminergic alteration in a murine model of Alzheimer's disease. *Int. J. Neuropsychopharmacol.* **18**, pyu020 (2014).
25. Rodriguez-Ortiz, C. J. et al. Neuronal-specific overexpression of a mutant valosin-containing protein associated with IBMPFD promotes aberrant ubiquitin and TDP-43 accumulation and cognitive dysfunction in transgenic mice. *Am. J. Pathol.* **183**, 504–515 (2013).
26. Billings, L. M., Oddo, S., Green, K. N., McGaugh, J. L. & LaFerla, F. M. Intraneuronal Abeta causes the onset of early Alzheimer's disease-related cognitive deficits in transgenic mice. *Neuron* **45**, 675–688 (2005).
27. Medina, D. X., Caccamo, A. & Oddo, S. Methylene blue reduces Aβ levels and rescues early cognitive deficit by increasing proteasome activity. *Brain. Pathol.* **21**, 140–149 (2011).
28. Tomasini, M. C. et al. Delta(9)-tetrahydrocannabinol increases endogenous extracellular glutamate levels in primary cultures of rat cerebral cortex neurons: involvement of CB(1) receptors. *J. Neurosci. Res.* **68**, 449–453 (2002).
29. Canese, R. et al. Peculiar response to methylphenidate in adolescent compared to adult rats: a phMRI study. *Psychopharmacol. (Berl.).* **203**, 143–153 (2009).
30. Cleveland, D. W., Hwo, S. Y. & Kirschner, M. W. Physical and chemical properties of purified tau factor and the role of tau in microtubule assembly. *J. Mol. Biol.* **116**, 227–247 (1977).
31. Aberle, H., Bauer, A., Stappert, J., Kispert, A. & Kemler, R. Beta-catenin is a target for the ubiquitin-proteasome pathway. *EMBO* **16**, 3797–3804 (1997).
32. Zhu, L. Q. et al. Activation of glycogen synthase kinase-3 inhibits long-term potentiation with synapse-associated impairments. *J. Neurosci.* **27**, 12211–12220 (2007).

33. Engel, T., Hernandez, F., Avila, J. & Lucas, J. J. Full reversal of Alzheimer's disease-like phenotype in a mouse model with conditional overexpression of glycogen synthase kinase-3. *J. Neurosci.* **26**, 5083–5090 (2006).
34. Grimes, C. A. & Jope, R. S. The multifaceted roles of glycogen synthase kinase 3beta in cellular signaling. *Prog. Neurobiol.* **65**, 391–426 (2001).
35. Jope, R. S., Yuskaitis, C. J. & Beurel, E. Glycogen synthase kinase-3 (GSK3): inflammation, diseases, and therapeutics. *Neurochem. Res.* **32**, 577–595 (2007).
36. Esposito, E., Impellizzeri, D., Mazzon, E., Paterniti, I. & Cuzzocrea, S. Neuroprotective activities of palmitoylethanolamide in an animal model of Parkinson's disease. *PLoS. One.* **7**, e41880 (2012).
37. Rahimi, A. et al. Interaction between the protective effects of cannabidiol and palmitoylethanolamide in experimental model of multiple sclerosis in C57BL/6 mice. *Neuroscience* **290**, 279–287 (2015).
38. Impellizzeri, D. et al. Micronized/ultramicronized palmitoylethanolamide displays superior oral efficacy compared to nonmicronized palmitoylethanolamide in a rat model of inflammatory pain. *J. Neuroinflamm.* **11**, 136 (2014).
39. Rodríguez, J. J., Olabarria, M., Chvatal, A. & Verkhratsky, A. Astroglia in dementia and Alzheimer's disease. *Cell. Death. Differ.* **16**, 378–385 (2009).
40. Verkhratsky, A. & Parpura, V. Astrogliopathology in neurological, neurodevelopmental and psychiatric disorders. *Neurobiol. Dis.* **85**, 254–261 (2016).
41. Orre, M. et al. Isolation of glia from Alzheimer's mice reveals inflammation and dysfunction. *Neurobiol. Aging* **35**, 2746–2760 (2014).
42. Wozniak, M. A., Itzhaki, R. F., Shipley, S. J. & Dobson, C. B. Herpes simplex virus infection causes cellular beta-amyloid accumulation and secretase upregulation. *Neurosci. Lett.* **429**, 95–100 (2007).
43. De Ferrari, G. V. & Inestrosa, N. C. Wnt signaling function in Alzheimer's disease. *Brain. Res. Rev.* **33**, 1–12 (2000).
44. Li, H. L. et al. Phosphorylation of tau antagonizes apoptosis by stabilizing beta-catenin, a mechanism involved in Alzheimer's neurodegeneration. *Proc. Natl. Acad. Sci. USA* **104**, 3591–3596 (2007).
45. Graff-Radford, J. & Kantarci, K. Magnetic resonance spectroscopy in Alzheimer's disease. *Neuropsychiatr. Dis. Treat.* **9**, 687–696 (2013).
46. Verkhratsky, A., Steardo, L., Peng, L. & Parpura, V. Astroglia, glutamatergic transmission and psychiatric diseases. *Adv. Neurobiol.* **13**, 307–326 (2016).
47. Scuderi, C. & Steardo, L. Neuroglial roots of neurodegenerative diseases: therapeutic potential of palmitoylethanolamide in models of Alzheimer's disease. *CNS Neurol. Disord. Drug. Targets* **12**, 62–69 (2013).

Preventing neuroinflammation with co-ultramicronized palmitoylethanolamide/luteolin in an animal model of prodromal Alzheimer's disease

Facchinetti Roberta[1#], Bronzuoli Maria Rosanna[1#], Valenza Marta[1,2#], Ratano Patrizia[1,3], Steardo Luca[1], Campolongo Patrizia[1] and Scuderi Caterina[1*]

[1]Department Physiology and Pharmacology "V. Erspamer" SAPIENZA University of Rome – P.le A. Moro, 5 – 00185 Rome – Italy

[2] Epitech Group SpA – 35030 Saccolongo (PD) – Italy

[3] Nanotechnology Institute, CNR-Nanotechnology Institute, SAPIENZA University of Rome

[#] These authors contributed equally to this manuscript

[*]Corresponding Author: Dr. Caterina Scuderi, Dept. Physiology and Pharmacology "V. Erspamer" SAPIENZA University of Rome – P.le A. Moro, 5 – 00185 Rome – Italy

phone +39 06 49912713 fax +39 06 49912480

email: caterina.scuderi@uniroma1.it

Abstract

Background: At the earliest stage of dementia, the cerebral alterations leading to the disease have already been triggered, despite patients are still asymptomatic. Both beta amyloid (Aβ) accumulation and a neuroinflammatory process have been documented in prodromal Alzheimer's disease (AD) patients. Therefore, targeting neuroinflammation at this earliest phase of the disease may be a valuable therapeutic strategy. The new combination of palmitoylethanolamide (PEA) and luteolin (Lut), ultramicronized together as a single formulation (co-ultra PEALut), has been recently studied for its analgesic, anti-inflammatory and neuroprotective effects. Moreover, co-ultra PEALut has been marked as safe in humans and already approved as dietary food for special medical purposes. **Methods:** Here we tested the anti-inflammatory and neuroprotective effects of chronic co-ultra PEALut treatment in an animal model of prodromal sporadic AD. Rats were unilaterally injected with $A\beta_{(1-42)}$(5 μg) in the dorsolateral hippocampus to model the very first modifications in Aβ amount into this brain area documented in prodromal AD, while control rats received vehicle. Co-ultra PEALut systemic administration (5 mg/kg or vehicle) was started on the day of intracerebral infusion and continued for 14 consecutive days, as treatment strategy for the earliest disease stage. On day 15, rats were sacrificed, and molecular analysis performed by immunofluorescence and real time-qPCR. **Results:** Results show that chronic co-ultra PEALut was able to dampen the astrogliosis and microgliosis observed in Aβ-treated rats. Here we provide the first *in vivo* evidence that co-ultra PEALut prevented the Aβ-induced upregulation in gene expression of pro-inflammatory cytokines and enzymes, as well as the reduction of mRNA levels of two neurotrophins, BDNF and GDNF, ultimately promoting neuronal survival in our experimental conditions.

Conclusions: Results here presented support the notion that targeting neuroinflammation during prodromal sporadic AD may be a valuable therapeutic strategy, and that chronic co-ultra PEALut treatment may be beneficial in prodromal AD patients.

Keywords

Neuroinflammation, reactive gliosis, palmitoylethanolamide, luteolin, co-ultramicronized PEALut, prodromal Alzheimer's disease, $A\beta_{(1-42)}$ intracerebral inoculation, western blot, immunofluorescence, PCR.

Background

Alzheimer's disease (AD) is a multifactorial neurodegenerative disease of the brain, clinically characterized by progressive memory loss and cognitive decline leading to dementia and functional disability [1, 2]. The onset of AD is insidious since clinical symptoms manifest years after structural alterations of the brain have already established. According to the 2011 guidelines published by the National Institute on Aging (NIA), AD is preceded by an early stage of dementia, named prodromal AD, in which the cellular and molecular alterations leading to the disease have been already triggered, but an affected person can be still asymptomatic, therefore independent and unaware of his clinical condition as well [3-5]. At the molecular level, AD lesions consist of deposits of beta amyloid (Aβ) peptides in the extracellular space and of neurofibrillary tangles inside neurons. Aβ accumulation has been documented in asymptomatic patients [6] and both histopathological and structural studies have shown that the hippocampus is one of the first brain areas affected [7, 8].

Currently approved therapies for AD are not curative and provide only symptom management, resulting in modest and/or transient benefits to a subset of patients. Since the start of an intervention at the earliest stage of the disease could have a powerful impact on slowing or blocking pathology progression [9-11], the prodromal phase of AD represents a temporal window in which it may be possible to reduce both risk and incidence of the disease [12-14]. However, few preclinical data are available using this specific time point as therapeutic strategy. With the aim to contribute in filling this gap, we designed an *in vivo* pharmacological study focused on this preclinical stage of the disease.

Together with abnormal protein deposits, it is now established that neuroinflammation represents the third hallmark found in AD patients' brains. This notion is supported by numerous neuropathological observations together with some recent genetic data [15-17]. Many scientists agree that the neuroinflammatory process begins at the earliest pre-symptomatic phase of AD, bringing both positive and negative consequences [15, 18-21]. Indeed, the brain immune system recognizes the abnormal accumulation of proteins as injurious stimuli, so it triggers a physiological reaction to defend the brain, called reactive gliosis, that includes activation of glial cells and release of proinflammatory molecules [22, 23]. When the neuroinflammatory process is protracted, it becomes detrimental promoting glial cell reactivity or atrophy and neuronal degeneration, thus fostering AD progression [24, 25]. However, some preclinical and clinical investigations have documented foci of activated microglia and astrocytes before any amyloid deposition, suggesting that neuroinflammation occurs first, followed by plaques formation [26, 27]. Based on these considerations, targeting pathological reactive gliosis at the very earliest stage of the disease seems to represent a valuable therapeutic approach [28-31].

Compounds able to control glial activation with a combination of neuroprotective and anti-inflammatory effects constitute a pool of possible therapeutic drugs to study. Among them, we and other groups have already shown that palmitoylethanolamide (PEA), a naturally occurring amide of ethanolamine and palmitic acid, exerts anti-inflammatory and neuroprotective properties in several preclinical models of AD [32-36].

In parallel, the flavonoid luteolin (3,4,5,7-tetrahydroxyflavone; Lut), found in different edible plants, showed antioxidant, anti-inflammatory as well as memory-improving properties [37-39].

Recent studies showed that a novel formulation containing both PEA and Lut, ultramicronized together at fixed doses (co-ultra PEALut; 10:1 by mass), exhibits good bioavailability [40, 41] and is more efficacious than the two compounds alone [42-44]. This is probably related to the inhibition of PEA crystallization process performed by Lut, ultimately leading to highly stable microparticles [45]. No data are available yet on the effects of co-ultraPEALut administration in an *in vivo* model of AD.

We have recently demonstrated the efficacy of a formulation of ultramicronized PEA (um-PEA) in reducing several molecular and behavioral signs of 3×Tg-AD mice at two different stages (mild and severe) of AD-like pathology[46]. Interestingly, the efficacy of um-PEA was particularly potent in younger mice, suggesting its potential as an early treatment. Therefore, our hypothesis was to test the efficacy of co-ultra PEALut in the early pre-symptomatic phase of the disease, focusing our attention on its ability in dampening neuroinflammation. To this aim, we decided to use a surgical model of AD. In fact, among the preclinical models, the 3×Tg-AD is considered the closest to the human disease [47]; however, it mainly recapitulates some features of the familial form of AD, which is the least frequent among the general population [2]. Keeping in mind that the common interest gravitates around the most frequent sporadic form of AD, in the present study we tested for the first time the potential anti-inflammatory and neuroprotective effects of co-ultra PEALut in a model of prodromal sporadic AD. Our animal model, obtained by a single intrahippocampal inoculation of $A\beta_{(1-42)}$ in adult rats, allows to study the Aβ-induced reactive gliosis [32, 48]. To model the prodromal stage of AD as a strategic therapeutic window for treatment, co-ultra PEALut systemic administration was started on the day of the surgical $A\beta_{(1-42)}$ peptide infusion, and continued daily for 14 consecutive days. This timing of treatment has been chosen because our intention was to test the efficacy of co-ultra PEALut during the pre-

symptomatic stage of the disease. In fact, we have already demonstrated that, in these experimental conditions, animals start to exhibit modest learning and memory deficits only 21 day after Aβ injection [32]. In agreement, no behavioral modifications were observed in the current study (data not shown). Gene and protein expression analyses of markers for astrocyte and microglia activation, as well as for parameters of neuroinflammation, were investigated in the hippocampi at the end of treatment. Further, since co-ultraPEALut exerted neuroprotective effects in models of neurological conditions that share some features with AD, such as cerebral ischemia, traumatic brain injuries and vascular dementia [44, 49-51], we studied both the healthy state of neurons and two markers for neuronal support. Indeed, neurotrophins are important regulators of neuronal survival and growth, pruning, differentiation and myelination, including the brain-derived neurotrophic factor (BDNF) and the glial cell line-derived neurotrophic factor (GDNF) [52]. Brains from AD patients as well as of asymptomatic patients during the prodromal stages of AD show reduced release of neurotrophic factors, which has been associated with cognitive deficits [53, 54]. Therefore, we investigated whether our model of prodromal AD showed altered release of both BDNF and GDNF, and if chronic administration of co-ultraPEALut was able to modulate it.

Results collected in the present study have translational relevance since co-ultra PEALut has already been licensed for human use (Glialia®) as a dietary food for special medical purposes. Co-ultra PEALut has demonstrated good safety and tolerability, thus representing a valid tool for a long-lasting treatment as AD requires. To the best of our knowledge, it has already been tested in patients with stroke undergoing neurorehabilitation as well as in a single patient with mild cognitive impairment [51, 55], resulting in beneficial effects.

Methods

Animals

Adult male Sprague-Dawley rats (250-275 g at the time of surgery; Charles River Laboratories, Calco, Italy) were individually housed in a 12-h light/dark cycle (lights ON at 7AM, OFF at 7PM) behavioral facility, at controlled conditions (20 ± 1 °C temperature), with *ad libitum* food and water.

All procedures involving animal care or treatments were approved by the Animal Care and Use Committee of the Italian Ministry of Health (prot.19/1/2012) and performed in compliance with the guidelines of the Directive 2010/63/EU of the European Community Council. All efforts were made to minimize animal suffering and to reduce the number of animals used.

Surgical procedures

Stereotaxic surgeries and $A\beta_{(1-42)}$ intracerebral inoculation were performed as previously published [32, 56] and shown in Fig. 1a. Briefly, rats (*n*=4-5 for each experimental group) were anesthetized with sodium pentobarbital 50 mg/kg, *i.p.*, and placed in a stereotaxic frame. An injector, connected to a tubing linked to a microsyringe mounted on a microdialysis pump, was lowered to reach the dorsal hippocampus (HPC), using the following coordinates relative to the bregma: AP - 3 mm; ML ± 2.2 mm, and DV - 2.8 mm [57]. A volume of 2.5 µl containing 5 µg of human fibrillary $A\beta_{(1-42)}$ was unilaterally inoculated at a 0.5 µl/min rate. To minimize backflow and facilitate diffusion, the needle was left in place for an additional 5-8 min after injection [56]. An equal volume of artificial cerebrospinal fluid (aCSF) was inoculated in control rats undergoing the same surgical procedure.

Drugs and drug treatment

Human $A\beta_{(1-42)}$ was purchased from Tocris Cookson (Bristol, UK). $A\beta_{(1-42)}$ was dissolved in sterile aCSF at the concentration of 2 µg/µl. The solution was incubated at 37°C for at least 24 h to obtain the peptide in its fibrillary form [32]. Five µg of fibrillary $A\beta_{(1-42)}$ were injected unilaterally into the dorsal hippocampus. Vehicle rats were similarly inoculated with an equal volume (2.5 µl) of aCSF, referred in all figures as vehicle (Veh).

A preparation containing co-ultramicronized PEA and Lut (co-ultraPEALut; 10:1, by mass; kind gift of Epitech Group SpA - Saccolongo, Italy) was dissolved in 10 % pluronic F-68 (Sigma-Aldrich, Saint Louis, MO, USA), solubilized in 90 % saline and injected intraperitoneally (*i.p.* 5 mg/kg; 1 ml/kg). Control rats received *i.p.* an equivalent volume of vehicle, referred in all figures as vehicle (Veh). Doses were chosen according to the literature [58] as well as pilot experiments (data not shown).

The timeline of the drug treatment schedule is reported in Fig. 1b. Rats underwent surgical intrahippocampal inoculation of human fibrillary $A\beta_{(1-42)}$ (5 µg or vehicle). Starting on the day of surgery, rats were treated *i.p*. with co-ultraPEALut (5 mg/kg or vehicle) once a day for 14 consecutive days. On day 15, rats were sacrificed, and brains extracted for molecular analyses.

Quantitative real-time polymerase chain reaction

Rats were sacrificed 24 h after the last co-ultraPEALut systemic injection. Each brain was rapidly extracted, the dorsal hippocampi isolated and stored at -80°C for subsequent RT-qPCR analysis.

mRNA isolation and analyses were performed as previously described [59, 60]. Briefly, total mRNA was isolated from hippocampi using TRI-Reagent (Sigma-Aldrich) following manufacturer's instructions. mRNA was quantified by D30 BioPhotometer spectrophotometer

(Eppendorf AG, Hamburg, Germany), detecting mRNA absorbance at 260 nm. 1 µg of mRNA was reverse transcribed to cDNA using the first-strand cDNA synthesis kit, in presence of 0.2 µM oligo(dT) and 0.05 µg/µl random primers (all from Promega, Promega Corporation, WI, USA). The thermal protocol included a step at 25°C for 10 min and one at 72°C for 65 min. Primers were custom designed specific for the cluster of differentiation 11b (CD11b), the inducible nitric oxide synthase (iNOS) (Bio-Rad, Hercules, CA, USA), the cyclooxygenase (COX)-2 (Bio-Fab laboratories, Rome, Italy), the interleukin (IL)-1β (BioRad), the IL-6 (Bio-Rad), the tumor necrosis factor (TNF)-α (Bio-Fab laboratories), the IL-10 (Bio-Rad), the glial-derived neurotrophic factor (GDNF) (Bio-Fab laboratories) and the brain-derived neurotrophic factor (BDNF) (Bio-Fab laboratories). Primers (500-800 nM) and cDNA (20 ng) were mixed with the iTaq Universal SYBR Green Supermix (Bio-Rad). The amount of each target amplicon was normalized to the mean mRNA of two reference genes, the TATA-box binding protein (TBP) and the hypoxanthine guanine phosphoribosyl transferase (HPRT) (Bio-Fab laboratories). All primers sequences and details are listed in Table 1. The thermal protocol used for amplification included an initial step at 95°C for 3 min and 40 cycles with one step at 95°C for 10 sec and one at 60°C for 30 sec. Primers efficiency was confirmed by the melting curve analysis of the amplification products, obtained at the end of the reaction of the amplification cycles increasing the temperature from 65 to 95°C with step of 0.5°C, carrying out the fluorescence reading at each step. The experiments were executed using the CFX96 Touch thermocycler (Bio-Rad). For each gene of interest, four independent experiments were performed in triplicate. Data are expressed as ΔΔCq, calculated using the CFX Manager software (Bio-Rad).

Table 1. List of primer sequences, general conditions and validation parameters used to perform real-time quantitative PCR

Gene		Primer (5' → 3')	Annealing (°C)	Efficiency (%)	R^2
CD11b	Forward	N/A (Cod. qRnoCID0002800, Bio-Rad)	60	94.0	.990
	Reverse				
iNOS	Forward	N/A (Cod. qRnoCED0020417, Bio-Rad)	60	98.0	.999
	Reverse				
COX-2	Forward	GATGACGAGCGACTGTTCCA	60	99.7	.991
	Reverse	TGGTAACCGCTCAGGTGTTG			
IL-1β	Forward	N/A (Cod. qRnoCID0004680, Bio-Rad)	60	98.0	.999
	Reverse				
IL-6	Forward	N/A (Cod. qRnoCID0053166, Bio-Rad)	60	94.0	.998
	Reverse				
TNF-α	Forward	CCACCACGCTCTTCTGTCTA	60	104.7	.984
	Reverse	CTTGTTGGGACCGATC ACCC			
IL-10	Forward	N/A (Cod. qRnoCID0005930, Bio-Rad)	60	98.0	.999
	Reverse				
GDNF	Forward	CACCAGATAAACAAGCGGCG	60	99.8	.989
	Reverse	TCGTAGCCCAAACCCAAGTC			
BDNF	Forward	GGGACTCTGGAGAGCGTGAA	60	103.8	.996
	Reverse	GTCAGACCTCTCGAACCTGC			
HPRT	Forward	TCCCAGCGTCGTGATTAGTGA	60	98.3	.992
	Reverse	CCTTCATGACATCTCGAGCAAG			
TBP	Forward	TGGGATTGTACCACAGCTCCA	60	99.7	.995
	Reverse	CTCATGATGACTGCAGCAAACC			

Immunofluorescence

Immunofluorescence analysis was performed as previously reported [60, 61]. Rats were sacrificed 24 h after the last co-ultra PEALut injection and brains were immediately extracted, flash frozen using 2-methylbutane, and stored at -80°C [62]. Coronal slices (20 μm thickness) containing the dorsal hippocampal regions were obtained using a cryostat (Thermo Fisher Scientific, Waltham, MA, USA) and immediately mounted on slides. Hippocampal slices were then fixed through a bath in 4% paraformaldehyde, prepared in 0.1M phosphate buffer saline (PBS), for 10 min at 4°C. Experimental conditions for immunofluorescence staining are summarized in Table 2. Briefly, sections were blocked in a solution of 5% bovine serum albumin (BSA) in PBS containing 0.25% Triton X-100 (PBS/Triton) for 60 min, at room temperature. Slices were incubated overnight at 4°C, in the same blocking solution in which one of the following primary antibodies was diluted: rabbit anti-glial fibrillary acidic protein (GFAP; 1:1000, Abcam, Cambridge, UK), rabbit anti-ionized calcium-binding adapter molecule 1 (Iba1; 1:1000, Wako, Pure Chemical Industries, Osaka, Japan), mouse anti-microtubule associated protein-2 (MAP-2; 1:250, Novus Biologicals, Littleton, CO, USA). After rinses (2x10 min plus 1x5 min) with PBS/Triton, sections were incubated in the proper secondary antibody (1:200, fluorescein-affinipure goat anti-rabbit IgG (H+L); 1:300, rhodamine-affinipure goat anti-mouse IgG (H+L), all from Jackson ImmunoResearch, Suffolk, UK) dissolved in fresh BSA-PBS/Triton solution for 2 h at room temperature. Nuclei were stained with Hoechst (Thermo Fisher Scientific) diluted 1:500 in double distilled water. Slides were mounted with Fluoromount aqueous mounting medium (Sigma Aldrich) and coverslipped. Fluorescent signal was detected by an Eclipse E600 microscope using Nikon Plan 10X/10.25 and Nikon Plan Fluor 20X/0.5 objectives (Nikon Instruments, Rome, Italy). Pictures were captured by a QImaging camera (Surrey, BC, Canada) with NISelements BR 3.2 64-

bit software (Nikon Instruments). Gain and time exposure were kept constant during all image acquisitions to prevent artifacts. Image analysis was performed using Fiji software. Data were expressed as the ratio of the difference between the mean target fluorescence signal and its background (ΔF) to the non-immunoreactive region signal (F_0).

Table 2. Immunofluorescence experimental conditions

Primary antibody	Brand	Dilution	Secondary antibody	Brand
Rabbit α-GFAP	Abcam	1:200 5% BSA in PBS/0.25% triton X-100	FITC conjugated goat anti-rabbit IgG (H+L) 1:200, 5% BSA in PBS/0.25% triton X-100	Jackson ImmunoResearch
Rabbit α-Iba1	Wako	1:1000 1% BSA in PBS/0.25% triton X-100	FITC conjugated goat anti-rabbit IgG (H+L) 1:200, 0.5% BSA in PBS/0.25% triton X-100	Jackson ImmunoResearch
Mouse α-MAP-2	Novus Biologicals	1:200 5% BSA in PBS/0.25% triton X-100	TRITC conjugated goat anti-mouse IgG (H+L) 1:200, 0.5% BSA in PBS/0.25% triton X-100	Jackson ImmunoResearch

Statistical analysis

Statistical analysis was performed using GraphPad Prism software version 6.0 (GraphPad Software, San Diego, CA, USA). Data were analyzed by two-way analysis of variance (ANOVA) and, upon detection of a main significant effect or interaction, multiple comparisons were carried out by the Bonferroni's post-*hoc* test. Differences between mean values were considered statistically significant when $p<0.05$.

Results

Co-ultraPEALut prevented protracted astrocyte activation induced by $A\beta_{(1-42)}$challenge

We tested the effects of chronic administration of co-ultra PEALut in modulating astrogliosis induced by a single intrahippocampal $A\beta_{(1-42)}$ peptide infusion. Among glial cells, astrocytes are the most abundant. They provide trophic, metabolic and synaptic support to neurons, contributing to brain homeostasis [63, 64]. Here, we assessed the astrocytic cytoskeletal protein GFAP to study the morphological changes occurring on astrocytes upon activation [65, 66].

As shown in Figure 2, a significantly stronger GFAP immunofluorescence signal was detected in $A\beta_{(1-42)}$-inoculated rats compared to the one detected in control rats, suggesting that astrocytes were still activated 15 days after a single Aβ peptide infusion. $A\beta_{(1-42)}$-inoculated rats that received daily systemic co-ultra PEALut showed significantly lower GFAP expression compared to rats systemically treated with the respective vehicle.

Co-ultraPEALut blocked microglia activation induced by $A\beta_{(1-42)}$challenge

We tested the effects of chronic administration of co-ultra PEALut in modulating activation of microglia induced by a single intrahippocampal $A\beta_{(1-42)}$peptide infusion. Microglia are the brain-resident phagocytes and antigen presenting cells [67]. We investigated microglial morphology studying the Iba1 and CD11b. The first is a marker for microglial cytoplasmic processes, which serve as the cell sensors for exploring their surroundings [68], while CD11bis a marker expressed by both activated local microglia and circulating monocytes, reaching the site of brain injury [64]. As shown in Fig. 3a and 3b, CA1 region of hippocampus from $A\beta_{(1-42)}$-inoculated rats showed higher level of Iba1 protein immunolabeling than the ones from their vehicle-infused counterparts.

Chronic *i.p.* administration with co-ultra PEALut completely blocked the raise in Iba1 protein fluorescent signal in $A\beta_{(1-42)}$-inoculated rats compared to rats that received systemic vehicle.

Moreover, CD11b gene expression was found higher in the hippocampi of rats that received a single $A\beta_{(1-42)}$ stereotaxic infusion compared to their respective vehicle rats (Fig. 3c). Chronic systemic administration of co-ultra PEALut, but not vehicle, prevented such increase.

Co-ultraPEALut administration prevented the gene expression upregulation of several proinflammatory compounds induced by $A\beta_{(1-42)}$challenge

We then examined the possible anti-inflammatory effect of chronically administered co-ultra PEALut on gene expression of several proinflammatory mediators involved in the pathological neuroinflammatory process. In different preclinical models of AD, we have already showed the $A\beta_{(1-42)}$-augmented expression of both iNOS and COX-2, two enzymes responsible for NO and prostaglandins production respectively, as well as of pro-inflammatory cytokines, such as IL-1β, IL-6 and TNF-α [33, 69, 70]. IL-1β is critically involved in AD pathophysiology since its production, stimulated by Aβ, promotes glial activation perpetuating its further release [71-73]. Low levels of anti-inflammatory mediators, such as IL-10, has been documented too [74].

As shown in Fig. 4a and 4b, gene expression of both iNOS and COX-2 was significantly higher in rats that received a single intrahippocampal $A\beta_{(1-42)}$ infusion compared to vehicle-injected rats. Chronic administration of co-ultra PEALut significantly prevented such increase, compared to $A\beta_{(1-42)}$-inoculated rats that received systemic vehicle.

Also, as shown in Fig. 4c, 4d and 4e, the gene expression of all pro-inflammatory cytokines here investigated was upregulated after $A\beta_{(1-42)}$ infusion compared to vehicle, and chronic co-ultra PEALut treatment was able to prevent it. Furthermore, $A\beta_{(1-42)}$-inoculated rats showed a

significantly lower IL-10 mRNA level, as shown in Fig. 4f. Daily co-ultra PEALut, but not its vehicle, administration significantly normalized it.

Co-ultraPEALut promoted neuronal survival impaired by Aβ(1-42)challenge

We also tested the hypothesis that systemic co-ultra PEALut, given concurrently with intracerebral Aβ(1-42)challenge and continued consecutively for two weeks, would prevent Aβ(1-42)-altered release of neurotrophins and the connected neuronal damage. GDNF is involved in neuronal survival and plasticity and it is produced by both neurons and astrocytes [75]. Activated astrocytes, after brain injury, may up-regulate GDNF production [76]. BDNF is a neurotrophin produced by neurons, but also expressed by astrocytes after brain injury [77], promoting neuronal growth and survival, and participating in the synaptic processes of memory [52].

Results from RT-qPCR analysis showed significantly lower levels of both GDNF and BDNF mRNA in the hippocampus of Aβ(1-42)-inoculated rats compared to vehicle-infused animals. Chronic treatment with co-ultra PEALut, but not vehicle, significantly prevented the reduced gene expression of both neurotrophins in Aβ(1-42)-treated rats.

To study the possible beneficial effect of chronic treatment with co-ultra PEALut on neurons, we labeled cells for MAP-2, a specific neuronal protein of the cytoskeleton, in the CA1 sub-region of the hippocampus. As shown in Fig. 6, protein immunoreactivity was significantly lower in Aβ(1-42)-inoculated rats compared to vehicle, possibly suggesting neuronal death. Chronic systemic treatment with co-ultra PEALut, but not vehicle, prevented the reduction of MAP-2 fluorescent signal detected in Aβ(1-42)-treated rats.

Discussion

The aim of the present study was to test for the first time *in vivo* the hypothesis that chronic systemic administration of co-ultra PEALut exerts anti-inflammatory and neuroprotective effects in a model of prodromal sporadic AD. Our data confirmed that a single intrahippocampal $A\beta_{(1-42)}$ infusion (5 μg) in adult rats was able to induce a prolonged neuroinflammatory response, such that we were able to detect local activation of astrocytes and microglia 15 days after surgical infusion, together with upregulated gene expression of pro-inflammatory cytokines and enzymes, reduced mRNA levels of the anti-inflammatory cytokine IL-10 and of two neurotrophins, BDNF and GDNF. We show here, for the first time, that chronic systemic administration of co-ultra PEALut (*i.p.* 5 mg/kg), started on the day of $A\beta_{(1-42)}$ challenge and continued for 14 consecutive days, prevented such molecular alterations in all parameters of neuroinflammation examined. Furthermore, systemic treatment with co-ultra PEALut displayed neuroprotective effects by upregulating gene expression of neurotrophins and promoting neuronal health in our experimental conditions.

To date, none of the drugs currently approved for AD are effective [2, 13]. Clinical research has mainly focused its efforts on inhibitors of the enzymes that cut APP and antibodies against various forms of Aβ without success [78, 79].Therefore, novel therapeutic strategies are needed. Several reports highlight the importance of starting AD therapeutic intervention as early as possible, targeting asymptomatic individuals but at risk of developing AD, in order to treat them before the onset of irreversible neuronal degeneration and cognitive deficits [12, 13, 80, 81]. Most of preclinical data available so far is based on experiments carried out in models of full-blown AD

neuropathology. Therefore, to answer this clinical need, we aimed at producing novel translational evidence supporting the pharmacological use of a novel drug in the pre-symptomatic stage of AD.

Among all molecular alterations occurring in AD patients, neuroinflammation is one of the first to take place and it has been documented in the prodromal phase of AD [18, 25, 82]. In the present study, we aimed at reproducing *in vivo* this pathological AD hallmark using our previously published surgical AD model, in which adult rats were challenged once with 5 μg human fibrillary $A\beta_{(1-42)}$ peptide in the hippocampus [32]. Damage in this cerebral area and its connected structures leads to difficulties to remember or learn new information, one of the most common symptoms of AD [83, 84]. One benefit of using this *in vivo* model is that it simulates some features of sporadic AD, the most frequent form affecting patients, in contrast to the genetic form, which accounts for the 5-10% of all AD cases, and partially reproduced by numerous genetic models available [46, 64]. We have previously shown that rats inoculated with fibrillary $A\beta_{(1-42)}$ into their hippocampus show reversal learning deficits three weeks after injection [32]. This rat behavioral impairment can be partially matched to working-like memory in humans [85, 86], which has been considered an early marker for AD [87, 88]. Our results confirmed the establishment of a marked neuroinflammatory process occurring in the rat hippocampi surgically infused with $A\beta_{(1-42)}$, since we found astrogliosis and microgliosis 15 days after $A\beta_{(1-42)}$ challenge, detected as increased immunofluorescent cells labeled with GFAP and Iba1, respectively. Further, gene expression of both iNOS and COX-2 enzymes as well as of TNF-α, IL-1β, IL-6 were found upregulated in $A\beta_{(1-42)}$ rats compared to control vehicle-inoculated rats. These results are in line with what we and other groups have reported in both *in vitro* and *in vivo* models of neuroinflammation in AD [69, 89, 90]. Interestingly, in a previous study carried out in a genetic model of AD, we detected the

presence of neuroinflammation in 6 months, but not 12 months, old 3×Tg-AD mice [46, 61]. This, together with the present data, supports our current hypothesis that treatment strategies directed to control reactive gliosis need to target the early phase of AD.

A growing body of evidence shows that PEA, an endogenous lipid messenger produced on demand in the brain by glial cells, displays analgesic, antidepressant, anti-inflammatory and neuroprotective effects in several preclinical models of a variety of diseases, including AD [91-94]. Indeed, we have previously demonstrated that acute PEA administration (10mg/kg) was effective *in vivo* in controlling parameters of astrocytosis and neuroinflammation, exerting neuroprotective properties as well [32]. Our group and others have also proposed a mechanism by which PEA modulates its actions involving the peroxisome proliferating receptor alfa (PPARα). The pharmacological blockade of this receptor was able to partially or completely suppress PEA effects in several *in vitro* and *in vivo* models [89, 95-100]. This mechanism of action was also confirmed by the partial or full absence of PEA-mediated responses in a murine model carrying the genetic ablation of the PPARα [101, 102].

To overcome the limits for administration imposed by its lipid structure, PEA has been ultramicronized and tested for oral bioavailability and pain relieving effect, demonstrating both superior absorption and efficacy compared to naïve formulations [41, 103]. Um-PEA also demonstrated anti-inflammatory properties reversing the upregulation of GFAP, iNOS, IL-1β, TNF-α, MAP-2 detected in 6 months old 3×Tg-AD mice [46, 104]. Um-PEA was more potent in younger mice than in older ones, suggesting its potential as an early treatment strategy. Recently, a different formulation has been synthetized where PEA was ultramicronized together with the

flavonoid Lut, which has mainly antioxidant properties [105]. Lut demonstrated efficacy in improving spatial learning and memory impairment in rats, relevant features detected in AD patients [106]. Lut alone effectively reduced the levels of inflammatory mediators and cytokines induced by fibrillary Aβ [107]. Superior properties of co-ultra PEALut compared to the two compounds alone has been shown [40, 42, 44]. Indeed, small quantities of Lut are sufficient to modify the crystallization behaviour of PEA, improving the physicochemical feature of the resulting co-ultramicronized composite [45]. Co-ultra PEALut has been recently tested *in vitro* showing efficacy in reducing GFAP, IL-1β, TNF-α, iNOS, GDNF and BDNF in both human neuronal cells and in rat hippocampal slice cultures challenged with Aβ [90]. Here we report the first *in vivo* evidence on the efficacy of chronic co-ultra PEALut treatment in blunting early signs of neuroinflammation in a model of prodromal sporadic AD.

Low levels of BDNF and GDNF have been documented in prodromal AD patients [53, 54]. Similarly, in the currently used animal model, an altered neurotrophic support from glial cells was detectable in the hippocampus of $A\beta_{(1-42)}$-inoculated rats even 15 days after infusion, as decreased gene expression levels of GDNF and BDNF compared to control vehicle-infused rats. Chronic systemic treatment with co-ultra PEALut was able to prevent such alteration. This neuroprotective effect of co-ultra PEALut is of particular importance since BDNF and GDNF are key neurotrophins regulating neuronal branching, synaptic plasticity, and supporting the growth and survival of several neuronal populations [108]. In accordance with the present data, Li et al. observed that PEA treatment was able to revert the decrease in BDNF and GDNF concentrations in the hippocampus through the participation of the PPARα signaling pathway, in a rodent model of stress-induced depression [94]. As consequence of the poor neurotrophic support,

intrahippocampal $A\beta_{(1-42)}$ injection was sufficient to induce neuronal damage in our experimental condition, detected as lower immunofluorescent signal of the neuronal marker MAP-2. Chronic treatment with co-ultra PEALut prevented the establishment of such alteration, thus promoting neuronal survival, as suggested by the normalized level of MAP-2 positive signal found in $A\beta_{(1-42)}$ rats chronically treated with co-ultra PEALut instead of vehicle. This is in line with data from Paterniti et al. [109] obtained *in vitro*.

Conclusions

Taken together our data expand the knowledge on the efficacy of chronic co-ultra PEALut administration as an anti-inflammatory and neuroprotective drug in an animal model of prodromal sporadic AD. Future studies will demonstrate *in vivo* the synergy of action and elucidate the mechanism underlying the association of PEA with Lut. The translational value of the present study is supported by the recent approval of co-ultra PEALut for human use as dietary food for special medical purposes(Glialia®). One report has already tested Glialia® (700 mg PEA/70 mg Lut daily for 9 months) in an asymptomatic 67-year-old woman affected by mild cognitive impairment, the clinical phase immediately before full-blown AD, resulting in a significant improvement of her neuropsychological performances [55]. Taken together with that report, our preclinical results impel towards a rapid translation of them into the clinical practice as a preventive therapeutic strategy for AD.

List of abbreviations

aCSF: artificial cerebrospinal fluid; AD: Alzheimer's disease; ANOVA: analysis of variance; APP: amyloid precursor protein; Aβ: beta amyloid; BDNF: brain derived neurotrophic factor; BSA: bovine serum albumin; CD: cluster of differentiation; COX-2: cyclooxygenase-2; FITC: fluorescein isothiocyanate;GDNF: glial derived neurotrophic factor; GFAP: glial fibrillary acidic protein; HPRT: hypoxanthine guanine phosphoribosyl transferase; *i.p.*: intraperitoneally; Iba1: ionized calcium-binding adapter molecule 1; IL: interleukin; iNOS: inducible nitric oxide synthase; Lut: luteolin; MAP-2: microtubule associated protein-2; PBS: phosphate buffer saline; PEA: palmitoylethanolamide; PPARα: peroxisome proliferating receptor alpha; TBP: TATA-box binding protein; TNF-α: tumor necrosis factor-alpha; TRITC: tetramethylrhodamine; um-PEA: ultramicronized-palmitoylethanolamide; Veh: vehicle.

Declarations

Ethics approval and consent to participate

All procedures involving animal care or treatments were approved by the Animal Care and Use Committee of the Italian Ministry of Health (prot.19/1/2012) and performed in compliance with the guidelines of the Directive 2010/63/EU of the European Community Council

Consent for publication

Not applicable

Availability of data and materials

The datasets generated during the current study are available from the corresponding author on reasonable request.

Competing interests

CS and MV disclose a collaboration with Epitech Group SpA, which had no role in study design, collection, analysis and interpretation of data, in the writing of the report, and in the decision to submit the paper for publication.

The other authors declare that they have no competing interests.

Funding

The present study was funded by SAPIENZA University of Rome grant n.MA116154CD981DAE (CS) and Epitech Group SpA (MV).

Authors'contributions

RF, MRB, MV and CS performed the molecular experiments and analysed the data. MV, PR and PC treated animals and performed the surgeries. LS, PC and CS supervised the experiments and discussed the results. RF, MRB, MV and CS wrote the manuscript. All authors contributed to and approved the final manuscript.

Acknowledgments

We gratefully thank Epitech Group SpA for providing us with co-ultra PEALut, as well as Dr. Dionysios Xenos for helpful consultation on immunofluorescence experiments.

References

1. Wortmann M: **Importance of national plans for Alzheimer's disease and dementia.***Alzheimers Res Ther* 2013, **5:**40.
2. ADAssociation: **2018 Alzheimer's disease facts and figures.***Alzheimers & Dementia* 2018, **14:**367-425.
3. Jack CR, Jr., Knopman DS, Jagust WJ, Petersen RC, Weiner MW, Aisen PS, Shaw LM, Vemuri P, Wiste HJ, Weigand SD, et al: **Tracking pathophysiological processes in Alzheimer's disease: an updated hypothetical model of dynamic biomarkers.***Lancet Neurol* 2013, **12:**207-216.
4. Hyman BT, Phelps CH, Beach TG, Bigio EH, Cairns NJ, Carrillo MC, Dickson DW, Duyckaerts C, Frosch MP, Masliah E, et al: **National Institute on Aging-Alzheimer's Association guidelines for the neuropathologic assessment of Alzheimer's disease.***Alzheimers & Dementia* 2012, **8:**1-13.
5. Irwin K, Sexton C, Daniel T, Lawlor B, Naci L: **Healthy Aging and Dementia: Two Roads Diverging in Midlife?***Front Aging Neurosci* 2018, **10:**275.
6. Price JL, McKeel DW, Jr., Buckles VD, Roe CM, Xiong C, Grundman M, Hansen LA, Petersen RC, Parisi JE, Dickson DW, et al: **Neuropathology of nondemented aging: presumptive evidence for preclinical Alzheimer disease.***Neurobiol Aging* 2009, **30:**1026-1036.
7. Braak H, Braak E: **Staging of Alzheimer's disease-related neurofibrillary changes.***Neurobiol Aging* 1995, **16:**271-278; discussion 278-284.
8. Delacourte A, David JP, Sergeant N, Buee L, Wattez A, Vermersch P, Ghozali F, Fallet-Bianco C, Pasquier F, Lebert F, et al: **The biochemical pathway of neurofibrillary degeneration in aging and Alzheimer's disease.***Neurology* 1999, **52:**1158-1165.
9. Williams JW, Plassman BL, Burke J, Benjamin S: **Preventing Alzheimer's disease and cognitive decline.***Evid Rep Technol Assess (Full Rep)* 2010**:**1-727.
10. Crous-Bou M, Minguillon C, Gramunt N, Molinuevo JL: **Alzheimer's disease prevention: from risk factors to early intervention.***Alzheimers Res Ther* 2017, **9:**71.
11. Kozauer N, Katz R: **Regulatory innovation and drug development for early-stage Alzheimer's disease.***N Engl J Med* 2013, **368:**1169-1171.
12. Dubois B, Hampel H, Feldman HH, Scheltens P, Aisen P, Andrieu S, Bakardjian H, Benali H, Bertram L, Blennow K, et al: **Preclinical Alzheimer's disease: Definition, natural history, and diagnostic criteria.***Alzheimers & Dementia* 2016, **12:**292-323.
13. EMA: **Guideline on the clinical investigation of medicines for the treatment of Alzheimer's disease.** European Medicines Agency - Science Medicines Health; 2018.
14. Scheltens P, Blennow K, Breteler MM, de Strooper B, Frisoni GB, Salloway S, Van der Flier WM: **Alzheimer's disease.***Lancet* 2016, **388:**505-517.
15. Heneka MT, Carson MJ, El Khoury J, Landreth GE, Brosseron F, Feinstein DL, Jacobs AH, Wyss-Coray T, Vitorica J, Ransohoff RM, et al: **Neuroinflammation in Alzheimer's disease.***Lancet Neurol* 2015, **14:**388-405.
16. Karch CM, Goate AM: **Alzheimer's disease risk genes and mechanisms of disease pathogenesis.***Biol Psychiatry* 2015, **77:**43-51.
17. Griciuc A, Serrano-Pozo A, Parrado AR, Lesinski AN, Asselin CN, Mullin K, Hooli B, Choi SH, Hyman BT, Tanzi RE: **Alzheimer's disease risk gene CD33 inhibits microglial uptake of amyloid beta.***Neuron* 2013, **78:**631-643.
18. Janelidze S, Mattsson N, Stomrud E, Lindberg O, Palmqvist S, Zetterberg H, Blennow K, Hansson O: **CSF biomarkers of neuroinflammation and cerebrovascular dysfunction in early Alzheimer disease.***Neurology* 2018, **91:**e867-e877.

19. Cribbs DH, Berchtold NC, Perreau V, Coleman PD, Rogers J, Tenner AJ, Cotman CW: **Extensive innate immune gene activation accompanies brain aging, increasing vulnerability to cognitive decline and neurodegeneration: a microarray study.***J Neuroinflammation* 2012, **9:**179.
20. Carter SF, Scholl M, Almkvist O, Wall A, Engler H, Langstrom B, Nordberg A: **Evidence for astrocytosis in prodromal Alzheimer disease provided by 11C-deuterium-L-deprenyl: a multitracer PET paradigm combining 11C-Pittsburgh compound B and 18F-FDG.***J Nucl Med* 2012, **53:**37-46.
21. Hoozemans JJ, Veerhuis R, Rozemuller JM, Eikelenboom P: **Neuroinflammation and regeneration in the early stages of Alzheimer's disease pathology.***Int J Dev Neurosci* 2006, **24:**157-165.
22. Osborn LM, Kamphuis W, Wadman WJ, Hol EM: **Astrogliosis: An integral player in the pathogenesis of Alzheimer's disease.***Prog Neurobiol* 2016, **144:**121-141.
23. Skaper SD: **The brain as a target for inflammatory processes and neuroprotective strategies.***Ann N Y Acad Sci* 2007, **1122:**23-34.
24. Heneka MT, O'Banion MK, Terwel D, Kummer MP: **Neuroinflammatory processes in Alzheimer's disease.***J Neural Transm (Vienna)* 2010, **117:**919-947.
25. Knezevic D, Mizrahi R: **Molecular imaging of neuroinflammation in Alzheimer's disease and mild cognitive impairment.***Prog Neuropsychopharmacol Biol Psychiatry* 2018, **80:**123-131.
26. Heneka MT, Sastre M, Dumitrescu-Ozimek L, Dewachter I, Walter J, Klockgether T, Van Leuven F: **Focal glial activation coincides with increased BACE1 activation and precedes amyloid plaque deposition in APP[V717I] transgenic mice.***J Neuroinflammation* 2005, **2:**22.
27. Frisoni GB, Fox NC, Jack CR, Jr., Scheltens P, Thompson PM: **The clinical use of structural MRI in Alzheimer disease.***Nat Rev Neurol* 2010, **6:**67-77.
28. Sawikr Y, Yarla NS, Peluso I, Kamal MA, Aliev G, Bishayee A: **Neuroinflammation in Alzheimer's Disease: The Preventive and Therapeutic Potential of Polyphenolic Nutraceuticals.***Adv Protein Chem Struct Biol* 2017, **108:**33-57.
29. Scuderi C, Steardo L: **Neuroglial roots of neurodegenerative diseases: therapeutic potential of palmitoylethanolamide in models of Alzheimer's disease.***CNS Neurol Disord Drug Targets* 2013, **12:**62-69.
30. Bronzuoli MR, Iacomino A, Steardo L, Scuderi C: **Targeting neuroinflammation in Alzheimer's disease.***J Inflamm Res* 2016, **9:**199-208.
31. Ralay Ranaivo H, Craft JM, Hu W, Guo L, Wing LK, Van Eldik LJ, Watterson DM: **Glia as a therapeutic target: selective suppression of human amyloid-beta-induced upregulation of brain proinflammatory cytokine production attenuates neurodegeneration.***J Neurosci* 2006, **26:**662-670.
32. Scuderi C, Stecca C, Valenza M, Ratano P, Bronzuoli MR, Bartoli S, Steardo L, Pompili E, Fumagalli L, Campolongo P, Steardo L: **Palmitoylethanolamide controls reactive gliosis and exerts neuroprotective functions in a rat model of Alzheimer's disease.***Cell Death Dis* 2014, **5:**e1419.
33. Scuderi C, Valenza M, Stecca C, Esposito G, Carratu MR, Steardo L: **Palmitoylethanolamide exerts neuroprotective effects in mixed neuroglial cultures and organotypic hippocampal slices via peroxisome proliferator-activated receptor-alpha.***J Neuroinflammation* 2012, **9:**49.
34. D'Agostino G, Russo R, Avagliano C, Cristiano C, Meli R, Calignano A: **Palmitoylethanolamide protects against the amyloid-beta25-35-induced learning and memory impairment in mice, an experimental model of Alzheimer disease.***Neuropsychopharmacology* 2012, **37:**1784-1792.
35. Tomasini MC, Borelli AC, Beggiato S, Ferraro L, Cassano T, Tanganelli S, Antonelli T: **Differential Effects of Palmitoylethanolamide against Amyloid-beta Induced Toxicity in Cortical Neuronal and Astrocytic Primary Cultures from Wild-Type and 3xTg-AD Mice.***J Alzheimers Dis* 2015, **46:**407-421.

36. Cipriano M, Esposito G, Negro L, Capoccia E, Sarnelli G, Scuderi C, De Filippis D, Steardo L, Iuvone T: **Palmitoylethanolamide Regulates Production of Pro-Angiogenic Mediators in a Model of beta Amyloid-Induced Astrogliosis In Vitro.***CNS Neurol Disord Drug Targets* 2015, **14:**828-837.
37. Lopez-Lazaro M: **Distribution and biological activities of the flavonoid luteolin.***Mini Rev Med Chem* 2009, **9:**31-59.
38. Seelinger G, Merfort I, Schempp CM: **Anti-oxidant, anti-inflammatory and anti-allergic activities of luteolin.***Planta Med* 2008, **74:**1667-1677.
39. Nabavi SF, Braidy N, Gortzi O, Sobarzo-Sanchez E, Daglia M, Skalicka-Wozniak K, Nabavi SM: **Luteolin as an anti-inflammatory and neuroprotective agent: A brief review.***Brain Res Bull* 2015, **119:**1-11.
40. Petrosino S, Di Marzo V: **The pharmacology of palmitoylethanolamide and first data on the therapeutic efficacy of some of its new formulations.***Br J Pharmacol* 2017, **174:**1349-1365.
41. Petrosino S, Cordaro M, Verde R, Schiano Moriello A, Marcolongo G, Schievano C, Siracusa R, Piscitelli F, Peritore AF, Crupi R, et al: **Oral Ultramicronized Palmitoylethanolamide: Plasma and Tissue Levels and Spinal Anti-hyperalgesic Effect.***Front Pharmacol* 2018, **9:**249.
42. Impellizzeri D, Esposito E, Di Paola R, Ahmad A, Campolo M, Peli A, Morittu VM, Britti D, Cuzzocrea S: **Palmitoylethanolamide and luteolin ameliorate development of arthritis caused by injection of collagen type II in mice.***Arthritis Res Ther* 2013, **15:**R192.
43. Skaper SD, Facci L, Barbierato M, Zusso M, Bruschetta G, Impellizzeri D, Cuzzocrea S, Giusti P: **N-Palmitoylethanolamine and Neuroinflammation: a Novel Therapeutic Strategy of Resolution.***Mol Neurobiol* 2015, **52:**1034-1042.
44. Parrella E, Porrini V, Iorio R, Benarese M, Lanzillotta A, Mota M, Fusco M, Tonin P, Spano P, Pizzi M: **PEA and luteolin synergistically reduce mast cell-mediated toxicity and elicit neuroprotection in cell-based models of brain ischemia.***Brain Res* 2016, **1648:**409-417.
45. Adami R, Liparoti S, Di Capua A, Scognamiglio M, Reverchon E: **Production of PEA composite microparticles with polyvinylpyrrolidone and luteolin using Supercritical Assisted Atomization.***The Journal of Supercritical Fluids* 2019, **143:**82-89.
46. Scuderi C, Bronzuoli MR, Facchinetti R, Pace L, Ferraro L, Broad KD, Serviddio G, Bellanti F, Palombelli G, Carpinelli G, et al: **Ultramicronized palmitoylethanolamide rescues learning and memory impairments in a triple transgenic mouse model of Alzheimer's disease by exerting anti-inflammatory and neuroprotective effects.***Transl Psychiatry* 2018, **8:**32.
47. Oddo S, Caccamo A, Shepherd JD, Murphy MP, Golde TE, Kayed R, Metherate R, Mattson MP, Akbari Y, LaFerla FM: **Triple-transgenic model of Alzheimer's disease with plaques and tangles: intracellular Abeta and synaptic dysfunction.***Neuron* 2003, **39:**409-421.
48. Jean YY, Baleriola J, Fa M, Hengst U, Troy CM: **Stereotaxic Infusion of Oligomeric Amyloid-beta into the Mouse Hippocampus.***J Vis Exp* 2015**:**e52805.
49. Cordaro M, Impellizzeri D, Paterniti I, Bruschetta G, Siracusa R, De Stefano D, Cuzzocrea S, Esposito E: **Neuroprotective Effects of Co-UltraPEALut on Secondary Inflammatory Process and Autophagy Involved in Traumatic Brain Injury.***J Neurotrauma* 2016, **33:**132-146.
50. Siracusa R, Impellizzeri D, Cordaro M, Crupi R, Esposito E, Petrosino S, Cuzzocrea S: **Anti-Inflammatory and Neuroprotective Effects of Co-UltraPEALut in a Mouse Model of Vascular Dementia.***Front Neurol* 2017, **8:**233.
51. Caltagirone C, Cisari C, Schievano C, Di Paola R, Cordaro M, Bruschetta G, Esposito E, Cuzzocrea S, Stroke Study G: **Co-ultramicronized Palmitoylethanolamide/Luteolin in the Treatment of Cerebral Ischemia: from Rodent to Man.***Transl Stroke Res* 2016, **7:**54-69.
52. Budni J, Bellettini-Santos T, Mina F, Garcez ML, Zugno AI: **The involvement of BDNF, NGF and GDNF in aging and Alzheimer's disease.***Aging Dis* 2015, **6:**331-341.

53. Peng S, Wuu J, Mufson EJ, Fahnestock M: **Precursor form of brain-derived neurotrophic factor and mature brain-derived neurotrophic factor are decreased in the pre-clinical stages of Alzheimer's disease.***J Neurochem* 2005, **93:**1412-1421.
54. Forlenza OV, Miranda AS, Guimar I, Talib LL, Diniz BS, Gattaz WF, Teixeira AL: **Decreased Neurotrophic Support is Associated with Cognitive Decline in Non-Demented Subjects.***J Alzheimers Dis* 2015, **46:**423-429.
55. Calabro RS, Naro A, De Luca R, Leonardi S, Russo M, Marra A, Bramanti P: **PEALut efficacy in mild cognitive impairment: evidence from a SPECT case study!***Aging Clin Exp Res* 2016, **28:**1279-1282.
56. Facchinetti R, Bronzuoli MR, Scuderi C: **An Animal Model of Alzheimer Disease Based on the Intrahippocampal Injection of Amyloid beta-Peptide (1-42).***Methods Mol Biol* 2018, **1727:**343-352.
57. Paxinos G, Watson C: *The rat brain in stereotaxic coordinates.* 6th edn. Amsterdam ; Boston ;: Academic Press/Elsevier; 2007.
58. Skaper SD, Barbierato M, Facci L, Borri M, Contarini G, Zusso M, Giusti P: **Co-Ultramicronized Palmitoylethanolamide/Luteolin Facilitates the Development of Differentiating and Undifferentiated Rat Oligodendrocyte Progenitor Cells.***Mol Neurobiol* 2018, **55:**103-114.
59. Valenza M, Picetti R, Yuferov V, Butelman ER, Kreek MJ: **Strain and cocaine-induced differential opioid gene expression may predispose Lewis but not Fischer rats to escalate cocaine self-administration.***Neuropharmacology* 2016, **105:**639-650.
60. Bronzuoli MR, Facchinetti R, Ingrassia D, Sarvadio M, Schiavi S, Steardo L, Verkhratsky A, Trezza V, Scuderi C: **Neuroglia in the autistic brain: evidence from a preclinical model.***Mol Autism* 2018, **9:**66.
61. Bronzuoli MR, Facchinetti R, Valenza M, Cassano T, Steardo L, Scuderi C: **Astrocyte Function Is Affected by Aging and Not Alzheimer's Disease: A Preliminary Investigation in Hippocampi of 3xTg-AD Mice.***Front Pharmacol* 2019, **10:**644.
62. Valenza M, Butelman ER, Kreek MJ: **"Effects of the novel relatively short-acting kappa opioid receptor antagonist LY2444296 in behaviors observed after chronic extended-access cocaine self-administration in rats".***Psychopharmacology (Berl)* 2017, **234:**2219-2231.
63. Banker GA: **Trophic interactions between astroglial cells and hippocampal neurons in culture.***Science* 1980, **209:**809-810.
64. Chun H, Marriott I, Lee CJ, Cho H: **Elucidating the Interactive Roles of Glia in Alzheimer's Disease Using Established and Newly Developed Experimental Models.***Front Neurol* 2018, **9:**797.
65. Zhang S, Wu M, Peng C, Zhao G, Gu R: **GFAP expression in injured astrocytes in rats.***Exp Ther Med* 2017, **14:**1905-1908.
66. Bronzuoli MR, Facchinetti R, Steardo L, Scuderi C: **Astrocyte: An Innovative Approach for Alzheimer's Disease Therapy.***Curr Pharm Des* 2017, **23:**4979-4989.
67. Kettenmann H, Hanisch UK, Noda M, Verkhratsky A: **Physiology of microglia.***Physiol Rev* 2011, **91:**461-553.
68. Ito D, Imai Y, Ohsawa K, Nakajima K, Fukuuchi Y, Kohsaka S: **Microglia-specific localisation of a novel calcium binding protein, Iba1.***Brain Res Mol Brain Res* 1998, **57:**1-9.
69. Esposito G, Scuderi C, Valenza M, Togna GI, Latina V, De Filippis D, Cipriano M, Carratu MR, Iuvone T, Steardo L: **Cannabidiol reduces Abeta-induced neuroinflammation and promotes hippocampal neurogenesis through PPARgamma involvement.***PLoS One* 2011, **6:**e28668.
70. Scuderi C, Stecca C, Bronzuoli MR, Rotili D, Valente S, Mai A, Steardo L: **Sirtuin modulators control reactive gliosis in an in vitro model of Alzheimer's disease.***Front Pharmacol* 2014, **5:**89.
71. Mrak RE, Griffin WS: **Interleukin-1, neuroinflammation, and Alzheimer's disease.***Neurobiol Aging* 2001, **22:**903-908.

72. Li C, Zhao R, Gao K, Wei Z, Yin MY, Lau LT, Chui D, Yu AC: **Astrocytes: implications for neuroinflammatory pathogenesis of Alzheimer's disease.***Curr Alzheimer Res* 2011, **8:**67-80.
73. Deniz-Naranjo MC, Munoz-Fernandez C, Alemany-Rodriguez MJ, Perez-Vieitez MC, Aladro-Benito Y, Irurita-Latasa J, Sanchez-Garcia F: **Cytokine IL-1 beta but not IL-1 alpha promoter polymorphism is associated with Alzheimer disease in a population from the Canary Islands, Spain.***Eur J Neurol* 2008, **15:**1080-1084.
74. Kempuraj D, Thangavel R, Selvakumar GP, Zaheer S, Ahmed ME, Raikwar SP, Zahoor H, Saeed D, Natteru PA, Iyer S, Zaheer A: **Brain and Peripheral Atypical Inflammatory Mediators Potentiate Neuroinflammation and Neurodegeneration.***Front Cell Neurosci* 2017, **11:**216.
75. Sun XL, Chen BY, Duan L, Xia Y, Luo ZJ, Wang JJ, Rao ZR, Chen LW: **The proform of glia cell line-derived neurotrophic factor: a potentially biologically active protein.***Mol Neurobiol* 2014, **49:**234-250.
76. Marco S, Canudas AM, Canals JM, Gavalda N, Perez-Navarro E, Alberch J: **Excitatory amino acids differentially regulate the expression of GDNF, neurturin, and their receptors in the adult rat striatum.***Exp Neurol* 2002, **174:**243-252.
77. Dougherty KD, Dreyfus CF, Black IB: **Brain-derived neurotrophic factor in astrocytes, oligodendrocytes, and microglia/macrophages after spinal cord injury.***Neurobiol Dis* 2000, **7:**574-585.
78. Honig LS, Vellas B, Woodward M, Boada M, Bullock R, Borrie M, Hager K, Andreasen N, Scarpini E, Liu-Seifert H, et al: **Trial of Solanezumab for Mild Dementia Due to Alzheimer's Disease.***N Engl J Med* 2018, **378:**321-330.
79. van Dyck CH: **Anti-Amyloid-beta Monoclonal Antibodies for Alzheimer's Disease: Pitfalls and Promise.***Biol Psychiatry* 2018, **83:**311-319.
80. Baazaoui N, Iqbal K: **Prevention of Amyloid-beta and Tau Pathologies, Associated Neurodegeneration, and Cognitive Deficit by Early Treatment with a Neurotrophic Compound.***J Alzheimers Dis* 2017, **58:**215-230.
81. Graham WV, Bonito-Oliva A, Sakmar TP: **Update on Alzheimer's Disease Therapy and Prevention Strategies.***Annu Rev Med* 2017, **68:**413-430.
82. Craft JM, Watterson DM, Van Eldik LJ: **Human amyloid beta-induced neuroinflammation is an early event in neurodegeneration.***Glia* 2006, **53:**484-490.
83. Jaroudi W, Garami J, Garrido S, Hornberger M, Keri S, Moustafa AA: **Factors underlying cognitive decline in old age and Alzheimer's disease: the role of the hippocampus.***Rev Neurosci* 2017, **28:**705-714.
84. Jahn H: **Memory loss in Alzheimer's disease.***Dialogues Clin Neurosci* 2013, **15:**445-454.
85. Morris RG: **Episodic-like memory in animals: psychological criteria, neural mechanisms and the value of episodic-like tasks to investigate animal models of neurodegenerative disease.***Philos Trans R Soc Lond B Biol Sci* 2001, **356:**1453-1465.
86. Savonenko A, Xu GM, Melnikova T, Morton JL, Gonzales V, Wong MP, Price DL, Tang F, Markowska AL, Borchelt DR: **Episodic-like memory deficits in the APPswe/PS1dE9 mouse model of Alzheimer's disease: relationships to beta-amyloid deposition and neurotransmitter abnormalities.***Neurobiol Dis* 2005, **18:**602-617.
87. Sexton CE, Mackay CE, Lonie JA, Bastin ME, Terriere E, O'Carroll RE, Ebmeier KP: **MRI correlates of episodic memory in Alzheimer's disease, mild cognitive impairment, and healthy aging.***Psychiatry Res* 2010, **184:**57-62.
88. Espinosa A, Alegret M, Valero S, Vinyes-Junque G, Hernandez I, Mauleon A, Rosende-Roca M, Ruiz A, Lopez O, Tarraga L, Boada M: **A longitudinal follow-up of 550 mild cognitive impairment patients: evidence for large conversion to dementia rates and detection of major risk factors involved.***J Alzheimers Dis* 2013, **34:**769-780.

89. Scuderi C, Esposito G, Blasio A, Valenza M, Arietti P, Steardo L, Jr., Carnuccio R, De Filippis D, Petrosino S, Iuvone T, et al: **Palmitoylethanolamide counteracts reactive astrogliosis induced by beta-amyloid peptide.***J Cell Mol Med* 2011, **15:**2664-2674.
90. Paterniti I, Cordaro M, Campolo M, Siracusa R, Cornelius C, Navarra M, Cuzzocrea S, Esposito E: **Neuroprotection by association of palmitoylethanolamide with luteolin in experimental Alzheimer's disease models: the control of neuroinflammation.***CNS Neurol Disord Drug Targets* 2014, **13:**1530-1541.
91. Petrosino S, Iuvone T, Di Marzo V: **N-palmitoyl-ethanolamine: Biochemistry and new therapeutic opportunities.***Biochimie* 2010, **92:**724-727.
92. Hoareau L, Buyse M, Festy F, Ravanan P, Gonthier MP, Matias I, Petrosino S, Tallet F, d'Hellencourt CL, Cesari M, et al: **Anti-inflammatory effect of palmitoylethanolamide on human adipocytes.***Obesity (Silver Spring)* 2009, **17:**431-438.
93. Koch M, Kreutz S, Bottger C, Benz A, Maronde E, Ghadban C, Korf HW, Dehghani F: **Palmitoylethanolamide protects dentate gyrus granule cells via peroxisome proliferator-activated receptor-alpha.***Neurotox Res* 2011, **19:**330-340.
94. Li MM, Wang D, Bi WP, Jiang ZE, Piao RL, Yu HL: **N-Palmitoylethanolamide exerts antidepressant-like effects in rats: involvement of PPAR-alpha pathway in the hippocampus.***J Pharmacol Exp Ther* 2019.
95. Lo Verme J, Fu J, Astarita G, La Rana G, Russo R, Calignano A, Piomelli D: **The nuclear receptor peroxisome proliferator-activated receptor-alpha mediates the anti-inflammatory actions of palmitoylethanolamide.***Mol Pharmacol* 2005, **67:**15-19.
96. D'Agostino G, La Rana G, Russo R, Sasso O, Iacono A, Esposito E, Raso GM, Cuzzocrea S, Lo Verme J, Piomelli D, et al: **Acute intracerebroventricular administration of palmitoylethanolamide, an endogenous peroxisome proliferator-activated receptor-alpha agonist, modulates carrageenan-induced paw edema in mice.***J Pharmacol Exp Ther* 2007, **322:**1137-1143.
97. Raso GM, Esposito E, Vitiello S, Iacono A, Santoro A, D'Agostino G, Sasso O, Russo R, Piazza PV, Calignano A, Meli R: **Palmitoylethanolamide stimulation induces allopregnanolone synthesis in C6 Cells and primary astrocytes: involvement of peroxisome-proliferator activated receptor-alpha.***J Neuroendocrinol* 2011, **23:**591-600.
98. Genovese T, Esposito E, Mazzon E, Di Paola R, Meli R, Bramanti P, Piomelli D, Calignano A, Cuzzocrea S: **Effects of palmitoylethanolamide on signaling pathways implicated in the development of spinal cord injury.***J Pharmacol Exp Ther* 2008, **326:**12-23.
99. Khasabova IA, Xiong Y, Coicou LG, Piomelli D, Seybold V: **Peroxisome proliferator-activated receptor alpha mediates acute effects of palmitoylethanolamide on sensory neurons.***J Neurosci* 2012, **32:**12735-12743.
100. Aldossary SA, Alsalem M, Kalbouneh H, Haddad M, Azab B, Al-Shboul O, Mustafa AG, Obiedat S, El-Salem K: **The role of transient receptor potential vanilloid receptor 1 and peroxisome proliferator-activated receptors-alpha in mediating the antinociceptive effects of palmitoylethanolamine in rats.***Neuroreport* 2019, **30:**32-37.
101. Esposito E, Impellizzeri D, Mazzon E, Paterniti I, Cuzzocrea S: **Neuroprotective activities of palmitoylethanolamide in an animal model of Parkinson's disease.***PLoS One* 2012, **7:**e41880.
102. Di Cesare Mannelli L, D'Agostino G, Pacini A, Russo R, Zanardelli M, Ghelardini C, Calignano A: **Palmitoylethanolamide is a disease-modifying agent in peripheral neuropathy: pain relief and neuroprotection share a PPAR-alpha-mediated mechanism.***Mediators Inflamm* 2013, **2013:**328797.
103. Impellizzeri D, Bruschetta G, Cordaro M, Crupi R, Siracusa R, Esposito E, Cuzzocrea S: **Micronized/ultramicronized palmitoylethanolamide displays superior oral efficacy compared to**

nonmicronized palmitoylethanolamide in a rat model of inflammatory pain.*J Neuroinflammation* 2014, **11:**136.
104. Bronzuoli MR, Facchinetti R, Steardo L, Jr., Romano A, Stecca C, Passarella S, Steardo L, Cassano T, Scuderi C: **Palmitoylethanolamide Dampens Reactive Astrogliosis and Improves Neuronal Trophic Support in a Triple Transgenic Model of Alzheimer's Disease: In Vitro and In Vivo Evidence.***Oxid Med Cell Longev* 2018, **2018:**4720532.
105. Ashaari Z, Hadjzadeh MA, Hassanzadeh G, Alizamir T, Yousefi B, Keshavarzi Z, Mokhtari T: **The Flavone Luteolin Improves Central Nervous System Disorders by Different Mechanisms: A Review.***J Mol Neurosci* 2018, **65:**491-506.
106. Wang H, Wang H, Cheng H, Che Z: **Ameliorating effect of luteolin on memory impairment in an Alzheimer's disease model.***Mol Med Rep* 2016, **13:**4215-4220.
107. Zhang JX, Xing JG, Wang LL, Jiang HL, Guo SL, Liu R: **Luteolin Inhibits Fibrillary beta-Amyloid1-40-Induced Inflammation in a Human Blood-Brain Barrier Model by Suppressing the p38 MAPK-Mediated NF-kappaB Signaling Pathways.***Molecules* 2017, **22**.
108. Halappa NG, Thirthalli J, Varambally S, Rao M, Christopher R, Nanjundaiah GB: **Improvement in neurocognitive functions and serum brain-derived neurotrophic factor levels in patients with depression treated with antidepressants and yoga.***Indian J Psychiatry* 2018, **60:**32-37.
109. Paterniti I, Impellizzeri D, Di Paola R, Navarra M, Cuzzocrea S, Esposito E: **A new co-ultramicronized composite including palmitoylethanolamide and luteolin to prevent neuroinflammation in spinal cord injury.***J Neuroinflammation* 2013, **10:**91.

Figure Legends

Fig. 1 Schematic representation of the experimental design. **a** Procedure for stereotaxic intracerebral injection in adult rats showing the positioning of the animal on the stereotaxic frame. The injector apparatus was composed by a needle connected to a tubing plugged into a Hamilton syringe mounted on a pump. **b** Timeline of the experiment showing schedule and doses of both treatments. Rats underwent a single intracranial injection of human fibrillary $A\beta_{(1-42)}$, or vehicle, into the dorsal hippocampus. Co-ultra PEALut 5 mg/kg, or vehicle, were administered *i.p.*to rats on the day of surgery and daily for 14 consecutive days. Twenty-four hours after the last systemic injection, rats were sacrificed, and brains extracted for molecular analyses.

Fig. 2 Chronic treatment with co-ultra PEALut reduces Aβ-induced astrocyte activation. **a** Representative fluorescent photomicrographs of GFAP (*green*) staining in the CA1 hippocampal

sub-region, ipsilateral to $A\beta_{(1–42)}$ (or vehicle) injection site, of rats chronically treated with co-ultra PEALut (5 mg/kg/die) or vehicle. Nuclei were stained with Hoechst (*blue*). Scale bar is 50 μm. **B** Quantification of GFAP fluorescent signal in both Veh- and$A\beta_{(1-42)}$-inoculated rats chronically treated with either co-ultraPEA/Lut or its vehicle. Data were expressed as the ratio of the difference between the mean fluorescence of the sample and the background (ΔF) to the fluorescence of the non-immunoreactive regions (F_0). Data are presented as mean ± SEM (*** $p< 0.001$ *versus*Veh/Veh; °° $p< 0.01$ *versus* Aβ/Veh) of four independent experiments performed in triplicate. Statistical analysis was performed by two-way ANOVA followed by Bonferroni's multiple comparisons test.

Fig. 3 Chronic treatment with co-ultraPEALut blocks Aβ-induced microglia activation. **a** Representative fluorescent photomicrographs of Iba1 (*green*) staining in the CA1 hippocampal sub-region, ipsilateral to $A\beta_{(1–42)}$ (or vehicle) injection site, obtained from rats chronically treated with either co-ultra PEALut (5 mg/kg/die) or vehicle. Nuclei were stained with Hoechst (*blue*). Scale bar is 30 μm. **B** Quantification of Iba1 fluorescent signal in both vehicle and$A\beta_{(1-42)}$-inoculated rats chronically treated with either co-ultra PEALut, or vehicle. Data were expressed as the ratio of the difference between the mean fluorescence of the sample and the background (ΔF) to the fluorescence of the non-immunoreactive regions (F_0). **C** Gene expression of CD11b in the hippocampus of both vehicle- and$A\beta_{(1-42)}$-inoculated rats chronically treated with either co-ultraPEALut or vehicle. CD11b mRNA was normalized to the mean mRNA of two reference genes, TBP and HPRT respectively, and expressed as $\Delta\Delta Cq$. Data are presented as mean ± SEM (** $p< 0.01$ *versus*Veh/Veh; °° $p< 0.01$ *versus* Aβ/Veh) of three independent experiments

performed in triplicate. Statistical analysis was performed by two-way ANOVA followed by Bonferroni's multiple comparisons test.

Fig. 4 Chronic treatment with co-ultraPEALut blunts gene expression of several markers of neuroinflammation triggered by intrahippocampal $A\beta_{(1-42)}$ injection. Panels show the relative mRNA concentrations of **a** iNOS, **b** COX-2, **c** IL-1β, **d** IL-6, **e** TNF-α and **f** IL-10 in the hippocampus of rats inoculated with $A\beta_{(1-42)}$-(or vehicle) and chronically treated with either co-ultraPEALut (5 mg/kg/die) or its vehicle. Data are presented as mean ± SEM (* $p< 0.05$ and *** $p< 0.001$ *versus*Veh/Veh; °°° $p< 0.001$ *versus* Aβ/Veh) of four independent experiments performed in triplicate. Statistical analysis was performed by two-way ANOVA followed by Bonferroni's multiple comparisons test.

Fig. 5 Chronic treatment with co-ultraPEALut increases gene expression of neurotrophic factors, lowered by intrahippocampal injection of $A\beta_{(1-42)}$. Panels show the relative mRNA concentration of **a** GDNF and **b** BDNF in the hippocampus of rats inoculated with $A\beta_{(1-42)}$,or vehicle, chronically treated with either co-ultra PEALut (5 mg/kg/die) or its vehicle. Data are presented as mean ±SEM (** $p< 0.01$ and *** $p< 0.001$ *versus*Veh/Veh; °°° $p< 0.001$ *versus*Aβ/Veh) of four independent experiments performed in triplicate. Statistical analysis was performed by two-way ANOVA followed by Bonferroni's multiple comparisons test.

Fig. 6 Chronic treatment with co-ultraPEALut promotes neuronal survival impaired by Aβ intracerebral injection. **a** Representative fluorescent photomicrographs of MAP-2 (*red*) staining in

the CA1 hippocampal sub-region ipsilateral to $A\beta_{(1–42)}$ (or vehicle) injection site obtained from rats chronically treated with either co-ultraPEALut (5 mg/kg/die) or vehicle. Nuclei were stained with Hoechst (*blue*). Scale bar is 100 µm. **b** Quantification of MAP-2 fluorescent signal in both vehicle and Aβ-inoculated rats, chronically treated with either co-ultra PEALut or vehicle. Data were expressed as the ratio of the difference between the mean fluorescence of the sample and the background (ΔF) to the fluorescence of the non-immunoreactive regions (F_0). Data are presented as mean ± SEM (* $p< 0.05$ *versus*Veh/Veh; °°° $p< 0.001$ *versus* Aβ/Veh) of four independent experiments performed in triplicate. Statistical analysis was performed by two-way ANOVA followed by Bonferroni's multiple comparisons test.

Figure 1

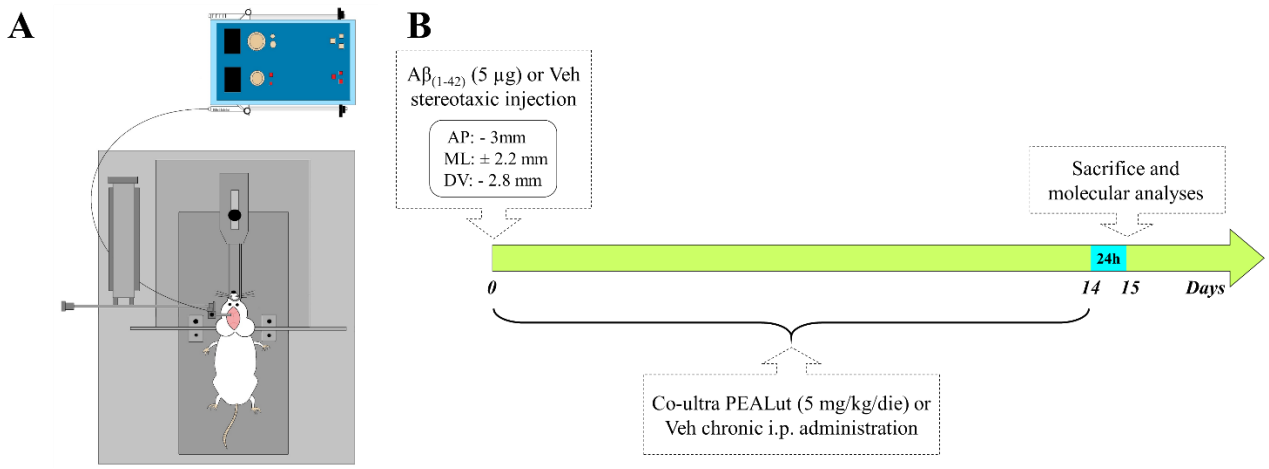

Figure 2

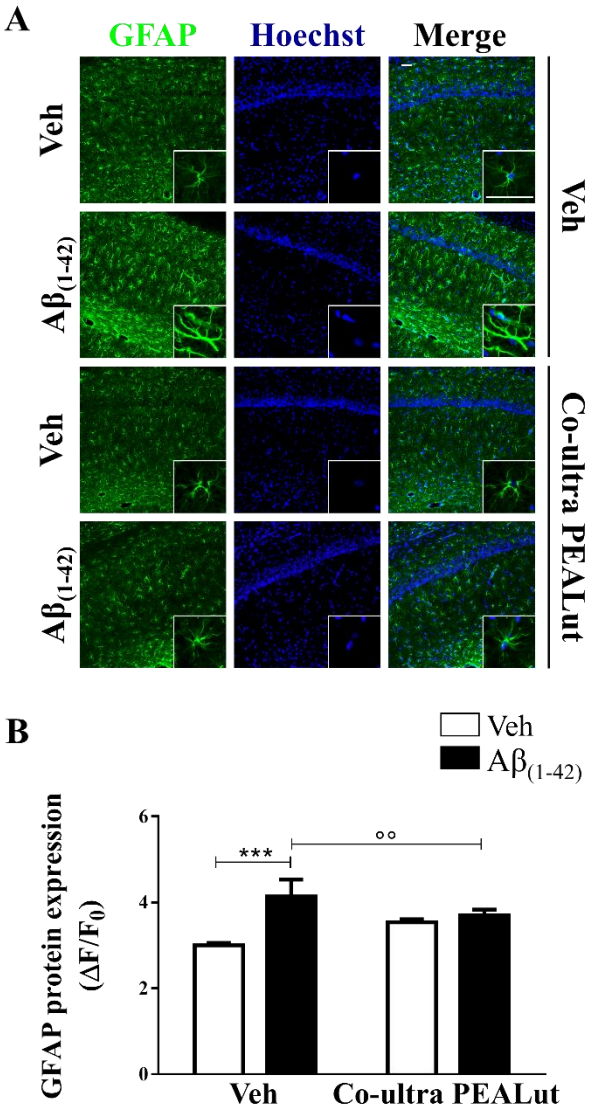
A
GFAP
Hoechst
Merge
Veh
Aβ(1-42)
Veh
Aβ(1-42)
Veh
Co-ultra PEALut
B
Veh
Aβ(1-42)
GFAP protein expression
(ΔF/F0)
***
°°
0
2
4
6
Veh
Co-ultra PEALut

Figure 3

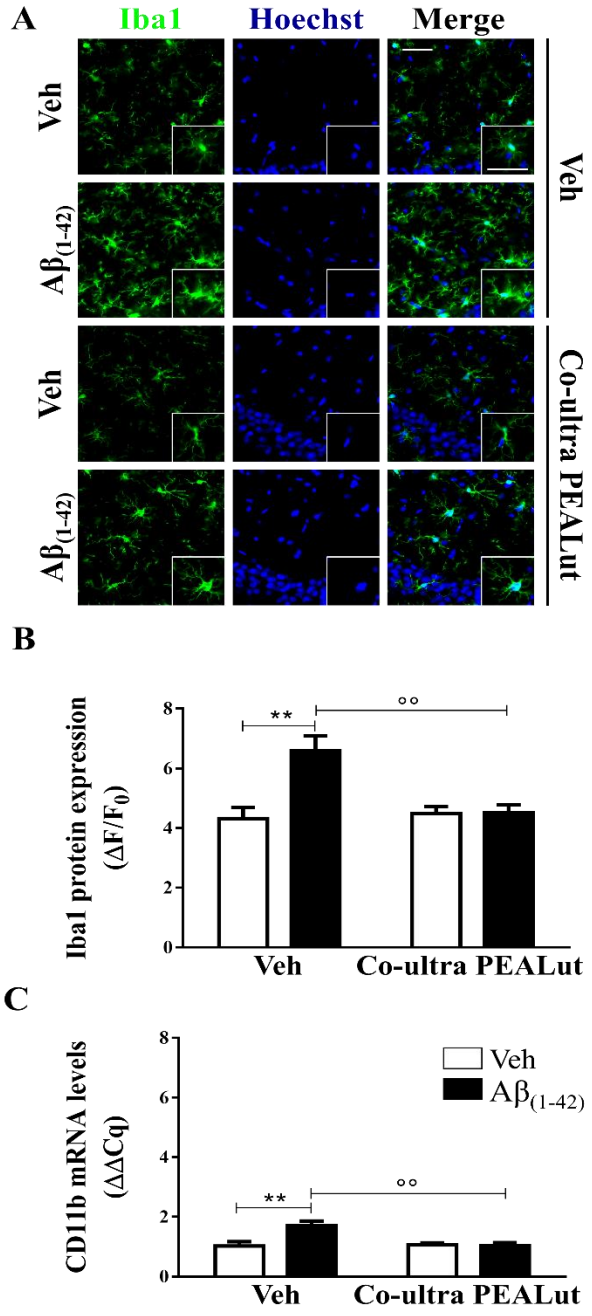
A
Iba1
Hoechst
Merge
Veh
Aβ(1-42)
Veh
Aβ(1-42)
Veh
Co-ultra PEALut
B
Iba1 protein expression
(ΔF/F0)
**
°°
Veh
Co-ultra PEALut
C
CD11b mRNA levels
(ΔΔCq)
Veh
Aβ(1-42)
**
°°
Veh
Co-ultra PEALut

Figure 4

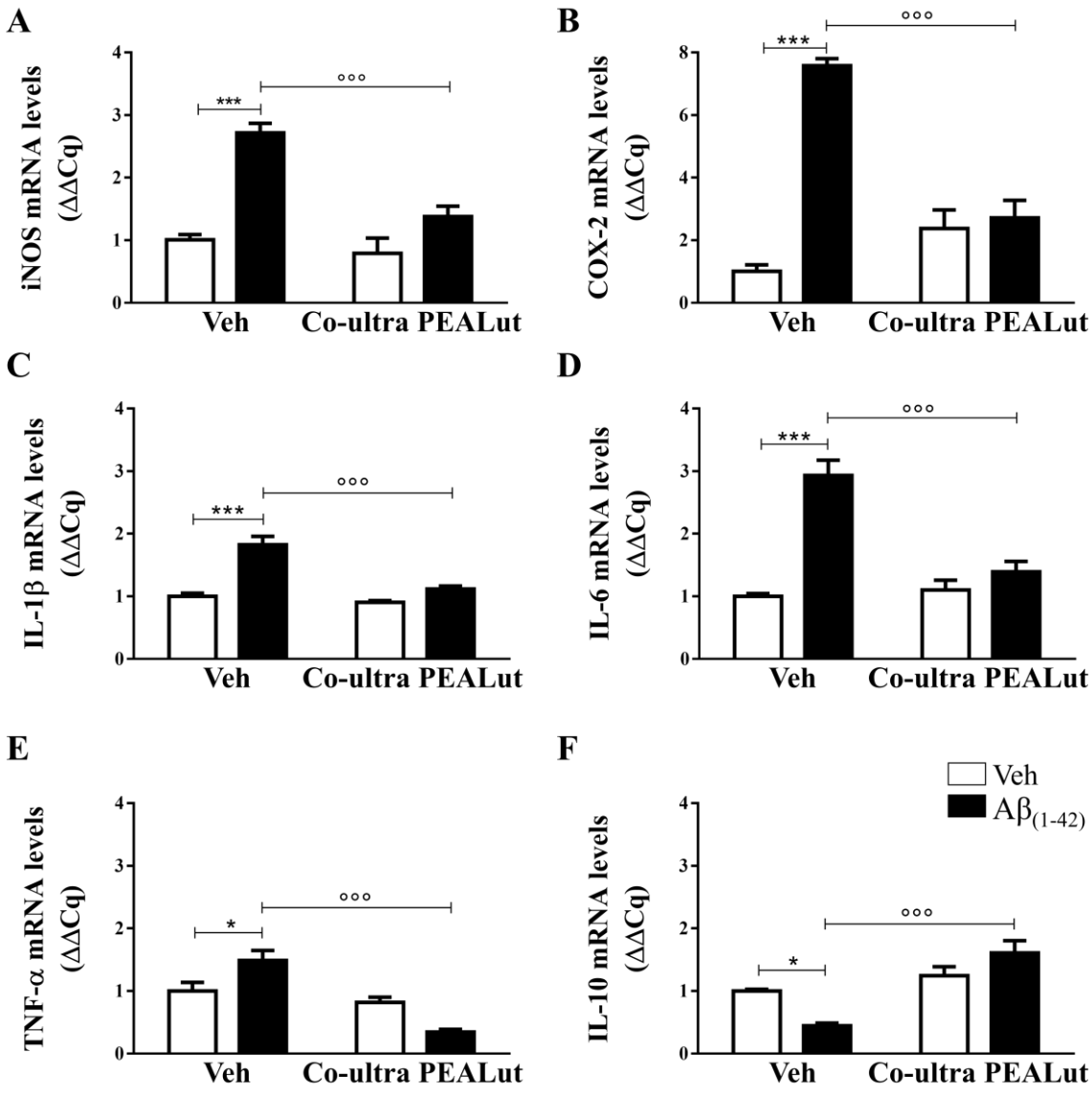
A
iNOS mRNA levels (ΔΔCq)
B
COX-2 mRNA levels (ΔΔCq)
C
IL-1β mRNA levels (ΔΔCq)
D
IL-6 mRNA levels (ΔΔCq)
E
TNF-α mRNA levels (ΔΔCq)
F
IL-10 mRNA levels (ΔΔCq)
Veh
Co-ultra PEALut
Veh
Aβ(1-42)
***
*
°°°

Figure 5

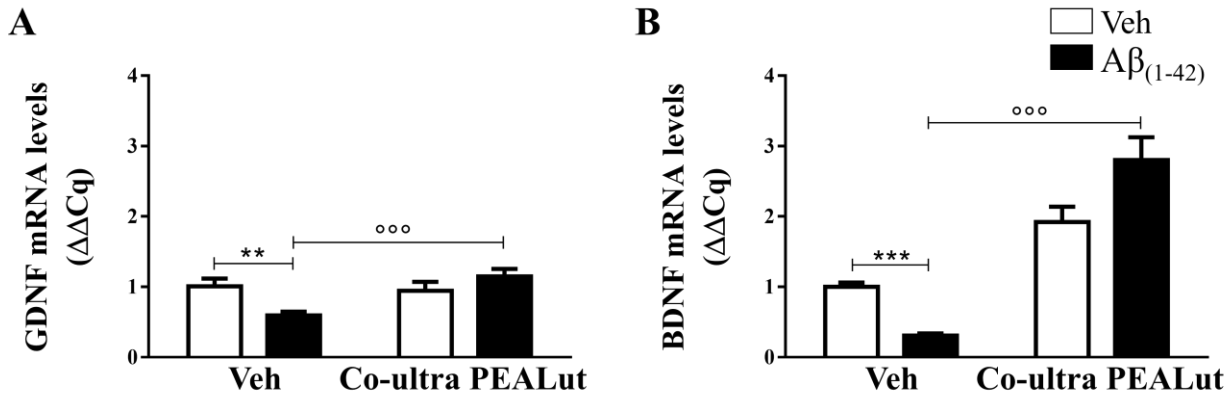
A
GDNF mRNA levels
(ΔΔCq)
4
3
2
1
0
**
°°°
Veh
Co-ultra PEALut
B
Veh
Aβ(1-42)
BDNF mRNA levels
(ΔΔCq)
4
3
2
1
0
***
°°°
Veh
Co-ultra PEALut

Figure 6

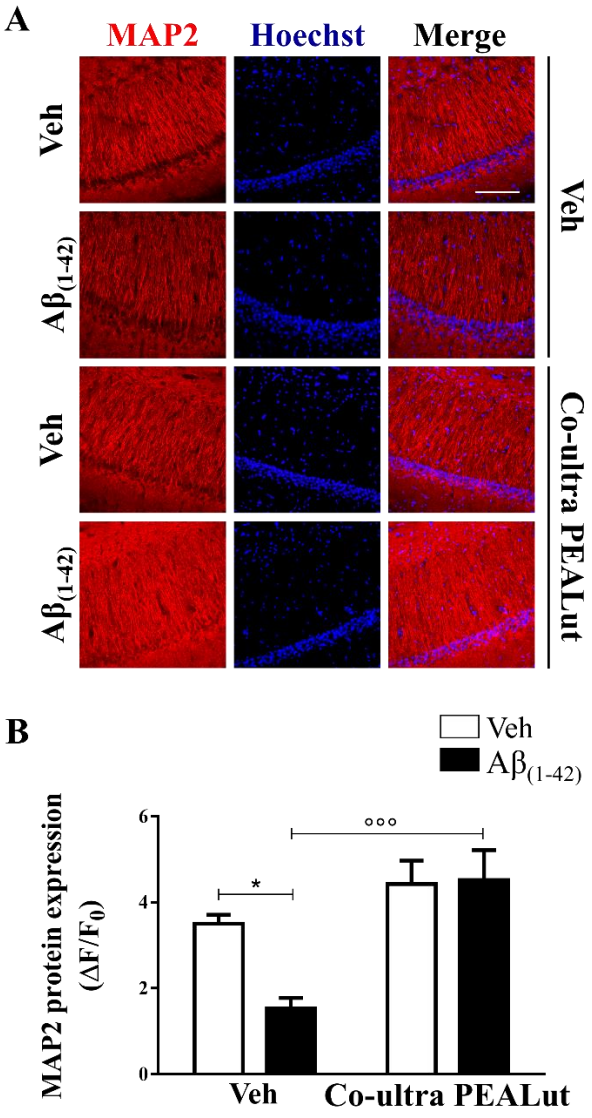
A
MAP2
Hoechst
Merge
Veh
Aβ(1-42)
Veh
Aβ(1-42)
Veh
Co-ultra PEALut
B
Veh
Aβ(1-42)
MAP2 protein expression
(ΔF/F0)
6
4
2
0
*
°°°
Veh
Co-ultra PEALut

frontiers in Pharmacology

BRIEF RESEARCH REPORT
published: 06 June 2019
doi: 10.3389/fphar.2019.00644

Astrocyte Function Is Affected by Aging and Not Alzheimer's Disease: A Preliminary Investigation in Hippocampi of 3xTg-AD Mice

*Maria Rosanna Bronzuoli[1], Roberta Facchinetti[1], Marta Valenza[1,2], Tommaso Cassano[3], Luca Steardo[1] and Caterina Scuderi[1]**

[1] Department of Physiology and Pharmacology "V. Erspamer," Sapienza University of Rome, Rome, Italy, [2] Epitech Group SpA, Saccolongo, Italy, [3] Department of Clinical and Experimental Medicine, University of Foggia, Foggia, Italy

Old age is a risk factor for Alzheimer's disease (AD), which is characterized by hippocampal impairment together with substantial changes in glial cell functions. Are these alterations due to the disease progression or are they a consequence of aging? To start addressing this issue, we studied the expression of specific astrocytic and microglial structural and functional proteins in a validated transgenic model of AD (3×Tg-AD). These mice develop both amyloid plaques and neurofibrillary tangles, and initial signs of the AD-like pathology have been documented as early as three months of age. We compared male 3×Tg-AD mice at 6 and 12 months of age with their wild-type age-matched counterparts. We also investigated neurons by examining the expression of both the microtubule-associated protein 2 (MAP2), a neuronal structural protein, and the brain-derived neurotrophic factor (BDNF). The latter is indeed a crucial indicator for synaptic plasticity and neurogenesis/neurodegeneration. Our results show that astrocytes are more susceptible to aging than microglia, regardless of mouse genotype. Moreover, we discovered significant age-dependent alterations in the expression of proteins responsible for astrocyte–astrocyte and astrocyte–neuron communication, as well as a significant age-dependent decline in BDNF expression. Our data promote further research on the unexplored role of astroglia in both physiological and pathological aging.

Keywords: aging, Alzheimer's disease, 3×Tg-AD mouse, astrocyte, connexin-43, AQP4, S100B, brain-derived neurotrophic factor

OPEN ACCESS

Edited by:
Cesare Mancuso, Catholic University of the Sacred Heart, Italy

Reviewed by:
Nicholas Castello, Gladstone Institutes, United States
Marco Milanese, University of Genoa, Italy

***Correspondence:**
Caterina Scuderi
caterina.scuderi@uniroma1.it

Specialty section:
This article was submitted to Experimental Pharmacology and Drug Discovery, a section of the journal Frontiers in Pharmacology

Received: *12 February 2019*
Accepted: *17 May 2019*
Published: *06 June 2019*

Citation:
Bronzuoli MR, Facchinetti R, Valenza M, Cassano T, Steardo L and Scuderi C (2019) Astrocyte Function Is Affected by Aging and Not Alzheimer's Disease: A Preliminary Investigation in Hippocampi of 3xTg-AD Mice. Front. Pharmacol. 10:644. doi: 10.3389/fphar.2019.00644

INTRODUCTION

Alzheimer's disease (AD) is currently considered a multifactorial disorder, although aging still remains its greatest risk factor (van der Flier and Scheltens, 2005; Hodson, 2018). Many targets are considered to design novel therapeutics. Glia represents one of them because of its contribution in the regulation of several highly specialized brain functions including glutamate, ions and water homeostasis, excitability and metabolic support of neurons, synaptic plasticity, brain blood flow, and neurotrophic support (Acosta et al., 2017; Bronzuoli et al., 2017). These functions are well integrated since astrocytes tightly communicate one to each other through gap junctions, comprised mainly of connexin-43 (CX43), that provide the structural basis for astrocyte networks (Bruzzone et al., 1996; Theis et al., 2005). These cells quickly respond to brain insults, synergistically working with

microglia, the intrinsic immune effector of the brain, to remove injurious stimuli thus restoring brain homeostasis (Gehrmann et al., 1995; Scuderi et al., 2013). For example, during reactive astrogliosis, an event well described in both aged and AD brains (Scuderi et al., 2014a; Steardo et al., 2015; Rodríguez-Arellano et al., 2016), astrocytes modify their structure, usually studied by detecting the cytoskeletal glial fibrillary acidic protein (GFAP) and connexin expression (Peters et al., 2009; Giaume et al., 2010). Connexins form a "honeycomb" organization that creates edges between the end-feet enwrapping blood vessels. Here, astrocytes through aquaporin-4 (AQP4) water channels coordinate water flux and the clearance of interstitial fluid and neurotoxic solutes, including beta amyloid (Aβ). When such a clearance is dysfunctional, Aβ deposition occurs facilitating neurodegeneration (Iliff et al., 2012).

Astrocytes support neurons by releasing several neurotrophins, like S100B and the brain-derived neurotrophic factor (BDNF) (Marshak, 1990; Wiese et al., 2012). In the event of an abnormal production, as in some diseases including AD, such molecules contribute to neuronal damage (Vondran et al., 2010; Scuderi et al., 2014a; Bronzuoli et al., 2016). Glia involvement in the onset and/or progression of AD has been demonstrated by our and other groups (Esposito et al., 2007a; Esposito et al., 2007b; Esposito et al., 2011; Scuderi et al., 2011; Scuderi et al., 2012; Scuderi et al., 2014b; Scuderi and Steardo, 2013; Cipriano et al., 2015; Salter and Stevens, 2017; Taipa et al., 2017). Less is known about their role during healthy aging. Therefore, in this brief research report, we provide a preliminary descriptive investigation of the effects of aging on morphology and functions of hippocampal astrocytes and microglia by comparing young adult (6-month-old) and aged (12-month-old) healthy (Non-Tg) and AD-like (3×Tg-AD) mice to model healthy and pathological aging, respectively. We explored the hippocampal expression of GFAP and S100B for astrocytes, and the ionized calcium binding adaptor molecule-1 (Iba1) and the cluster of differentiation 11b/c (CD11b/c) for microglia. Moreover, we examined deeper astrocyte functions by exploring AQP4 and CX43 expression. Since one of the most important astrocytes functions is the neurotrophic support (Kimelberg and Nedergaard, 2010), we also investigated BDNF production and the dendritic microtubule-associated protein 2 (MAP2).

Collectively, our findings reveal that aging negatively alters astrocytic functions, including their neurotrophic support. A main effect of aging and not of genotype was detected in all astrocytic markers here studied, thus suggesting that observed alterations to astroglia functions were related to aging itself rather than AD.

MATERIALS AND METHODS

All procedures involving animals were approved by the Italian Ministry of Health (Rome, Italy) and performed in compliance with the guidelines of the Directive 2010/63/EU of the European Parliament, and the D.L. 26/2014 of Italian Ministry of Health.

Animals

Six- and 12-month-old male 3×Tg-AD mice (homozygous for $PS1_{M146V}$ and homozygous for the co-injected APP_{swe}, tau_{P301L} transgenes) were used as model of pathological aging. This mutant mouse exhibits, indeed, AD-like plaques and tangles associated with synaptic dysfunction (Oddo et al., 2003a), observed also in our experimental conditions (see **Supplementary Figure S1**). To reproduce a condition of healthy aging, age-matched wild-type littermates (Non-Tg) (C57BL6/129SvJ) were used. Mice were housed in an enriched environment at controlled conditions (22 ± 2°C temperature, 12-h light/12-h dark cycle, 50–60% humidity), with *ad libitum* food and water. Six male mice per group were decapitated, and their brains rapidly isolated and either flash frozen in 2-methylbutane to perform immunofluorescences or dissected to isolate hippocampi for western blot analyses. Tissues were stored at −80°C.

Western Blot

Hippocampi were processed as previously described (Scuderi et al., 2018a). Briefly, tissues were homogenized in ice-cold hypotonic lysis buffer and then centrifuged. Fifty micrograms of proteins was resolved on 12% acrylamide SDS-PAGE gels and then transferred onto nitrocellulose membranes, which were blocked for 1 h with either 5% bovine serum albumin (BSA) (Fitzgerald, MA) or non-fat dry milk (Bio-Rad, Italy) in tris-buffered saline-0.1% tween-20 (Corning, NY). Membranes were then incubated overnight with one of the following primary antibodies: rabbit anti-GFAP (1:25,000; Abcam, UK), rabbit anti-S100B (1:1,000; Novus Biological, CO), rabbit anti-Iba1 (1:1,000; Abcam), rabbit anti-CD11b/c (1:1,000; Bioss, MA), mouse anti-CX43 (1:500; EMD Millipore, MA), mouse anti-AQP4 (1:500; Santa Cruz, TX), rabbit anti-BDNF (1:1,000; Abcam), mouse anti-β-amyloid (1:200; Millipore, Germany), rabbit anti-p[Ser396]tau (1:1,000; Thermo Fisher Scientific, MA). Rabbit anti-β-actin (1:1,500, Santa Cruz) was used as loading control. After rinses, membranes were incubated with the proper secondary horseradish peroxidase (HRP)-conjugated antibody (1:10,000–1:30,000; Jackson ImmunoResearch, UK), and immunocomplexes detected by an ECL kit (GE Healthcare Life Sciences, Italy). Signals were analyzed by ImageJ.

Immunofluorescence

As previously described (Bronzuoli et al., 2018), hippocampal coronal slices (12-μm thickness) obtained at a cryostat were post-fixed with 4% paraformaldehyde (Sigma-Aldrich). After blockage in 1% BSA dissolved in PBS/0.25% triton X-100, slices were incubated overnight with one of the following primary antibodies: mouse anti-CX43 (1:50, EMD Millipore), mouse anti-AQP4 (1:50, Santa Cruz), rabbit anti-GFAP (1:1000, Abcam), mouse anti-MAP2 (1:250, Novus Biologicals). Sections were rinsed in PBS and incubated for 2 h with the proper secondary antibody [1:200 fluorescine-affinipure goat anti-rabbit IgG (H+L); 1:300-1:400 rhodamine-affinipure goat anti-mouse IgG (H+L) (Jackson ImmunoResearch)] and DAPI (1:75,000, Sigma-Aldrich). Fluorescence was detected by an Eclipse E600 microscope (Nikon, Japan). To avoid the observation of differences among groups caused by artifacts, the exposure parameters, including gain and time, were kept uniform during image acquisitions. Pictures were captured by a QImaging camera and analyzed by

ImageJ. Immunofluorescence quantifications are expressed as $\Delta F/F_0 = [(F- F_0)/F_0]$, where F is the mean fluorescence intensity and F_0 is the mean background fluorescence. We performed immunofluorescence experiments in the hippocampus, focusing our analyses on the Ammon's horn 1 (CA1) subregion because this area is one of the most vulnerable to AD, in both patients (Rössler et al., 2002; Mueller et al., 2010) and 3×Tg-AD mice (Oddo et al., 2003a). We analyzed three serial coronal sections per animal (between −1.82 and −1.94 mm from bregma) spaced 36 μm apart, analyzing four ROIs in the stratum radiatum of each section (200 × 100 μm).

Statistics

Data were analyzed by two-way ANOVA using GraphPad Prism6. When applicable, Bonferroni's *post hoc* test was used. Data were expressed as mean ± standard error of the mean (SEM) of percentage of control (6-month-old/Non-Tg mice).

RESULTS

Aging Affects Morphology and Functions of Hippocampal Astrocytes, Independent of Genotype

Results from Western blot experiments, performed in homogenates of hippocampi of Non-Tg and 3×Tg AD mice, showed that age significantly affects astrocyte morphology and functions. In fact, we observed a significant reduction of the cytoskeletal protein GFAP and the neurotrophin S100B in 12-month-old mice compared with 6-month-old mice, irrespective of genotype (**Figure 1A**, **B**, **C**). Moreover, we found a significant genotype-by-age interaction on GFAP data ($p = 0.0357$). By immunofluorescence, we observed a significant reduction of GFAP in the hippocampal CA1 subregion of 12-month-old mice compared with 6-month-old mice, independently of genotype (**Figure 1F**, **G**, **H**). In addition, results from immunofluorescence and Western blot revealed that aging impacts on astrocyte functions. Indeed, we found a significant decrease of CX43 expression in 12-month-old mice compared with 6-month-old mice, independently of genotype (**Figure 1A**, **D**, **F**, **I**). Moreover, in the same experimental conditions, we observed an increased expression of AQP4 in the hippocampi of aged mice regardless of genotype (**Figure 1A**, **E**, **G**, **L**). For both AQP4 and CX43, no genotype-by-age interaction was detected.

Aging Does Not Significantly Affect Hippocampal Microglia

In hippocampal homogenates of Non-Tg and 3×Tg-AD mice, we performed Western blot experiments for Iba1, a calcium-binding protein constitutively expressed by both surveillant and activated microglia, and CD11b/c, a marker of proliferative reactivity. Obtained results showed that the expression of Iba1 was not affected by either age or genotype (**Figure 2A**, **B**). However, we observed a significant increase of CD11b/c in 6-month-old 3×Tg-AD mice in comparison with their age-matched Non-Tg littermates, indicative of a potential microglial activation in young transgenic animals, but not in aged ones (**Figure 2A**, **C**).

Aging Reduces Hippocampal Expression of BDNF, With No Significant Impact on Neuronal Loss, Independent of Genotype

The neurotrophic factor BDNF is produced by neurons and, only under pathological circumstances, by astrocytes (Parpura and Zorec, 2010; Fulmer et al., 2014). Therefore, we tested whether aging could affect BDNF production and, in turn, cause neuronal loss. Results from Western blot experiments, performed in homogenates of hippocampi of Non-Tg and 3×Tg AD mice, showed a significant age-related decrease in BDNF production, irrespective of genotype (**Figure 3A**, **B**). Despite the observed reduction of this important neurotrophic factor, the hippocampal expression of the dendritic marker MAP2, analyzed by immunofluorescence, was not significantly different between all experimental groups (**Figure 3C**, **D**).

DISCUSSION

In the present study, we provide the first preliminary evidence of the effect of aging on structure and functions of hippocampal glial cells. Our primary goal was to study the impact of age on glial cells in conditions of physiological and pathological, AD-like, aging. To start addressing this issue, we used young adult and aged Non-Tg and 3×Tg-AD mice to simulate healthy and pathological aging, respectively. Collectively, our results indicate that aging affects astrocytes with no significant differences between the two genotypes.

The importance of glia in maintaining brain homeostasis and cerebral metabolism is well documented (Parpura and Haydon, 2008; Dzamba et al., 2016). Growing evidence demonstrate the fundamental role of these cells in the etiopathogenesis of several neuropsychiatric disorders thus opening new scenarios to the development of glia-targeted drugs (Bronzuoli et al., 2017; Bronzuoli et al., 2018; Bronzuoli et al., 2019; Cartocci et al., 2018; Scuderi et al., 2018a). The role of glia in healthy aging is still poorly investigated. No data are yet available elucidating whether glial abnormalities involved in neurodegeneration were due to disease progression or they were just a consequence of aging itself. Therefore, we compared young adult (6-month-old) and aged (12-month-old) healthy (Non-Tg) and AD-like (3×Tg-AD) mice. 3×Tg-AD mice progressively and hierarchically develop Aβ plaques and neurofibrillary tangles in AD-relevant brain regions (cortex, hippocampus, and amygdala) and show an age-related cognitive decline that closely mimics the human AD progression (Oddo et al., 2003b; Cassano et al., 2011; Cassano et al., 2012; Romano et al., 2014; Coughlan et al., 2018). Here, we demonstrate that aging affects glial cells, especially modifying astrocyte structure and functions. In our experimental conditions, we observed that aging reduces the expression of the cytoskeletal GFAP and the neurotrophin S100B, regardless of mice genotype. The age-dependent increase in astrocyte reactivity has been well documented (Beach et al., 1989; David et al., 1997; Janota et al., 2015).

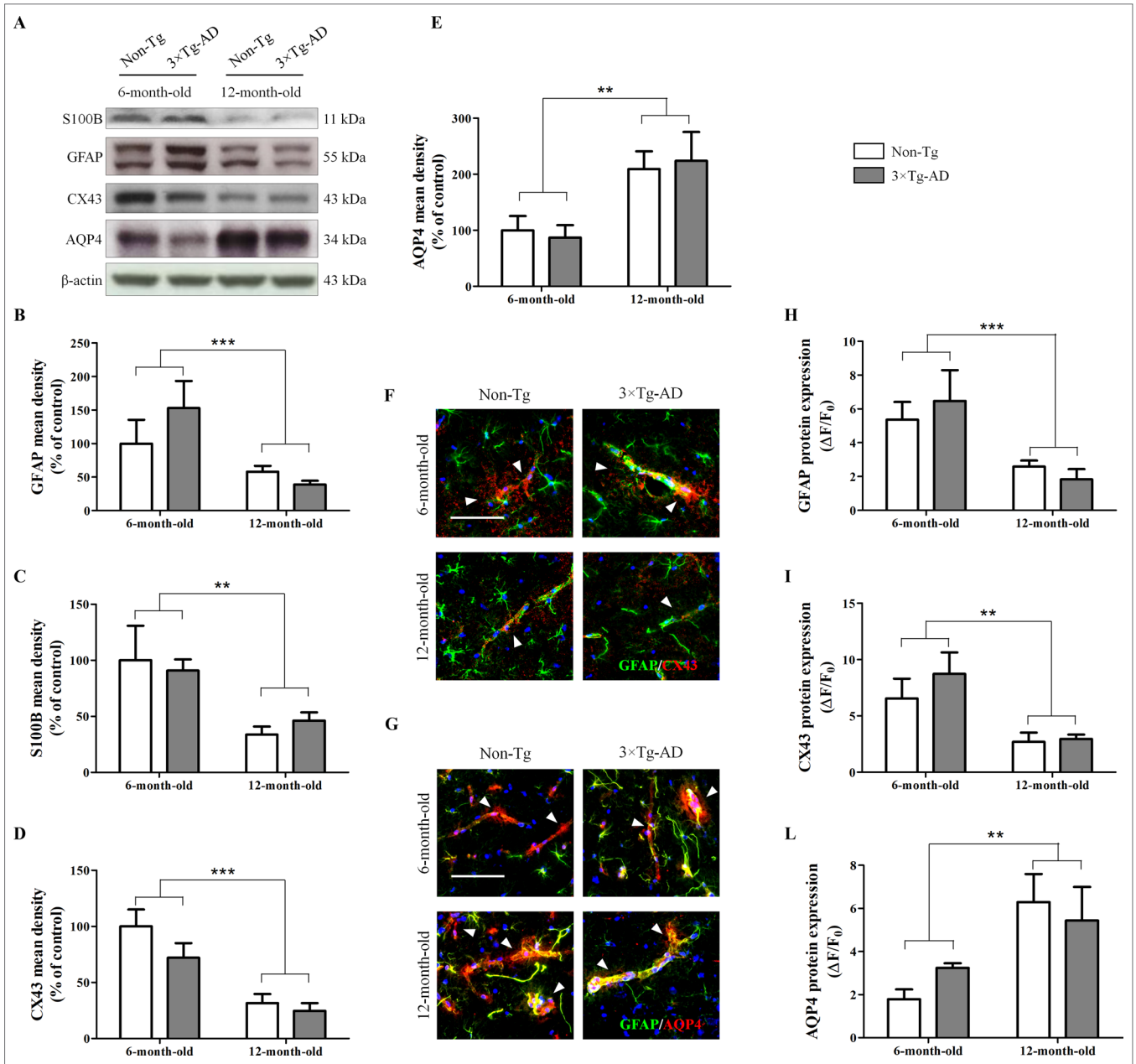

FIGURE 1 | Effects of aging on morphology and functions of hippocampal astrocytes. **(A)** Representative western blots for GFAP, S100B, CX43 and AQP4 and **(B**, **C**, **D**, **E)** densitometric analyses normalized to β-actin loading control. Results are expressed as means ± SEM of percentage of controls (6-month-old/Non-Tg) (N = 3, in triplicate). **(F)** Representative fluorescent photomicrographs of CX43 (red) and GFAP (green) in the hippocampal CA1 region of both 6- and 12-month-old Non-Tg and 3×Tg-AD mice. White arrows indicate CX43 mainly expressed in astrocytes enveloping blood vessels. **(G)** Representative fluorescent photomicrographs of AQP4 (red) and GFAP (green) in the hippocampal CA1 region of both 6- and 12-month-old Non-Tg and 3×Tg-AD mice. White arrows indicate AQP4 expressed in astrocyte end-feet surrounding blood vessels. Fluorescence analyses of **(H)** GFAP, **(I)** CX43 and **(L)** AQP4 are expressed as $\Delta F/F_0 = [(F- F_0)/F_0]$, where F is the mean fluorescence intensity and F_0 is the mean background fluorescence. Nuclei were stained with DAPI (blue). Scale bar 50 μm. Statistical analysis was performed by two-way ANOVA followed by Bonferroni's *post hoc* test (**$p < 0.01$; ***$p < 0.001$, 6-month-old vs 12-month-old).

However, data obtained from both human material and animal models demonstrate the existence of a complex and region-specific glial response in AD and aging that can be crudely summarized in glial reactivity or glial degeneration, atrophy, and loss of functions (Rodríguez et al., 2016; Verkhratsky et al., 2016; Scuderi et al., 2018b). Our findings are apparently in contrast with the evidence indicating an age-matched astrogliosis in 3×Tg-AD mice (Oddo et al., 2003a; Zaheer et al., 2013). However, Oddo and colleagues analyzed cortical and hippocampal levels of GFAP in both 3×Tg-AD and Non-Tg mice showing no substantial difference between genotype in the hippocampal levels of GFAP in agreement with the results of the present paper (Oddo et al., 2003a). GFAP expression

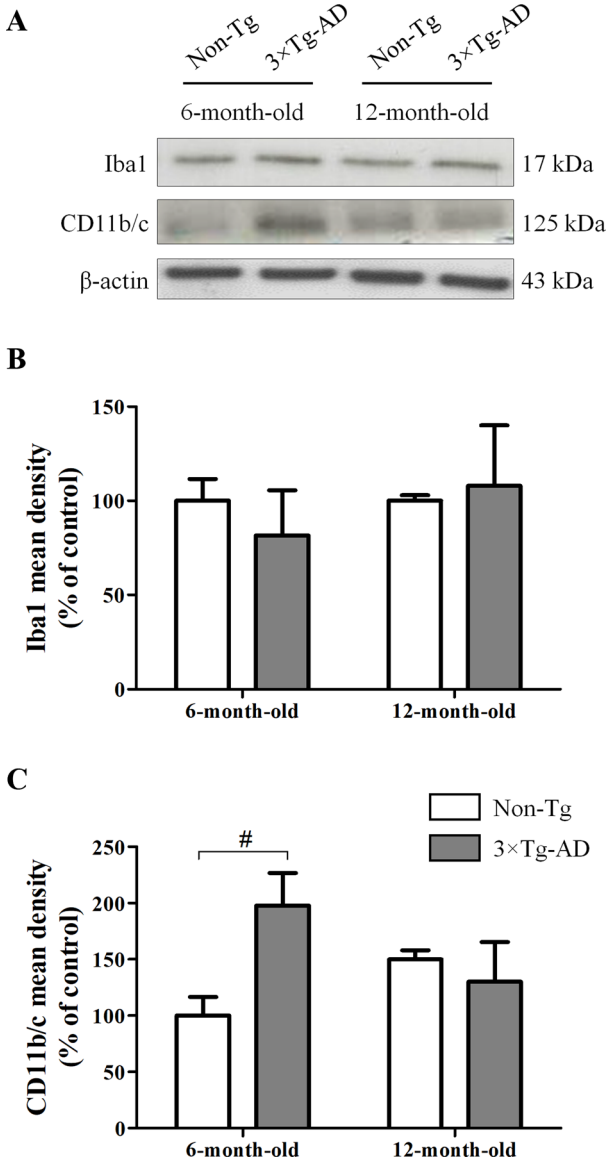

FIGURE 2 | Effects of aging on hippocampal microglia of 3×Tg-AD and Non-Tg mice. **(A)** Representative Western blots for Iba1 and CD11b/c and **(B, C)** densitometric analyses normalized to β-actin loading control. Results are expressed as means ± SEM of percentage of controls (6-month-old/Non-Tg) (N = 3, in triplicate). Statistical analysis was performed by two-way ANOVA followed by Bonferroni's *post hoc* test ($^{\#}p < 0.05$, 6-month-old/3×Tg-AD vs 6-month-old/Non-Tg).

showed a trend toward being upregulated with increasing age in their experimental conditions; however, they compared 2-month-old mice with 16-month-old mice. The different age chosen for comparison could explain the discrepancy with the present data. 3×Tg-AD mice show activated astrocytes and microglia as age increases and the majority of the studies detected them near amyloid plaques (Oddo et al., 2003a; Zaheer et al., 2013; Rodríguez-Arellano et al., 2016). Interestingly, numerous investigators reported the concomitant occurrence of astrogliosis and astroglial atrophy, demonstrating that the latter appears as a generalized process, whereas astrogliosis is triggered by senile plaques and Aβ aggregates (Rodríguez et al., 2009; Olabarria et al., 2010; Heneka et al., 2010; Verkhratsky et al., 2010; Yeh et al., 2011). In parallel with activation, the AD progression is also associated with astrodegeneration. Accordingly, atrophic astrocytes have been observed in the hippocampus, prefrontal and entorhinal cortices of mouse models of AD (Verkhratsky et al., 2016). In line with these observations, our group has recently demonstrated a reduction of GFAP in the hippocampus of aged 3×Tg-AD mice (Scuderi et al., 2018a). Interestingly, Hoozemans and colleagues (2011) showed lower GFAP immunostaining in post-mortem brains from old AD patients (>80 years) compared with younger AD cases, concluding that the occurrence of astrocyte activation decreases with increasing age in AD dementia.

In our experimental conditions, aging negatively affected astrocyte functions, with particular regard to some of their homeostatic and neurotrophic roles. We found, in both 3×Tg-AD and Non-Tg mice, a significant reduction of CX43 expression, one of the major gap junction proteins that allow an efficient communication among astrocytes. Our data are in line with those obtained by Cotrina and collaborators (2001) demonstrating an age-dependent CX43 reduction in C57Bl/6 mice. The impairments observed in our experimental conditions seems to be caused by aging; in fact, we did not observe any significant differences between the two genotypes. We speculate that this finding together with the aforementioned astrocyte atrophy could be due to a reduced communication among astrocytes. This communication is usually mediated by endogenous peptides, growth factors, neurotransmitters, bioactive lipids, and structural proteins widely expressed in the astrocytic end-feet enveloping blood vessels (Rouach et al., 2002). Interestingly, some authors demonstrated that CX43 reduction boosts Aβ deposits (Koulakoff et al., 2012). In this context, our data could suggest a mechanism responsible for the observed deposition of a huge amount of Aβ in the brain of healthy subjects not affected by AD (Chételat et al., 2013).

AQP4 is another astrocytic protein implicated in the CNS lymphatic drainage and clearance of interstitial solutes, including Aβ (Cotrina et al., 2001; Iliff et al., 2012; Yang et al., 2016). We found that aging is responsible for the augmented AQP4 expression, independent of genotype. Accordingly, AQP4 is highly expressed near Aβ plaques in amyloidopathies (Moftakhar et al., 2010). The raise in AQP4 expression could be a compensatory process aimed at keeping water and ion homeostasis, and at encouraging the clearance of the interstitial fluid in the CNS in both physiological and pathological aging (Gupta and Kanungo, 2013). Interestingly, our data on CX43 and AQP4 are in line with those we obtained on $A\beta_{(1\text{-}42)}$ levels (Supplementary Figure S1). Indeed, we found higher hippocampal $A\beta_{(1\text{-}42)}$ levels in aged mice of both genotypes. We also observed a significant increase of $A\beta_{(1\text{-}42)}$ expression in 3×Tg-AD mice in comparison to Non-Tg animals, at both ages. Given these results, further experiments are required to look for a correlation between severity of pathology and astrocyte protein expression, also investigating other areas crucially involved in AD.

Quite unexpectedly, we did not observe significant structural modifications in microglia in our experimental conditions, except for a significant activation in young transgenic mice, supposedly indicative of the presence of an early

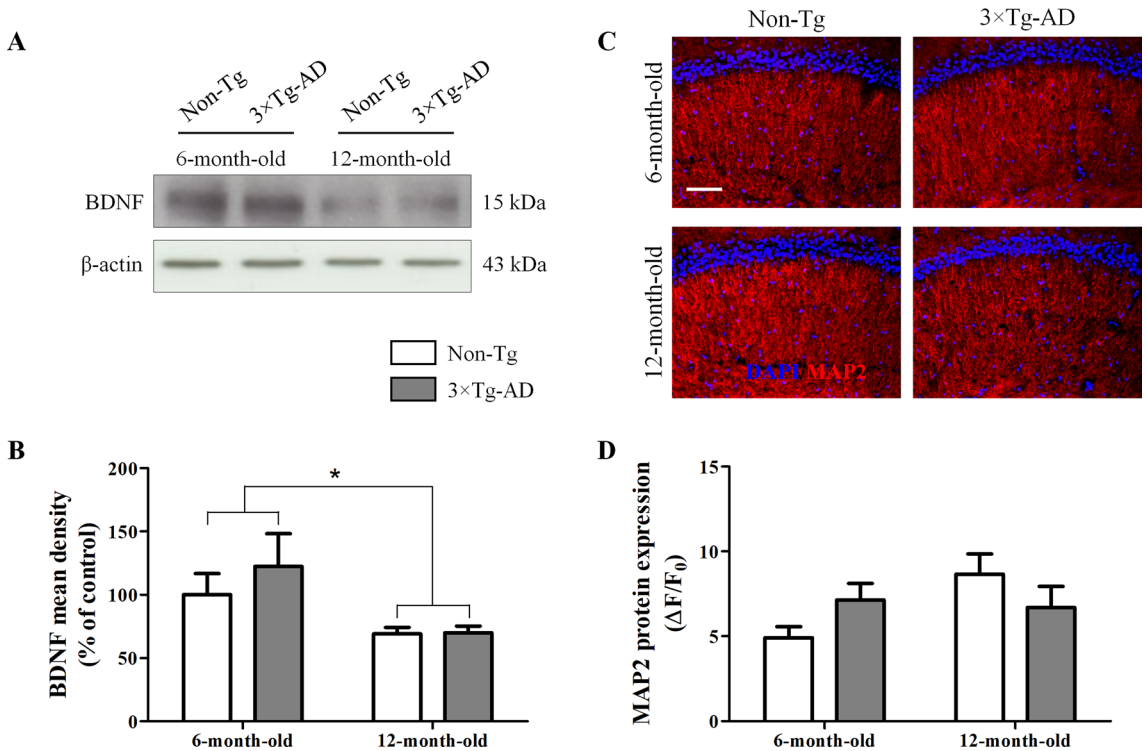

FIGURE 3 | Effects of aging on BDNF and MAP2 expression in hippocampus of 3×Tg-AD and Non-Tg mice. **(A)** Representative Western blots for BDNF and **(B)** densitometric analysis normalized to β-actin as loading control. Results are expressed as means ± SEM of percentage of controls (6-month-old/Non-Tg) (N = 3, in triplicate). **(C)** Representative fluorescent photomicrographs of MAP2 (red) in the hippocampal CA1 region of both 6- and 12-month-old Non-Tg and 3×Tg-AD mice. **(D)** MAP2 fluorescence analysis is expressed as $\Delta F/F_0 = [(F - F_0)/F_0]$, where F is the mean fluorescence intensity and F_0 is the mean background fluorescence. Nuclei were stained with DAPI (blue). Scale bar 50 μm. Statistical analysis was performed by two-way ANOVA followed by Bonferroni's *post hoc* test (*$p < 0.05$; 6-month-old vs 12-month-old).

pro-inflammatory status which disappears in adult mice. These findings are in line with those previously obtained in 3×Tg-AD mice showing that neuroinflammation occurs early in AD-like pathology (Bronzuoli et al., 2018; Scuderi et al., 2018a), and with some authors suggesting that neuroinflammation becomes less and less evident and spread as the disease progresses, remaining detectable in the proximity of Aβ plaques and neurofibrillary tangles (Yeh et al., 2011; Rodríguez-Arellano et al., 2016; Verkhratsky et al., 2016).

The role of microglia in aging and AD is complex and not fully elucidated. Microglial pro-inflammatory markers, including fractalkine and receptors, are reduced in the brain of aged mice compared to adult controls (Wynne et al., 2010), and microglia in aged animals appear irregularly distributed, with variable morphology of both cell bodies and processes, occupying smaller territories (Tremblay et al., 2012). Moreover, it has been demonstrated that 3×Tg-AD mice at 2, 3, and 6 months progressively show significant microglia activation in the entorhinal cortex but not in the hippocampus (Janelsins et al., 2005), as well as a significant increase of activated microglia at 18 months of age compared to 3×Tg-AD mice at 9 months, but not at 12 months of age (Rodríguez et al., 2013). Conversely, very recently Belfiore and colleagues (2019) have demonstrate an age-dependent activation of hippocampal microglia in female 3×Tg-AD mice, from 6 up to 20 months of age. The heterogeneity of these results confirms that categorizing microgliosis is still particularly challenging. Nowadays, several authors hypothesize the presence of diverse microglial reactions to different disease stages, suggesting that the complete characterization of these processes may open new avenues for therapeutic intervention (Mosher and Wyss-Coray, 2014; Sarlus and Heneka, 2017). Based on these considerations and keeping in mind that our study is preliminary, we believe that further experiments using more specific markers will be required to better characterize the microglia phenotype and its correlations with the neuroinflammatory process also investigating other brain areas importantly affected by AD.

Astrocytes produce and release several neurotrophins, including S100B and BDNF. S100B is a calcium-binding protein mainly involved in cell cycle progression and differentiation as well as neurite outgrowth (Scotto et al., 1998; Sen and Belli, 2007). BDNF is produced mainly by astrocytes over neurons under pathological conditions (Dougherty et al., 2000). We found a significant reduction of both BDNF and S100B in aged mice, irrespective of genotype. Since BDNF regulates the astrocytic expression of S100B and both together are required to support at least serotonergic neurons (Ye et al., 2011), further studies would elucidate the cross-talk between astrocytes and

neuronal cells. Despite the reduced neurotrophic support, we did not detect neuronal impairment, as assessed by MAP2.

In conclusion, in this brief research report, we provide preliminary data demonstrating that aging rather than AD progression importantly affects morphology and functions of hippocampal glial cells. In our experimental conditions, the most vulnerable cells were the astrocytes whose structure and functions appear profoundly modified. Additional studies are required to further reveal the role of astrocytes and microglia in both physiological and pathological aging, using more specific markers for the detection of changes in their morphology and/or functions, and extending such observations in other brain regions. Avoiding any superficial projection to human disease and keeping in mind that human astrocytes are more complex than their murine counterparts, these data open novel perspective in the field of astrocyte functions in health and disease.

DATA AVAILABILITY STATEMENT

Datasets are available on request. Requests to access the datasets should be directed to caterina.scuderi@uniroma1.it.

ETHICS STATEMENT

All procedures involving animals were approved by the Italian Ministry of Health (Rome, Italy) and performed in compliance with the guidelines of the Directive 2010/63/EU of the European Parliament, and the D.L. 26/2014 of Italian Ministry of Health.

AUTHOR CONTRIBUTIONS

MB, RF, MV, and CS performed most of the molecular experiments and analyzed the data. TC housed and raised the animals. LS, TC, and CS supervised the experiments and discussed the results. MB, RF, MV, and CS wrote the manuscript. All authors contributed to and approved the final manuscript.

FUNDING

This work was supported by the Italian Ministry of Instruction, University and Research (MIUR) to LS (PON01-02512, PRIN prot. 2009NKZCNX, PRIN prot. 2015HRE757) and to CS (PRIN prot. 2015KP7T2Y_002); the SAPIENZA University of Rome to CS (prot. C26A15X58E and prot. MA116154CD981DAE) and MB (prot. C26N15BHZZ).

SUPPLEMENTARY MATERIAL

The Supplementary Material for this article can be found online at: https://www.frontiersin.org/articles/10.3389/fphar.2019.00644/full#supplementary-material

FIGURE S1 | Effects of aging on $A\beta_{(1-42)}$ production and tau protein phosphorylation in hippocampus of 3×Tg-AD and Non-Tg mice. **(A)** Representative Western blots for $A\beta_{(1-42)}$ and p[Ser396]tau and **(B**, **C)** densitometric analyses normalized to β-actin as loading control. Results are expressed as means ± SEM of percentage of controls (6-month-old/Non-Tg) (N = 3, in triplicate). Statistical analysis was performed by two-way ANOVA followed by Bonferroni's *post hoc* test (**$p < 0.01$; ***$p < 0.001$, 6-month-old vs 12-month-old; ##$p < 0.01$, 6-month-old/3×Tg-AD vs 6-month-old/Non-Tg; ###$p < 0.001$, 12-month-old/3×Tg-AD vs 12-month-old/Non-Tg).

REFERENCES

Acosta, C., Anderson, H. D., and Anderson, C. M. (2017). Astrocyte dysfunction in Alzheimer disease. *J. Neurosci. Res.* 95 (12), 2430–2447. doi: 10.1002/jnr.24075

Beach, T. G., Walker, R., and McGeer, E. G. (1989). Patterns of gliosis in Alzheimer's disease and aging cerebrum. *Glia* 2, 420–436. doi: 10.1002/glia.440020605

Belfiore, R., Rodin, A., Ferreira, E., Velazquez, R., Branca, C., Caccamo, A., et al. (2019). Temporal and regional progression of Alzheimer's disease-like pathology in 3xTg-AD mice. *Aging Cell* 18 (1), e12873. doi: 10.1111/acel.12873

Bronzuoli, M. R., Facchinetti, R., Ingrassia, D., Sarvadio, M., Schiavi, S., Steardo, L., et al. (2019). Neuroglia in the autistic brain: evidence from a preclinical model. *Mol. Autism* 9, 66. doi: 10.1186/s13229-018-0254-0

Bronzuoli, M. R., Facchinetti, R., Steardo, L. Jr., Romano, A., Stecca, C., Passarella, S., et al. (2018). Palmitoylethanolamide dampens reactive astrogliosis and improves neuronal trophic support in a triple transgenic model of Alzheimer's disease: *in vitro* and *in vivo* evidence. *Oxid. Med. Cell. Longev.* 2018, 4720532. doi: 10.1155/2018/4720532

Bronzuoli, M. R., Facchinetti, R., Steardo, L., and Scuderi, C. (2017). Astrocyte: an innovative approach for Alzheimer's disease therapy. *Curr. Pharm Des.* 23 (33), 4979–4989. doi: 10.2174/1381612823666170710163411

Bronzuoli, M. R., Iacomino, A., Steardo, L., and Scuderi, C. (2016). Targeting neuroinflammation in Alzheimer's disease. *J. Inflamm Res* 9, 199–208. doi: 10.2147/JIR.S86958

Bruzzone, R., White, T. W., and Paul, D. L. (1996). Connections with connexins: the molecular basis of direct intercellular signaling. *Eur. J. Biochem.* 238 (1), 1–27. doi: 10.1111/j.1432-1033.1996.0001q.x

Cartocci, V., Catallo, M., Tempestilli, M., Segatto, M., Pfrieger, F. W., Bronzuoli, M. R., et al. (2018). Altered brain cholesterol/isoprenoid metabolism in a rat model of autism spectrum disorders. *Neuroscience* 372, 27–37. doi: 10.1016/j.neuroscience.2017.12.053

Cassano, T., Romano, A., Macheda, T., Colangeli, R., Cimmino, C. S., Petrella, A., et al. (2011). Olfactory memory is impaired in a triple transgenic model of Alzheimer disease. *Behav. Brain Res.* 224 (2), 408–412. doi: 10.1016/j.bbr.2011.06.029

Cassano, T., Serviddio, G., Gaetani, S., Romano, A., Dipasquale, P., Cianci, S., et al. (2012). Glutamatergic alterations and mitochondrial impairment in a murine model of Alzheimer disease. *Neurobiol. Aging* 33 (6), 1121.e1–12. doi: 10.1016/j.neurobiolaging.2011.09.021

Chételat, G., La Joie, R., Villain, N., Perrotin, A., de La Sayette, V., Eustache, F., et al. (2013). Amyloid imaging in cognitively normal individuals, at-risk populations and preclinical Alzheimer's disease. *Neuroimage Clin.* 2, 356–365. doi: 10.1016/j.nicl.2013.02.006

Cipriano, M., Esposito, G., Negro, L., Capoccia, E., Sarnelli, G., Scuderi, C., et al. (2015). Palmitoylethanolamide regulates production of pro-angiogenic mediators in a model of β amyloid-induced astrogliosis *in vitro*. *CNS Neurol Disord Drug Targets* 14 (7), 828–837. doi: 10.2174/1871527314666150317224155

Cotrina, M. L., Gao, Q., Lin, J. H., and Nedergaard, M. (2001). Expression and function of astrocytic gap junctions in aging. *Brain Res.* 901 (1–2), 55–61. doi: 10.1016/S0006-8993(01)02258-2

Coughlan, G., Laczó, J., Hort, J., Minihane, A. M., and Hornberger, M. (2018). Spatial navigation deficits - overlooked cognitive marker for preclinical Alzheimer disease? *Nat. Rev. Neurol.* 14 (8), 496–506. doi: 10.1038/s41582-018-0031-x

David, J. P., Ghozali, F., Fallet-Bianco, C., Wattez, A., Delaine, S., Boniface, B., et al. (1997). Glial reaction in the hippocampal formation is highly correlated with aging in the human brain. *Neurosci. Lett.* 235, 53–56. doi: 10.1016/S0304-3940(97)00708-8

Dougherty, K. D., Dreyfus, C. F., and Black, I. B. (2000). Brain-derived neurotrophic factor in astrocytes, oligodendrocytes, and microglia/macrophages after spinal cord injury. *Neurobiol. Dis.* 7, 574–585. doi: 10.1006/nbdi.2000.0318

Dzamba, D., Harantova, L., Butenko, O., and Anderova, M. (2016). Glial cells—the key elements of Alzheimer´s disease. *Curr. Alzheimer Res.* 13 (8), 894–911. doi: 10.2174/1567205013666160129095924

Esposito, G., Iuvone, T., Savani, C., Scuderi, C., De Filippis, D., Papa, M., et al. (2007b). Opposing control of cannabinoid receptor stimulation on amyloid-beta-induced reactive gliosis: *in vitro* and *in vivo* evidence. *J. Pharmacol. Exp. Ther.* 322 (3), 1144–1152. doi: 10.1124/jpet.107.121566

Esposito, G., Scuderi, C., Savani, C., Scuderi, C., De Filippis, D., Papa, M., et al. (2007a). Cannabidiol *in vivo* blunts beta-amyloid induced neuroinflammation by suppressing IL-1beta and iNOS expression. *Br. J. Pharmacol.* 151 (8), 1272–1279. doi: 10.1038/sj.bjp.0707337

Esposito, G., Scuderi, C., Valenza, M., Togna, G. I., Latina, V., De Filippis, D., et al. (2011). Cannabidiol reduces Aβ-induced neuroinflammation and promotes hippocampal neurogenesis through PPARγ involvement. *PLoS One* 6 (12), e28668. doi: 10.1371/journal.pone.0028668

Fulmer, C. G., VonDran, M. W., Stillman, A. A., Huang, Y., Hempstead, B. L., and Dreyfus, C. F. (2014). Astrocyte-derived BDNF supports myelin protein synthesis after cuprizone-induced demyelination. *J. Neurosci.* 34 (24), 8186–8196. doi: 10.1523/JNEUROSCI.4267-13.2014

Gehrmann, J., Matsumoto, Y., and Kreutzberg, G. W. (1995). Microglia: intrinsic immune effector cell of the brain. *Brain Res. Rev.* 20 (3), 269–287. doi: 10.1016/0165-0173(94)00015-H

Giaume, C., Koulakoff, A., Roux, L., Holcman, D., and Rouach, N. (2010). Astroglial networks: a step further in neuroglial and gliovascular interactions. *Nat. Rev. Neurosci.* 11 (2), 87–99. doi: 10.1038/nrn2757

Gupta, R. K., and Kanungo, M. (2013). Glial molecular alterations with mouse brain development and aging: up-regulation of the Kir4.1 and aquaporin-4. *Age (Dordr)* 35 (1), 59–67. doi: 10.1007/s11357-011-9330-5

Heneka, M. T., Rodríguez, J. J., and Verkhratsky, A. (2010). Neuroglia in neurodegeneration. *Brain Res. Rev.* 63 (1–2), 189–211. doi: 10.1016/j.brainresrev.2009.11.004

Hodson, R. (2018). Alzheimer's disease. *Nature* 559 (7715), S1. doi: 10.1038/d41586-018-05717-6

Hoozemans, J. J., Rozemuller, A. J., van Haastert, E. S., Eikelenboom, P., and van Gool, W. A. (2011). Neuroinflammation in Alzheimer's disease wanes with age. *J. Neuroinflammation* 8, 171. doi: 10.1186/1742-2094-8-171

Iliff, J. J., Wang, M., Liao, Y., Plogg, B. A., Peng, W., Gundersen, G. A., et al. (2012). A paravascular pathway facilitates CSF flow through the brain parenchyma and the clearance of interstitial solutes, including amyloid β. *Sci. Transl. Med.* 4 (147), 147ra111. doi: 10.1126/scitranslmed.3003748

Janelsins, M. C., Mastrangelo, M. A., Oddo, S., LaFerla, F. M., Federoff, H. J., and Bowers, W. J. (2005). Early correlation of microglial activation with enhanced tumor necrosis factor-alpha and monocyte chemoattractant protein-1 expression specifically within the entorhinal cortex of triple transgenic Alzheimer's disease mice. *J. Neuroinflammation* 18 (2), 23. doi: 10.1186/1742-2094-2-23

Janota, C. S., Brites, D., Lemere, C. A., and Brito, M. A. (2015). Glio-vascular changes during ageing in wild-type and Alzheimer's disease-like APP/PS1 mice. *Brain Res.* 1620, 153–168. doi: 10.1016/j.brainres.2015.04.056

Kimelberg, H. K., and Nedergaard, M. (2010). Functions of astrocytes and their potential as therapeutic targets. *Neurotherapeutics* 7, 338–353. doi: 10.1016/j.nurt.2010.07.006

Koulakoff, A., Mei, X., Orellana, J. A., Sáez, J. C., and Giaume, C. (2012). Glial connexin expression and function in the context of Alzheimer's disease. *Biochim. Biophys. Acta* 1818 (8), 2048–2057. doi: 10.1016/j.bbamem.2011.10.001

Marshak, D. R. (1990). S100 beta as a neurotrophic factor. *Prog. Brain Res.* 86, 169–181. doi: 10.1016/S0079-6123(08)63175-1

Moftakhar, P., Lynch, M. D., Pomakian, J. L., and Vinters, H. V. (2010). Aquaporin expression in the brains of patients with or without cerebral amyloid angiopathy. *J. Neuropathol. Exp. Neurol.* 69 (12), 1201–1209. doi: 10.1097/NEN.0b013e3181fd252c

Mosher, K. I., and Wyss-Coray, T. (2014). Microglial dysfunction in brain aging and Alzheimer's disease. *Biochem. Pharmacol.* 88 (4), 594–604. doi: 10.1016/j.bcp.2014.01.008

Mueller, S. G., Schuff, N., Yaffe, K., Madison, C., Miller, B., and Weiner, M. W. (2010). Hippocampal atrophy patterns in mild cognitive impairment and Alzheimer's disease. *Hum. Brain Mapp.* 31, 1339–1347. doi: 10.1002/hbm.20934

Oddo, S., Caccamo, A., Kitazawa, M., Tseng, B. P., and LaFerla, F. M. (2003a). Amyloid deposition precedes tangle formation in a triple transgenic model of Alzheimer's disease. *Neurobiol. Aging* 24 (8), 1063–470. doi: 10.1016/j.neurobiolaging.2003.08.012

Oddo, S., Caccamo, A., Shepherd, J. D., Murphy, M. P., Golde, T. E., Kayed, R., et al. (2003b). Triple-transgenic model of Alzheimer's disease with plaques and tangles: intracellular Abeta and synaptic dysfunction. *Neuron* 39 (3), 409–421. doi: 10.1016/S0896-6273(03)00434-3

Olabarria, M., Noristani, H. N., Verkhratsky, A., and Rodríguez, J. J. (2010). Concomitant astroglial atrophy and astrogliosis in a triple transgenic animal model of Alzheimer's disease. *Glia* 58 (7), 831–838. doi: 10.1002/glia.20967

Parpura, V., and Haydon, P. G. (2008). *Astrocytes in (patho)physiology of the nervous system.* Germany: Springer Science & Business Media.

Parpura, V., and Zorec, R. (2010). Gliotransmission: Exocytotic release from astrocytes. *Brain Res. Rev.* 63 (1–2), 83–92. doi: 10.1016/j.brainresrev.2009.11.008

Peters, O., Schipke, C. G., Philipps, A., Haas, B., Pannasch, U., Wang, L. P., et al. (2009). Astrocyte function is modified by Alzheimer's disease-like pathology in aged mice. *J. Alzheimers Dis.* 18 (1), 177–189. doi: 10.3233/JAD-2009-1140

Rodríguez, J. J., Olabarria, M., Chvatal, A., and Verkhratsky, A. (2009). Astroglia in dementia and Alzheimer's disease. *Cell Death Differ.* 16 (3), 378–385. doi: 10.1038/cdd.2008.172

Rodríguez, J. J., Noristani, H. N., Hilditch, T., Olabarria, M., Yeh, C. Y., Witton, J., et al. (2013). Increased densities of resting and activated microglia in the dentate gyrus follow senile plaque formation in the CA1 subfield of the hippocampus in the triple transgenic model of Alzheimer's disease. *Neurosci. Lett.* 27 (552), 129–134. doi: 10.1016/j.neulet.2013.06.036

Rodríguez, J. J., Butt, A. M., Gardenal, E., Parpura, V., and Verkhratsky, A. (2016). Complex and differential glial responses in Alzheimer's disease and ageing. *Curr. Alzheimer Res.* 13 (4), 343–358. doi: 10.2174/1567205013666160229112911

Rodríguez-Arellano, J. J., Parpura, V., Zorec, R., and Verkhratsky, A. (2016). Astrocytes in physiological aging and Alzheimer's disease. *Neuroscience* 323, 170–182. doi: 10.1016/j.neuroscience.2015.01.007

Romano, A., Pace, L., Tempesta, B., Lavecchia, A. M., Macheda, T., Bedse, G., et al. (2014). Depressive-like behavior is paired to monoaminergic alteration in a murine model of Alzheimer's disease. *Int. J. Neuropsychopharmacol.* 18 (4), pyu020 doi: 10.1093/ijnp/pyu020

Rössler, M., Zarski, R., Bohl, J., and Ohm, T. G. (2002). Stage-dependent and sector-specific neuronal loss in hippocampus during Alzheimer's disease. *Acta Neuropathol.* 103, 363–369. doi: 10.1007/s00401-001-0475-7

Rouach, N., Avignone, E., Même, W., Koulakoff, A., Venance, L., Blomstrand, F., et al. (2002). Gap junctions and connexin expression in the normal and pathological central nervous system. *Biol. Cell* 94 (7-8), 457–475. doi: 10.1016/S0248-4900(02)00016-3

Salter, M. W., and Stevens, B. (2017). Microglia emerge as central players in brain disease. *Nat. Med.* 23 (9), 1018–1027. doi: 10.1038/nm.4397

Sarlus, H., and Heneka, M. T. (2017). Microglia in Alzheimer's disease. *J. Clin. Invest* 127 (9), 3240–3249. doi: 10.1172/JCI90606

Scotto, C., Deloulme, J. C., Rousseau, D., Chambaz, E., and Baudier, J. (1998). Calcium and S100B regulation of p53-dependent cell growth arrest and apoptosis. *Mol. Cell Biol.* 18 (7), 4272–4281. doi: 10.1128/MCB.18.7.4272

Scuderi, C., Bronzuoli, M. R., Facchinetti, R., Pace, L., Ferraro, L., Broad, K. D., et al. (2018a). Ultramicronized palmitoylethanolamide rescues learning and memory impairments in a triple transgenic mouse model of Alzheimer's disease by exerting anti-inflammatory and neuroprotective effects. *Transl. Psychiatry* 8 (1), 32. doi: 10.1038/s41398-017-0076-4

Scuderi, C., Noda, M., and Verkhratsky, A. (2018b). Editorial: neuroglia molecular mechanisms in psychiatric disorders. *Front. Mol. Neurosci.* 31 (11), 407. doi: 10.3389/fnmol.2018.00407

Scuderi, C., Esposito, G., Blasio, A., Valenza, M., Arietti, P., Steardo, L. Jr., et al. (2011). Palmitoylethanolamide counteracts reactive astrogliosis induced by β-amyloid peptide. *J. Cell Mol. Med.* 15 (12), 2664–2674. doi: 10.1111/j.1582-4934.2011.01267.x

Scuderi, C., and Steardo, L. (2013). Neuroglial roots of neurodegenerative diseases: therapeutic potential of palmitoylethanolamide in models of

Alzheimer's disease. *CNS Neuro. Disord. Drug Targets* 12 (1), 62–69. doi: 10.2174/1871527311312010011

Scuderi, C., Stecca, C., Bronzuoli, M. R., Rotili, D., Valente, S., Mai, A., et al. (2014b). Sirtuin modulators control reactive gliosis in an *in vitro* model of Alzheimer's disease. *Front. Pharmacol.* 5, 89. doi: 10.3389/fphar.2014.00089

Scuderi, C., Stecca, C., Iacomino, A., and Steardo, L. (2013). Role of astrocytes in major neurological disorders: the evidence and implications. *IUBMB Life* 65 (12), 957–961. doi: 10.1002/iub.1223

Scuderi, C., Stecca, C., Valenza, M., Ratano, P., Bronzuoli, M. R., Bartoli, S., et al. (2014a). Palmitoylethanolamide controls reactive gliosis and exerts neuroprotective functions in a rat model of Alzheimer's disease. *Cell Death Dis.* 5, e1419. doi: 10.1038/cddis.2014.376

Scuderi, C., Valenza, M., Stecca, C., Esposito, G., Carratù, M. R., and Steardo, L. (2012). Palmitoylethanolamide exerts neuroprotective effects in mixed neuroglial cultures and organotypic hippocampal slices *via* peroxisome proliferator-activated receptor-α. *J. Neuroinflammation* 9, 49. doi: 10.1186/1742-2094-9-21

Sen, J., and Belli, A. (2007). S100B in neuropathologic states: the CRP of the brain? *J. Neurosci. Res.* 85 (7), 1373–1380. doi: 10.1002/jnr.21211

Steardo, L. Jr., Bronzuoli, M. R., Iacomino, A., Esposito, G., Steardo, L., and Scuderi, C. (2015). Does neuroinflammation turn on the flame in Alzheimer's disease? Focus on astrocytes. *Front. Neurosci.* 9, 259. doi: 10.3389/fnins.2015.00259

Taipa, R., Ferreira, V., Brochado, P., Robinson, A., Reis, I., Marques, F., et al. (2017). Inflammatory pathology markers (activated microglia and reactive astrocytes) in early and late onset Alzheimer disease: a post-mortem study. *Neuropathol. Appl. Neurobiol.* 44 (3), 298–313. doi: 10.1111/nan.12445

Theis, M., Söhl, G., Eiberger, J., and Willecke, K. (2005). Emerging complexities in identity and function of glial connexins. *Trends Neurosci.* 28 (4), 188–195. doi: 10.1016/j.tins.2005.02.006

Tremblay, M.È., Zettel, M. L., Ison, J. R., Allen, P. D., and Majewska, A. K. (2012). Effects of aging and sensory loss on glial cells in mouse visual and auditory cortices. *Glia* 60 (4), 541–558. doi: 10.1002/glia.22287

van der Flier, W. M., and Scheltens, P. (2005). Epidemiology and risk factors of dementia. *J. Neurol. Neurosurg. Psychiatry* 76 (Suppl V), v2–v7. doi: 10.1136/jnnp.2005.082867

Verkhratsky, A., Olabarria, M., Noristani, H. N., Yeh, C. Y., and Rodríguez, J. J. (2010). Astrocytes in Alzheimer's disease. *Neurotherapeutics* 7, 399–412. doi: 10.1016/j.nurt.2010.05.017

Verkhratsky, A., Zorec, R., Rodríguez, J. J., and Parpura, V. (2016). Astroglia dynamics in ageing and Alzheimer's disease. *Curr. Opin. Pharmacol.* 26, 74–79. doi: 10.1016/j.coph.2015.09.011

Vondran, M. W., Clinton-Luke, P., Honeywell, J. Z., and Dreyfus, C. F. (2010). BDNF+/- mice exhibit deficits in oligodendrocyte lineage cells of the basal forebrain. *Glia* 58 (7), 848–856. doi: 10.1002/glia.20969

Wiese, S., Karus, M., and Faissner, A. (2012). Astrocytes as a source for extracellular matrix molecules and cytokines. *Front. Pharmacol.* 3, 120. doi: 10.3389/fphar.2012.00120

Wynne, A. M., Henry, C. J., Huang, Y., Cleland, A., and Godbout, J. P. (2010). Protracted downregulation of CX3CR1 on microglia of aged mice after lipopolysaccharide challenge. *Brain Behav. Immun.* 24 (7), 1190–1201. doi: 10.1016/j.bbi.2010.05.011

Yang, C., Huang, X., Huang, X., Mai, H., Li, J., Jiang, T., et al. (2016). Aquaporin-4 and Alzheimer's Disease. *J. Alzheimers Dis.* 52 (2), 391–402. doi: 10.3233/JAD-150949

Ye, Y., Wang, G., Wang, H., and Wang, X. (2011). Brain-derived neurotrophic factor (BDNF) infusion restored astrocytic plasticity in the hippocampus of a rat model of depression. *Neurosci. Lett.* 503 (1), 15–19. doi: 10.1016/j.neulet.2011.07.055

Yeh, C. Y., Vadhwana, B., Verkhratsky, A., and Rodríguez, J. J. (2011). Early astrocytic atrophy in the entorhinal cortex of a triple transgenic animal model of Alzheimer's disease. *ASN Neuro* 3 (5), 271–279. doi: 10.1042/AN20110025

Zaheer, S., Thangavel, R., Wu, Y., Khan, M. M., Kempuraj, D., and Zaheer, A. (2013). Enhanced expression of glia maturation factor correlates with glial activation in the brain of triple transgenic Alzheimer's disease mice. *Neurochem. Res.* 38 (1), 218–225. doi: 10.1007/s11064-012-0913-z

Conflict of Interest Statement: MV is currently employed by company Epitech Group SpA, which had no role in study design, collection, analysis, and interpretation of data, in the writing of the report, and in the decision to submit the paper for publication. The remaining authors declare that the research was conducted in the absence of any commercial or financial relationships that could be construed as a potential conflict of interest.

Bronzuoli et al. Molecular Autism (2018) 9:66
https://doi.org/10.1186/s13229-018-0254-0

Molecular Autism

RESEARCH Open Access

Neuroglia in the autistic brain: evidence from a preclinical model

Maria Rosanna Bronzuoli[1†], Roberta Facchinetti[1†], Davide Ingrassia[1], Michela Sarvadio[2], Sara Schiavi[2], Luca Steardo[1], Alexei Verkhratsky[3,4,5], Viviana Trezza[2] and Caterina Scuderi[1*]

Abstract

Background: Neuroglial cells that provide homeostatic support and form defence of the nervous system contribute to all neurological disorders. We analyzed three major types of neuroglia, astrocytes, oligodendrocytes, and microglia in the brains of an animal model of autism spectrum disorder, in which rats were exposed prenatally to antiepileptic and mood stabilizer drug valproic acid; this model being of acknowledged clinical relevance.

Methods: We tested the autistic-like behaviors of valproic acid-prenatally exposed male rats by performing isolation-induced ultrasonic vocalizations, the three-chamber test, and the hole board test. To account for human infancy, adolescence, and adulthood, such tasks were performed at postnatal day 13, postnatal day 35, and postnatal day 90, respectively. After sacrifice, we examined gene and protein expression of specific markers of neuroglia in hippocampus, prefrontal cortex, and cerebellum, these brain regions being associated with autism spectrum disorder pathogenesis.

Results: Infant offspring of VPA-exposed dams emitted less ultrasonic vocalizations when isolated from their mothers and siblings and, in adolescence and adulthood, they showed altered sociability in the three chamber test and increased stereotypic behavior in the hole board test. Molecular analyses indicate that prenatal valproic acid exposure affects all types of neuroglia, mainly causing transcriptional modifications. The most prominent changes occur in prefrontal cortex and in the hippocampus of autistic-like animals; these changes are particularly evident during infancy and adolescence, while they appear to be mitigated in adulthood.

Conclusions: Neuroglial pathological phenotype in autism spectrum disorder rat model appears to be rather mild with little signs of widespread and chronic neuroinflammation.

Keywords: Autism spectrum disorder, Astrocyte, Microglia, Oligodendrocyte, Valproic acid

Background

Autism spectrum disorder (ASD) is a heterogeneous set of neurodevelopmental disorders characterized by deficits in social communication and social interaction, stereotypies, and reduced patterns of behaviors [1, 2]. Even though ASD can be diagnosed at any age, symptoms generally appear in the childhood and last throughout a person's life. Although about 1% of the world population suffers from ASD [3], little is known on ASD etiology and pathogenesis. Genetic predispositions, maternal stressors, environmental factors, infectious agents, and the intake of specific drugs during pregnancy all have some degree of association with ASD [4]. One of the common environmental factors involved in the pathogenesis of ASD is maternal exposure to the antiepileptic and mood stabilizer drug valproic acid (VPA). When given during pregnancy, VPA was reported to induce various congenital malformations [5, 6] including autistic-like features in the exposed children, such as impaired communication, reduced sociability and stereotyped behaviors [7, 8]. Based on these clinical observations, prenatal VPA exposure in rodents has been developed and became a widely used environmental preclinical model of ASD with face and construct validity [9–11].

Recent findings highlight contribution of neuroglia to the ASD pathophysiology. Glial cells are non-excitable

* Correspondence: caterina.scuderi@uniroma1.it
†Maria Rosanna Bronzuoli and Roberta Facchinetti contributed equally to this work.
[1]Department of Physiology and Pharmacology, "Vittorio Erspamer" SAPIENZA University of Rome, 00185 Rome, Italy
Full list of author information is available at the end of the article

homeostatic cells of the central nervous system (CNS), sub-classified into astrocytes, oligodendrocytes and their precursors (also known as NG-2 glia) and microglia; all types of glia sustain vital brain functions [12]. Specifically, astroglial cells are key cellular contributors to the homeostasis of the nervous tissue and the brain as an organ [13–16]. Astrocytes regulate pH and ion homeostasis, regulate functional hyperaemia and provide trophic and metabolic support to neurones. Astrocytes are important elements of the cytoarchitecture of the brain. These cells are essential for synaptogenesis [17, 18] as well as synaptic remodeling and are likely to contribute to various aspects of memory formation, storage, and retention [19]. Oligodendrocytes form the myelin sheath, thus maintaining the functional connectome of the brain and contributing to the optimal information processing in complex neural networks [20]. Microglia provide the immune and cellular defence in the brain. Through several surveillance mechanisms, microglia detect diverse pathological extracellular signals, and respond to them to protect the brain. These cells also contribute to the development of the nervous tissue, shaping neuronal ensembles and synaptic plasticity [21–24].

Increasing appreciation of the multifaceted physiological roles of glia in the developing and mature CNS suggests that abnormalities in glial functions contribute to neuropathology. Several preclinical models of diseases revealed the role of glia in neurodevelopmental diseases, from ASD to neuropsychiatric disorders. Pathological changes in neuroglia are complex and can be classified into reactive response (astrogliosis, activation of microglia, and Wallerian remodeling of oligodendrocytes), degeneration with atrophy and loss of function (characteristic for astrocytes and microglia), and pathological remodeling [25–27]. The contribution of glial cells to pathological development of cognitive and neuropsychiatric disorders, such as Alzheimer's disease, Parkinson's disease, depression, schizophrenia, and others, has been demonstrated [28–36]. The role of glia in ASD however is not clear and often the data available are limited to their involvement in the inflammatory response.

In this study, we performed an in-depth analysis of gene and protein expression of specific markers of astrocytes, oligodendrocytes, and microglia in the rats prenatally exposed to VPA (ASD animal model). We studied brain areas critically involved in ASD, namely, hippocampus (HPC), prefrontal cortex (PfC), and cerebellum (Cb) [37–39]. To account for human infancy, adolescence, and adulthood, brain tissues were analyzed at three different ages, at postnatal day (PND) 13, PND 35, and PND 90. Our results indicate that prenatal VPA exposure affects all types of neuroglia, mainly causing transcriptional modifications. The most significant changes occur in PfC and in the HPC of autistic-like animals; these changes are particularly evident during infancy and adolescence, while they appear to be mitigated in adulthood.

Methods

All animal procedures were performed in agreement with the guidelines of the Italian Ministry of Health (D.L. 26/2014) and with the European Parliament directive 2010/63/EU.

Animals

The offspring born from VPA-exposed dams was obtained as described previously [40]. Adult female Wistar rats (Charles River, Arbresle, France) were housed and raised under controlled conditions (22 ± 2 °C temperature, 55–65% relative humidity, 12-h light/12-h dark cycle with lights on at 07:00 h) in an enriched environment, with food and water available ad libitum. Rats weighing 250 ± 15 g were mated overnight, and the morning when spermatozoa were found was assigned as gestational day 1 (GD 1). Pregnant rats, singly placed in Macrolon cages (40 × 26 × 20 cm), on GD 12.5, received an intraperitoneal injection of either VPA (500 mg/kg in saline) or saline (Veh). This dose of VPA, administered at this developmental time point, is known to induce autistic-like traits in the exposed rat offspring at infancy, adolescence, and adulthood [41]. The day after birth (PND 1), the litters were culled to six males and two females to reduce the litter size-induced variability in the growth and development of pups during the postnatal period. However, epidemiological studies report a higher incidence of ASD in boys than in girls, and it has been shown that the autistic-like-behaviors displayed by rats prenatally exposed to VPA are more pronounced in the male than in the female offspring [42, 43]. For these reasons, only the male offspring was used in this study. After weaning on PND 21, pups were weaned and housed in groups of three. In order to perform the molecular analysis of the brains in infancy, adolescence, and adulthood, the male offspring (one rat/litter/treatment) was sacrificed on PND 13, PND 35, and PND 90, respectively. After decapitation, PfC, HPC, and Cb were rapidly isolated to perform western blot and real time-quantitative PCR (RT-qPCR); whereas, whole brains for immunofluorescence were flash-frozen in 2-methylbutane and stored at − 80 °C. The experimental design is outlined in Fig. 1a.

Behavioral tests

Isolation-induced ultrasonic vocalizations (USVs)

On PND 13, the USVs emitted by each pup removed from the nest and placed into a Plexiglas arena were detected for 3 min by an ultrasound microphone (Avisoft Bioacoustics, Germany) sensitive to frequencies between

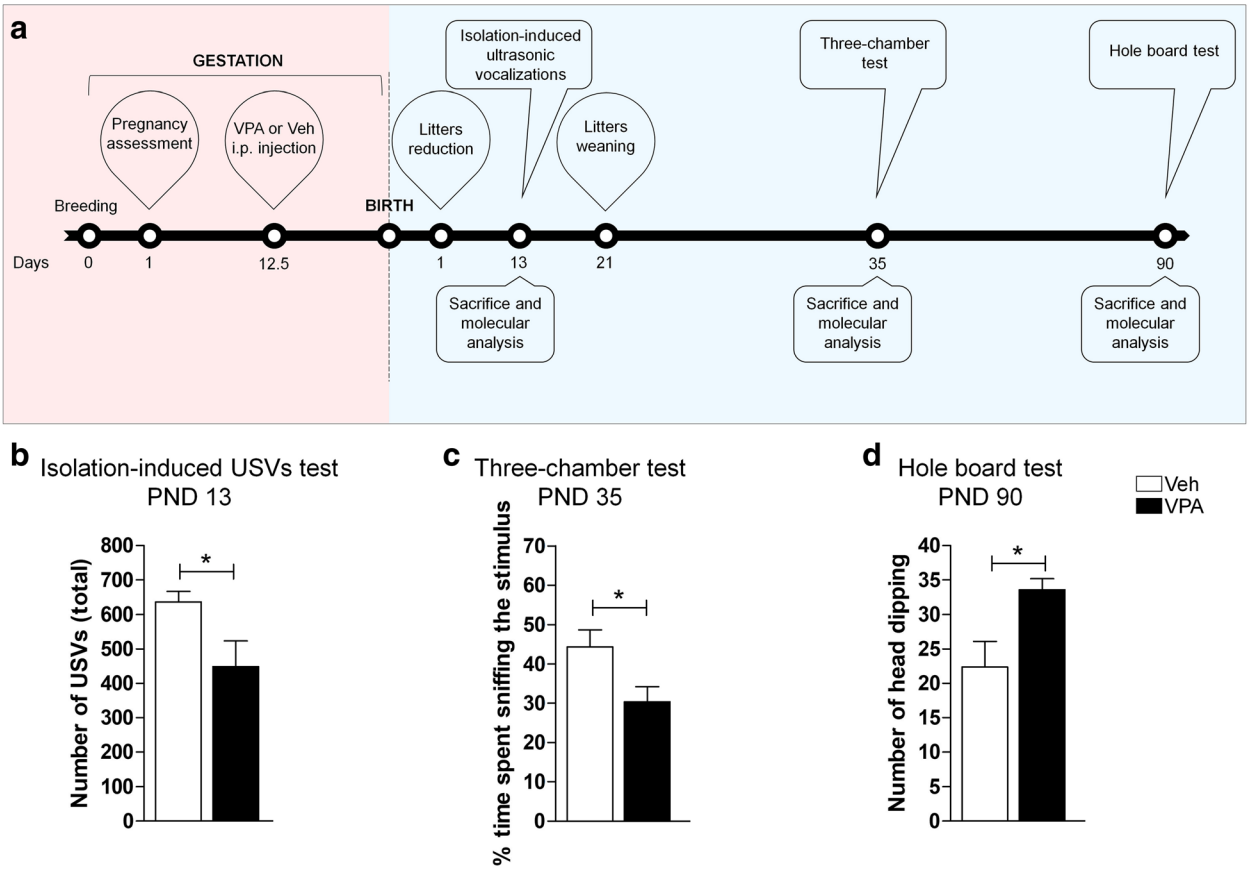

Fig. 1 Effect of prenatal VPA exposure on animals' behavior. Schematic representation of the experimental design (**a**). Assessment of the autistic-like phenotype in prenatally VPA-exposed rats through reduced isolation-induced USV emission at PND 13 (**b**), sociability in the three-chamber test at PND 35 (**c**), and induced stereotypic behavior in the hole-board test at PND 90 (**d**) (Veh $n = 5$, VPA $n = 5$). Data represent mean ± SEM. Statistical analysis was performed by t test (*$p < 0.05$ vs Veh group)

10 and 200 kHz. The USVs were analyzed quantitatively using Avisoft Recorder software (Version 5.1).

Three-chamber test

The test was performed as previously described [40]. The apparatus was a rectangular three-chamber box, with two lateral chambers (30 l × 35 w × 35 h cm) connected to a central chamber (15 l × 35 w × 35 h cm). Each lateral chamber contained a small Plexiglas cylindrical cage. At PND 35, each experimental rat was individually allowed to explore the three-chamber apparatus for 10 min, and then confined in the central compartment. An unfamiliar stimulus animal was confined in a cage located in one chamber of the apparatus, while the cage in the other chamber was left empty. Both doors to the side chambers were then opened, allowing the experimental animal to explore the apparatus for 10 min. The percent of time spent in social approach (sniffing the stimulus animal) were scored using the Observer 3.0 software (Noldus, The Netherlands).

Hole board test

The apparatus was a gray square metal table (40 l × 40 w × 10 h cm) with 16 evenly spaced holes (4 cm in diameter), inserted in a Plexiglas arena (40 l × 40 w × 60 h cm). At PND 90, rats were individually placed in the apparatus and their behavior was observed for 5 min. Dipping behavior was scored by the number of times an animal inserted its head into a hole at least up to the eye level. Each session was recorded with a camera positioned above the apparatus for subsequent behavioral analysis performed using the Observer 3.0 software (Noldus Information Technology).

Real-time quantitative PCR (RT-qPCR)

Total mRNA of PfC, HPC, and Cb was isolated by TRI-Reagent (Sigma-Aldrich, Saint Louis, MO, USA) following the manufacturer's instructions. For each brain tissue, the total amount of the mRNA was quantified by D30 BioPhotometer spectrophotometer (Eppendorf AG, Hamburg, Germany). The first-strand cDNA synthesis kit, adding oligo (dT) 0.2 μM and random primers 0.05 μg/μl was

used to perform revers transcription of 1 μg mRNA to obtain cDNA (Promega, Promega Corporation, WI, USA). Reverse transcription was carried out with the following thermal protocol: + 25 °C for 10 min and + 72 °C for 65 min. Samples were stored at + 4 °C and then processed for mRNA encoding for S100B, glial fibrillary acidic protein (GFAP), Olig2, Iba1 (Bio-Fab laboratories, Rome, Italy), and the cluster of differentiation 11b (CD11b) (Bio-Rad, Hercules, CA, USA).

To confirm pair's primers efficiency, the amplification products from each primer pair were tested with the melting curve analyses. The amounts of the amplicons were normalized against TATA-box binding protein (TBP) and hypoxanthine guanine phosphoribosyl transferase (HPRT) used as reference genes (all primers sequences are listed in Table 1). All amplifications were performed dissolving 500–800 nM primers and 75 ng cDNA in the iTaq Universal SYBR Green Supermix (Bio-Rad) using a CFX96 Touch thermocycler (Bio-Rad) according to the manufacturer's instructions. The detection of the fluorescent signals was assessed at the end of the + 60 °C extension period. For each sequence of interest, three independent experiments were performed in triplicate. Data are expressed as the fold difference in mRNA expression (ΔΔCq) calculated according to the Pflaffl method.

Western blot

Total protein amount of PfC, HPC, and Cb was isolated and processed as previously described [29, 30, 34]. Brain tissues were mechanically lysed in ice-cold hypotonic lysis buffer containing 50 mM Tris/HCl pH 7.5, 150 mM NaCl, 1 mM ethylenediamenetetraacetic acid (EDTA), 1% triton X-100, 1 mM phenylmethylsulfonyl fluoride (PMSF), 10 μg/ml aprotinin, and 0.1 mM leupeptin (all from Sigma-Aldrich), and then incubated for 40 min at + 4 °C. After centrifugation at 14000 rpm for 30 min, supernatants were collected and stored at − 80 °C. Protein concentration was calculated by Bradford assay to resolve an equal amount of proteins for each sample. Thirty micrograms were resolved through 12% acrylamide SDS-PAGE gel and then transferred onto nitrocellulose membranes with a trans-blot semi-dry transfer cell (Bio-Rad). From this step on, membranes were treated on an orbital shaker. Unspecific bound of the antibodies was avoided by incubating membranes for 1 h at room temperature in a blocking solution containing either 5% non-fat dry milk (Bio-Rad) or 5% bovine serum albumin (BSA, Sigma-Aldrich) in tris-buffered saline (TBS) (Corning, NY, USA) 0.1% tween 20 (TBS-T). Then, an overnight incubation with the proper primary antibodies against S100B, GFAP, Olig2, CD11b, or Iba1 was performed at + 4 °C (experimental conditions are reported in Table 2).

After removing the excess of antibody solution, the membranes were rinsed in TBS-T 0.05% and incubated for 1 h at room temperature with a specific secondary horseradish peroxidase (HRP)-conjugated antibody (Table 2) to detect immunocomplexes by an enhanced chemiluminescence (ECL) kit (GE Healthcare Life Sciences, Milan, Italy). Immunocomplexes were visualized using a Chemidoc XRS + and Image Lab software (Bio-Rad), and then quantified by ImageJ software. Values were normalized to those of β-actin.

For each protein of interest, three independent experiments were performed in triplicate. Data are expressed as percentage of control.

Table 1 Primer sequences and general conditions used to perform real-time qPCR

GENE	Primer (5′ → 3′)		Annealing (°C)	Efficiency (%)	R^2
S100B	Forward	TCAGGGAGAGAGGGTGACAA	60	94.6	.998
	Reverse	ACACTCCCCATCCCCATCTT			
GFAP	Forward	CGGCTCTGAGAGAGATTCGC	60	105.0	.989
	Reverse	GCAAACTTGGACCGATACCA			
Olig2	Forward	CCCGATGATCTTTTTCTGCC	60	98.8	.990
	Reverse	GCTTCTTATCTTTCTTGGTG			
CD11b	Forward	N/A (Cod. qRnoCID0002800, Bio-Rad)	60	94.0	.990
	Reverse				
Iba1	Forward	GTCCTTGAAGCGAATGCTGG	60	95.6	.994
	Reverse	CATTCTCAAGATGGCAGATC			
HPRT	Forward	TCCCAGCGTCGTGATTAGTGA	60	98.3	.992
	Reverse	CCTTCATGACATCTCGAGCAAG			
TBP	Forward	TGGGATTGTACCACAGCTCCA	60	99.7	.995
	Reverse	CTCATGATGACTGCAGCAAACC			

GFAP glial fibrillary acidic protein; *CD11b* cluster of differentiation 11b; *HPRT* hypoxanthine guanine phosphoribosyl transferase; *TBP* TATA-box binding protein

Table 2 Experimental conditions used to perform western blot experiments

Primary antibody	Brand/cat #	Dilution	Secondary antibody	Brand/cat #
Rabbit α-S100B	Genetex	1:1000	HRP conjugated goat anti-rabbit IgG 1:10000	Jackson ImmunoResearch
	GTX129573	5% BSA in TBS-T 0.1%	5% BSA in TBS-T 0.1%	111-035-045
Rabbit α-GFAP	Abcam	1:25000	HRP conjugated goat anti-rabbit IgG 1:10000	Jackson ImmunoResearch
	ab7260	5% milk in TBS-T 0.1%	5% milk in TBS-T 0.1%	111-035-045
Rabbit α-Olig2	Santa Cruz	1:500	HRP conjugated goat anti-rabbit IgG 1: 10000	Jackson ImmunoResearch
	sc-48817	5% milk in TBS-T 0.1%	5% milk in TBS-T 0.1%	111-035-045
Rabbit α-CD11b	Bioss	1:1000	HRP conjugated goat anti-rabbit IgG 1:10000	Jackson ImmunoResearch
	bs-1014R	5% BSA in TBS-T 0.1%	5% BSA in TBS-T 0.1%	111-035-045
Rabbit α-Iba1	Abcam	1:1000	HRP conjugated goat anti-rabbit IgG 1:10000	Jackson ImmunoResearch
	ab178846	5% milk in TBS-T 0.1%	5% milk in TBS-T 0.1%	111-035-045
Rabbit α-β-actin	Santa Cruz	1:1000	HRP conjugated goat anti-rabbit IgG 1:20000	Jackson ImmunoResearch
	sc-1616R	5% milk in TBS-T 0.1%	5% milk in TBS-T 0.1%	111-035-045

GFAP glial fibrillary acidic protein; *CD11b* cluster of differentiation 11b; *MAP2* microtubule associated protein; *BSA* bovine serum albumin; *TBS-T* tris buffered saline tween 20; *HRP* horseradish peroxidase

Immunofluorescence

Immunofluorescence was performed as previously described [30, 34, 44]. The assay was performed on 12-μm-thick coronal slices of PfC, HPC, and Cb. Tissues were rinsed in phosphate-buffered saline (PBS) and post-fixed with 4% paraformaldehyde (PFA). After the blocking step lasting 90 min at room temperature in 1% BSA dissolved in PBS/0.25% triton X-100, sections were incubated overnight with the primary antibody recognizing GFAP, Olig2, or Iba1 at + 4 °C. Primary antibodies were diluted in 0.5% BSA in PBS/0.25% triton X-100. Tissues were rinsed in PBS and incubated for 2 h at room temperature with the proper secondary antibody. The staining of nuclei was performed with Hoechst (1:5000, Thermo Fisher Scientific, MA, USA). After rinses in PBS slices were mounted with Fluoromount aqueous mounting medium (Sigma-Aldrich). The experimental conditions are summarized in Table 3.

Cell count analysis

Cells labeled with the different markers were quantified in 4 serial coronal 12 μm sections, spaced 48 μm apart, in each brain region for each animal. We used three rats per experimental group ($N = 3$ vehicle and $N = 3$ VPA) for each age, for a total of 18 rats. The brain regions analyzed were the PfC, the molecular layer (ML) and the granular cell layer (GL) of the Cb, the stratum radiatum of the Ammon's horn 1 (CA1), CA2, CA3, and hilus of the dentate gyrus (DG) of the HPC. Nuclei were stained with Hoechst dye. Cells were identified as positive for a marker if they expressed immunoreactivity visually deemed to be above background. Images were captured using a × 20/0.50 magnification objective, and digitization was executed with a wide-field microscope (Eclipse E600; Nikon Instruments, Rome, Italy) connected to a QImaging camera with NIS-Elements BR 3.2 64-bit software. We used a 200 × 100 × 12 μm capture field of view to analyze the number of immunopositive cells within each field using the multi-point button of the Fiji Is Just ImageJ (FIJI) software. Cell count analyses, expressed as number of antibody positive cells in 2.4×10^5 μm^3 of tissue, were carried out by a blind observer.

Statistical analysis

GraphPad Prism 6 software (GraphPad Software, San Diego, CA, USA) was used for the statistical analyses. Student's t test was used to compare Veh and VPA

Table 3 Experimental conditions used to perform immunofluorescence

Primary antibody	Brand/cat #	Dilution	Secondary antibody	Brand/cat #
Rabbit α-GFAP	Abcam	1:200	FITC conjugated goat anti-rabbit IgG (H + L) 1:200, 5% BSA in PBS/0.25% triton X-100	Jackson ImmunoResearch
	ab7260	5% BSA in PBS/0.25% triton X-100		111-095-003
Rabbit α-Olig2	Santa Cruz	1:250	FITC conjugated goat anti-rabbit IgG (H + L) 1:200, 0.5% BSA in PBS/0.25% triton X-100	Jackson ImmunoResearch
	sc-48817	0.5% BSA in PBS/0.25% triton X-100		111-095-003
Rabbit α-Iba1	Wako	1:1000	FITC conjugated goat anti-rabbit IgG (H + L) 1:200, 0.5% BSA in PBS/0.25% triton X-100	Jackson ImmunoResearch
	019-19741	0.5% BSA in PBS/0.25% triton X-100		111-095-003

GFAP glial fibrillary acidic protein; *MAP2* microtubule associated protein; *BSA* bovine serum albumin; *FITC* fluorescein isothiocyanate; *PBS* phosphate buffered saline

groups. Data are presented as mean ± SEM. Differences between means were considered as significant at $p < 0.05$.

Results

Behavioral tests

Animals prenatally exposed to VPA showed enduring impairments in the three core symptoms of autism. At infancy, VPA-exposed pups separated from the dam and siblings vocalized significantly less compared to Veh-exposed pups ($t = 2.334$; $p < 0.05$; df = 8, Fig. 1b). At adolescence, VPA-exposed rats showed decreased sociability in the three-chamber test, since they spent less time sniffing the stimulus animal compared to Veh-exposed animals ($t = -2.436$; $p < 0.05$; df = 8, Fig. 1c). At adulthood, VPA-exposed rats showed stereotypic behaviors in the hole board test, since they made more head dipping at PND 90 ($t = -2.781$; $p < 0.05$; df = 8, Fig. 1d).

In their entirety, these results confirm that prenatal exposure to VPA causes the manifestation of autistic-like behaviors that persist from infancy to early adulthood.

Astrocytes in ASD model rats

To investigate the effect of prenatal VPA exposure on astrocyte phenotype, we analyzed transcription and expression of the archetypal astroglial markers GFAP and the neurotrophin/Ca^{2+} binding protein S100B. At PND 13, we observed a significant reduction of S100B mRNA in the HPC of VPA-exposed rats compared to control animals, with no significant modification in its protein expression (Fig. 2a, b). At the same age, we detected a significant increase of GFAP mRNA in the HPC of VPA-exposed rats (Fig. 2c). No changes in GFAP protein were observed among all groups by western blot (Fig. 2d); however, immunofluorescence experiments revealed a significant increase of GFAP-positive cells in the PfC of VPA-exposed rats (Fig. 2e, f).

At PND 35 rats showed higher levels of S100B mRNA in both PfC and HPC of VPA-exposed rats, with a significant reduction in the Cb (Fig. 3a). A decreased level of GFAP mRNA was found in the PfC and in the Cb of VPA animals compared to controls (Fig. 3c). No modifications of S100B levels were found at protein level (Fig. 3b), whereas GFAP protein expression was higher in the PfC of VPA-exposed rats (Fig. 3d).The number of GFAP-positive cells was decreased in the GL of the Cb, and in the CA1 and DG hippocampal sub-regions, while a significant increase of GFAP-positive astrocytes was observed in the CA3 of VPA-exposed rats (Fig. 3e, f). Results obtained in adult rats demonstrate transcriptional modifications and some alterations in protein content. At PND 90, VPA-exposed animals showed higher levels of S100B mRNA in Cb and HPC (Fig. 4a). Conversely, GFAP mRNA was lower in the HPC and higher in the Cb of VPA-exposed rats compared to Veh animals (Fig. 4c). No changes in the protein expression of GFAP and S100B were detected (Fig. 4b, d). Finally, significantly higher number of GFAP-positive cells in the ML of the Cb and CA2 of the HPC of VPA-exposed rats was documented (Fig. 4e, f).

In summary, prenatal exposure to VPA differentially affects astrocytes in different brain regions, and causes transcriptional modifications of S100B and GFAP, which are particularly evident in adolescent and adult rats, where modified GFAP expression is also observed.

Oligodendrocytes in ASD model rats

We examined the effects of prenatal exposure to VPA on oligodendrocytes by testing Olig2, a transcriptional factor essential for oligodendrocyte development. Infant VPA-exposed rats showed higher levels of Olig2 mRNA in PfC and HPC, and a trend toward an increase of Olig2 protein expression (+ 76.77%) in PfC compared to age-matched control animals (Fig. 5a, b). No changes of Olig2-positive cells density were observed, except for the CA3 sub-region of the HPC where a significant decrease of their population was detected (Fig. 5c, d).

The RT-qPCR analysis revealed a significant increase of Olig2 in the PfC of VPA-exposed rats at PND 35, with a decrease of this transcription factor in the HPC of the same animals (Fig. 6a). These modifications were evident also at a protein level. In adolescent VPA-exposed rats, we observed a statistically significant increase of Olig2 protein expression in the PfC, a significant decrease in the Cb, and a trend toward a decrease in the HPC (– 27.24%) (Fig. 6b). A more detailed analysis of the brain areas revealed subtler modifications in Olig2-positive cells distribution. In particular, in VPA-exposed rats we observed a significant increase in the number of Olig2-positive cells in the GL of the Cb and in the DG of the HPC, and a statistically significant reduction of Olig2-positive cells in the CA1 and CA2 of the same animals (Fig. 6c, d). In adult (PND 90) rats prenatally exposed to VPA, a significant decrease of Olig2 mRNA was observed solely in the HPC (Fig. 7a). On the contrary, the Olig2 protein was increased in the HPC of these animals (Fig. 7b). The VPA-exposed rats also showed more Olig2-positive cells in the ML of the Cb and in the CA1 (Fig. 7c, d).

Collectively, these results demonstrate that the prenatal exposure to VPA modifies oligodendrocytes at both the transcriptional and translational levels, and that these changes occur mainly in the PfC and in the HPC. Of note, these alterations are particularly evident during adolescence, but seem to be compensated in adulthood.

Microglia in ASD model rats

To characterize microglia in this rat model of ASD, we analyzed transcription and expression of CD11b, a

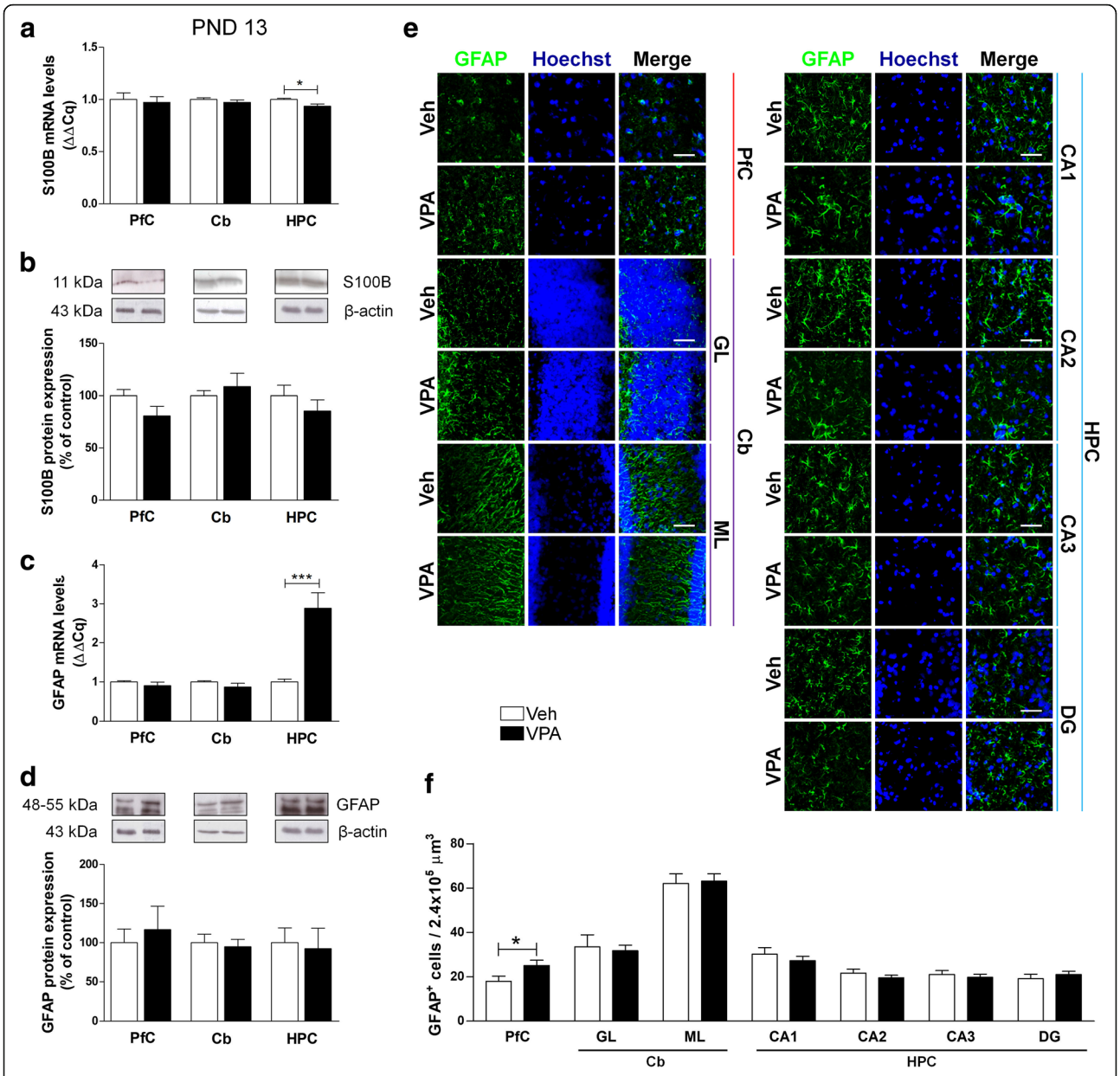

Fig. 2 Effect of prenatal VPA exposure on astrocytes in infancy. Analysis of the neurotrophin S100B and the GFAP in the PfC, Cb, and HPC of healthy- (open bars, Veh) and autistic-like (black bars, VPA) infant rats (PND 13). Representation of the relative concentration of S100B (**a**) and GFAP (**c**) in VPA animals compared to control (Veh), normalized to both TBP and HPRT (ΔΔCq; $N = 3$, in triplicate). Representative western blots for S100B (**b**) and GFAP (**d**) proteins, and densitometric analyses are normalized to β-actin used as loading control. Results are expressed as percentage of control (Veh) ($N = 3$, in triplicate). Representative fluorescence micrographs of GFAP (green) staining in the PfCGL and MLof Cb, and CA1, CA2, CA3, and the hilus of the DG of the HPC. Nuclei were stained with Hoechst (blue) (**e**). The images have been analyzed by counting the number of GFAP-positive cells in 2.4×10^5 μm^3 (scale bar 50 μm; $N = 3$, 4 times) (**f**). All data are presented as means ± SEM. Statistical analysis was performed by *t* test (*$p < 0.05$; ***$p < 0.001$ vs Veh group)

marker of microglia activation, and Iba1, a Ca^{2+}-binding protein constitutively expressed by both surveillant and activated microglia. In VPA-exposed rats at PND 13, we observed a significant increase of CD11b mRNA in PfC and HPC, and no substantial change in the protein expression except for a trend toward an increase of this marker in PfC (+ 54.36%) (Fig. 8a, b). At the same age, we detected a significant increase of Iba1 mRNA in the Cb of VPA-exposed rats (Fig. 8c). We also found a significant increase in the number of Iba-positive cells in the ML of the Cb of VPA-exposed rats with a significant decrease in the CA3 of the same animals (Fig. 8e, f).

Adolescent (PND 35) rats displayed more pronounced modifications. A significant increase of both transcription

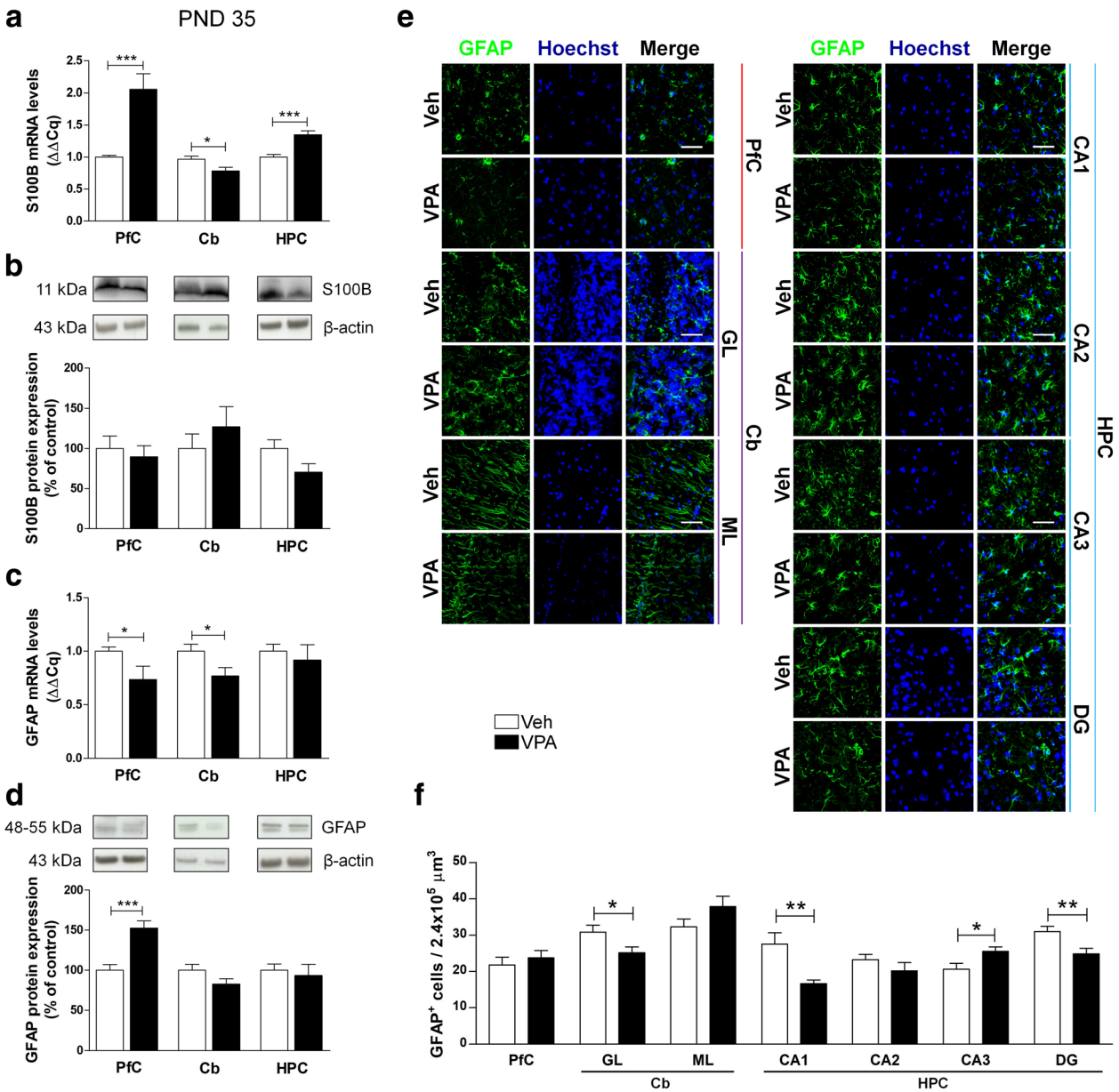

Fig. 3 Effect of the prenatal VPA exposure on astrocytes in adolescence. Evaluation of the neurotrophin S100B and the cytoskeletal GFAP in the PfC, Cb, and HPC of healthy- (open bars, Veh) and autistic-like (black bars, VPA) adolescent rats (PND 35). Representation of the relative concentration of S100B (**a**) and GFAP (**c**) in VPA animals compared to control (Veh), normalized to both TBP and HPRT (**ΔΔ**Cq; *N* = 3, in triplicate). Representative western blots for S100B (**b**) and GFAP (**d**) proteins, and densitometric analyses normalized to β-actin used as loading control. Results are expressed as percentage of control (Veh) (*N* = 3, in triplicate). Representative fluorescence micrographs of GFAP (green) staining in the PfC, GL and ML of Cb, and stratum radiatum of CA1, CA2, CA3, and the hilus of the DG of the HPC. Nuclei were stained with Hoechst (blue) (**e**). The images have been analyzed by counting the number of GFAP-positive cells in 2.4×10^5 µm^3 (scale bar 50 µm; *N* = 3, 4 times) (**f**). All data are presented as means ± SEM. Statistical analysis was performed by *t* test (*$p < 0.05$; **$p < 0.01$; ***$p < 0.001$ vs Veh group)

and expression of CD11b in the PfC of VPA-exposed animals compared to control rats was detected (Fig. 9a, b). Moreover, a significant increase of Iba1 mRNA was found in the PfC of VPA-exposed rats, whereas, in the same animals, we observed reduced transcription in the HPC (Fig. 9c). No changes of protein expression of Iba1 were observed (Fig. 9d). The number of Iba1-positive cells increased in the GL of the Cb and in the CA1 of adolescent (PND 35) VPA-exposed rats (Fig. 9e, f).

In adult rats (PND 90), no modifications of CD11b and Iba1 protein transcription and expression was observed, except for a trend toward an increase of CD11b expression in PfC (+ 47.04%) and Cb (+ 41.26%), and a significant decrease of Iba1 mRNA in the HPC of the

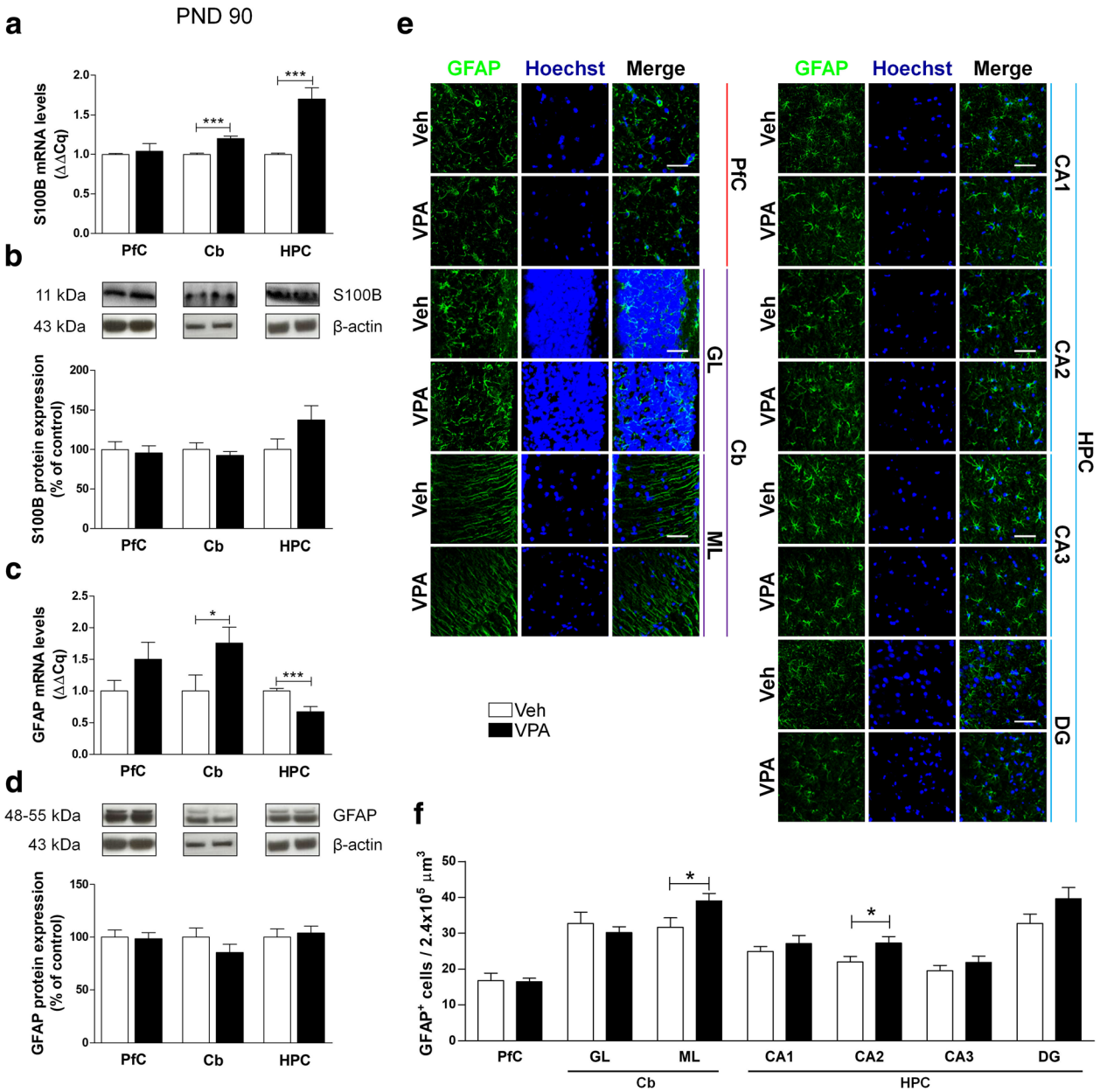

Fig. 4 Effect of the prenatal VPA exposure on astrocytes in adulthood. Evaluation of the neurotrophin S100B and the cytoskeletal GFAP in the PfC, Cb, and HPC of healthy- (open bars, Veh) and autistic-like (black bars, VPA) adult rats (PND 90). Representation of the relative concentration of S100B (**a**) and GFAP (**c**) in VPA animals compared to control (Veh), normalized to both TBP and HPRT (**ΔΔ**Cq; $N = 3$, in triplicate). Representative western blots for S100B (**b**) and GFAP (**d**) proteins, and densitometric analyses normalized to β-actin used as loading control. Results are expressed as percentage of control (Veh) ($N = 3$, in triplicate). Representative fluorescence micrographs of GFAP (green) staining in the PfC, GL and ML of Cb, and stratum radiatum of CA1, CA2, CA3, and the hilus of the DG of the HPC. Nuclei were stained with Hoechst (blue) (**e**). The images have been analyzed by counting the number of GFAP-positive cells in 2.4×10^5 µm^3 (scale bar 50 µm; $N = 3$, 4 times) (**f**). All data are presented as means ± SEM. Statistical analysis was performed by *t* test (*$p < 0.05$; ***$p < 0.001$ vs Veh group)

same animals (Fig. 10a–d). At PND 90, the number of Iba1-positive cells was significantly reduced in PfC, CA1, and CA2 of rats prenatally exposed to VPA, while more Iba1-positive cells were detected in the GL of the Cb of the same animals (Fig. 10e, f).

Taken together, these results indicate that the prenatal VPA exposure modifies microglia and that these changes occur mainly in the PfC and in the HPC. Moreover, we observed that the prenatal VPA exposure switches microglial phenotypes from resting to activated in infant

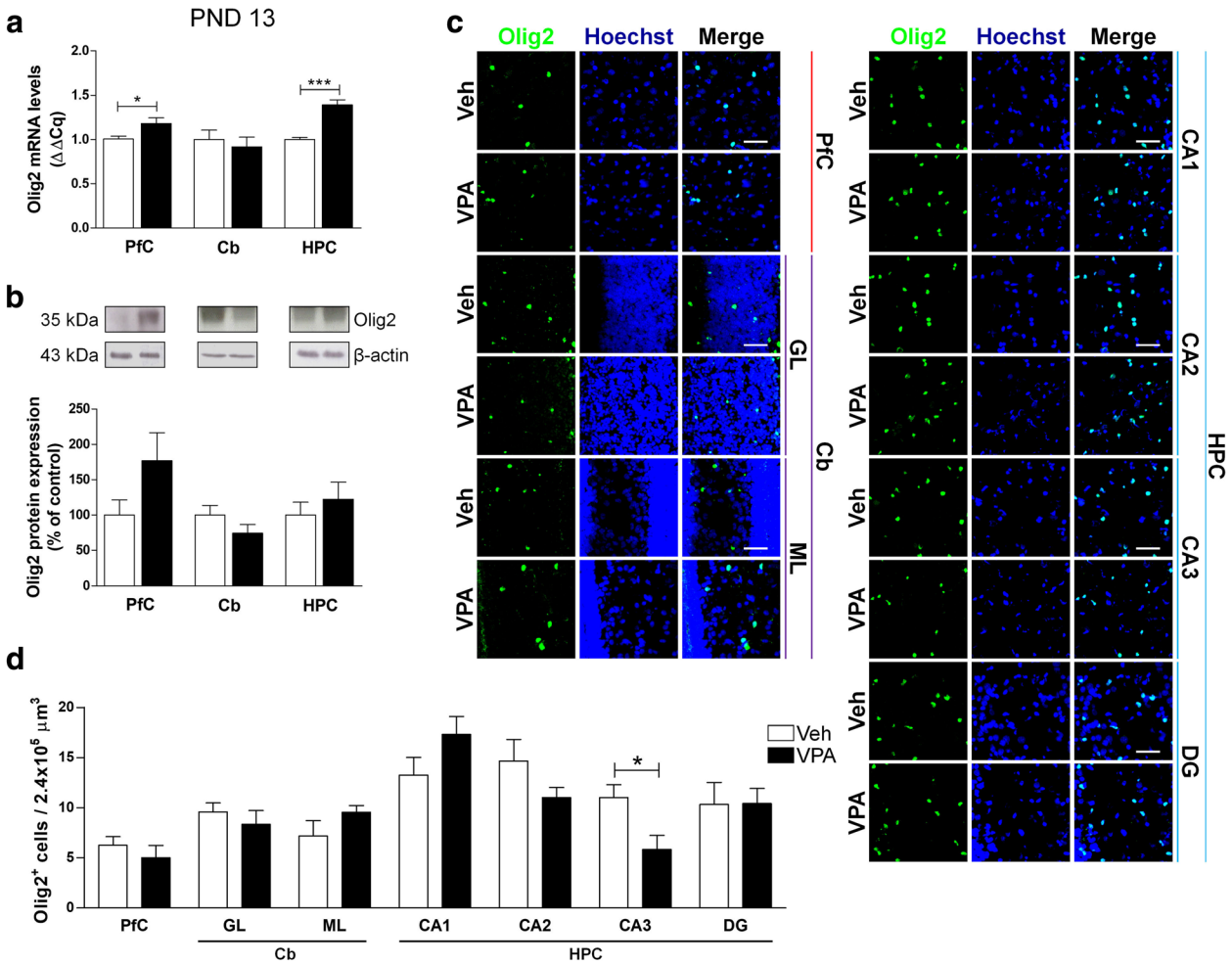

Fig. 5 Effect of the prenatal VPA exposure on oligodendrocytes in infancy. Evaluation of the transcription factor Olig2 in the PfC, Cb, and HPC of healthy- (open bars, Veh) and autistic-like (black bars, VPA) infant rats (PND 13). Representation of the relative concentration of Olig2 (**a**) in VPA animals compared to control (Veh), normalized to both TBP and HPRT (**ΔΔ**Cq; $N = 3$, in triplicate). Representative western blots for Olig2 protein and densitometric analyses normalized to β-actin used as loading control (**b**). Results are expressed as percentage of control (Veh) ($N = 3$, in triplicate). Representative fluorescence micrographs of Olig2 (green) staining in the PfC, GL and ML of Cb, and stratum radiatum of CA1, CA2, CA3, and the hilus of the DG of the HPC. Nuclei were stained with Hoechst (blue) (**c**). The images have been analyzed by counting the number of Olig2-positive cells in 2.4×10^5 µm^3 (scale bar 50 µm; $N = 3$, 4 times) (**d**). All data are presented as means ± SEM. Statistical analysis was performed by *t* test (*$p < 0.05$; ***$p < 0.001$ vs Veh group)

and adolescent rats while this phenomenon is somewhat mitigated in adulthood.

Discussion

All three types of neuroglia are critically important for normal development of the CNS and for formation of neuronal ensembles. Astrocytes assist synaptogenesis [17, 18], while astrocytes together with microglia shape neuronal networks through synaptic pruning and removal of redundant synaptic contacts [45–47]. Functional insufficiency of neuroglia leads to neurodevelopmental pathologies [48, 49]. The role of neuroglial components in ASD has received much attention recently, when several lines of evidence have demonstrated glia-specific alterations in animal models of ASD as well as in patients suffering from this disorder (for recent reviews see [48, 49]). The transcriptome analysis of the brains of ASD patients identified significant association of the pathology with genes linked to reactive gliosis and neuroinflammation [50]. Increased expression of astroglia-specific proteins aquaporin-4 and connexin43 has been found in the autistic human tissue [51]; increase in GFAP expression and astroglial hypertrophy was also observed with cerebellum demonstrating most prominent changes [52]. Microglial activation and increase in pro-inflammatory factors were other characteristic features of ASD brain tissue [52–54].

These findings support the notion of glia-related pathological developments that may exacerbate or even

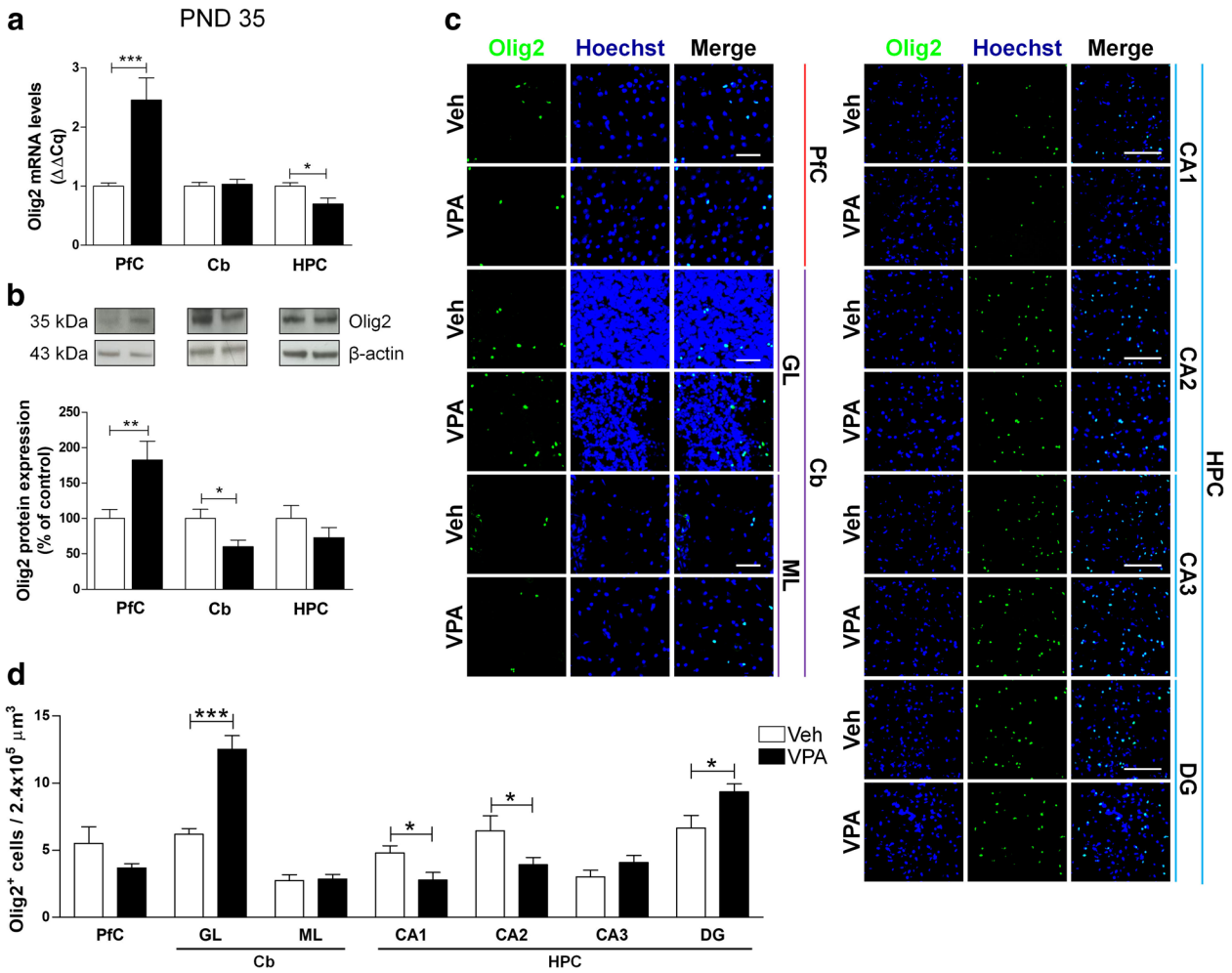

Fig. 6 Effect of the prenatal VPA exposure on oligodendrocytes in adolescence. Evaluation of the transcription factor Olig2 in the PfC, Cb, and HPC of healthy- (open bars, Veh) and autistic-like (black bars, VPA) adolescent rats (PND 35). Representation of the relative concentration of Olig2 (**a**) in VPA animals compared to control (Veh), normalized to both TBP and HPRT (**ΔΔ**Cq; $N = 3$, in triplicate). Representative western blots for Olig2 protein and densitometric analyses normalized to β-actin used as loading control (**b**). Results are expressed as percentage of control (Veh) ($N = 3$, in triplicate). Representative fluorescence micrographs of Olig2 (green) staining in the PfC, GL and ML of Cb, and stratum radiatum of CA1, CA2, CA3, and the hilus of the DG of the HPC. Nuclei were stained with Hoechst (blue) (**c**). The images have been analyzed by counting the number of Olig2-positive cells in 2.4×10^5 µm^3 (scale bar 50 µm; $N = 3$, 4 times) (**d**). All data are presented as means ± SEM. Statistical analysis was performed by *t* test (*$p < 0.05$; **$p < 0.01$; ***$p < 0.001$ vs Veh group)

drive ASD evolution. Indeed, the autistic brain is affected already at the early developmental stages, when loss of function of microglia and astrocytes can affect formation of synaptically connected neuronal networks. Equally important could be the contribution of oligodendrocytes, which shape the brain connectome. Expression of specific markers associated with cells of oligodendroglial lineage (including for example oligodendrocyte transcription factor 1/2 or myelin basic protein) is increased in the cerebella of autistic patients [55]. The single nucleotide polymorphisms of the central oligodendroglial differentiation regulator gene DUSP15 were identified in the brains of ASD patients [56], while many components of a molecular network associated with ASD are specifically enriched in oligodendroglia and white matter [57]. Changes in oligodendroglia and hence changes in white matter may be linked to a rather characteristic ASD-associated increase in the brain size (see for examples [58, 59]).

Astroglial as well as microglial abnormalities have been detected in animal models of several types of ASD associated with expression of pathologically modified genes; these include the Rett syndrome, fragile X syndrome, and tuberous sclerosis. In the Rett syndrome that arises from loss-of-function mutations in the X-linked MeCP2 encoding methyl-CpG-binding protein 2, the glial pathological phenotype has been clearly revealed. Microglial cells lacking MeCP2 triggered excitotoxicity

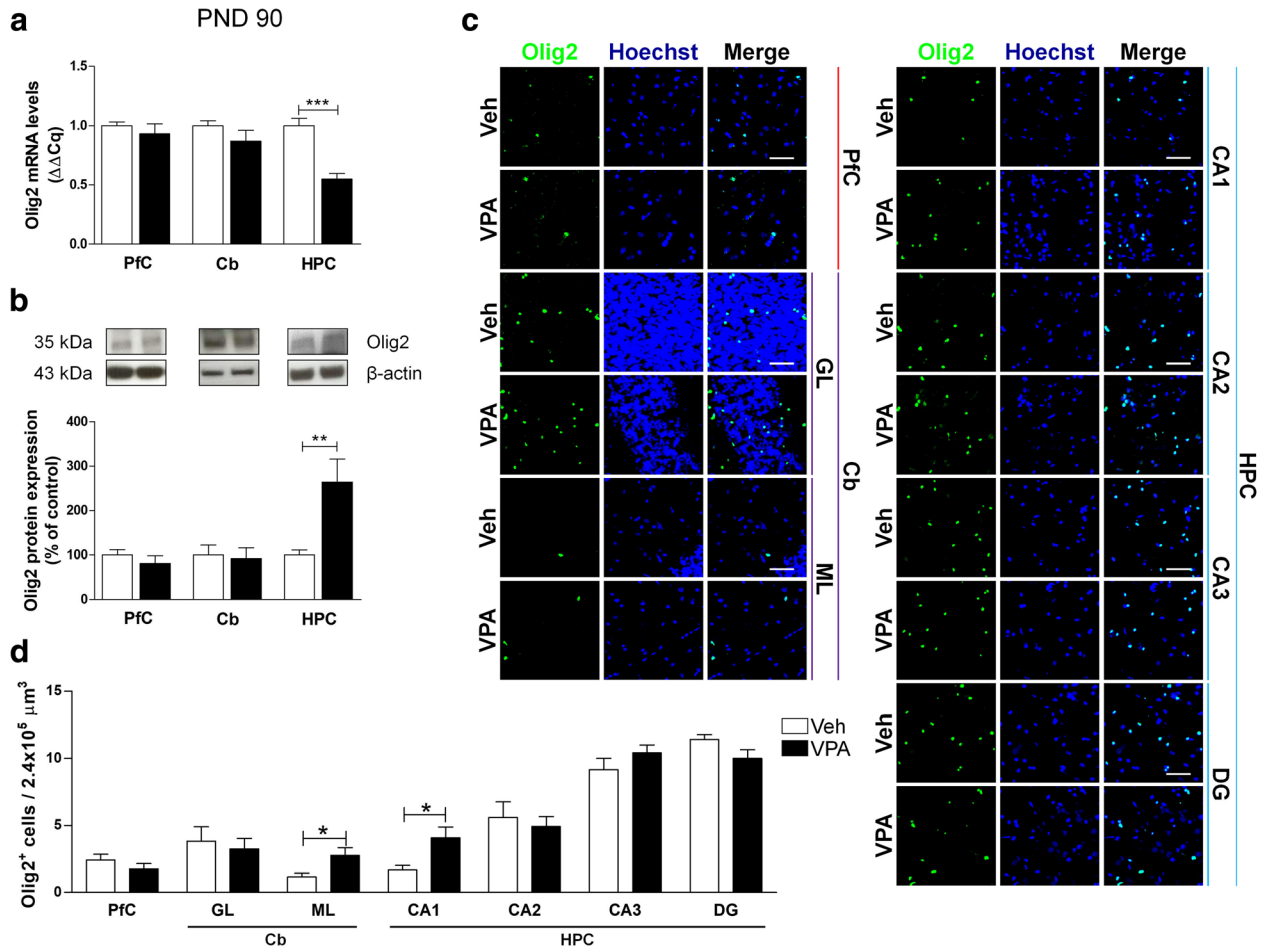

Fig. 7 Effect of the prenatal VPA exposure on oligodendrocytes in adulthood. Evaluation of the transcription factor Olig2 in the PfC, Cb, and HPC of healthy- (open bars, Veh) and autistic-like (black bars, VPA) adult rats (PND 90). Representation of the relative concentration of Olig2 (**a**) in VPA animals compared to control (Veh), normalized to both TBP and HPRT (**ΔΔ**Cq; $N = 3$, in triplicate). Representative western blots for Olig2 protein and densitometric analyses normalized to β-actin used as loading control (**b**). Results are expressed as percentage of control (Veh) ($N = 3$, in triplicate). Representative fluorescence micrographs of Olig2 (green) staining in the PfC, GL and ML of Cb, and stratum radiatum of CA1, CA2, CA3, and the hilus of the DG of the HPC. Nuclei were stained with Hoechst (blue) (**c**). The images have been analyzed by counting the number of Olig2-positive cells in 2.4×10^5 µm^3(scale bar 50 µm; $N = 3$, 4 times) (**d**). All data are presented as means ± SEM. Statistical analysis was performed by *t* test (*$p < 0.05$; **$p < 0.01$; ***$p < 0.001$ vs Veh group)

through excessive release of glutamate [60]; whereas MeCP2-deficient astrocytes lost their ability to support neuronal growth and dendritic ramifications in vitro [61]. In the fragile X syndrome (which results from the loss of Fmr1 gene function), increased astroglial reactivity has been observed (in mice with genetic deletion of Fmr1 gene) [62].

To summarize, the gliopathology in the ASD context is mainly represented by glial reactivity, which further highlights the contribution of neuroinflammation with both processes apparently having pathological significance. In this context, we asked ourselves whether the same reactive changes are pronounced in a rodent model of ASD resulting from in utero exposure to VPA, a widely used antiepileptic drug. The use of VPA has clinical significance as indeed VPA treatment during pregnancy has been related with a higher risk of ASD in the exposed children [7, 8]. Despite this evidence, recent epidemiological studies show that the public awareness of such an association is still limited [63].

Rodents prenatally exposed to VPA are widely used as a preclinical model of ASD [9, 11, 64]. The VPA-treated animals display several ASD-like symptoms in the course of development. These animals show impairment of the communicative capabilities, alteration of the social repertoire, stereotypical behavior, and anxiety [40, 65]. In particular, in line with previous studies [66, 67], we found that the infant male offspring born from VPA-treated rats exhibit reduced ability to interact with their mothers, since they emit less ultrasonic vocalizations when isolated

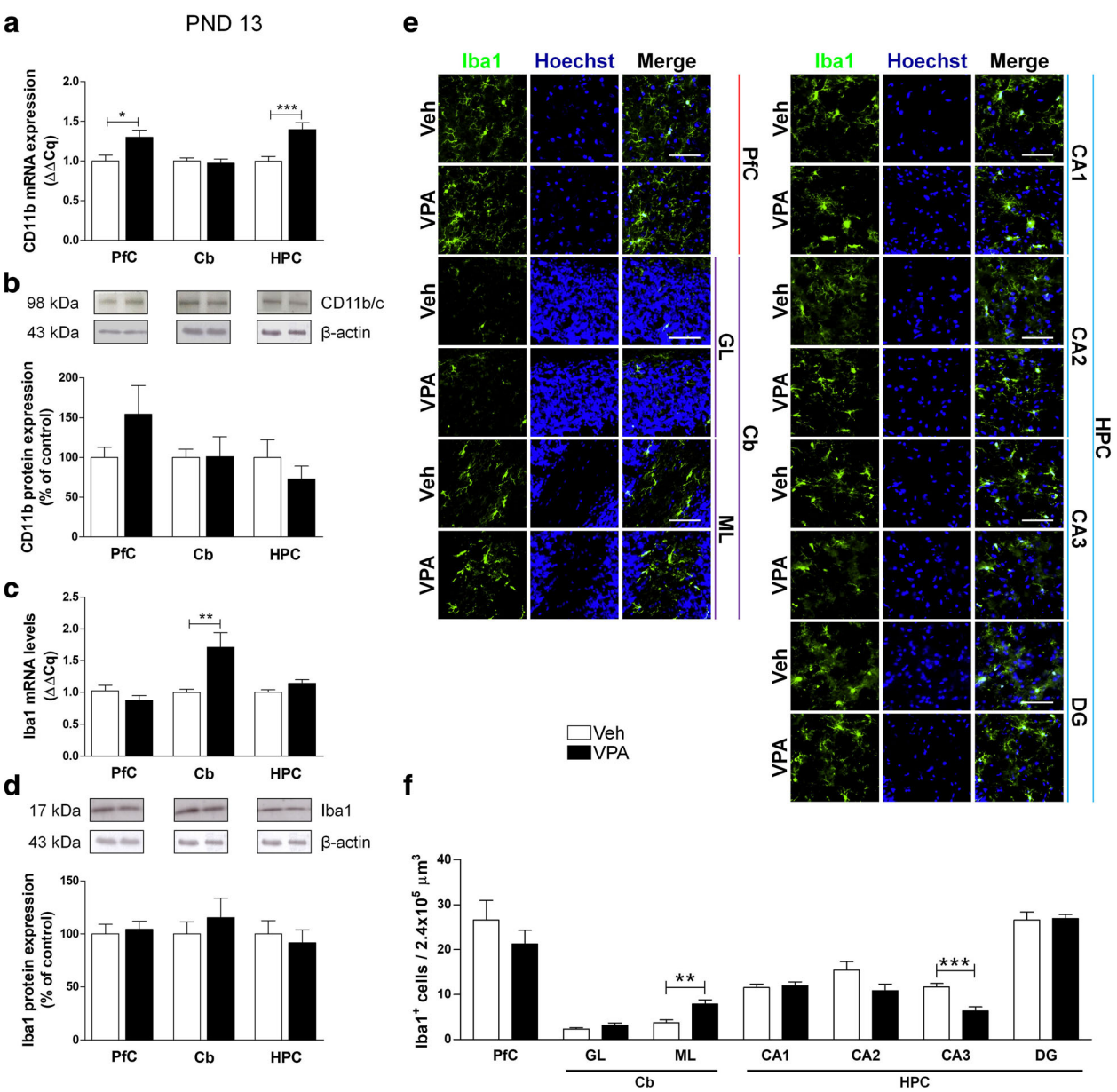

Fig. 8 Effect of the prenatal VPA exposure on microglia in infancy. Evaluation of the cluster of differentiation 11b (CD11b) and Iba1 in the PfC, Cb, and HPC of healthy- (open bars, Veh) and autistic-like (black bars, VPA) infant rats (PND 13). Representation of the relative concentration of CD11b (**a**) and Iba1 (**c**) in VPA animals compared to control (Veh), normalized to both TBP and HPRT (ΔΔCq; $N = 3$, in triplicate). Representative western blots for CD11b (**b**) and Iba1 (**d**) proteins, and densitometric analyses normalized to β-actin used as loading control. Results are expressed as percentage of control (Veh) ($N = 3$, in triplicate). Representative fluorescence micrographs of Iba1 (green) staining in the PfC, GL and ML of Cb, and stratum radiatum of CA1, CA2, CA3, and the hilus of the DG of the HPC. Nuclei were stained with Hoechst (blue) (**e**). The images have been analyzed by counting the number of Iba1-positive cells in 2.4×10^5 µm^3 (scale bar 50 µm; $N = 3$, 4 times) (**f**). All data are presented as means ± SEM. Statistical analysis was performed by *t* test (*$p < 0.05$; **$p < 0.01$; ***$p < 0.001$ vs Veh group)

from their mothers and siblings. This feature is accompanied by the inability of VPA-exposed pups to recognize familiar from unfamiliar odors, this being an early sign of the impairment in social recognition [66, 68, 69]. All these aspects negatively affect the social postnatal development of the VPA-exposed offspring and persist through adolescence and adulthood [40]. Indeed, VPA-exposed rats showed altered sociability in the three chamber test and increased stereotypic behavior in the hole board test. Our results are in agreement with those obtained by other researchers showing that a single injection of VPA to pregnant rats [65, 68, 70, 71] or mice [66, 72] on gestational day 12.5 yielded offspring with a behavioral pattern strikingly similar to that observed in autism. Beside behavioral

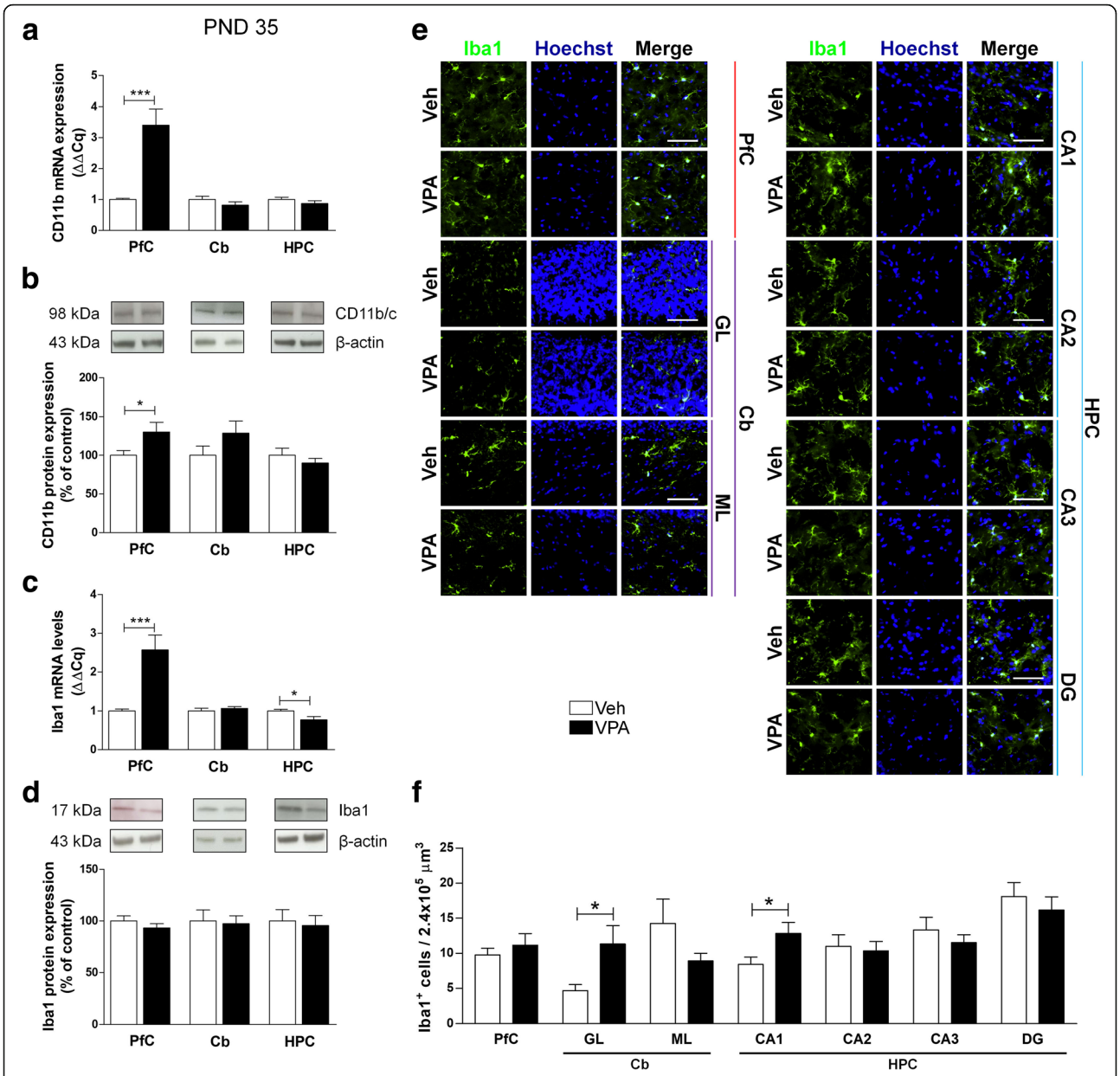

Fig. 9 Effect of the prenatal VPA exposure on microglia in adolescence. Evaluation of the cluster of differentiation 11b (CD11b) and Iba1 in the PfC, Cb, and HPC of healthy- (open bars, Veh) and autistic-like (black bars, VPA) adolescent rats (PND 35). Representation of the relative concentration of CD11b (**a**) and Iba1 (**c**) in VPA animals compared to control (Veh), normalized to both TBP and HPRT (**ΔΔ**Cq; *N* = 3, in triplicate). Representative western blots for CD11b (**b**) and Iba1 (**d**) proteins, and densitometric analyses normalized to β-actin used as loading control. Results are expressed as percentage of control (Veh) (*N* = 3, in triplicate). Representative fluorescence micrographs of Iba1 (green) staining in the PfC, GL and ML of Cb, and stratum radiatum of CA1, CA2, CA3, and the hilus of the DG of the HPC. Nuclei were stained with Hoechst (blue) (**e**). The images have been analyzed by counting the number of Iba1-positive cells in 2.4×10^5 µm^3 (scale bar 50 µm; *N* = 3, 4 times) (**f**). All data are presented as means ± SEM. Statistical analysis was performed by *t* test (*$p < 0.05$; **$p < 0.01$; ***$p < 0.001$ vs Veh group)

alterations, rats exposed to VPA in utero demonstrate molecular and metabolic abnormalities. Very recent experiments demonstrated that VPA exposure impairs repair of DNA damage [41], modifies cholesterol/isoprenoid metabolism, and reduces the number of oligodendrocytes leading to lower myelin and cholesterol levels in the HPC of adolescent VPA-exposed rats [44].

Conclusions

Here, we extend this scenario by showing that prenatal VPA exposure induces autistic-like behaviors and does affect neuroglia. Modifications identified are brain region- and age-dependent. The changes in glia which we observed in VPA-exposed rats have been rather modest and occurred mostly at young ages; moreover, the

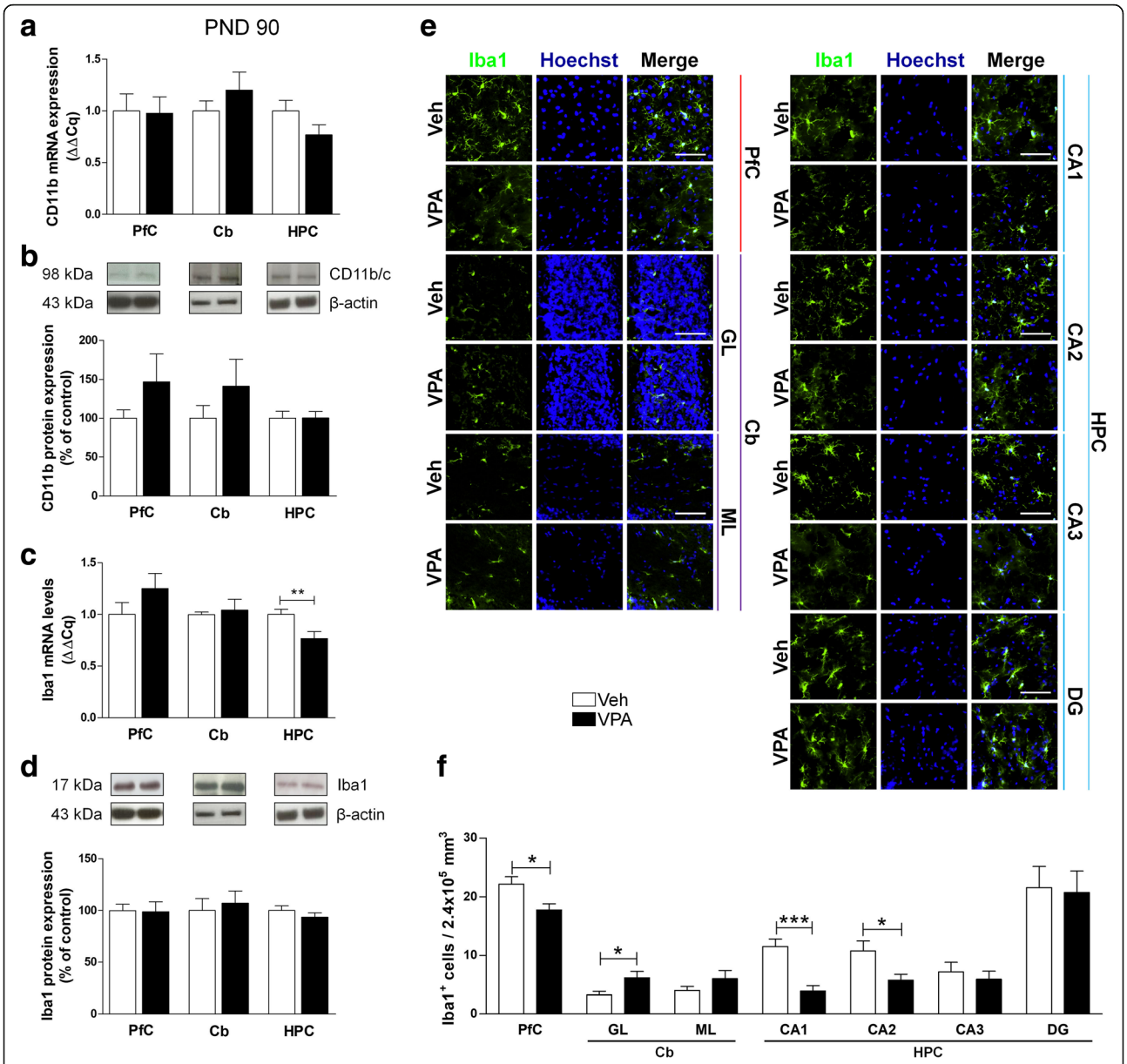

Fig. 10 Effect of the prenatal exposure to VPA on microglia in adulthood. Evaluation of the cluster of differentiation 11b (CD11b) and Iba1 in the PfC, Cb, and HPC of healthy- (open bars, Veh) and autistic-like (black bars, VPA) adult rats (PND 90). Representation of the relative concentration of CD11b (**a**) and Iba1 (**c**) in VPA animals compared to control (Veh), normalized to both TBP and HPRT (**ΔΔ**Cq; $N = 3$, in triplicate). Representative western blots for CD11b (**b**) and Iba1 (**d**) proteins, and densitometric analyses normalized to β-actin used as loading control. Results are expressed as percentage of control (Veh) ($N = 3$, in triplicate). Representative fluorescence micrographs of Iba1 (green) staining in the PfC, GL and ML of Cb, and stratum radiatum of CA1, CA2, CA3, and the hilus of the DG of the HPC. Nuclei were stained with Hoechst (blue) (**e**). The images have been analyzed by counting the number of Iba1-positive cells in 2.4×10^5 μm^3 (scale bar 50 μm; $N = 3$, 4 times) (**f**). All data are presented as means ± SEM. Statistical analysis was performed by *t* test (*$p < 0.05$; **$p < 0.01$; ***$p < 0.001$ vs Veh group)

changes were quite heterogeneous as they differ between brain regions, and often we have not seen obvious correlation between expression of mRNA and respective protein. In line with previous findings [24, 71], some hints for astrogliotic response were found in young animals, in which the density of GFAP-positive astrocytes has increased in the cortical regions. This increase went in parallel with elevated GFAP mRNA, without however changes in protein content. In adult rats, the number of GFAP-positive astrocytes was increased in CA3 but decreased in CA1 region and in cerebellum. Finally, in the mature rats, numbers of GFAP-positive cells were increased in Cb and CA2 hippocampal area, with no changes in expression of GFAP and S100B at a protein

level. At the same time, the changes in expression of neuroglial markers seem to be rather mild, with neuroinflammatory phenotype being present mainly in young ages and being ameliorated in adulthood.

All in all, the results we obtained in VPA-exposed rats are heterogeneous and intricate and reflect the complexity of the molecular and cellular mechanisms underlying ASD. Indeed, autism is a complex disease, whose clinic features are multifaceted and intricate like equally complex and subtle should be the molecular changes causing these phenotypes.

Abbreviations

ASD: Autism spectrum disorder; BSA: Bovine serum albumin; Cb: Cerebellum; CD11b: Cluster of differentiation 11b; CNS: Central nervous system; DG: Dentate gyrus; ECL: Enhanced chemiluminescence; EDTA: Ethylenediaminetetraacetic acid; GD: Gestational day; GFAP: Glial fibrillary acidic protein; GL: Granular layer; HPC: Hippocampus; HPRT: Hypoxanthine guanine phosphoribosyl transferase; HRP: Secondary horseradish peroxidase; ML: Molecular layer; PBS: Phosphate-buffered saline; PFA: Paraformaldehyde; PfC: Prefrontal cortex; PMSF: Phenylmethylsulfonyl fluoride; PND: Postnatal day; RT-qPCR: Real-time quantitative PCR; TBP: TATA-box binding protein; TBS-T: Tris-buffered saline 0.1% tween 20; USVs: Isolation-induced ultrasonic vocalizations; Veh: Saline; VPA: Valproic acid

Funding

This work was supported by SAPIENZA University of Rome grant n.MA116154CD981DAE (CS), Marie Curie Career Reintegration Grant PCIG09-GA-2011-293589 (VT) and the Jerome Lejeune Foundation Research grant #1674 (VT).

Availability of data and materials

The datasets used and/or analyzed during the current study are available from the corresponding author on reasonable request.

Authors' contributions

MRB, RF, DI, and CS performed most of the molecular experiments and analyzed the data. MS, SS, and VT treated and housed the animals, and performed the behavioral tasks. VT, LS, AV, and CS supervised the experiments and discussed the results. MRB, RF, VT, AV, and CS wrote the manuscript. All authors contributed to and approved the final manuscript.

Ethics approval

All procedures involving animals were performed in accordance with the guidelines of the Italian Ministry of Health (D.L. 26/2014) and with the European Parliament directive 2010/63/EU.

Consent for publication

Not applicable.

Competing interests

The authors declare that they have no competing interests.

Publisher's Note

Author details

[1]Department of Physiology and Pharmacology, "Vittorio Erspamer" SAPIENZA University of Rome, 00185 Rome, Italy. [2]Department of Science, Section of Biomedical Sciences and Technologies, University "Roma Tre", 00154 Rome, Italy. [3]Faculty of Biology, Medicine and Health, The University of Manchester, Manchester M13 9PT, UK. [4]Center for Basic and Translational Neuroscience, Faculty of Health and Medical Sciences, University of Copenhagen, 2200 Copenhagen, Denmark. [5]Achucarro Center for Neuroscience, IKERBASQUE, Basque Foundation for Science, 48011 Bilbao, Spain.

Received: 19 September 2018 Accepted: 10 December 2018
Published online: 27 December 2018

References

1. Gillott A, Standen PJ. Levels of anxiety and sources of stress in adults with autism. J Intellect Disabil. 2007;11(4):359–70.
2. Lai MC, Lombardo MV, Baron-Cohen S. Autism. Lancet. 2014;383(9920):896–910.
3. Christensen DL, Bilder DA, Zahorodny W, Pettygrove S, Durkin MS, Fitzgerald RT, et al. Prevalence and characteristics of autism spectrum disorder among 4-year-old children in the autism and developmental disabilities monitoring network. J Dev BehavPediatr. 2016;37(1):1–8.
4. Dietert RR, Dietert JM, Dewitt JC. Environmental risk factors for autism. Emerg Health Threats J. 2011;4:7111.
5. Kini U, Adab N, Vinten J, Fryer A, Clayton-Smith J. Liverpool and Manchester neurodevelopmental study group. Dysmorphic features: an important clue to the diagnosis and severity of fetal anticonvulsant syndromes. Arch Dis Child Fetal Neonatal. 2006;91:F90–5.
6. Kozma C. Valproic acid embryopathy: report of two siblings with further expansion of the phenotypic abnormalities and a review of the literature. Am J Med Genet. 2001;98(2):168–75.
7. Williams PG, Hersh JH. A male with fetal valproate syndrome and autism. Dev Med Child Neurol. 1997;39(9):632–4.
8. Williams G, King J, Cunningham M, Stephan M, Kerr B, Hersh JH. Fetal valproate syndrome and autism: additional evidence of an association. Dev Med Child Neurol. 2001;43(3):202–6.
9. Roullet FI, Lai JK, Foster JA. In utero exposure to valproic acid and autism--a current review of clinical and animal studies. Neurotoxicol Teratol. 2013;36:47–56.
10. Servadio M, Vanderschuren LJ, Trezza V. Modeling autism-relevant behavioral phenotypes in rats and mice: do 'autistic' rodents exist? Behav Pharmacol. 2015;26(6):522–40.
11. Nicolini C, Fahnestock M. The valproic acid-induced rodent model of autism. Exp Neurol. 2018;299:217–27.
12. Verkhratsky A, Butt AM. Glial physiology and pathophysiology. 1st ed: Wiley-Blackwell; 2013. Hoboken (NJ), USA
13. Wang DD, Bordey A. The astrocyte odyssey. Prog Neurobiol. 2008;86(4):342–67.
14. Parpura V, Heneka MT, Montana V, Oliet SH, Schousboe A, Haydon PG, et al. Glial cells in (patho)physiology. J Neurochem. 2012;121(1):4–27.
15. Verkhratsky A, Nedergaard M. The homeostatic astroglia emerges from evolutionary specialization of neural cells. Philos Trans R Soc Lond B Biol Sci. 2016;371(1700). https://doi.org/10.1098/rstb.2015.0428.
16. Verkhratsky A, Nedergaard M. Physiology of astroglia. Physiol Rev. 2018;98:239–389.
17. Eroglu C, Barres BA. Regulation of synaptic connectivity by glia. Nature. 2010;468:223–31.
18. Verkhratsky A, Nedergaard M. Astroglial cradle in the life of the synapse. Philos Trans R Soc Lond Ser B Biol Sci. 2014;369:20130595.
19. Zorec R, Horvat A, Vardjan N, Verkhratsky A. Memory formation shaped by astroglia. Front Integr Neurosci. 2015;9:56.
20. Nave KA. Myelination and support of axonal integrity by glia. Nature. 2010;468(7321):244–52.
21. Bessis A, Béchade C, Bernard D, Roumier A. Microglial control of neuronal death and synaptic properties. Glia. 2007;55(3):233–8.
22. Wake H, Moorhouse AJ, Jinno S, Kohsaka S, Nabekura J. Resting microglia directly monitor the functional state of synapses in vivo and determine the fate of ischemic terminals. J Neurosci. 2009;29(13):3974–80.
23. Kettenmann H, Hanisch UK, Noda M, Verkhratsky A. Physiology of microglia. Physiol Rev. 2011;91:461–553.
24. Salter MW, Stevens B. Microglia emerge as central players in brain disease. Nat Med. 2017;23(9):1018–27.
25. Pekny M, Pekna M, Messing A, Steinhauser C, Lee JM, Parpura V, et al. Astrocytes: a central element in neurological diseases. Acta Neuropathol. 2016;131:323–45.
26. Ferrer I. Diversity of astroglial responses across human neurodegenerative disorders and brain aging. Brain Pathol. 2017;27:645–74.
27. Verkhratsky A, Zorec R, Parpura V. Stratification of astrocytes in healthy and diseased brain. Brain Pathol. 2017;27:629–44.
28. Blank T, Prinz M. Microglia as modulators of cognition and neuropsychiatric disorders. Glia. 2013;61(1):62–70.

29. Scuderi C, Stecca C, Valenza M, Ratano P, Bronzuoli MR, Bartoli S, et al. Palmitoylethanolamide controls reactive gliosis and exerts neuroprotective functions in a rat model of Alzheimer's disease. Cell Death Dis. 2014;5:e1419.
30. Scuderi C, Bronzuoli MR, Facchinetti R, Pace L, Ferraro L, Broad KD, et al. Ultramicronized palmitoylethanolamide rescues learning and memory impairments in a triple transgenic mouse model of Alzheimer's disease by exerting anti-inflammatory and neuroprotective effects. Transl Psychiatry. 2018;8(1):32.
31. Verkhratsky A, Parpura V. Astrogliopathology in neurological, neurodevelopmental and psychiatric disorders. Neurobiol Dis. 2016;85:254–61.
32. Verkhratsky A, Zorec R, Rodriguez JJ, Parpura V. Astroglia dynamics in ageing and Alzheimer's disease. Curr Opin Pharmacol. 2016;26:74–9.
33. Zorec R, Parpura V, Vardjan N, Verkhratsky A. Astrocytic face of Alzheimer's disease. Behav Brain Res. 2017;322(Pt B):250–7.
34. Bronzuoli MR, Facchinetti R, Steardo L Jr, Romano A, Stecca C, Passarella S, et al. Palmitoylethanolamide dampens reactive astrogliosis and improves neuronal trophic support in a triple transgenic model of Alzheimer's disease: in vitro and in vivo evidence. Oxid Med Cell Longev. 2018;2018: 4720532.
35. Monzón M, Hernández RS, Garcés M, Sarasa R, Badiola JJ. Glial alterations in human prion diseases: a correlative study of astroglia, reactive microglia, protein deposition, and neuropathological lesions. Medicine (Baltimore). 2018;97(15):e0320.
36. Villadiego J, Labrador-Garrido A, Franco JM, Leal-Lasarte M, De Genst EJ, Dobson CM, et al. Immunization with α-synuclein/Grp94 reshapes peripheral immunity and suppresses microgliosis in a chronic Parkinsonism model. Glia. 2018;66(1):191–205.
37. Dichter GS, Felder JN, Green SR, Rittenberg AM, Sasson NJ, Bodfish JW. Reward circuitry function in autism spectrum disorders. Soc Cogn Affect Neurosci. 2012;7(2):160–72.
38. Donovan AP, Basson MA. The neuroanatomy of autism—a developmental perspective. J Anat. 2017;230(1):4–15.
39. Reim D, Distler U, Halbedl S, Verpelli C, Sala C, Bockmann J, et al. Proteomic analysis of post-synaptic density fractions from shank3 mutant mice reveals brain region specific changes relevant to autism spectrum disorder. Front Mol Neurosci. 2017;10:26.
40. Servadio M, Melancia F, Manduca A, di Masi A, Schiavi S, Cartocci V, et al. Targeting anandamide metabolism rescues core and associated autistic-like symptoms in rats prenatally exposed to valproic acid. Transl Psychiatry. 2016;6(9):e902.
41. Servadio M, Manduca A, Melancia F, Leboffe L, Schiavi S, Campolongo P, et al. Impaired repair of DNA damage is associated with autistic-like traits in rats prenatally exposed to valproic acid. Eur Neuropsychopharmacol. 2018; 28(1):85–96.
42. Kim KC, Kim P, Go HS, Choi CS, Park JH, Kim HJ, et al. Male-specific alteration in excitatory post-synaptic development and social interaction in pre-natal valproic acid exposure model of autism spectrum disorder. J Neurochem. 2013;124(6):832–43.
43. Melancia F, Schiavi S, Servadio M, Cartocci V, Campolongo P, Palmery M, et al. Sex-specific autistic endophenotypes induced by prenatal exposure to valproic acid involve anandamide signalling. Br J Pharmacol. 2018;175(18):3699–712.
44. Cartocci V, Catallo M, Tempestilli M, Segatto M, Pfrieger FW, Bronzuoli MR, et al. Altered brain cholesterol/isoprenoid metabolism in a rat model of autism spectrum disorders. Neuroscience. 2018;372:27–37.
45. Paolicelli RC, Bolasco G, Pagani F, Maggi L, Scianni M, Panzanelli P, et al. Synaptic pruning by microglia is necessary for normal brain development. Science. 2011;333:1456–8.
46. Tremblay ME, Stevens B, Sierra A, Wake H, Bessis A, Nimmerjahn A. The role of microglia in the healthy brain. J Neurosci. 2011;31:16064–9.
47. Kettenmann H, Kirchhoff F, Verkhratsky A. Microglia: new roles for the synaptic stripper. Neuron. 2013;77:10–8.
48. Zeidan-Chulia F, Salmina AB, Malinovskaya NA, Noda M, Verkhratsky A, Moreira JC. The glial perspective of autism spectrum disorders. Neurosci Biobehav Rev. 2014;38:160–72.
49. Petrelli F, Pucci L, Bezzi P. Astrocytes and microglia and their potential link with autism spectrum disorders. Front Cell Neurosci. 2016;10:21.
50. Voineagu I, Wang X, Johnston P, Lowe JK, Tian Y, Horvath S, et al. Transcriptomic analysis of autistic brain reveals convergent molecular pathology. Nature. 2011;474:380–4.
51. Fatemi SH, Folsom TD, Reutiman TJ, Lee S. Expression of astrocytic markers aquaporin 4 and connexin 43 is altered in brains of subjects with autism. Synapse. 2008;62:501–7.
52. Vargas DL, Nascimbene C, Krishnan C, Zimmerman AW, Pardo CA. Neuroglial activation and neuroinflammation in the brain of patients with autism. Ann Neurol. 2005;57:67–81.
53. Edmonson C, Ziats MN, Rennert OM. Altered glial marker expression in autistic post-mortem prefrontal cortex and cerebellum. Mol Autism. 2014;5:3.
54. Tetreault NA, Hakeem AY, Jiang S, Williams BA, Allman E, Wold BJ, et al. Microglia in the cerebralcortex in autism. J Autism Dev Disord. 2012;42: 2569–84.
55. Zeidan-Chulia F, de Oliveira BN, Casanova MF, Casanova EL, Noda M, Salmina AB, et al. Up-regulation of oligodendrocyte lineage markers in the cerebellum of autistic patients: evidence from network analysis of gene expression. Mol Neurobiol. 2016;53:4019–25.
56. Tian Y, Wang L, Jia M, Lu T, Ruan Y, Wu Z, et al. Association of oligodendrocytes differentiation regulator gene DUSP15 with autism. World J Biol Psychiatry. 2017;18:143–50.
57. Li J, Shi M, Ma Z, Zhao S, Euskirchen G, Ziskin J, et al. Integrated systems analysis reveals a molecular network underlying autism spectrum disorders. Mol Syst Biol. 2014;10:774.
58. Hardan AY, Libove RA, Keshavan MS, Melhem NM, Minshew NJ. A preliminary longitudinal magnetic resonance imaging study of brain volume and cortical thickness in autism. Biol Psychiatry. 2009;66:320–6.
59. Freitag CM, Luders E, Hulst HE, Narr KL, Thompson PM, Toga AW, et al. Total brain volume and corpus callosum size in medication-naive adolescents and young adults with autism spectrum disorder. Biol Psychiatry. 2009;66: 316–9.
60. Maezawa I, Jin LW. Rett syndrome microglia damage dendrites and synapses by the elevated release of glutamate. J Neurosci. 2010;30:5346–56.
61. Ballas N, Lioy DT, Grunseich C, Mandel G. Non-cell autonomous influence of MeCP2-deficient glia on neuronal dendritic morphology. Nat Neurosci. 2009; 12:311–7.
62. Yuskaitis CJ, Beurel E, Jope RS. Evidence of reactive astrocytes but not peripheral immune system activation in a mouse model of fragile X syndrome. Biochim Biophys Acta. 1802;2010:1006–12.
63. European Medicines Agency (EMA) New measures to avoid valproate exposure in pregnancy endorsed EMA/375438/2018. 2017. http://www.ema.europa.eu/docs/en_GB/document_library/Referrals_document/Valproate_2017_31/European_Commission_final_decision/WC500250216.pdf. Accessed 31 May 2018.
64. Ranger P, Ellenbroek BA. Perinatal influences of valproate on brain and behaviour: an animal model for autism. Curr Top BehavNeurosci. 2016;29: 363–86.
65. Markram K, Rinaldi T, La Mendola D, Sandi C, Markram H. Abnormal fear conditioning and amygdala processing in an animal model of autism. Neuropsychopharmacology. 2008;33:901–12.
66. Moldrich RX, Leanage G, She D, Dolan-Evans E, Nelson M, Reza N, et al. Inhibition of histone deacetylase in utero causes sociability deficits in postnatal mice. Behav Brain Res. 2013;257:253–64.
67. Wohr M, Schwarting RK. Affective communication in rodents: ultrasonic vocalizations as a tool for research on emotion and motivation. Cell Tissue Res. 2013;354:81–97.
68. Schneider T, Przewlocki R. Behavioral alterations in rats prenatally exposed to valproic acid: animal model of autism. Neuropsychopharmacology. 2005; 30:80–9.
69. Melo AI, Lovic V, Gonzalez A, Madden M, Sinopoli K, Fleming AS. Maternal and littermate deprivation disrupts maternal behavior and social-learning of food preference in adulthood: tactile stimulation, nest odor, and social rearing prevent these effects. Dev Psychobiol. 2006;48:209–19.
70. Schneider T, Turczak J, Przewlocki R. Environmental enrichment reverses behavioral alterations in rats prenatally exposed to valproic acid: issues for a therapeutic approach in autism. Neuropsychopharmacology. 2006;31:36–46.
71. Lucchina L, Depino AM. Altered peripheral and central inflammatory responses in a mouse model of autism. Autism Res. 2014;7(2):273–89.
72. Codagnone MG, Podestá MF, Uccelli NA, Reinés A. Differential local connectivity and neuroinflammation profiles in the medial prefrontal cortex and hippocampus in the valproic acid rat model of autism. Dev Neurosci. 2015;37(3):215–31.

1.7 Preliminary results on the role of glial cells in acute stress

2.7.1 Introduction

Stress is one of the major risk factors in psychiatric and neurodegenerative diseases, which constitute one of the most urgent and complex therapeutic challenges of the XXI century (Radley et al., 2011). When stress response is physiologically activated and then inactivated, it can promote adaptive plasticity; the subjects characterized by such a response are defined as resilient (RES). When the response is excessive or unregulated, it can induce maladaptive harmful effects; on the contrary, these subjects are defined as vulnerable (VUL) (Musazzi and Marrocco, 2016). Therefore, it is important to understand the mechanisms capable of modifying an adaptive physiological response to a maladaptive one. Changes in the neuroarchitecture of specific brain areas, like HPC and PfC, have been found in psychiatric patients and rodents exposed to chronic stress (CS) (Musazzi et al., 2013; Murrough et al., 2017). Findings suggest that these modifications are caused by the enhancement of glutamate release and excitatory transmission induced by stress (Musazzi et al., 2010, 2013), but clear evidence is still needed. Moreover, it has been also demonstrated that glia impairment after CS directly affects the glutamatergic homeostasis, thus contributing to a maladaptive stress response (Tynan et al., 2013; Mayhew et al., 2015).

Recent evidence hypothesizes that rapid and sustained changes in cerebral neuroarchitecture are also caused by acute stress (AS) (Nava et al., 2014; Treccani et al., 2014; Musazzi et al., 2017, 2019). Despite it is known that glial cells are the main regulators of the CNS given their important homeostatic functions, the effects of AS on these cells are still not well investigated. Astrocytes, also known as astroglia, are the most abundant cells of the human brain, performing heterogeneous functions including composing the blood brain barrier, provision of nutrients to the neurons, maintenance of extracellular ion balance, and damage repair (Allen and Eroglu, 2017).

Specific markers are used to identify and visualize astrocytes in the CNS (Verkhratsky et al., 2017). The most commonly used marker for immunostaining of astrocytes is the glial fibrillary acidic protein (GFAP), a structural marker which detects only a sub-population of these cell type with a regional and developmental heterogeneity. Immunoreactivity for another astrocytic marker, the glutamine synthetase (GS), responsible of the conversion of glutamate in glutamine, is usually detected in fibrous and protoplasmic astrocytes, in radial glia, Bergmann glia, retinal Müller glia, tanycytes and ependymal cells; interestingly, GS labels many GFAP-negative astrocytes. For example, in the mouse entorhinal cortex, 78% of all labelled glial cells are GS-positive, 12% GFAP-positive and only 10% are positive for both GS and GFAP (Yeh et al., 2013). Similarly, in the HPC, the double staining showed that only 60% of the cells immunoreactive for GS were positive also for GFAP (Walz and Lang, 1998).

The aim of this study is to investigate the role of glial cells in stress response. In particular, it intends to investigate if AS causes structural and functional alterations of these cells in the PrL, an area importantly involved in the stress response, and whether these modifications are similar in both RES and VUL animals. The results will allow to identify effectors that may become targets for innovative drug treatments.

The first experiments performed were conducted with the effort of characterizing the involvement and the response to AS of three different astrocytic subpopulations, marked with GFAP, GS and GFAP+GS in both RES and VUL animals.

2.7.2. Materials and Methods

Animals and experimental design

Experiments were performed on adult male Sprague-Dawley rats (100g ± 20g). Rodents were housed in groups of four/cage and constantly monitored in order to protect their welfare. All experiments were conducted in accordance with the guidelines for the correct use of laboratory animals, as reported by the Ministry of Health in the L.D. 4 March 2014, n.26 and in the Directive of the European Community 2010/63/EU. The housing conditions included a 12h light/12h dark life cycle (light on at 07:00 AM), room temperature at 22°C, and *ad libitum* water and food.

Starting at the second experimental day, animals were exposed to a 1% sucrose solution for two hours. Rats were then subjected to a period of habituation to sucrose until day 35 exposing them, twice a week, for 1 hour a day (from 10:00 to 11:00 AM) to two bottles, one containing tap water and the other a 0.5% sucrose solution.

Water and sucrose consumptions were measured by weighing the respective bottles before and after the exposure, obtaining the basal level of sucrose preference. 24 hours after the end of the habituation period, half of the rats were exposed to a footshock (FS) protocol (Musazzi et al., 2010); the other animals were considered as controls (not stressed, NS).

After the FS session, animals were placed in their own cages and, after 24 hours, subjected to the sucrose preference test (SPT). In the middle of the test, bottles were exchanged in order to eliminate the bias due to their position in the cage. On the basis of the results obtained from the SPT, animals were divided into RES and VUL rats. Specifically, rats were considered RES when the intake of sucrose was below 10% compared to the basal consumption, or VUL if this reduction exceeded 25%. After the test, rats were sacrificed and the brain of each animal rapidly isolated and stored at -80°C, until subsequent molecular biology analyses. The experimental design is shown in detail in Fig.7.

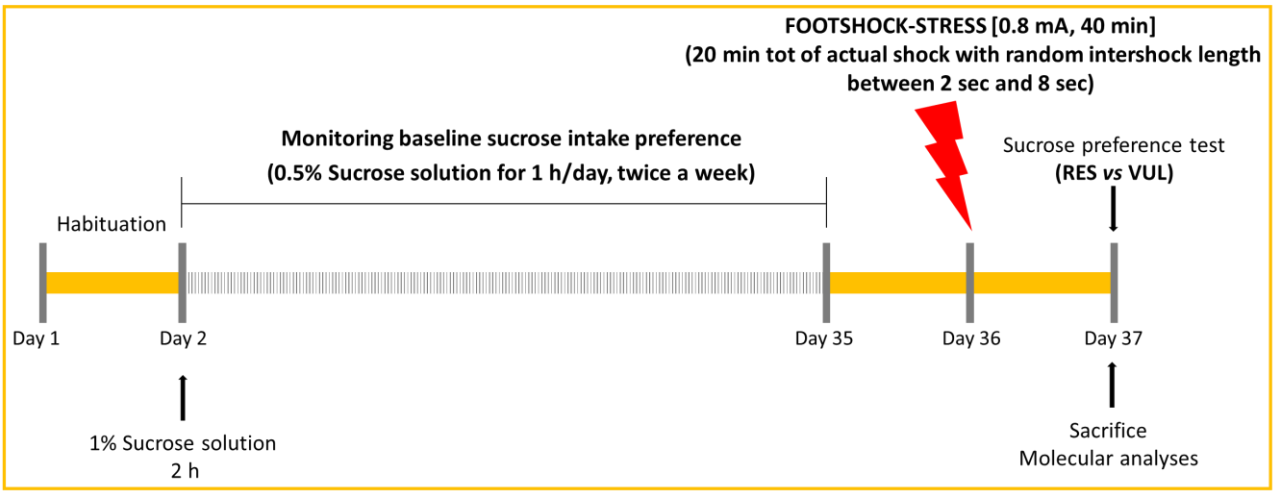

Fig. 7. Schematic representation of the experimental design.

Immunofluorescence

Animals were perfused with 4% paraformaldehyde (PFA) and immunofluorescence was performed on brain 20-µm-thick coronal slices containing the PrL. Perfused tissues were rinsed in phosphate-buffered saline (PBS) and antigen-retrival was performed at 95°C in sodium citrate. After the blocking step, lasting 60 min at room temperature in 5% BSA dissolved in PBS/0.25% triton X-100, sections were incubated overnight with the primary antibody recognizing GFAP and GS at + 4 °C. Primary antibodies were diluted in 5% BSA in PBS/ 0.25% triton X-100. Tissues were rinsed in PBS and incubated for 2 h at room temperature with the proper secondary antibody. The staining of nuclei was performed with Hoechst (1:5000, Thermo Fisher Scientific, MA, USA). After rinses in PBS, slices were mounted with Fluoromount aqueous mounting medium (Sigma-Aldrich). Fluorescent signal was detected by an Eclipse E600 microscope using a Nikon Plan Fluor 20X/0.5 objective (Nikon Instruments, Rome, Italy). Pictures were captured by a QImaging camera (Surrey, BC, Canada) with NISelements BR 3.2 64-bit software (Nikon Instruments). For each slice three images were acquired, in order to analyze the whole area. The immunopositive cell count was calculated in a volume of 1,57 x 10^6 µm^3, deriving from the sum of the three areas acquired, multiplied by the thickness of the slice. The experimental conditions are summarized in Table 1.

Table 1. Experimental conditions used for immunofluorescence.

Primary antibody	Brand	Dilution	Secondary antibody	Brand
Rabbit α-GFAP	Abcam	1:200 5% BSA in PBS/0.25% triton X-100	FITC conjugated goat anti-rabbit IgG (H+L) 1:200, 5% BSA in PBS/0.25% triton X-100	Jackson ImmunoResearch
Rabbit α-GS	Millipore	1:1000 5% BSA in PBS/0.25% triton X-100	FITC conjugated goat anti-mouse IgG (H+L) 1:200, 5% BSA in PBS/0.25% triton X-100	Jackson ImmunoResearch

2.7.3 Results

To characterize the astrocytic component in this model of AS and investigate the role of astrocytes in the resilient or vulnerable response to stress, GFAP-positive cells, GS-positive cells and GFAP+GS-positive cells were counted in NS, RES and VUL animals. Data obtained from the immunofluorescence analyses showed a reduction of the total amount of astrocytes in the PrL of stressed animals, independently from their resilient or vulnerable response to AS (RES, ****p < 0,0001 *vs* NS and VUL, ***p < 0,001 *vs* NS). Surprisingly, the three astrocytic components behaved differently between RES and VUL animals. In particular, only VUL animals showed statistically significant increased levels of GFAP-positive cells respect to NS rats (*p < 0,05). Concerning the enzyme responsible of the conversion of glutamate in glutamine, we found a decreased number of GS-positive cells again in VUL subjects compared to NS animals (*p < 0,05). GS+GFAP-double positive cells markedly decreased their number in both RES and VUL animals (***p < 0,001) (Fig. 8).

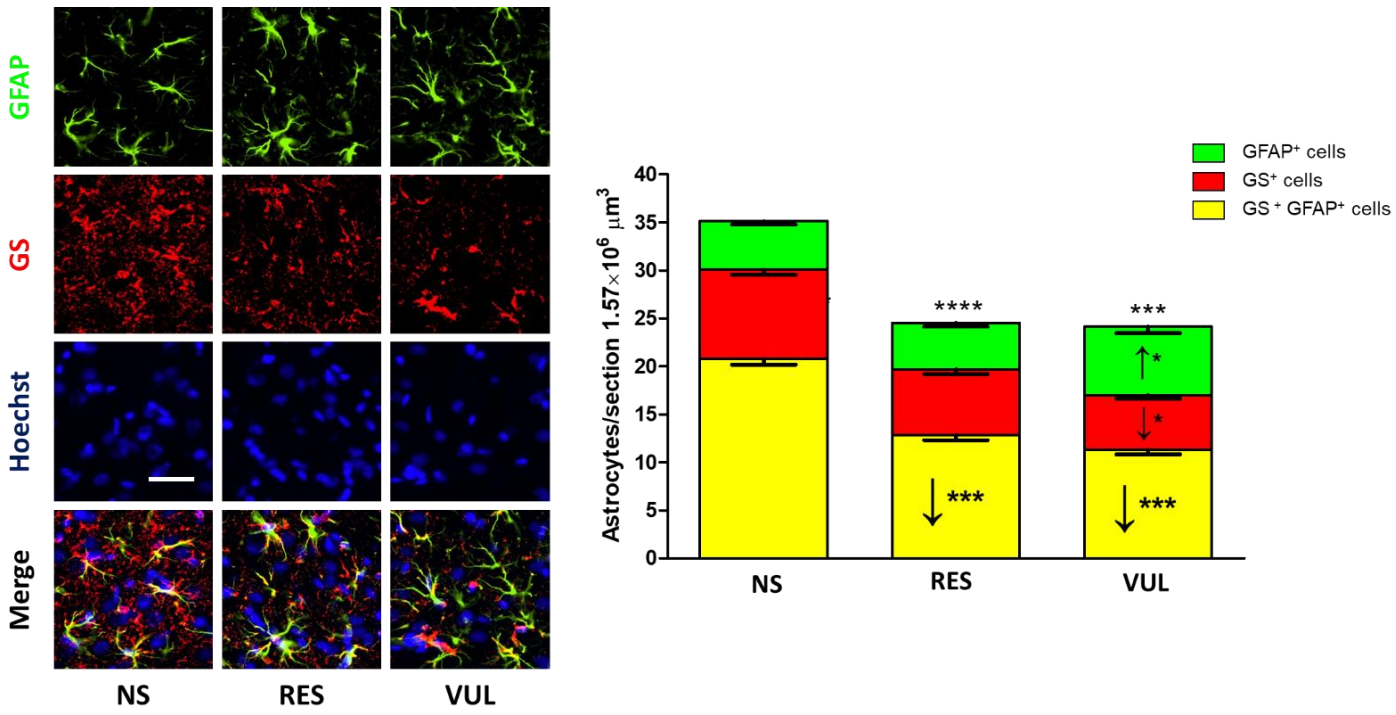

Fig.8. Acute stress decreases the total number of astrocytes and induces a rearrangement in the three astrocytic subpopulations investigated in both RES and VUL animals. Representative fluorescent photomicrographs of GFAP (*green*), GS (*red*) and GFAP+GS (*yellow*) staining in the PrL of Sprague-Dawley rats 24 hours after acute stress. Nuclei were stained with Hoechst (*blue*). Scale bar is 20 µm.

2.7.4 Discussion and conclusions

To date, literature is still poor of data on acute stress despite this is a topic of recent interest since acute stress-related events, like earthquakes, are more and more frequent. Moreover, the individual predisposition to the stress resilient or vulnerable response is still underinvestigated. Therefore, our interest has focused on glial cells and, in particular, on astrocytes because of their key role in the maintenance of the homeostasis of the brain. Our initial investigations show that a short, unpredictable, AS is able to induce a marked astrocytic death, independently from their resilient or vulnerable response to stress and, mostly, independently from the subpopulation investigated. More interestingly, with these preliminary results we characterized, for the first time in a preclinical model, the different behavior of three different astrocytic subpopulations in the resilient or vulnerable response to stress in the PrL. What comes to the attention in the graph here presented is an overall rearrangement of the astrocytic subpopulations between RES and VUL animals respect to NS rats. However, the most prominent changes are clearly visible in VUL rats, the experimental group in which all the three subpopulations investigated are rearranged in different directions respect to control subjects. These initial results suggest the abundant heterogeneity of the astrocytic component and that both structural and functional alterations can affect these cells after an AS. This could be the starting point towards an identification of the different predispositions of individuals to traumatic events, aiming at a future personalized pharmacological approach to treat stress-related neuropsychiatric disorders.

2.7.5 References

Allen NJ, Eroglu C. Cell Biology of Astrocyte-Synapse Interactions. *Neuron*. 2017;96(3):697–708.

Marrocco J, Reynaert ML, Gatta E, et al. The effects of antidepressant treatment in prenatally stressed rats support the glutamatergic hypothesis of stress-related disorders. *J Neurosci*. 2014; 34(6):2015–2024.

Mayhew J, Beart PM, Walker FR. Astrocyte and microglial control of glutamatergic signalling: a primer on understanding the disruptive role of chronic stress. *J Neuroendocrinol*. 2015;27(6):498-506.

Murrough JW, Abdallah CG, Mathew SJ. Targeting glutamate signalling in depression: progress and prospects. *Nat Rev Drug Discov*. 2017;16(7):472-486.

Musazzi L, Marrocco J. The Many Faces of Stress: Implications for Neuropsychiatric Disorders. *Neural Plast*. 2016;2016:8389737.

Musazzi L, Milanese M, Farisello P, et al. Acute stress increases depolarization-evoked glutamate release in the rat prefrontal/frontal cortex: the dampening action of antidepressants. *PLoS One*. 2010;5(1): e8566.

Musazzi L, Sala N, Tornese P, et al. Acute Inescapable Stress Rapidly Increases Synaptic Energy Metabolism in Prefrontal Cortex and Alters Working Memory Performance. *Cereb Cortex*. 2019; pii: bhz034.

Musazzi L, Treccani G, Mallei A, et al. The action of antidepressants on the glutamate system: regulation of glutamate release and glutamate receptors. *Biol Psychiatry*. 2013;73(12):1180-8.

Nava N, Treccani G, Liebenberg N, et al. Chronic desipramine prevents acute stress-induced reorganization of medial prefrontal cortex architecture by blocking glutamate vescicle accumulation and excitatory synapse increase. *Int J Neuropsychopharmacol*. 2014;18(3): pyu085.

Radley JJ, Kabbaj M, Jacobson L, Heydendael W, Yehuda R, Herman JP. Stress risk factors and stress-related pathology: neuroplasticity, epigenetics and endophenotypes. *Stress*. 2011;14(5):481–497.

Treccani G, Musazzi L, Perego C, et al. Stress and corticosterone increase the readily releasable pool of glutamate vesicles in synaptic terminals of prefrontal and frontal cortex. *Mol Psychiatry*. 2014;19(4):433-43.

Tynan RJ, Beynon SB, Hinwood M, et al. Chronic stress-induced disruption of the astrocyte network is driven by structural atrophy and not loss of astrocytes. *Acta Neuropathol*. 2013;126(1):75-91.

Verkhratsky A, Zorec R, Parpura V. Stratification of astrocytes in healthy and diseased brain. *Brain Pathol*. 2017;27(5):629–644.

Walz W, Lang MK. Immunocytochemical evidence for a distinct GFAP-negative subpopulation of astrocytes in the adult rat hippocampus. *Neurosci Lett.* 1998;257(3):127-30.

Yeh CY, Verkhratsky A, Terzieva S, et al. Glutamine synthetase in astrocytes from entorhinal cortex of the triple transgenic animal model of Alzheimer's disease is not affected by pathological progression. *Biogerontology*. 2013;14(6):777-87.

Chapter 25

An Animal Model of Alzheimer Disease Based on the Intrahippocampal Injection of Amyloid β-Peptide (1–42)

Roberta Facchinetti, Maria Rosanna Bronzuoli, and Caterina Scuderi

Abstract

The intrahippocampal injection of amyloid beta peptide (1–42) ($A\beta_{(1–42)}$) represents one of the most useful animal models of Alzheimer disease. Since none of these available models fully represents the main pathological hallmarks of Alzheimer disease, stereotaxic $A\beta_{(1–42)}$ infusion provides researchers with an in vivo alternative paradigm. When performed by well-trained individuals, this model is the best-suited one for short-term studies focusing on the effects of $A\beta_{(1–42)}$ on a specific brain region or circuitry. Here, we describe all methodological phases of such a model.

Key words Stereotaxic infusion, Hippocampus, Beta-amyloid, Alzheimer disease, In vivo experiments

1 Introduction

Alzheimer disease (AD) is, without question, one of the most economically burdensome health conditions facing today's society [1]. Histopathologically, one of the main AD features is the deposition of extracellular neuritic amyloid β-peptide (Aβ) that eventually forms senile plaques. These deposits are present mainly in the hippocampal and cortical regions [2]. The hippocampal stereotaxic infusion of oligomeric Aβ in rats (mice can be used as well [3]) is a method involving the direct infusion of Aβ oligomeric species into the brain parenchyma. Usually, the infusion target is the CA1 subregion of the hippocampus [4], since this brain region is one of the areas most affected by neurodegeneration in AD; alternatively, this peptide can be infused into the neocortex [5], according to the experimental aim. The infusion of oligomeric $A\beta_{(1–42)}$ into the brain of wild-type rat provides an excellent in vivo model which replicates the amyloidopathy and consequent neuronal cell death

Stephen D. Skaper (ed.), *Neurotrophic Factors: Methods and Protocols*, Methods in Molecular Biology, vol. 1727, https://doi.org/10.1007/978-1-4939-7571-6_25,

[6–8]. This method allows one to replicate the increase of Aβ peptide in a spatial and temporal manner, preventing any compensatory or side effects that may be encountered with transgenic lines [3]. Despite the advantages of this model, the $A\beta_{(1–42)}$ infusion method has its limitations. First, this model attempts to reproduce only the effects of $A\beta_{(1–42)}$ in just a specific brain region. Second, during the procedure, the needle itself (used for $A\beta_{(1–42)}$ infusion) causes damage in the injection site, thus provoking additional cell death and gliosis. Here, we describe all steps required to establish this model starting from determining injection coordinates, performing the surgery, and $A\beta_{(1–42)}$ infusion and, at the end, postoperative animal care.

2 Materials

All steps are carried out at room temperature unless otherwise described in sterile conditions. Wear lab coat and gloves.

1. 70° ethanol: to prepare 1 kg (sterile conditions are not required) measure in a cylinder 320 g 96° ethanol and 680 g deionized distilled H_2O (*see* **Note 1**).
2. 0.9% NaCl solution (saline solution): to prepare 1 L, dissolve 9 g NaCl in 600 mL of ultrapure H_2O in a beaker and mix thoroughly with the help of stirrer. Make up to 1000 mL with ultrapure H_2O and mix again. Sterilize the solution by filtering through a 0.22 μm filter or by autoclaving for 20 min at 15 psi (1.05 kg/cm^2) on liquid cycle.
3. Artificial cerebrospinal fluid (aCSF): 12.4 mM NaCl, 1.1 mM glucose, 0.25 mM KCl, 0.25 mM $CaCl_2$ dihydrate, 0.13 mM $MgCl_2$ hexahydrate, 0.1 mM NaH_2PO_4 monohydrate, and 2.6 mM $NaHCO_3$. Prepare two 10× stock solutions (*see* **Note 2**). To prepare 1 L of 10× stock solution 1, weigh out 72.46 g NaCl, 19.82 g glucose, 1.25 g KCl, 0.65 g $MgCl_2$ hexahydrate, and 0.5 g NaH_2PO_4 monohydrate, transfer to a graduated cylinder, make up to 1 L with ultrapure H_2O, and mix thoroughly with the help of a magnetic stirrer. To prepare 1 L of 10× stock solution 2, weigh out 13 g $NaHCO_3$, transfer to a graduated cylinder, and make up to 1 L with ultrapure H_2O. Mix thoroughly until completely dissolved. Store both stock solutions at +4 °C for a maximum of 2 months. To prepare 1 L of 1× aCSF working solution, transfer 100 mL each of stocks 1 and 2 into a graduated cylinder and bring to 1 L with ultrapure H_2O (*see* **Note 3**).
4. $A\beta_{(1–42)}$ solution: the concentration suggested for rats is 2 μg/μL $A\beta_{(1–42)}$ [4] (*see* **Note 4**). Solubilize 300 μg $A\beta_{(1–42)}$ in 150 μL of aCSF (*see* **Note 5**).

5. Sodium pentobarbital (recommended dosage for rats is 50 mg/kg): to prepare 50 mL, weigh 2500 mg of sodium pentobarbital into a beaker and suspend in ultrapure H_2O with stirring (*see* **Note 6**). Add dry NaOH (1–2 pellets) so that the pH of the solution is between 12 and 12.5. Adjust the pH to approximately 9.8 (i.e., until the drug barely goes into solution) by adding 10 M HCl dropwise. Adjust the volume of the drug solution so that it is 50% of the final desired volume. Add 20 mL of propylene glycol (40% of total volume), followed by 5 mL of ethanol (10% of total volume) and mix with a stirrer until the solution is homogeneous. Filter the solution into a sterile bottle using a 0.22 μm filter. Store the solution in a locked drawer at room temperature until use [9] (*see* **Note 7**).
6. Buprenorphine (recommended dosage for rats is 0.05 mg/kg): dilute 1 mL of buprenorphine (0.3 mg/mL) in 5 mL 0.9% NaCl. Mix with a stirrer. The solution is light-sensitive; store in a dark place and protect from light. The diluted buprenorphine solution should be used within 30 days of preparation [11].
7. Chlorhexidine 2%: to prepare 50 mL, dissolve 1 g of chlorhexidine digluconate in ultrapure H_2O by mixing with a stirrer. Sterilize the solution by filtering it through a 0.22 μm filter.
8. Lidocaine chlorhydrate: to prepare 5 mL, weigh 50 mg of lidocaine chlorhydrate and 30 mg of sodium chloride. Bring to volume with ultrapure H_2O. Mix with a stirrer. Sterilize the solution by filtering it through a 0.22 μm filter.

3 Methods

To prevent any animal infections during surgical procedures, wearing a surgical face mask, a clean lab coat, and sterile surgical gloves is suggested. All procedures should be carried out in compliance with appropriate governmental and institutional guidelines for the care and use of laboratory animals.

3.1 Preparation of Surgical Tools

1. Autoclave all surgical tools.
2. Attach the 29 G needle to the Hamilton syringe.
3. Clean the interior of Hamilton syringe and the needle by withdrawing and ejecting ultrapure H_2O repeatedly for 1 min.
4. Remove the plunger and needle from the Hamilton syringe. Air-dry the parts in a laminar flow hood overnight.
5. Irradiate the needle and syringe with ultraviolet light for 30 min before use.

3.2 Stereotaxic Frame Setup

1. Wipe down the stereotaxic instrument and rat adaptor with 70° ethanol (*see* **Note 8**).
2. Place the stereotaxic instrument with rat adaptor on the surgical bench over which has been placed a sterile surgical towel (*see* **Note 9**).
3. With 70° ethanol wipe the rat heating pad (*see* **Note 10**) and position it over the stereotaxic frame bed (*see* **Note 11**).
4. Switch on the heating pad and set to 37 °C and wait until it reaches the temperature.

3.3 Animal Preparation

1. Determine the weight of the rat (*see* **Note 12**).
2. Anesthetize the rat with sodium pentobarbital (50 mg/kg) intraperitoneally (*see* **Note 13** and **14**).
3. Monitor the depth of anesthesia by the loss of toe pinch reflex (*see* **Note 15**).
4. After the rat is sedated, use the hair clipper and shave its head to expose the skin over the skull.
5. Place the animal on top of the heating pad placed over the stereotaxic bed (*see* **Note 16**).
6. Use a spatula to open the mouth, and a tweezer to take out the tongue to prevent choking. Place the incisor teeth inside the appropriate hole. Secure the nosepiece above the face of the rat. Clamp it down gently, but not too tight (*see* **Note 17**).
7. Position the bilateral ear crossbars into auditory meatus to secure the head. Move each crossbar until they hit the skull, and then turn the screw to lock it (*see* **Note 18**).
8. Apply eye drops on each eye to keep them wet (*see* **Note 19**). Insert the anal thermometer in the rat (Fig. 1a) (*see* **Note 20**).

3.4 Surgery and Infusion

1. Disinfect the surgical site using cotton swabs to apply 2% chlorhexidine (*see* **Note 21**) over the shaved skin, followed by 70° ethanol. Repeat this procedure three times (*see* **Note 22**).
2. Administer subcutaneously lidocaine chlorhydrate (1–2%), enough to create a bubble between the skin and the skull (*see* **Note 23**).
3. Use a scalpel to make an incision in the midline of the scalp (*see* **Note 24**) and, if necessary, use a straight fine scissors to extend the incision line to expose the sagittal suture, bregma, and lambda, landmarks based on stereotaxic coordinates.
4. Dry the skull with cotton swabs, trying to keep the skin apart (*see* **Note 25**).
5. Fix a 0.8 mm drill head to the drill. Take the drill with both hands, set elbows on the surface of the table for stability, and position the drill head slightly above the sharpie (*see* **Note 26**).

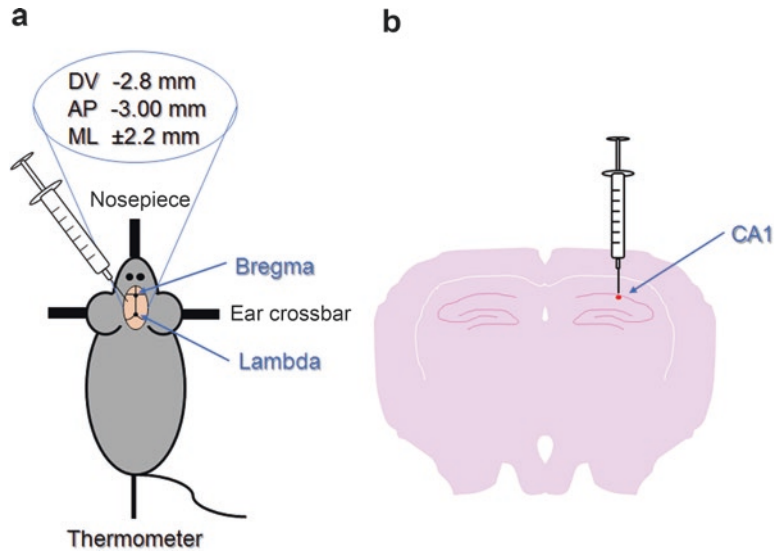

Fig. 1 (**a**) Animal preparation after shaving its head to expose the skin over the skull: use the spatula to open the mouth and place the incisor teeth inside the appropriate hole; position the bilateral ear crossbars into auditory meatus to secure the head; insert the anal thermometer in the rat. (**b**) DV, ML and AP coordinates (respectively −2.8 mm, ±2.2 mm and −3.00) to find the CA1 subregion of the hippocampus of an adult rat

6. Use the stereotaxic micromanipulator to position the drill (*see* **Note 27**).
7. Be sure that the head of the rat is perfectly parallel to the floor (*see* **Note 28**).
8. Move the drill bit on the AP axis so that the tip touches first the lambda and then the bregma point and the DV coordinates are the same (accept a difference within 0.5 mm).
9. Do the same to check that also the ML axis is perfectly horizontal: move the drill bit on the ML axes of the same distances from the bregma (e.g., −1.0 and +1.0); make sure that the DV coordinates are the same at both ML axes (accept a difference within 0.5 mm).
10. Now that the skull is in the right position, starting from bregma, move the drill in the ML and AP directions according to the coordinates needed (*see* **Note 29**).
11. With a sterile marker, draw a dot in the precise region of interest at both left and right ML coordinates (*see* **Note 30**).
12. With the help of a micromanipulator, lower the tip of the drill onto the skull surface and activate the drill to create a hole in the skull (*see* **Note 31**, **32** and **33**).
13. Move far from the injection site and disassemble the drill from the stereotaxic frame.

14. Mount the Hamilton syringe on the stereotaxic frame.
15. Starting again with the tip of the 29G needle above the bregma, move the Hamilton syringe according to AP and ML coordinates (*see* **Note 34**).
16. Lower the Hamilton needle through the hole and find the DV, ML, and AP coordinates (in this case, respectively −2.8 mm, ±2.2 mm and −3.00) to find the CA1 of the adult rat (Fig. 1).
17. Activate the stereotaxic injector pump connected to the Hamilton syringe to release 2.5 μL $A\beta_{(1–42)}$ at a rate of 0.5 μL/min (*see* **Note 35**).
18. Slowly, move the needle out of the brain with the micromanipulator (*see* **Note 36**).
19. Close the wound with resorbable suture wire.

3.5 Animal Removal from Stereotactic Frame and Postoperative Care

1. Unscrew the ear bars and face/nose guard.
2. Remove the anal thermometer.
3. Remove the rat from the stereotactic frame.
4. Inject the rat intraperitoneally with 1 mL of sterile saline for hydration.
5. Inject buprenorphine (0.01–0.05 mg/kg) subcutaneously to relieve pain over the next 24 h.
6. Maintain the rat in a clean empty cage equipped with a hot plate until it wakens (*see* **Note 37**).
7. Return the rat to its housing cage with food and water ad libitum (*see* **Note 38**).
8. Administer buprenorphine subcutaneously every 12 h for 3 days for pain relief.
9. Usually, the animal can be sacrificed 7–14 days after surgery [3].
10. According to the experimental design, treatment can be started and the animal perfused with 4% paraformaldehyde, the brain removed and processed for cryosectioning. Alternatively, behavioral studies can be performed.

4 Notes

1. % w/w 70° ethanol is 62.46 and % w/w 96° ethanol is 93.82.
2. Avoid preparing a unique 10× stock solution because the powders would never dissolve.
3. Prepare the aCSF working solution the day of the experiments.

4. Choose $A\beta_{(1–42)}$ dose according to literature.
5. This preparation allows to prepare a soluble $A\beta_{(1–42)}$ solution. Since Aβ is toxic not only in this form but also in the oligomeric and fibrillary forms, it is possible to generate the latter two species with different protocols. For further information, see [13].
6. Sodium pentobarbital will not dissolve completely in water at neutral pH; a suspension will be obtained.
7. Alternatively, the animal can be anesthetized with ketamine/xylazine cocktail: 100 mg/mL ketamine, 100 mg/mL xylazine. To prepare 10 mL: mix 3.75 mL ketamine and 0.5 mL xylazine in 5.75 mL of ultrapure H_2O in a sterile 10 mL bottle closed with a rubber stopper. Keep the ketamine/xylazine cocktail up to 7 days at +4 °C. Select the earliest expiration date between ketamine or xylazine, for a maximum of 3 months. Shake well before use. Another way to anesthetize the rat is through the inhalation of isoflurane. In a chamber of 1 L, use 0.26 mL of liquid isoflurane to achieve a 5% concentration, and 0.10 mL to have 2% [10].
8. Choose the size of the tools according to the age of the animal and to the animal itself, e.g., mice need a smaller stereotaxic frame and ear bars to hold the head.
9. When using isoflurane, remember to work under a vertical flow hood in order to avoid inhalation of the drug by the operator.
10. We recommend using a heating pad with built-in anal thermometer to check the animal's temperature. Body temperature should be maintained at 37 ± 0.5 °C.
11. Use general purpose laboratory labeling tape to attach the heating pad over the mouse adaptor bed.
12. The animal's weight is important to calculate the dose of anesthetic.
13. If you are using the ketamine/xylazine cocktail, the dosage is 40–100 mg/kg (i.p.) (ketamine) and 5–13 mg/kg (i.p.) (xylazine); if you are using isoflurane, the dosage of up to 5% in oxygen may be used for induction and approximately 2% in oxygen for maintenance.
14. Right after administration, leave the animal in a dark box to facilitate relaxation and a faster sleep induction.
15. Check reflexes once the animal appears to be anesthetized; causing pain too early slows down the process of anesthesia.
16. Animals under anesthesia are unable to control their body temperature, and it is important to monitor and regulate it to avoid death from hypothermia.

17. Be careful not to choke the animal while performing this procedure.
18. To make sure the head is secured use the index finger to gently push it down. A properly secured head should not move at all.
19. Make sure the eyes are moist throughout the surgical procedure; constantly monitor that the eyes are covered with the drops because long-term dry eyes could lead to blindness.
20. To avoid the thermometer moving during the procedure, fix it with tape parallel to the tail.
21. Alternatively, also betadine or iodine solution can be used.
22. Apply 2% chlorhexidine circling from future incision site outward to free the surgical area of dirt.
23. Do not exceed 10 mg/kg, the toxic dose.
24. To perform a single and precise cut, use two fingers to stretch the skin over the head of the animal.
25. Use micro clamps to keep the skin apart, if necessary.
26. We recommend using a stereoscope to be as accurate as possible during all procedures from this step on.
27. Use the adult rat brain atlas [12] to determine the precise anterior-posterior (AP), medial-lateral (ML), and dorsal-ventral (DV) coordinates to reach the region of interest (to illustrate the technique we considered the CA1 of the adult rat hippocampus). The following coordinates from the bregma have been taken into consideration: AP −3.00 mm, ML ±2.2 mm, DV −2.8 mm [4]. The negative sign preceding the AP value indicates that it is 2.00 mm posterior of the bregma. The ± sign preceding the medial-lateral value indicates left (−) and right (+) direction from the center. Lastly, the negative sign preceding the DV indicates a ventral direction from the surface of the brain [3].
28. Adjust the skull in order to have the same DV coordinates in both bregma and lambda with the help of a micromanipulator; this would mean that the AP axis is perfectly parallel to the floor.
29. Before starting the actual procedure, we recommend practicing the injections in few animals with a dye (e.g., Evan's blue); after sacrifice, cut slices at the vibratome and check under a dissection microscope if the dye is in the correct position. This is particularly important when injecting young animals.
30. $A\beta_{(1–42)}$ can also be inoculated unilaterally or bilaterally, according to experimental aims.
31. It is important to pay attention to the depth of the hole to avoid bleeding. We recommend drilling a little, then raising the drill bit and checking with a needle the presence or absence

of the bone. Repeat until the hole is created and the needle touches the brain without puncturing it.

32. Use a clean dry cotton swab to dab the blood in the case of bleeding.
33. In case of bilateral inoculation, repeat this step for the contralateral side.
34. When executed properly, the needle will be perfectly above the hole in the skull.
35. When the infusion is complete, leave the needle in place for an additional 5–8 min to minimize backflow of $A\beta_{(1-42)}$ solution out of the injection site and to facilitate its diffusion.
36. Oligomeric $A\beta_{(1-42)}$ solutions can be injected on each side of the brain allowing comparisons to be made between the left and right hemispheres [6]; in this case, remember to restart the surgical protocol from step number 5.
37. 10–20 min before putting rats inside the cage, remember to turn on the hot plate setting it at +42 °C.
38. Animals that underwent surgery should be housed separately or with others that had undergone the same procedure in the last 12–24 h. There is a high risk that the operated animal may be attacked/bitten, or even killed if left together with a rat that has not undergone any procedure.

Acknowledgment

This work was supported by SAPIENZA University Grant to CS (prot. C26A15X58E).

References

1. Gaugler J, James B, Johnson T, Scholz K, Weuve J (2015) Alzheimer's disease facts and figures. Alzheimer's Dement 11(3):267–282
2. Braak H, Braak E (1988) Neuropil threads occur in dendrites of tangle-bearing nerve cells. Neuropathol Appl Neurobiol 14:39–44
3. Jean YY, Baleriola J, Fà M, Hengst U, Troy CM (2015) Stereotaxic infusion of oligomeric amyloid-beta into the mouse hippocampus. J Vis Exp 100:e52805. https://doi.org/10.3791/52805
4. Scuderi C, Stecca C, Valenza M, Ratano P, Bronzuoli MR, Bartoli S et al (2014) Palmitoylethanolamide controls reactive gliosis and exerts neuroprotective functions in a rat model of Alzheimer's disease. Cell Death Dis 5:e1419. https://doi.org/10.1038/cddis.2014.376
5. Bolmont T, Clavaguera F, Meyer-Luehmann M, Herzig M, Radde R, Staufenbiel M et al (2007) Induction of tau pathology by intracerebral infusion of amyloid-β-containing brain extract and by amyloid-β deposition in APP × tau transgenic mice. Am J Pathol 171(6):2012–2020. https://doi.org/10.2353/ajpath.2007.070403
6. Baleriola J, Walker CA, Jean YY, Crary JF, Troy CM, Nagy PL et al (2014) Axonally synthesized ATF4 transmits a neurodegenerative signal across brain regions. Cell 158(5):1159–1172. https://doi.org/10.1016/j.cell.2014.07.001

7. Jean YY, Ribe EM, Pero ME, Moskalenko M, Iqbal Z, Marks LJ et al (2013) Caspase-2 is essential for c-Jun transcriptional activation and Bim induction in neuron death. Biochem J 455(1):15–25. https://doi.org/10.1042/BJ20130556
8. Sotthibundhu A, Sykes AM, Fox B, Underwood CK, Thangnipon W, Coulson EJ (2008) Beta-amyloid (1-42) induces neuronal death through the p75 neurotrophin receptor. J Neurosci 28(15):3941–3946. https://doi.org/10.1523/JNEUROSCI.0350-08.2008
9. Priest SM, Geisbuhler TP (2015) Injectable sodium pentobarbital: stability at room temperature. J Pharmacol Toxicol Methods 76:38–42. https://doi.org/10.1016/j.vascn.2015.07.012
10. Office of Animal Resources (2017) Institutional Animal Care and Use Committee. https://animal.research.uiowa.edu. Accessed 7 Apr 2017
11. Thompson AC, Kristal MB, Sallaj A, Acheson A, Martin LB, Martin T (2004) Analgesic efficacy of orally administered buprenorphine in rats: methodologic considerations. Comp Med 54(3):293–300
12. Paxinos G, Watson C (1998) The rat brain in stereotaxic coordinates, 4th De Luxe edn. Elsevier Science Publishing Co Inc., San Diego
13. Stine WB, Jungbauer L, Yu C, LaDu MJ (2011) Preparing synthetic Aβ in different aggregation states. Methods Mol Biol 670:13–32. https://doi.org/10.1007/978-1-60761-744-0_2

Chapter 24

Preparation of Rat Hippocampal Organotypic Cultures and Application to Study Amyloid β-Peptide Toxicity

Maria Rosanna Bronzuoli, Roberta Facchinetti, and Caterina Scuderi

Abstract

Hippocampal organotypic cultures constitute a very easy but delicate method widely used to study amyloid β-peptide toxicity. This ex vivo technique is performed on tissues isolated from newborn rats. Here, we describe a protocol for the preparation and culture of hippocampal organotypic slices that can be maintained for 14–21 days and their application to the study of amyloid β-peptide toxicity.

Key words Organotypic culture, Hippocampus, β-Amyloid, Toxicity, Brain slices, Ex vivo, Rat, Neuropharmacology

1 Introduction

The concept of organotypic cultures comes from the need to study functional activity of the central nervous system in a more complex environment that is not represented by dissociated cell cultures. The term organotypic was first used in 1954 [1]. Since then, hippocampal organotypic cultures have found wide application in providing a bridge between in vitro and in vivo systems to investigate important neuronal and glial features in health and disease [2–4]. These allow the investigator to maintain the three-dimensional organization of cerebral tissue and thereby study structural and synaptic organization—even glial cell modifications. With this technique, most neuronal circuits, along with their physiology and receptor distribution, are preserved, especially in hippocampal organotypic cultures [5]. The latter can be easily grown for several weeks without particular difficulty, requiring only refreshing the culture medium when necessary. This method achieved optimization in 1991 [6] and has been adapted over the years [1, 7–10]. In particular, organotypic hippocampal cultures have become a helpful tool to study neurodegenerative disorders that often affect this

Stephen D. Skaper (ed.), *Neurotrophic Factors: Methods and Protocols*, Methods in Molecular Biology, vol. 1727, https://doi.org/10.1007/978-1-4939-7571-6_24,

cerebral region, such as Alzheimer disease [11], one of whose main neuropathological characteristics is the presence of amyloid β-peptide (Aβ) deposition [12].

Cerebral tissues from newborn rats and mice are commonly used. Here, we describe the preparation of organotypic hippocampal cultures and provide an example of their use to study Aβ neurotoxicity. This model can also be applied to physiological studies, live imaging, confocal time-lapse imaging, or immunohistochemical labeling with fluorescent dyes.

2 Materials

Prepare all the solutions in sterile conditions wearing lab coat and gloves.

1. Dissecting solution: Hanks' balanced salt solution (HBSS) with 20 mM 4-(2-hydroxyethyl)piperazine-1-ethanesulfonic acid, *N*-(2-hydroxyethyl)piperzine-*N*′-(2-ethanesulfonic acid) (HEPES), and 6% D-glucose. Weight 30 g D-glucose and 2.4 g HEPES and transfer to a cylinder. Add 100 mL HBSS and mix. Make up to 500 mL with HBSS. Sterilize the solution by passage through 0.22 μm filter and aliquot in 50 mL tubes. Store at +4 °C for no longer than 2 months (*see* **Note 1**).
2. Slice culture medium: 48.5% Dulbecco's Modified Eagle Medium (DMEM), 25% HBSS, 25% heat-inactivated horse serum (*see* **Note 2**), 20 mM HEPES, and 1.5% penicillin-streptomycin. Weight 2.4 g HEPES and transfer to the cylinder. Add 100 mL HBSS and mix. Add 125 mL heat-inactivated horse serum, 125 mL HBSS, and 7.5 mL penicillin-streptomycin. Make up to 500 mL with DMEM. Sterilize the solution by passage through 0.22 μm filter and aliquot in 50 mL tubes. Store at +4 °C for no longer than 2 months (*see* **Note 3**).
3. Aβ solution: 1 μg/mL $A\beta_{(1–42)}$ (*see* **Notes 4** and **5**). To prepare 10 mL: weight 0.01 mg soluble $A\beta_{(1–42)}$ and transfer to a cylinder. Make up to 10 mL with slice culture medium (*see* **Notes 6**, **7**, and **8**).
4. Phosphate-buffered saline (PBS): (*see* **Note 9**) A 10× stock solution can be prepared and then diluted 1:10 in sterile deionized H_2O to obtain the working solution. To prepare 1 L of 10× PBS, dissolve 80 g NaCl (1.37 M), 2.0 g KCl (27 mM), 14.4 g Na_2HPO_4 (100 mM), and 2.4 g KH_2PO_4 (18 mM) in 700 mL of deionized H_2O. Transfer the solution into a cylinder and make up to 1 L with deionized H_2O (*see* **Note 10**). Sterilize the solution by autoclaving for 20 min at 15 psi (1.05 kg/cm^2), and store it at +4 °C for no longer than 2 months. To prepare the 1× PBS working solution, put 100 mL of 10× stock solution

into a cylinder and add 800 mL of sterile deionized H_2O. Check the pH with a pH meter and, if necessary, adjust the pH to 7.4 with HCl. Make up to 1 L with deionized H_2O. Sterilize the solution by autoclaving for 20 min at 15 psi (1.05 kg/cm^2) on liquid cycle or by filter sterilization. Store at +4 °C for no longer than 2 months (*see* **Note 11**).

5. Four percent paraformaldehyde (PFA): (*see* **Notes 12** and **13**) weight 40 g of PFA powder and in the meantime heat 800 mL of 1× PBS working solution (prepared as described in **item 4** above) while stirring into a flask to approximately +60 °C using a hot plate (*see* **Note 14**). The powder will take few minutes to dissolve (*see* **Note 15**). Drop by drop add 1 N NaOH until the solution clears. Cool the solution, filter and cover with foil to protect from light. Make up to 1 L with 1× PBS working solution and check once again the pH and, if necessary, adjust to pH 6.9 with small drops of diluted HCl. Aliquot the solution and store frozen at −20 °C or store at +4 °C for up to 1 month.

3 Methods

All steps are carried out at room temperature unless otherwise described and in sterile conditions. The protocol below should be performed rapidly (*see* **Note 16**). Wear lab coat and gloves (*see* **Note 17**).

3.1 Hippocampal Slice Preparation

1. Prepare the dissecting area with paper over aluminum foil so to contain the spread of blood.
2. Clean the laminar flow hood with 70% ethanol and place inside the vibratome, stereoscope (to use in case of the alternative method, *see* **Note 18**), and dissecting tools for 15–20 min with UV light on.
3. Put the dissecting solution into a 200 mL beaker and leave for 10–20 min at −80 °C (*see* **Note 19**).
4. Sacrifice a postnatal day 1–7 Sprague-Dawley or Wistar rat pup (*see* **Note 20**) by decapitation with sharp scissors (*see* **Notes 21** and **22**). All procedures have to be carried out in compliance with appropriate governmental and institutional guidelines for the care and use of laboratory animals.
5. With a scalpel cut the skin to expose the skull, and cut the cerebellum away with a blade or a scalpel. Then, with small scissors, cut the skull from lambda to bregma along the midsagittal plane (*see* **Note 23**). With the help of pointed tweezers, remove the bones and quickly delve the brain with a

Fig. 1 Steps to prepare and fix the brain in the vibratome. (**a**) Eliminate one quarter of the cerebral rostral frontal lobe with a scalpel; (**b**) secure the brain over the holder with glue; (**c**) move the tissue over the chamber filled with cold dissecting solution and cut along the transversal plane

micro spatula from the frontal region. In a 100 mm Petri dish, with a scalpel, remove one quarter of the rostral frontal lobe (*see* **Note 18**) (Fig. 1a).

6. Fill the chamber that will contain the tissue with cold dissecting solution (*see* **Note 24**), and fill the surrounding chamber (if present) with ice (*see* **Note 25**).
7. For a few seconds, gently and slightly dry the brain on a piece of paper and fix the tissue over the holder with glue (Fig. 1b).
8. Transfer the tissue holder with the brain attached into the vibratome chamber containing the cold dissecting solution (Fig. 1c).
9. Mount a new blade at the vibratome (*see* **Note 26**). With the vibratome, cut the brain (or the hippocampus) along the transversal plane with the following parameters: 0.8 mm/s speed, 1.45 mm amplitude, and 350–400 μm thickness (*see* **Note 27**). Use the hippocampal slice collector (to use in case of the alternative method, *see* **Note 18**) to collect only slices containing the hippocampal region (*see* **Note 28**).
10. Fill a 100 mm Petri dish with chilled slice culture medium and transfer slices with a cut plastic Pasteur pipette (*see* **Note 29**) to avoid making bubbles (*see* **Note 30**).
11. Discard damaged slices.

3.2 Hippocampal Slices Culture

The use of sterile conditions applies also to this part.

1. Prepare a 6-well plate by adding 1.2 mL of slice culture medium (*see* **Note 11**) to each well and then place a semi-porous insert (0.4 μm pore size) into each well (*see* **Note 31**) and leave in the 37 °C and 5%CO_2/95%O_2 incubator to equilibrate.
2. Retrieve from the incubator the 6-well plate containing the semi-porous inserts submerged in slice culture medium, trans-

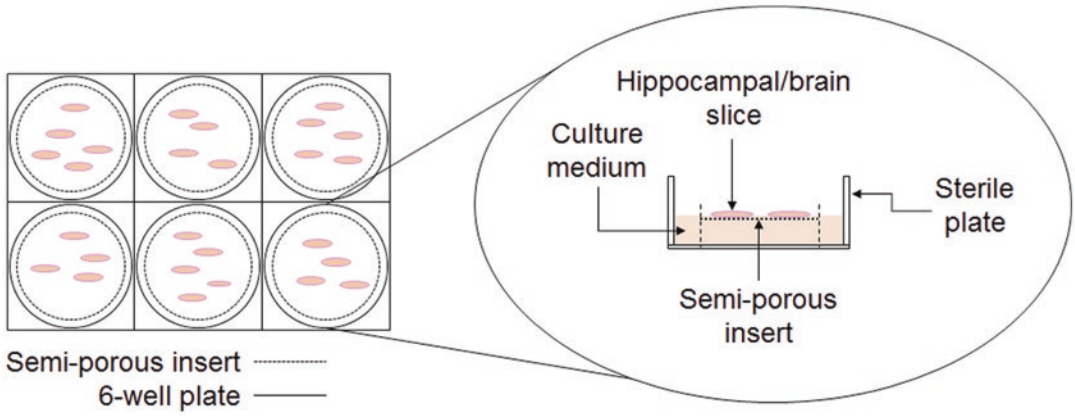

Fig. 2 Assembly of semi-porous inserts for hippocampal slice culture in a 6-well plate. The insert is located on the bottom of the well which is filled with culture medium avoiding bubbles. Hippocampal slices are positioned over the insert

fer 4–5 slices onto each membrane insert using a cut Pasteur pipette (*see* **Notes 29** and **32**); avoid making bubbles (Fig. 2). Return the 6-well plate to the incubator (*see* **Note 33**).

3. Refresh culture medium as needed, in general every 48 h (*see* **Notes 34** and **35**).

3.3 Aβ Toxicity in Hippocampal Slice Cultures

The use of sterile conditions applies also to this part.

1. On day 14–21 of culturing (*see* **Note 36**), remove the organotypic hippocampal slices from the incubator.
2. With the help of a vacuum pump, discard slice culture medium.
3. Treat the slices with 1.2 mL Aβ solution and/or any treatment solution to test.
4. Return slices to the 37 °C incubator.
5. Leave the organotypic hippocampal slices for 24 h in the incubator with test solutions (*see* **Note 37**).
6. After the desired period of incubation (*see* **Note 38**), with the help of a vacuum pump, discard the treatment solution.
7. Rinse slices twice with 1.2 mL 1× PBS.
8. Remove 1× PBS with the help of a vacuum pump.
9. Fix hippocampal slides for 24 h within 4% PFA at +4 °C (*see* **Note 39**).
10. Gently remove hippocampal slides from inserts with a cut Pasteur pipette made of plastic (*see* **Note 28**) and proceed with morphological evaluation.

4 Notes

1. Different solutions are available; for example, it is possible to use a low Na^+ artificial cerebrospinal fluid with the following composition: 1 mM $CaCl_2$ (0.055 g), 10 mM D-glucose (0.901 g), 4 mM KCl (0.149 g), 4 mM $MgCl_2$ (0.19 g), 26 mM $NaHCO_3$ (1.092 g), 234 mM sucrose (40 g), and 0.1% (v) phenol red solution in Dulbecco's phosphate-buffered saline. Make up to 500 mL with sterile deionized H_2O [13].
2. Horse serum inactivation is needed to inactivate complement. This is done by placing the serum in a water bath at 56° for 30 min. Aliquot and store at −20 °C for no longer than 18 months.
3. Alternatively, one can use 48.5% Minimum Essential Medium Eagle (MEM), 25% heat-inactivated horse serum, 25% HBSS, 20 mM HEPES, 1 mM glutamine, and 5 mg/mL glucose. To prepare 500 mL of solution: weight 2.4 g HEPES, 2.5 g D-glucose, and 73 mg glutamine and transfer to a cylinder. Add 100 mL MEM and mix. Add 125 mL heat-inactivated horse serum, 125 mL HBSS, and 7.5 mL penicillin-streptomycin. Make up to 500 mL with MEM. Sterilize the solution by passage through 0.22 μm filter and aliquot in 50 mL tubes. Store at +4 °C for no longer than 2 months.
4. Prepare the solution fresh on the day of the experiment unless otherwise specified.
5. Since $A\beta_{(1–42)}$ is not the only toxic amyloidogenic peptide, even $A\beta_{(25–35)}$ or $A\beta_{(1–40)}$ fragments can also be used, according to the experimental aim. Choose concentrations referring to the literature.
6. Warm the solution at 37 °C for around 10–15 min before treating slices. Longer times can lead to oligomerization, which should be avoided unless experimentally required.
7. This preparation allows to prepare a soluble $A\beta_{(1–42)}$ solution. Since Aβ is toxic not only in this form but also in the oligomeric and fibrillary forms, it is possible to reproduce these last with different protocols. For example, working in a fume hood, dissolve 10 mg lyophilized $A\beta_{(1–42)}$ in 2.217 mL 100% hexafluoroisopropanol (HFIP) to obtain a 1 mM solution. Allow the HFIP to evaporate overnight after preparing 10 μL aliquots (0.045 mg of $A\beta_{(1–42)}$), and store the peptide at −20 °C. Resuspend the peptide in 20 μL dimethyl sulfoxide (DMSO) to obtain a 5 mM solution. To obtain oligomers, dilute 60 μL of 5 mM Aβ in DMSO in 1140 μL of the culture medium to achieve the final concentration of 100 μM, and incubate at +4 °C for 24 h. To generate fibrils, dilute 60 μL of

5 mM Aβ in DMSO in 1140 μL of 10 mM HCl to reach the final concentration of 100 μM, and then incubate the solution for 24 h at +37 °C. For further information, see [14].

8. Some groups, instead of buying Aβ, use cell lines overexpressing Aβ species, and then collect the medium enriched in these species.
9. It is possible to buy ready-to-use 10× and 1× PBS solutions.
10. The pH of the PBS stock solution is around 6.8.
11. Warm the working solution in a +37 °C water bath before using with slices.
12. PFA is highly toxic, and personal protective equipment (appropriate mask and safety glasses) is recommended, along with preparing the solution inside a fume hood.
13. For each compound, especially with toxic ones, read carefully safety data sheets provided by the manufacturer before manipulation.
14. The solution must not boil. Check temperature with a thermometer. Do not heat the solution above 70 °C, otherwise the beaker will break.
15. Some fine particles will not go away.
16. Speed should not come at the expense of precision and accuracy!
17. To prevent any further culture contamination, wearing of a facemask is suggested.
18. Alternatively, it is possible to work with only hippocampi, isolating them from the cortex. In this case, place the brain in the ice-cold dissecting solution for 0.5–1 min, and then transfer it into a 100 mm Petri dish containing ice-cold dissecting solution, paying attention to completely cover the tissue. Move to the stereoscope, and place the brain in order to hold it at the midline with the forceps pressing over the surface of the 100 mm Petri dish. Work with one hemisphere at a time. With the hippocampus dissecting tool, remove the midbrain, and separate the hemispheres avoiding damage to the tissue. The hippocampi are then exposed, and it is possible to gently scoop them out with the tool. Remember to clean the hippocampus as much as possible.
19. Just before starting slice isolation, bubble the solution with 5% CO_2/95% O_2 until saturated (10–20 min) in order to prevent oxygenation of the tissue during the isolation.
20. It is possible to perform this technique with up to three animals at the same time.
21. Perform the cut rapidly, with no hesitation in order to prevent pain to the animal and reduce the presence of blood in the tissue.

22. The smell of blood can make rats very nervous; we recommend performing the decapitation in a room different from the one in which they are housed.
23. An alternative approach is to cut the interaural line and then along the sagittal suture.
24. Make sure to fill the chamber enough to completely cover both brain and blade, otherwise the vibratome will not be able to cut the tissue properly.
25. Alternatively, use a vibratome that chills the tissue by itself.
26. Some vibratomes allow you to check blade position and vibration. In this case, do not ignore this step, and perform it every time a new blade is inserted.
27. The use of less thick slices makes more unlikely the presence of entirely healthy neuronal cell projections; thicker slices increase the risk of hypoxia in the more central regions of the slice. In either case, tissue health would be compromised.
28. Refer to Paxinos & Watson atlas: for rats (IV edition) from Tables 29 to 38 [15] and for mice (II edition) from Tables 42 to 53 [16].
29. Alternatively, broken glass Pasteur pipettes or snipped tips of a P1000 filter pipette tips can be used. Although the use of a thin brush is also often proposed, we suggest avoiding this so as to touch tissues as little as possible.
30. With a spatula gently separate slices one from the other.
31. Make sure the inserts are completely wet with no bubbles underneath.
32. Pay attention to not place slices either close to the insert perimeter or to each other in order to prevent oxygenation of the tissues.
33. Keep cultures at a stable temperature above 30 °C.
34. Keep working in sterile conditions.
35. Pre-warm the slice culture medium at 37 °C. Aspirate the medium with the help of a vacuum pump or with a Pasteur pipette. Add 1.2 mL of fresh slice culture medium making sure not to create bubbles underneath the inserts.
36. Over the course of the culture period, the slices become thinner.
37. Selection of experimental conditions should be based on the literature.
38. Experiments should be designed with not too long an incubation time to prevent slice deterioration. We suggest not to exceed 24 h of incubation.

39. If live hippocampal slices are needed, such as for electrophysiological procedures, avoid this step and perform the experiments.

Acknowledgement

This work was supported by SAPIENZA University Grant to CS (prot. C26A15X58E).

References

1. Reinbold R (1954) Organotypic differentiation of the eye of the chick embryo in vitro. C R Seances Soc Biol Fil 148:1493–1495
2. Scuderi C, Valenza M, Stecca C et al (2012) Palmitoylethanolamide exerts neuroprotective effects in mixed neuroglial cultures and organotypic hippocampal slices via peroxisome proliferator-activated receptor-α. J Neuroinflammation 9:49. https://doi.org/10.1186/1742-2094-9-21
3. Harwell CS, Coleman MP (2016) Synaptophysin depletion and intraneuronal Aβ in organotypic hippocampal slice cultures from huAPP transgenic mice. Mol Neurodegener 11:44. https://doi.org/10.1186/s13024-016-0110-7
4. Müller M, Gähwiler BH, Rietschin L et al (1993) Reversible loss of dendritic spines and altered excitability after chronic epilepsy in hippocampal slice cultures. Proc Natl Acad Sci U S A 90:257–261
5. Gähwiler BH, Capogna M, Debanne D et al (1997) Organotypic slice cultures: a technique has come of age. Trends Neurosci 20:471–477
6. Stoppini L, Buchs PA, Muller D (1991) A simple method for organotypic cultures of nervous tissue. J Neurosci Methods 37:173–182
7. Shamir ER, Ewald AJ (2014) Three-dimensional organotypic culture: experimental models of mammalian biology and disease. Nat Rev Mol Cell Biol 15:647–664. https://doi.org/10.1038/nrm3873
8. Ullrich C, Daschil N, Humpel C (2011) Organotypic vibrosections: novel whole sagittal brain cultures. J Neurosci Methods 201:131–141. https://doi.org/10.1016/j.jneumeth.2011.07.021
9. Pellegrini-Giampietro DE, Cozzi A, Peruginelli F et al (1999) 1-Aminoindan-1,5-dicarboxylic acid and (S)-(+)-2-(3′-carboxybicyclo[1,1,1]pentyl)-glycine, two mGlu1 receptor-preferring antagonists, reduce neuronal death in in vitro and in vivo models of cerebral ischemia. Eur J Neurosci 11:3637–3647. https://doi.org/10.1046/j.1460-9568.1999.00786.x
10. Finley M, Fairman D, Liu D et al (2004) Functional validation of adult hippocampal organotypic cultures as an in vitro model of brain injury. Brain Res 100:125–132
11. Scuderi C, Steardo L (2013) Neuroglial roots of neurodegenerative diseases: therapeutic potential of palmitoylethanolamide in models of Alzheimer's disease. CNS Neurol Disord Drug Targets 12:62–69
12. Hardy J, Selkoe DJ (2002) The amyloid hypothesis of Alzheimer's disease: progress and problems on the road to therapeutics. Science 297:353–356
13. Opitz-Araya X, Barria A (2011) Organotypic hippocampal slice cultures. J Vis Exp 48:2462. https://doi.org/10.3791/2462
14. Stine WB, Jungbauer L, Yu C, LaDu MJ (2011) Preparing synthetic Aβ in different aggregation states. Methods Mol Biol 670:13–32. https://doi.org/10.1007/978-1-60761-744-0_2
15. Paxinos G, Watson C (1998) The rat brain in stereotaxic coordinates, 4th De Luxe edn. Elsevier Science Publishing Co Inc., San Diego
16. Franklin KBJ, Paxinos G (2001) The mouse brain in stereotaxic coordinates, 2nd revised edn. Elsevier Science Publishing Co Inc, San Diego

3. Conclusions

According to their physiological role, glial cells respond quickly right after any brain trauma. Despite this knowledge, research evidence still lacks an exhaustive comprehension of the molecular mechanisms involved in such glial response. Therefore, during the three years of PhD program in Pharmacology and Toxicology, I focused my research studies on this issue. I studied three different neuropsychiatric conditions, such as AD, ASD and AS, obtaining interesting results. My experiments contributed indeed to demonstrate the huge heterogeneity and complexity of the glial responses.

I observed that these cells, when activated, can assume a plethora of different behaviors that are dependent on the brain region investigated, the stage of the pathology, and the age of the animals.

Unexpectedly, the greatest alteration in glial cells were observed in PfC and HPC compared to other brain regions in all three neuropsychiatric disorders investigated, thus suggesting a strong region-dependent behavior of these cells.

The heterogeneity of the obtained results, which reflect the complexity of the pathologies I studied, should encourage further investigations of the cellular and molecular mechanisms involved in the onset and/or progression of AD, ASD, and AS. These conditions are indeed still incurable and extremely expensive for the society and governments.

The new “gliocentric vision” of neuropsychiatric disorders represents a new and intriguing direction in the neuroscience field, opening new horizons towards innovative pharmacological treatments.

In support of this hypothesis, it is worth highlighting that some drugs and supplements, already licensed for human use, act restoring glial cells dysfunctions. Among them, there are several PEA-containing products (Normast®, Glialia®, Nevamast®, Adolene®, Visimast®, Mastocol®, and Pelvilen®), already approved for human use especially in inflammatory pain, and drugs like Gylenia® (Fingolimod), approved for relapsing-remitting multiple sclerosis.

The data collected in this dissertation converge in indicating glial cells as main actors in the scenario of neuropsychiatric disorders. However, further studies are absolutely required to thoroughly characterize the mechanisms. Glial cells are fundamental for the brain homeostasis and, for this reason, the manipulation of their functions should be made within the context of precision medicine.